The Role of the ArcA Metabolic Regulator in Gram-Negative Bacteremia

by

Aric N. Brown

A dissertation submitted in partial fulfillment
of the requirements for the degree of
Doctor of Philosophy
(Microbiology and Immunology)
in the University of Michigan
2023

Doctoral Committee:

Professor Harry L. T. Mobley, Chair
Research Assistant Professor Mark T. Anderson
Professor Maria Sandkvist
Associate Professor Anthony Vecchiarelli

Aric N. Brown

arnbrown@umich.edu

ORCID iD: 0000-0003-1455-4736

Dedication

This dissertation is dedicated to my mom and dad, who are very kind.

Acknowledgements

Personal Acknowledgements

Firstly, I would like to thank Dr. Harry Mobley for the opportunity to train in such an esteemed and high-impact research program. This experience has afforded me the ability to learn and perform research alongside some of the finest scientists in the field of bacteriology. I cannot describe the educational value that the diversity in research in the Mobley lab has provided me. Your mentorship has allowed me to grow as a scientist and has fostered independence and creativity. I thank you for trusting me with managing my project and for listening to my office rants regarding convoluted metabolic processes.

I must give extensive credit to Dr. Mark Anderson for his guidance, insight, and support for the entire duration of this project. My graduate school tenure would not have been nearly as fruitful or impactful without your mentorship. Thank you for teaching me the first step of troubleshooting is not doubting yourself. I also extend gratitude to my other committee members, Dr. Maria Sandkvist and Dr. Anthony Vecchiarelli. Maria, your clever suggestions always came at the right time, and your high standards for research have encouraged me from the start. I thank you Anthony for always being enthusiastic about my research and reminding me to appreciate the novelty.

I express my deep appreciation for the time and energy of the many educators whom I have had the pleasure of learning from over the past 25 years. I would like to especially acknowledge Ms. Stacey Falk for believing in me, Dr. Judith Atzler for teaching me values beyond science, and Dr. Anupama Shanmuganathan for inspiring me to be the best student and

scientist I can be.

This research would not have been completed the same way without the professional and personal support of my many, many labmates. Thank you especially to Stephanie Himpsl for fostering a productive research environment.

I thank my friends, old and new, for letting me be me.

I acknowledge the unwavering (but maybe sometimes wavering) support of my family. To my brothers, thank you for reminding me to lighten up. To my sister, I cherish the value of our friendship over time and space. Thank you to my sisters-in-law for reminding me to come home. Thank you to my brother-in-law for understanding the relentless culture of academia. And thank you to my nieces and nephews even though you fail to grasp basic concepts of microbiology such as the differences between bacteria and viruses.

Thank you mom for teaching me the importance of education, thank you dad for teaching me the value of hard work, and thank you both for instilling in me our faith.

And lastly I acknowledge those along the way who made all the difference.

Financial Acknowledgements

This work was supported in part by the American Heart Association through a pre-doctoral fellowship (828854) and the University of Michigan Rackham Graduate School through pre-and post-candidate grants to Aric N. Brown. Support was also received from Public Health Service awards AI148767 to Mark T. Anderson and AI134731 to Harry L. T. Mobley and Michael A. Bachman from the National Institutes of Health. Financial assistance was also received from the Department of Microbiology and Immunology.

Table of Contents

List of Tables

List of Figures

List of Abbreviations

AUC: Area under curve
ATP: Adenosine triphosphate
CCCP: Carbonyl cyanide m-chlorophenyl hydrazone
CFU: Colony forming unit
CI: Competitive index
DIP: 2,2′-Bipyridine (Dipyridyl)
DMSO: Dimethyl sulfoxide
ETC: Electron transport chain
h.p.i.: Hours post-infection
LB: Luria broth
LC-MS: Liquid chromatography-mass spectrophotometry
LDH: Lactate dehydrogenase
OD: Optical density
PBS: Phosphate buffered saline
PCR: Polymerase chain reaction
PMF: Proton motive force
PMB: Polymyxin B
RT-qPCR: Real-time quantitative polymerase chain reaction
TCA: Tricarboxylic acid
wHTH: Winged helix-turn-helix

Abstract

Infections of the bloodstream are life-threatening and can result in sepsis. Gram-negative bacteria cause a significant portion of bloodstream infections, which is also referred to as bacteremia. The long-term goal of this work is to understand how such bacteria establish and maintain infection during bacteremia. Our research group has previously identified the transcription factor ArcA, which promotes fermentation in bacteria, as a likely contributor to the growth and survival of bacteria in this environment. Here, I study ArcA in the Gram-negative species *Citrobacter freundii*, *Klebsiella pneumoniae,* and *Serratia marcescens* and demonstrate that this transcription factor which represses aerobic respiration is necessary when cells encounter decreased oxygen levels, iron limitation, and perturbations to the membrane. Based on the requirement of ArcA, I hypothesized pathways underpinning aerobic respiration would be dispensable for these species during bacteremia but necessary for *Escherichia coli* for which ArcA is not a bacteremia fitness factor. Expendability of ubiquinone synthesis, a key pathway of aerobic respiration, did not correlate with essentiality of ArcA during bacteremia, suggesting that ArcA function does not necessitate absence of aerobic respiration and further species-specific metabolic activity needs to be explored. My findings overall aid in determining how bacteria sense their environment, utilize nutrients, and generate energy while countering the host immune system. This information is critical for understanding how ArcA promotes fitness during pathogenesis.

Chapter 1 Introduction

1.1 Bacteremia

Bacteremia refers to the presence of bacteria in the bloodstream. By some definitions, bacteria transiently entering the bloodstream, such as from a minor cut or brushing one's teeth, is an occurrence of bacteremia (1). Here, bacteremia will be studied as cases where bacteria in the mammalian bloodstream propagate, disseminate, and ultimately cause infection within the host. A robust immune response is necessary to counter bacteremia, but an overwhelming immune response can damage the host. Such injury is particularly relevant to the bloodstream where mediators of the innate immune system can quickly accumulate and activate. This instance of systemic inflammatory response syndrome because of infection is referred to as sepsis (2). Criteria for sepsis in the clinic can be difficult to identify, but cases are often characterized by a change in body temperature, increased heart rate, and rapid breathing (2). Sepsis cases marked by worsening clinical outcomes are referred to as severe sepsis and eventually septic shock in which extremely low blood pressure is coupled with multi-organ failure. Sepsis cases account for 1 in 5 deaths worldwide with a high proportion of mortalities in the pediatric population (3). Sepsis is also the highest contributor to nosocomial deaths, hospital readmissions, and healthcare costs per adverse event among all health conditions(4–6). Bacteremia can develop quickly and is the leading cause of sepsis (7). The severity of bacteremia and sepsis require a better understanding of the causative pathogens to understand these infections and associated clinical outcomes more fully.

Bacteremia is a complex infection that can arise from a multitude of circumstances. Direct entry of bacteria into the bloodstream is referred to as primary bacteremia, which may occur from intravenous needle use for instance. More common is secondary bacteremia where bacteria from a primary infection site cross into the bloodstream environment (8). The initial infection site is highly dependent on the bacterial species. Gram-negative cases tend to result from infections of the gastrointestinal and urogenital tracts whereas primary sites of Gram-positive bacteremia are more frequently skin, wounds, and sites of catheterization (9). The prevalence of Gram-negative bacteremia cases relative to Gram-positive has varied historically. Gram-negative species were initially recognized as the classic causative agent of bacteremia (10). The surge of staphylococcal infections in the community in the 1990s coincided with an increase in bacteremia cases of Gram-positive bacteria (11, 12). The antibiotic resistance crisis that marks this century has now provided an avenue for a resurgence of Gram-negative cases (13–15).

The distinct etiologies of Gram-negative and Gram-positive bacteremia have long been recognized (16), and one general difference is the toxins produced by the bacteria (17). Lipopolysaccharide (LPS) in the outer membrane of Gram-negative species is the "initiating factor" of infection, serving as a highly immunogenic endotoxin. Gram-positive species instead rely on the production of exotoxins such as staphylococcal enterotoxins. While some studies have reported the host response during sepsis does not differ between Gram-positive and Gram-negative cases (18), a growing body of experimental and clinical evidence has challenged this idea (9, 19, 20). At the cellular level, Gram-negative species are targeted by complement and antimicrobial peptides at their outer membrane while Gram-positive species are controlled by intracellular killing by neutrophils and macrophages (9). As this study will demonstrate, defining

the host response to different pathogens provides essential context for the stressors bacteria must counter.

Cases of Gram-negative bacteremia originate in the community and in the hospital in equal proportions (21). The most commonly isolated Gram-negative pathogens of bacteremia include *Escherichia coli*, *Klebsiella pneumoniae, Pseudomonas aeruginosa*, and *Acinetobacter baumannii*, and the prevalence of each species differs based on community and nosocomial settings. A large proportion of bacteremia causing neonatal sepsis (>70% in some studies) are Gram-negative, and these cases are associated with worse clinical outcomes relative to Gram-positive cases (20, 22, 23). In studies identifying the most commonly isolated Gram-negative species in bacteremia cases, at least 80% of the species are classified as facultative anaerobes with a majority being in Order *Enterobacterales* while *P. aeruginosa* and *A. baumannii* are strict aerobes dominating the remainder of cases (14, 21, 24, 25). Among Gram-negative pathogens, we have shown the temporal dynamic of bacteremia studies in a murine model differ by species and anatomical site (**Fig. S1.5)**. In order to build comprehensive models of pathogenesis, it is pertinent to understand why and how Gram-negative facultative anaerobes are so successful in colonizing the bloodstream. Given the rise of Gram-negative bacteremic infections in the era of the antibiotic resistance crisis, new therapies are needed (13, 26). Understanding the implications of metabolic flexibility during infection by Gram-negative bacteria during bacteremia can inform more robust models of pathogenesis and in turn therapeutic development.

1.2 Metabolic capabilities of Gram-negative facultative anaerobes

From existing in the external environment to disseminating to different organs within the host, pathogens causing bacteremia are likely to encounter vastly different conditions with regard to nutrient and electron acceptor availability. The facultatively anaerobic Gram-negative species

causing such infections have the metabolic flexibility to adapt to such conditions (27). These bacteria can generate energy with or without the use of oxygen as an electron acceptor, a distinct advantage over species that can only use oxygen (strict aerobes) and species that cannot tolerate oxidative damage in the presence of oxygen (strict anaerobes) (28). The three main mechanisms by which facultative anaerobes generate ATP are aerobic respiration, anaerobic respiration, and fermentation with multiple pathways being shared between them. The efficiency of these processes as measured by ATP produced per molecule of glucose is listed in descending order. To this end, aerobic respiration is generally presented as the favored pathway by which this group of bacteria generate energy under "normal" oxygen conditions (29). However, the dynamic host environment can present complex challenges to bacterial cells that affect the carbon sources available for energy production, molecules present as electron acceptors, and the machinery required for metabolism. The cell must ultimately balance the use of intermediate molecules for ATP production by catabolism *versus* macromolecular synthesis by anabolism (30). This balance requires careful regulation of metabolic pathways to meet the changing needs of the cell. Following the postulate that facultative anaerobes are successful pathogens because of their diverse and flexible metabolic capabilities, the metabolic regulators the pathogens utilize to optimize growth are an important aspect of infection to define. To this end, the goal of this research overall is to understand how Gram-negative bacteria regulate metabolism during bacteremia and determine if such mechanisms are shared among species.

1.3 Metabolic regulation during bacterial infection

The importance of understanding metabolic networks employed by pathogens during infection is well-established, but the utilization and regulation of metabolic pathways during bacteremia are understudied (31–33). Metabolism fuels the ability to grow, an imperative for

bacterial cells in the bloodstream environment which rely on rapid replication for fitness (34). Metabolism also underpins virulence, a pathogen's ability to cause disease, as virulence mechanisms also rely on cellular resources (35). Metabolism and virulence are ultimately co-dependent in bacteremia as virulence provides the general ability to survive and acquire nutrients in the hostile host environment. Studies that have uncovered the intricacies of metabolic networks have almost always been completed under standard lab conditions(36, 37), so it remains to be determined if certain metabolic processes are utilized or regulated differently in the context of infection.

To capture the three main metabolic processes facultative anaerobes use during infection, studying the metabolic regulators controlling expression of genes encoding the pathways underlying these processes is a useful strategy. The regulators can control multiple pathways at once, and the stimuli in which the regulators respond to can be used to infer conditions in the host. Important global regulators of carbon metabolism in *E. coli* include ArcAB, Cra, CreBC, Crp, FNR, and Rob (38). Transcription factors of these regulatory systems work in a hierarchical fashion to control the expression of glycolysis, the tricarboxylic cycle, and the pentose phosphate pathway. Hypotheses regarding which metabolic regulators are active during infection can be generated from existing data sets studying abundance of bacterial mutants in host models to input mutant libraries. Transposon sequencing (Tn-seq) is a useful screening method for identifying which genes contribute to fitness, or the ability of the bacteria to survive and propagate, in infection (39). Such fitness factors were identified in a murine model of bacteremia with Tn-seq for *C. freundii*, *E. coli*, *K. pneumoniae*, and *S. marcescens* (40–43). The results of the screens were compared to determine if any of the aforementioned global regulators of carbon metabolism were identified as fitness factors for multiple species (**Table 1**). A majority of the

transposon insertion global regulator mutants were dispensable to fitness, meaning the proportion of the regulator mutants did not significantly decrease when comparing the insert pool with the bacteria recovered from the murine spleen. A notable outlier is the two-component regulatory system ArcAB. At least one of genes encoding this system was found to be significant in each species except *E. coli*. The goal of this work is to understand how ArcAB contributes to bacterial fitness in the mammalian bloodstream environment and determine if this role is shared among species of clinical importance.

Table 1: Contribution of Global Metabolic Regulators to Bacteremia Fitness in Tn-Seq

Species	Strain	Transposon Library Mutants	Global regulators of carbon metabolism						Ref.
			ArcAB	Cra	CreBC	Crp	FNR	Rob	
C. freundii	UMH14	>44,000							(40)
E. coli	CFT073	360,000							(42)
K. pneumoniae	KPPR1	~25,000							(43)
S. marcescens	UMH9	~32,000							(41)
Dispensable			**Fitness Factor**					**Not Screened**	

1.4 Overview of the ArcAB two-component regulatory system[1]

The ability to regulate and optimize metabolism based on environmental conditions is a hallmark of life. The metabolic capacity of bacteria is extremely diverse and for facultative anaerobes can include mechanisms for aerobic respiration, anaerobic respiration, and fermentation to generate energy in the form of ATP (27). Accordingly, many genes encoding metabolic functions are transcriptionally regulated by multiple systems to optimize metabolism

[1]Components of this section are modified from the following publication:
Brown AN, Anderson MT, Bachman MA, Mobley HLT. The ArcAB Two-Component System: Function in Metabolism, Redox Control, and Infection. *Microbiol Mol Biol Rev*. 2022 Jun 15;86(2):e0011021. doi: 10.1128/mmbr.00110-21. Epub 2022 Apr 20. PMID: 35442087; PMCID: PMC9199408.

depending on the substrates and electron acceptors available (44).

The average bacterial species encodes 30 two-component regulatory systems, but extreme examples have been described with more than 200 systems encoded in a single genome (45, 46). A canonical two-component system consists of a sensor kinase and a response regulator. Upon recognizing a specific stimulus through a sensor domain or by interaction with an adaptor molecule, the sensor kinase phosphorylates and thus activates the response regulator. Once activated, the response regulator can bind DNA, RNA, or other proteins, or act as an enzyme itself depending on the system (47). Hundreds of two-component regulatory systems have been characterized and regulate a multitude of processes including pathogenesis, stress responses, and symbiotic interactions (48, 49). Despite substantial advancements in understanding bacterial two-component regulatory systems, there is still much to learn about specific systems and the processes they regulate.

The anoxic redox control (or aerobic respiration control) (Arc) two-component regulatory system senses the modulation of oxygen availability for use as an electron receptor (50). The Arc system is found in facultatively anaerobic bacteria that can switch from utilizing aerobic respiration to fermentation or anaerobic respiration when oxygen is not being consumed. During fermentation and anaerobic respiration, bacteria continue to utilize glycolysis, but intermediate metabolites are shuttled to different pathways depending on the availability of alternative electron acceptors. The Arc system is involved in mediating the switch to fermentation and was touted early for its potential for global control of gene expression (51, 52). The sensor kinase ArcB is typically described as sensing microaerobic and anaerobic conditions, and after autophosphorylation, ArcB transphosphorylates the response regulator ArcA (53–55). Phosphorylated ArcA promotes fermentation as a primary energy-generating pathway by mainly

repressing pathways associated with aerobic respiration. The active form of ArcA, often denoted as P-ArcA, is a cytosolic transcription factor and is projected to regulate over 1,100 genes directly or indirectly in *Escherichia coli* (**Table 2)** (56). Together, these proteins are referred to as the ArcAB or ArcBA system **(Fig. 1.1)**. In an analysis of 698 bacterial species, >110 orthologs of ArcA and >130 orthologs of ArcB have been identified (57). Genomes have also been identified in which only ArcA or ArcB are encoded, but the significance of this finding remains unclear (57). These instances of only *arcA* or *arcB* being present could implicate other sensor kinases or response regulators interacting with ArcA and ArcB, respectively, or *arcA* and *arcB* were not putatively identified due to extensive differences in sequences.

Table 2: Studies Defining the ArcA Regulon

Study	Species	Media	Oxygenation	Methods	Results
Iyer 2021 (36)	*Escherichia coli*	M9 minimal medium + glucose	Anaerobic	RNA-sequencing	119 genes downregulated, 61 genes upregulated
Jiang 2015 (58)	*Escherichia coli*	Duck serum, LB	Microaerobic	RNA-sequencing	81 genes downregulated, 48 genes upregulated
Federowicz 2014 (30)	*Escherichia coli*	M9 minimal medium + glucose + ammonium chloride	Fermentative and nitrate respiratory conditions	ChIP-chip	Fermentative: 47/21 operons repressed/activated Nitrate respiration: 67/47 operons repressed/activated
Park 2013 (59)	*Escherichia coli*	MOPS minimal medium + glucose	Anaerobic	ChIP-chip, ChIP- seq, DNase I footprinting assay	Directly repress 74 operons, directly activate 11 operons, 229 operons differentially expressed, 176 chromosomal binding regions
Morales 2013 (60)	*Salmonella* Typhimurium	LB	Aerobic	Microarrays, footprinting	Aerobic conditions: 220/122 genes upregulated/downregulated H_2O_2: 117/175 genes upregulated/downregulated
Yun 2012 (61)	*Mannheimia succiniciproducens*	TSB	10% CO_2	Microarrays	82 genes upregulated, 79 genes downregulated
Evans 2011 (62)	*Salmonella* Typhimurium	MOPS-buffered LB + xylose	Anaerobic	Microarrays	147 genes upregulated, 245 genes downregulated

Gao 2010 (63)	*Shewanella oneidensis*	*In silico*	N/A	Regulatory Sequence Analysis Tools	214 genes with ArcA-binding motif
Wong 2007 (64)	*Haemophilus influenzae*	Brain Heart Infusion + NAD + hemin	Anaerobic	Microarrays	23/1697 genes differentially regulated
Salmon 2005 (56)	*Escherichia coli*	MOPS medium + glucose	Aerobic & Anaerobic	Microarrays	1,139 genes predicted to be directly/indirectly regulated
Liu 2004 (65)	*Escherichia coli*	MOPS-buffered LB + xylose	Anaerobic	Microarrays, Footprinting	~85 operons in ArcA regulon

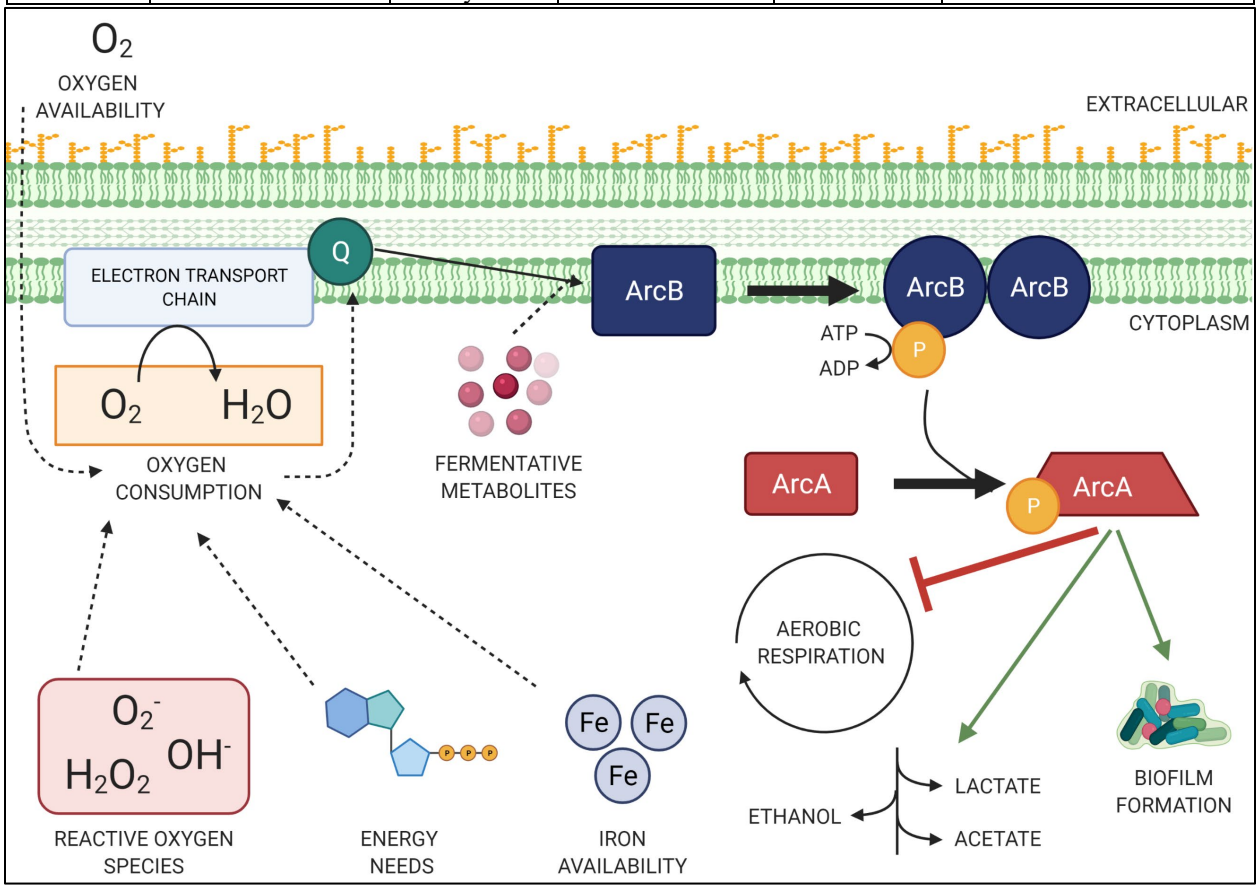

Figure 1.1: Working model of ArcAB in detecting oxygen consumption for redox maintenance. The two-component regulatory system ArcAB responds to changes in oxygen consumption within the bacterial cell. Oxygen consumption can be influenced by a multitude of factors including oxygen availability and energetic needs of the cell. As activity at the electron transport chain decreases, quinones (Q) interact with sensor kinase ArcB, causing a confirmational change and homodimerization. Now active, ArcB autophosphorylates and transphosphorylates response regulator ArcA via a phosphoryl relay. In turn, phosphorylated ArcA multimerizes and serves as a global transcription factor suppressing aerobic metabolic pathways and promoting fermentation among other processes.

ArcAB has been the subject of extensive research over the past 35 years. Most of this

work was conducted in *E. coli* and has uncovered the structure and function of the Arc system (66). Since ArcB is often referred to as a sensor of anaerobic and microaerobic conditions, the system is implied to be primarily relevant to bacteria when encountering low oxygen conditions. An increasing number of recent studies, however, have reported phenotypes for ArcAB mutants in higher oxygen conditions, establishing that ArcAB is responsive to more than oxygen availability alone (67, 68). In strains in which the genes encoding terminal oxidases are removed, ArcA is activated in aerobic conditions due to the inability of the cell to utilize oxygen as a terminal electron acceptor (69, 70). Accordingly, ArcB has been more accurately described as sensing the oxygen consumption rate or the degree to which bacteria acquire and utilize oxygen, rather than simply dissolved oxygen concentrations (71). Oxygen consumption may decrease even when abundant oxygen is available, so this distinction is important when considering the context of ArcA regulation. ArcAB has been described as not only a sensor of oxygen consumption but also as a general redox sensor (72). Metabolic activity and redox regulation are intimately linked processes, making these varying descriptions of ArcAB compatible (73). Many studies included in this review report functions of ArcAB in microaerobic and anaerobic conditions, but these findings may apply to other instances where oxygen consumption is also affected. ArcAB functions in conjunction with multiple other transcriptional regulators of metabolism, especially the fumarate and nitrate reductase regulator (FNR) (74, 75). Since they are often studied together, the relationship between ArcAB and FNR will specifically be reviewed here.

An exciting area of current research aims to determine how ArcAB is activated and deactivated. Some groups report that the system is controlled by the cellular pool of quinones, while others suggest different modulators including fermentation products (76–80). These

competing hypotheses indicate that ArcAB is at the intersection of multiple signaling pathways and underscores again that this system may be active in multiple conditions, including aerobiosis. Because of its extensive regulatory capabilities, ArcAB systems have been linked to a wide array of cellular processes beyond central metabolism in recent years including bacterial conjugation, acid tolerance, biofilm formation, and even bioluminescence (81–85). ArcAB may govern the elegant coordination of these processes with the appropriate metabolic pathways to provide the energy and resources cells require to perform them (59, 86, 36, 30). The significance of ArcAB regulation is perhaps especially evident during infection, an instance where pathogens must balance metabolic needs with survival in the host environment. Over the last 35 years since the discovery of ArcAB in *E. coli*, much progress has been made in understanding this complex regulatory system in multiple bacterial species. Here, I explore the seminal discoveries made along the way and highlight active and future areas of ArcAB research.

1.4.1 Organization of the Arc System

Expression of arcB and arcA

E. coli cells have approximately 1,088-8,000 molecules of ArcA and 85-226 copies of ArcB in each cell, depending on media and experimental techniques (78, 87–89). The two genes encoding these proteins are not found together in the same operon in contrast with many other two-component systems (49, 90, 91). Their expression and regulation must therefore be considered independently. The *arcB* gene encoding the sensor kinase was initially thought to be expressed constitutively and not influenced by respiration (92). It is intuitive that at basal level of *arcB* expression is needed to ensure that at least some amount of sensor is present and responsive to stimulus (49). More recently, however, *arcB* transcription was shown to be increased at lower oxygen concentrations (3.3 fold higher at 1% O_2 *versus* 10% O_2 in the headspace of cultures),

and ArcA itself may be a regulator of *arcB* transcription (93). Expression of *arcB* is also known to be affected following treatment with antibiotics including gentamicin and polymyxin B, suggesting that cell envelope stress influences ArcAB activity (88, 94). The small regulatory RNA ArcZ can destabilize *arcB* mRNA in aerobic conditions, which demonstrates post-transcriptional control of *arcB* is also possible and provides a potential mechanism by which ArcAB activity is limited (95).

The *arcA* gene is under the control of FNR, as well as ArcA itself, and is upregulated about four-fold once *E. coli* encounters increasingly anaerobic levels (93, 96, 97). FNR and ArcAB respond to oxygen availability and consumption, respectively (71, 98, 99). Regulation of *arcA* by FNR thus demonstrates a coordinated response to related stimuli. Interestingly, a study simultaneously analyzing the regulons of ArcA, FNR, and IHF (integration host factor) found that *arcA* expression was upregulated in the *ihf* mutant but not the *fnr* mutant, a contradiction suggesting additional levels of regulation are likely present (36). Expression of *arcA* is also upregulated in acidic relative to neutral microaerobic conditions, which is further indicative of ArcAB's role as responding to redox changes (100). The degree to which changes in ArcA abundance affect activity remains an open question since contrary evidence has shown that ArcA protein levels do not change between aerobic and anaerobic conditions (78, 101). Groisman describes in a review of mechanisms of two-component system regulation the potential impact of length of stimulus exposure on response regulators' autoregulatory abilities (49). It is unknown if ArcA autoregulation is also temporally dependent, but this type of mechanism could explain the difference here. Although regulation of the expression of ArcA may influence overall activity, the primary determinant of ArcA regulatory activity is likely its phosphorylation state.

Structure of ArcB

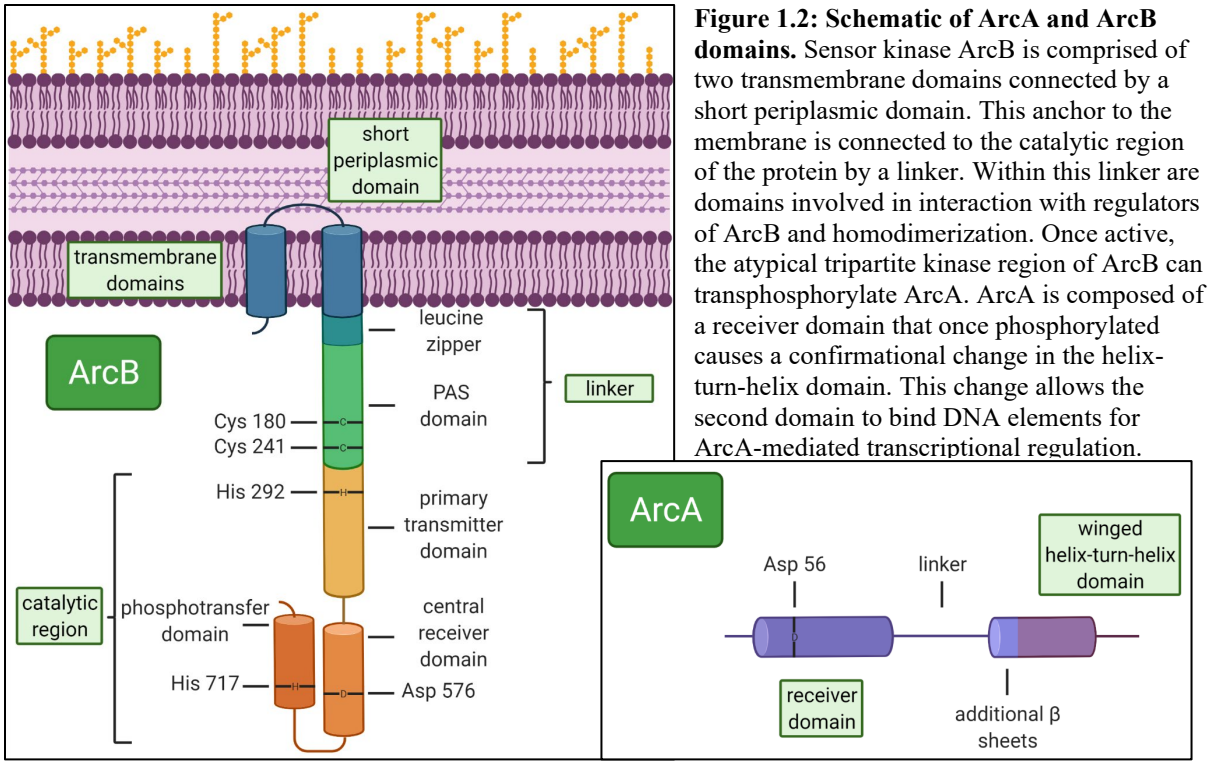

Figure 1.2: Schematic of ArcA and ArcB domains. Sensor kinase ArcB is comprised of two transmembrane domains connected by a short periplasmic domain. This anchor to the membrane is connected to the catalytic region of the protein by a linker. Within this linker are domains involved in interaction with regulators of ArcB and homodimerization. Once active, the atypical tripartite kinase region of ArcB can transphosphorylate ArcA. ArcA is composed of a receiver domain that once phosphorylated causes a confirmational change in the helix-turn-helix domain. This change allows the second domain to bind DNA elements for ArcA-mediated transcriptional regulation.

ArcB's structure is atypically configured compared to canonical sensor kinases **(Fig. 1.2)** (53). It has two transmembrane helices that function solely as an anchor into the membrane (102, 103). The intramembrane domains are connected by a conspicuously short periplasmic domain of only 16 amino acids (104). Many sensor kinases that are directly involved in interacting with external stimuli have more complex periplasmic domains (105). The periplasmic bridge of ArcB's two intramembrane domains has been shown not to be involved in signaling, providing evidence that ArcB requires interactions with adaptor molecules to ultimately sense stimuli (102). Canonical sensor kinases have a single domain with an invariant histidine residue for autophosphorylation whereas ArcB is a tripartite sensor kinase, meaning it has two additional domains (106–110). These domains have an additional histidine residue and an aspartate residue to participate in the phosphorylation process. Early studies examining the structure and phosphorylation of ArcB were indeed confounded by three domains participating in the enzymatic reaction (79, 92, 111, 112). The catalytic region of the protein was subsequently

identified to be composed of a primary transmitter domain, a central receiver domain, and a secondary transmitter (or phosphotransfer) domain (113). A single residue in each of these domains was later determined to play a role in phosphorylation and were identified as His292, Asp576, and His717, respectively (54, 79). The membrane anchor domain of ArcB is connected to these three catalytic domains by a linker slightly less than 200 amino acids in length. Within the linker are a leucine zipper, which is necessary for ArcB homodimer formation, and a Per-Arnt-Sim (PAS) domain, which is important for signal transduction (114–117). Within the PAS domain are two redox-sensitive cysteine residues (Cys180 and Cys241), which are in proximity with the cysteine residues of a second ArcB protein (104, 114). The oxidation state of these residues determines whether ArcB functions as a kinase or phosphatase (104). Two intermolecular disulfide bridges form between adjacent ArcB proteins when the cysteines are oxidized, preventing kinase activity. In contrast, the ArcB proteins can homodimerize to facilitate kinase function when the cysteine residues in the PAS domain are reduced and disulfide bridges are absent. Notably, mutation of both cysteine residues to alanine results in constitutively high ArcB kinase activity (104). Interestingly, the PAS domain is not present in the ArcB of *Haemophilus influenzae*, suggesting that activation and deactivation of this homology is accomplished via a different mechanism than *E. coli* (118).

Structure of ArcA

ArcA is configured in a manner characteristic of the OmpR/PhoB superfamily of two-component system response regulators (reviewed by Nguyen *et al*. (119)) **(Fig. 1.2)**. At the N-terminus of ArcA is a receiver domain (also referred to as a regulatory domain) where the protein is phosphorylated and dephosphorylated by ArcB at an aspartate residue (Asp54) (51, 79, 111). The receiver domain is connected to the C-terminal output or effector domain consisting of a

helix-turn-helix (HTH) for DNA binding (119, 120). Phosphorylation of the ArcA receiver domain results in a conformational change that allows the effector domain to bind DNA targets (121). Connecting the receiver and effector domains is a short linker of unknown function (119). The output domain can further be described as a winged HTH domain as with other OmpR-like regulators (122–124). The wings refer to additional small β sheets that can impact the DNA binding properties of the response regulator. The HTH motif subtype of the OmpR superfamily is further identifiable by a characteristic string of 4 additional β strands, forming an anti-parallel β sheet, in front of the prototypical winged HTH. Variation in residues contained within these β strands is proposed to be instrumental in determining which DNA sequences the domain can bind (119, 125). Techniques have thus been developed to predict sequence binding by these transcription factors based on residue differences (119, 125).

The ArcB to ArcA Phosphorelay

The passage of phosphoryl groups from ArcB to ArcA, known as a phosphorelay, results in the activation of ArcA and has been well characterized (54, 55, 108, 111). Under reducing conditions and subsequent homodimerization, ArcB autophosphorylates via an intramolecular reaction with ATP as the phospho-donor (126). In a study comparing 25 histidine kinases, a population of ArcB was able to autophosphorylate most quickly (91). Relative to the other kinases, ArcB had a considerably lower level of saturation, referring to the percentage of the ArcB population that ultimately is phosphorylated. Yamamoto *et al.* suggested rapid autophosphorylation coupled with a low level of saturation implies ArcB is also quickly dephosphorylated. Following autophosphorylation, ArcB transphosphorylates ArcA via a $ArcB_1^{His292} \rightarrow ArcB_1^{Asp576} \rightarrow ArcB_2^{His717} \rightarrow ArcA^{Asp54}$ phosphorelay, ending in P-ArcA activation (55, 127). Early findings suggested His292 of ArcB could directly phosphorylate

Asp54 of ArcA, bypassing the other catalytic domains, but no evidence was found later to support this transfer (54, 55). The molecular mechanism of this phosphorelay, including the uncovering of intramolecular *versus* intermolecular interactions of the homodimers, was described by Teran-Melo *et al.* (127). Under conditions that activate ArcB kinase activity, the phosphoryl group is initially passed from the primary transmitter domain (His292) to the central receiver domain (Asp576) of the same ArcB molecule. Then, the phosphoryl group is transferred to the phosphotransfer domain of another proximal ArcB molecule (His717), which further illustrates the importance of homodimerization. From here, the phosphoryl group is passed to the receiver domain of ArcA (Asp56). In some cases the phosphotransfer to the receiver domain of ArcA has been described as a dynamic process requiring catalytic contributions from ArcA (128). ArcA can in fact be autophosphorylated in the presence carbamoyl phosphate and acetyl phosphate, but this connection has not been found to be physiologically relevant (129–131).

DNA Binding by ArcA

Initial studies of ArcA-DNA complexes at the promoters of ArcA-controlled genes predicted that ArcA binds to multiple sites or that ArcA multimerizes following phosphorylation (129, 132). The ability of ArcA to multimerize has since been shown to be dependent on both the receiver domain and DNA binding domain and may be a requirement before proper DNA binding (120, 133). The ArcA dimer ultimately forms at the α_4-β_5-α_5 faces within the DNA binding domain with α referring to alpha helixes and β to beta strands (119, 120). Multiple studies have provided additional evidence that ArcA forms dimers, but it is possible that higher orders of oligomerization also exist (119, 133). Only phosphorylated forms of ArcA are thought to form higher order oligomers (120, 134). Other evidence suggests that nonphosphorylated ArcA can form dimers and bind regulatory regions, though this has been attributed to nonspecific

binding by some groups (133, 134). Regulation is dependent on phosphorylated ArcA binding to multiple repeats in the promoter of target genes, but it has not yet been fully determined to what extent dimers of P-ArcA interact with one another at these direct repeat binding sites (101). P-ArcA has been shown to bind the -35 and -10 elements of promoters, at the transcription start site itself, and even at loci almost 500 nucleotides upstream, depending on the target gene being regulated (30, 59). The consensus ArcA binding box, the DNA motif to which activated ArcA binds, has been extensively studied (30, 59, 62, 65, 121, 135–140). The prototypical ArcA consensus binding motif is approximately 15 base pairs in length and is highly conserved. The most common consensus sequence 5'-3' GTTAATTAAATGTTA has been identified in multiple species including *E. coli*, *Salmonella enterica*, and *Shewanella oneidensis* (62, 137–139). Within this sequence are two direct repeats (GTTA). Notably, the oscillation of the motif (11 base pairs) aligns well with the length of helical turns of DNA (10.5 base pairs) (30, 125). Park and colleagues noted that binding sequences longer than 15 nucleotides have been identified with more advanced techniques and further described an extended 18 base pair consensus sequence in *E. coli* (59). Analysis from this study showed that sites bound by ArcA contain up to five direct repeats with various lengths of space between each repeat. The amount of phosphorylated ArcA at each repeat can be variable and appears to be related to the number of repeats present (59). Bidirectional transcriptional regulation by ArcA has also been reported and can result in dual activation/repression or inverse regulation of opposing operons sharing a promoter region (30).

Dephosphorylation of ArcAB

The ability of cells to deactivate regulatory systems is as important as the mechanisms required to turn them on. During signal decay, ArcB kinase activity ceases, and ArcB in turn acts as a phosphatase to directly dephosphorylate ArcA (79). P-ArcA is dephosphorylated via an

$ArcA^{Asp56}$ → $ArcB_1{}^{His717}$ → $ArcB_1{}^{Asp576}$ → P_i intermolecular phosphorelay in which the domains of only a single ArcB protein are involved (141, 142). The phosphoryl group is transferred from the ArcA receiver domain (Asp56) back to the phosphotransfer domain (His717) of ArcB during this process. From here, the signal is passed to the central receiver domain (Asp576) of the same ArcB molecule before finally being released as inorganic phosphate. Following cessation of the stimulus, ArcB likely dephosphorylates due to the instability of the phosphoryl group bound at the aspartate residue in the central receiver domain (Asp576) (54, 142). Evidence has been described that ArcB can also be dephosphorylated by SixA during this process (143–145). SixA, a phosphohistidine phosphatase, is one of the first proteins described to have this enzymatic ability. However, a recent study challenges the connection of SixA to the ArcAB system, demonstrating that deletion of *sixA* did not impact a P-ArcA reporter assay (146). Pending further studies, the role of SixA in the dephosphorylation of ArcB remains open but highlights the potential for modulation of ArcAB by additional regulatory components. If SixA can dephosphorylate ArcB, more research will be needed to determine if SixA activity is condition-dependent and if it works in tandem with spontaneous release of the phosphoryl group. It is unlikely that ArcB-independent spontaneous hydrolysis of the phosphoryl group from ArcA contributes significantly to the decay pathway as the half-life of phosphorylated ArcA is long (30 minutes to longer than 1 hour) (91, 133, 141).

1.4.2 Regulation by Quinone Pools

The nature of the signal for the Arc system has been a consistent focus of the field since the initial identification and characterization of the protein components themselves. *arcA* and *arcB* were identified in an *E. coli* genetic screen performed under anaerobic conditions for the purpose of identifying mutants that upregulate *sdh*, an operon that is normally repressed in the

absence of oxygen (51, 52). The genes subsequently determined to comprise the ArcA regulon suggested that ArcAB was involved in regulating metabolism during anaerobiosis (53). *arcA* was also determined to be the same gene previously identified as *dye*, so named because loss of *dye/arcA* resulted in increased sensitivity to toluidine blue (51, 147). Toluidine blue induces photosensitizer-mediated oxidative stress and further served as an indication that ArcAB is linked to redox control or metabolism (51, 52, 148, 149). The short length of the periplasmic domain of ArcB and lack of potential redox reaction sites in this region suggested that sensor kinase does not directly interact with a molecular signal, such as oxygen (104). Molecular oxygen was subsequently discounted as the signal because ArcA activity was shown to also decrease when alternative electron acceptors are present (51). Fermentation products were found to enhance ArcB kinase activity and inhibit phosphatase activity in anaerobic conditions, which supported ArcAB as a two component system for anaerobiosis (78, 79, 150, 151). In this model, fermentative metabolites such as D-lactate, acetate, and pyruvate are the dominating influence on ArcB activity and thus serve as the signal for the system. Initial studies reported inhibition of ArcB phosphatase by such metabolites as an important mechanism by which ArcB transphosphorylates ArcA following autophosphorylation in anaerobic conditions (79). D-lactate was also found to amplify ArcB kinase activity but ultimately was not alone sufficient for activation, suggesting other layers of regulation (151). Along these lines, Georgellis *et al.* highlighted that the genuine signal needs to be able to suppress ArcB kinase under oxidizing conditions (80). While fermentative metabolites may enhance ArcB kinase activity, the absence of these metabolites under most oxidizing conditions likely disqualifies them from being the primary contributors to regulation.

Identification of Quinone Involvement

The observed de-repression of an ArcA-regulated promoter during anaerobic respiration indicated that a reduced component of the electron transport chain such as quinol may be the stimulus for ArcB (152). Quinones are comprised of a hydrophobic isoprenoid tail attached to a polar head group with a characteristic cyclic dione moiety (153). Quinones were considered good candidates for modulating ArcB since they are intricately linked to the redox state of the cell and located at the membrane. Indeed, the connection between quinones and ArcAB was firmly established in the early 2000s following a key set of experiments (80, 104). Radiolabeled ATP was used to track ArcB autophosphorylation, which was shown to be inhibited in the presence of soluble analogs of ubiquinone and menaquinone (80). When the quinones were reduced in the presence of hydrosulfite, they no longer inhibited ArcB kinase activity. Conclusively, oxidized forms of quinones were shown to repress ArcB autophosphorylation. These results ushered in a new focus of ArcAB research in which different quinone species were tested for their capability of interacting with ArcB.

Overview of Quinone Structure and Role

A combination of ubiquinone (UQ), menaquinone (MK), and demethylmenaquinone (DMK) are typically found in Gram-negative facultative anaerobes (154). UQ is classified as a benzoquinone and MK and DMK as naphthoquinones based on their variable head groups (155, 156). UQ is the dominant quinone during aerobiosis while MK and DMK are the major quinones during fermentation and anaerobic respiration. Each type interacts with different enzymes to modulate aerobic and anaerobic respiratory pathways (29, 157). The structure and function of quinones aligns well with the role of these molecules as excellent candidate transmitters of the cellular redox state to ArcB. The small size of quinones in general and overall hydrophobic nature allow for movement within the cellular membrane; the hydrophilic ringed head group can

then interact with proteins imbedded within the membrane (153). As part of the electron transport chain (ETC), quinones accept both electrons and protons but only donate electrons. Quinones receive electrons from dehydrogenases specific to substrates such as NADH and succinate (158). The electrons are then shuttled to various reductases depending on the quinone and the electron acceptor. For example, UQ passes electrons to cytochrome bo_3 which reduces oxygen to water and MK can pass electrons to fumarate via fumarate reductase (158–160). The quinone pool is an important component in the ETC, which supports the notion that quinones rapidly reflect the redox conditions within the cell. In turn, quinones can interact with ArcB, resulting in a response to changes in metabolic activity. Notably, ArcA downregulates expression of the *nuo* and *sdh* operons, which encode the dehydrogenases at the beginning of Complexes I and II, respectively (36, 59). As Complexes I and II feed directly into the quinone pool, ArcA regulation of these complexes serves as example of a feedback loop linking metabolic activity with maintenance of the ETC, a concept that warrants further interrogation.

When oxygen is present, the quinone pool is oxidized as electrons are shuttled through to terminal oxidoreductases (oxidases), ultimately reducing oxygen to water (158). Oxidized quinones function as a negative signal and prevent ArcB kinase activity under aerobic conditions (80). The two aforementioned redox-sensitive cysteines in the linker region of ArcB are the site of quinone-mediated regulation (104). The redox state of the quinone pool becomes reduced when electron acceptors are absent and cannot complete the ETC. Under anaerobic conditions, reduced quinones (quinols) reduce the cysteines of the PAS domain, resulting in the breakage of disulfide bonds between ArcB homodimers. When oxygen is not being utilized as an electron acceptor, ArcB's kinase is "on," resulting in autophosphorylation and subsequent transphosphorylation of ArcA. In contrast, oxidized quinones turn "off" the ArcAB system as

electrons are transferred from the cysteine residues to the quinones. The pool of oxidized quinones is theoretically maintained under conditions where electrons are continuously transferred to oxygen (80). The maintenance of the disulfide bonds between the ArcB cysteines silences kinase activity (104). The position of the cysteines in relation to the inner membrane of the cell ensures proximity to quinones and further supports the working model of the adaptor molecule of ArcB activation being kept in or close to the inner membrane (80, 161). Quinones are also hypothesized to be reduced under conditions in which an abundance of carbon sources results in flooding of the ETC with electrons, which may be an avenue by which ArcAB becomes activated in aerobic conditions (134). Overall, the proposed regulation of ArcAB by the quinone pool couples ETC activity with transcriptional regulation and provides a mechanism by which ArcAB receives and transmits respiratory activity by an organism.

Modelling Quinone-based Regulation of ArcAB

Although a compelling link has been established between the redox state of quinones and the activity of ArcB, there are discrepancies regarding which subsets in the quinone pool are the sensor kinase and when they do so (76, 77, 162). Quinones are difficult to isolate in the laboratory due to their hydrophobic nature, and in instances where they can be isolated from bacterial cells, maintaining the native oxidation state *ex vivo* has proven to be challenging (77, 163, 164). Characterizing the overall quinone profile of cells cultured in different conditions is therefore not trivial. Many studies rely on the analysis of mutants lacking specific species of quinones (76, 77, 162). These studies utilizing quinone mutants are complicated by the fact that different species of quinones share precursor molecules and biosynthesis pathway components. DMK for example is a direct precursor for MK, making it difficult to separate the roles of these quinone molecules (162). Furthermore, UbiE, the enzyme catalyzing the conversion of DMK to

MK, is also required in the UQ synthesis pathway (77, 165). When studying mutant strains lacking specific quinones, the possibility of redundancy and compensation should be considered. *E. coli* mutants lacking ubiquinone have been shown to have higher levels of menaquinone and demethylmenaquinone for example (157). Functional substitutions by these quinones could impact how the different species interact with ArcB in mutant strains. There is also the concern that mutation of synthesis genes (ex. *ubiE*) to engineer strains lacking specific quinones may result in the accumulation of quinone intermediates (77). The ability of these intermediates to interact with ArcB is unknown. Despite these experimental considerations, two prevailing models regarding regulation of the Arc system by the quinone pool have been developed.

Model A

Model A (**Fig. 1.3)** is based on comparing reduction potentials ($E°_{red}$) of the quinone species with ArcB (76). $E°_{red}$ of UQ, MK, and DMK are approximately +110mV, -80mV, and +36mV, respectively (160). Based on its cysteine residues, the midpoint potential of ArcB was calculated to be -41mV (76). MK is the only quinone of the three species to have a more negative reduction potential than ArcB. When menaquinol (reduced state) and ArcB interact,

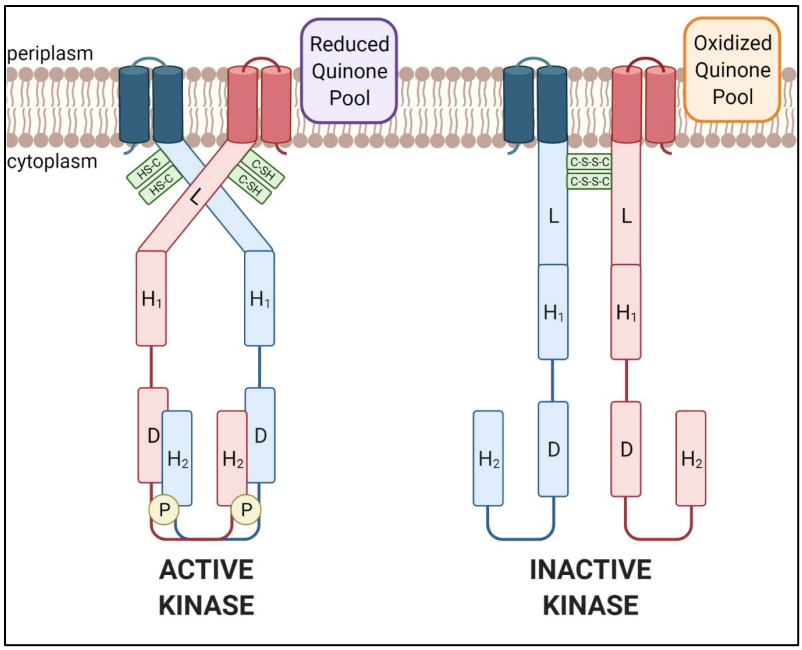

Figure 1.3: Quinone regulation of ArcAB. Activity of the sensor kinase ArcB is controlled by redox sensitive cysteine residues within its linker domain. Quinones are a major determinant of the oxidation state of the cysteine residues. In reducing conditions (*e.g.*, anaerobic culture), quinones reduces these residues, allowing for ArcB homodimerization. ArcB then functions as a kinase, and a phosphorelay ends with phosphorylation of the phosphotransfer domain of the partner ArcB molecule. In oxidizing conditions (*e.g.*, aerobic culture), quinones oxidize the cysteines, which form disulfide bonds with the corresponding cysteines of a neighboring ArcB molecule. This formation silences ArcB kinase activity and phosphorylation does not occur. Ubiquinone, menaquinone, and demethylmenaquinone can activate or inactivate ArcB kinase activity depending on their own oxidation state and abundance. See text for further details.

Key: C-S-H – reduced cysteine residue, C-S-S-C – disulfide bond, L – linker domain, H_1 – primary transmitter domain, D – central receiver domain, H_2 – phosphotransfer domain

This model has been adapted from Alvarez et al. (26) and Bekker et al. (119) with permission.

electrons flow from menaquinol to ArcB, reducing the ArcB cysteine residues and activating kinase activity. MK is the dominant species in anaerobic conditions, so the redox coupling of MK and ArcB would provide a mechanism for how ArcB can be activated in the absence of oxygen consumption. Conversely, when ubiquinone (oxidized state) and ArcB are in proximity, electrons flow from ArcB to ubiquinone as the $E°_{red}$ of ubiquinone is more positive (76). The result of such an interaction would be an oxidation of ArcB and silencing of kinase activity. UQ is the most abundant quinone under aerobic conditions, and it is expected that the UQ pools leads to repression of ArcAB function as the cell utilizes oxygen (29). This model therefore relies on the abundance of reduced MK relative to oxidized UQ for ArcAB to be active in anaerobic conditions. DMK can also be reduced by ArcB based on reduction potentials and thereby inactivate ArcB kinase activity. At first glance, this interaction appears counterintuitive since DMK is associated with anaerobic conditions in which ArcB should be active. In cells transitioning into anaerobic conditions in minimal media, the DMK pool increases more rapidly compared to MK pool (164). One may hypothesize that DMK serves as a direct counter to MK and that this may be important in fine tuning ArcB activity in microaerobic conditions where ArcB could be partially active and UQ is not as abundant (76). Such a relationship is consistent with the notion that the overall enzymatic activity of ArcB as a kinase or phosphatase functions on a continuum. Activity of the ArcAB system can therefore not be simplified to function as an

on/off switch, especially in intermediate conditions. The shift from UQ to MK in the quinone pool during anaerobiosis and the subsequent effect on ArcAB activity was shown previously (69). The same change in relative abundance of quinone species and activation of the Arc system was also seen in aerobic conditions in *E. coli* strains lacking terminal oxidases, providing more evidence that it is the utilization rather than the presence of oxygen that impacts the quinone profile of the cell and its interaction with ArcB (69). In support of this model is a study that measured ArcA activity as a readout of quinone modulation using an expression reporter system and included promoters for which ArcA acts as either an activator (*cydA*) or a repressor (*sdh*) (76). ArcA phosphorylation levels are not measured directly in these experiments, so there is a possibility of other regulators interfering with the reporter expression. An ArcA-P specific promoter system edited to remove binding sites of co-regulator FNR was not used in this case but may be useful in addressing these concerns (163).

Model B

The next model (**Fig. 1.3)** operates under the hypothesis that any quinone species can reduce or be reduced by ArcAB (77). In this model, the redox reaction is dependent on the overall redox potential of the quinone and ArcB complex rather than just the midpoint potential of the individual cysteines of the ArcB linker region (77). The first study reporting that ArcB autophosphorylation is blocked by quinones demonstrated this relationship with both ubiquinone-0 and menadione (80). Multiple quinone species simultaneously contributing to the redox state of ArcB could help explain findings that there is not a linear correlation between oxygen availability and ArcA activity (71, 72, 163, 166). In utilizing single quinone mutants, van Beilen and Hellingwerf demonstrated that ArcA can still be phosphorylated and dephosphorylated in response to aerobic transitions, referred to as the “ArcB

activation/deactivation" cycle (77, 162). A strength of the latest study is the use of a nitrogen gas sparging system to capture quinone composition of *E. coli* cells during the transition from aerobic to anaerobic conditions (77, 162, 163). The timing of ArcA phosphorylation here clearly correlates with the changes in the quinone profile of wild-type *E. coli*. While the study demonstrates that three mutant strains, each employing a different quinone, can still phosphorylate ArcA during changes in oxygen availability, the rate at which the different oxidized quinone species activate ArcB has not yet been determined. This model is therefore contingent on the overall amount of the quinone pool with the possibility that individual quinone species may differ in magnitude of effect on ArcB. Since the study relied on phosphorylation status of ArcA as a readout of system activity, additional investigation of target gene transcription activity would provide additional support for this model. All the quinone mutant strains in this study showed stunted growth during the sparging experiment, so the overall physiology of the mutant strains may also need further analysis.

Consolidation of ArcAB Regulation Data

While the above two models share some commonalities with regard to quinone function in ArcB activation, variations in growth phenotypes of quinone mutants and specific roles of quinone species currently limit consolidation of these studies. Importantly, mutation of *arcA* and *arcB* did not impact the quinone profile of cells in either aerobic or anaerobic conditions, ruling out the possibility of direct regulation of quinone production by ArcAB (167). Mutants lacking UQ have been shown by others to have normal levels of ArcA phosphorylation in aerobic conditions (157). This finding is in opposition to both models which agree that UQ is necessary to inhibit ArcB kinase function in aerobic conditions and thus prevent ArcA phosphorylation (76, 77). The same group also reported nearly normal fermentative growth in anaerobic conditions in

the mutant strains lacking UQ despite lower ArcA phosphorylation levels (157). The authors note these discrepancies and speculate that the differences may be due to effects of short-term *vs* long-term changes to aerobiosis. Disrupting quinone production affected ArcA phosphorylation only in anaerobic conditions in this study and was contingent on the presence of MK or MK and DMK. The requirement of MK for ArcA phosphorylation in anaerobic conditions may lend support to either model. Model A relies on MK as being the sole quinone capable of reducing ArcB, and MK is the dominant anaerobic quinone in facultative anaerobes. Model B infers that MK must be the quinone reducing ArcB as it is the most abundant quinone in anaerobic conditions in which ArcB is activated. Furthermore, the follow up study by Nietzsche and colleagues demonstrates the importance of all three quinone species for proper growth in aerobic and anaerobic conditions and highlights that the single quinone mutants likely do not reflect quinone activity of wild-type strains (157).

Modulation of ArcA-P activity through ArcB phosphatase activity has not been fully explored but should not be discounted because ArcA can be phosphorylated even in relatively aerobic conditions (78). In this scenario, ArcB would constitutively phosphorylate ArcA, and the changes in ArcB phosphatase activity would ultimately control ArcA. This case is not likely to be the main mechanism of regulation given the extended evidence that ArcB kinase activity is indeed inhibited by quinones. The phosphatase function of ArcB should still be studied in the context of quinone-based regulation to more fully encompass the physiological continuum of ArcB function. The discrepancies between various models of ArcAB regulation may also be due to the use of different strains of *E. coli*, culture conditions, or the presence or absence of additional regulators. Multiple questions certainly remain regarding regulation of ArcAB. Are quinones the main regulator of ArcB function in species other than *E. coli*? Which quinones

modulate ArcAB activity in periods of transition during anaerobiosis such as from fermentation to anaerobic respiration? Which other factors impact the redox state of quinones and ultimately their interaction with ArcB?

1.4.3 Control of Central Metabolism

ArcA meets the definition of a global regulator set forth by Martínez-Antonio and Collado-Vides based on the large number of operons under its control and its ability to regulate diverse metabolic pathways (168). Global regulation of metabolism by ArcA is thought to be achievable because of the flexibility of its DNA-binding architecture (101). Up to 150 different operons across various networks are under the direct control of ArcA in *E. coli* (59, 65). ArcA co-regulates these networks not only in conjunction with specific transcription factors but also with other global regulators (37, 59, 168, 169). Indeed, ArcA has been identified as one of five major global regulators of anaerobic fermentation in *E. coli*. (reviewed by Kargeti and Venkatesh (170)). Further complicating this global regulatory network is the regulation of other transcription factors by ArcA. Park and colleagues determined that seventeen transcription factors are under direct regulatory control of ArcA in strict anaerobic conditions (59). Analysis of ArcA's influence of vital cellular processes includes energy production and redox balance, demonstrating the importance of this global regulator. Catabolism of carbon sources to generate usable energy is highly dependent on the availability of electron acceptors and thus is presented as three possibilities: dependency on oxygen (aerobic respiration), dependency on alternative acceptors for the ETC (anaerobic respiration), or fermentation. It is important to consider, however, that the switch between aerobiosis and anaerobiosis works on a continuum and regulatory systems allow for fine tuning of the response to these changes (171). The activity of the Arc system has an inverse linear correlation to increasing aerobiosis, conferring maximal

ArcA regulation under total anaerobic conditions (78). This description is somewhat at odds with earlier reports that found ArcA activity was most relevant in microaerobic conditions (166, 72). Once again, the observed differences may be due to variable laboratory methods that impact oxygen consumption and testing metrics. A review of the literature regarding ArcAB contributions to growth phenotypes reveals a wide range of results for *arcA* and *arcB* mutants across multiple species and in various conditions. For example, one study demonstrated growth defects with *E. coli arcB* deletion mutants in aerobic conditions in contrast to another that showed *arcB* deletion mutants of *E. coli* did not exhibit growth defects in these conditions (172, 173). Despite some lab-to-lab discrepancies in defining ArcAB regulon function, much progress has been made toward the study of metabolism controlled by the Arc system.

The ArcA Regulon

Because of ArcA's extensive regulatory network, studies exploring global gene expression have been important in pinpointing the control of metabolism by this transcription factor **(Table 2).** Many of these studies are performed in aerobic or anaerobic conditions, but ArcA's role is perhaps best showcased during periods of transition when the availability of electron acceptors varies (30). The presence of alternative electron acceptors such as nitrate have indeed been shown to heavily influence activity of ArcA and the ArcA regulon independent of oxygen availability, providing yet further evidence that ArcAB is more closely linked to the redox state of the cell than oxygen availability alone (30, 174). Key themes of ArcA's regulatory function have emerged and will be covered in depth here. The most notable function of ArcA is repression of oxidative metabolic pathways. Closer inspection of the ArcA regulon reveals a role for ArcA in promoting fermentative pathways, the stress response, contributing to acquisition and utilization of the key elements nitrogen and iron, and metabolic overflow. Despite reportedly

high homology of ArcA proteins and conservation of its binding consensus sequence, the ArcA regulon can be highly variable between bacterial species. For example, only six genes are shared between the *E. coli* and *S. oneidensis* ArcA regulons (139). It is therefore pertinent to reiterate that the metabolic themes described here apply largely to work done in the model *E. coli* system and that the regulons of other species are currently less well defined.

Repression of Carbon Oxidation Pathways

ArcA represses genes of multiple pathways needed for the oxidation of carbon sources. In studies in which glucose is the sole carbon source for cells cultured anaerobically, ArcA directly downregulates catabolism of fatty acids, aromatic compounds, amino acids, and polyamines, among other compounds (59, 175). These pathways can all feed into the tricarboxylic acid (TCA) cycle, which is noteworthy as ArcA represses each gene corresponding to an active enzyme in the oxidative TCA cycle (30). Repression by ArcA thus targets pathways needed for the catabolism of carbon sources downstream of glycolysis. Notably, ArcA regulation has been tied to maintenance of the NADH:NAD^+ ratio, an electron carrier and critical cofactor that connects pathways of central metabolism (72, 176). Furthermore, this ratio has been linked to metabolic flexibility and the redox state of the cell – concepts that have already been described in the context of ArcAB regulation (73). After exposure to increasingly aerobic conditions, *arcA* mutants had a significantly higher NADH:NAD^+ ratio in comparison to wild-type cells (72). This effect of a skewed NADH:NAD^+ ratio on metabolism in *arcA* mutants is evident by elevated levels of acetate production, which can be prevented by overexpression of NADH hydrogenase (176). Intriguingly, there is evidence of diminished activity in the TCA cycle in *arcA* mutants even though ArcA is a prominent repressor of key genes in this pathway (36). While there are inherent difficulties in measuring metabolic flux alongside transcriptional regulation, these

results nevertheless serve as foundational evidence for two important points. First, global regulators of metabolism, including ArcA, cooperate to optimize metabolism, and impairment of only one such regulator can have dramatic consequences. Indeed, deletion of *arcA* results in increased flux through the TCA cycle in anaerobic conditions rather than fermentation, wasting metabolic substrates and energy (30, 177). Second, metabolism is regulated not only at the transcriptional level but also at the enzymatic level (*i.e.,* by post-translational modification and allosteric control). Predicting metabolic activity based on gene regulation alone is therefore difficult, especially when regulation by multiple transcriptional factors is considered. Application of different approaches including transcriptomics and metabolomics must be employed in multidisciplinary studies to understand the role of ArcA and other global regulators at the cellular level.

Promotion of Fermentation

In addition to repression of pathways necessary for oxidation of non-glycolytic carbon sources, P-ArcA promotes expression of genes involved in mixed acid fermentation, the primary metabolic pathway of *E. coli* cells that are unable to respire (178). Glycolysis is the main energy-producing pathway of fermentation, and certain enzymes in the glycolytic pathway are in fact upregulated by ArcA (30). Some groups have manipulated (or suggested the manipulation of) the ArcAB system in industry and biotechnology for over-producing a variety of fermentative compounds such as derivatives of acetyl-CoA (38, 69, 179–185). In a strain of *E. coli* engineered to overproduce ArcA, fermentative pathways were induced based on an increased secretion of acetate (180). As expected, *arcA* and *arcB* mutant strains of *E. coli* produce less acetate relative to wild-type strains (177, 179). Deletion of *arcA* had been shown earlier to negatively affect expression of *ackA*, the gene that encodes the second enzyme in the acetyl CoA to acetate

pathway. Regulatory control of the genes in this pathway are more directly under the control of FNR. ArcA has, however, been well documented to strongly repress production of acetyl-coenzyme A synthetase, which ultimately would prevent the conversion of acetate back to acetyl CoA (36, 59). A decrease in acetate production in *arcA* and *arcB* mutants is thus likely a combinatorial effect of an increase in carbon flux through non-glycolytic pathways and decrease in expression of acetate-related genes.

Dysregulation of fermentation is also evident in *E. coli* strains lacking *arcA* or *arcB* through increased secretion of succinate and lactate relative to the isogenic wild-type strains (177, 179, 184). *E. coli* strains lacking ubiquinone also produce more lactate relative to the wild-type strain during changes in oxygen availability, which supports the notion that disruption of the ArcA activation pathway impacts fermentation based on the close link previously described between ArcB and quinones (77). The change in fermentative products for mutant strains indicates a skew towards reduction reactions regenerating NAD+ (*e.g.*, pyruvate to lactate) over oxidation reactions producing ATP via substrate-level phosphorylation (acetyl-CoA to acetate) (179). These changes in metabolic flux of *arcA* and *arcB* mutants underscore the link between redox state and metabolic activity as well as the difficulty in predicting metabolic activity of global regulator mutants (36, 179, 186). One might expect all fermentative products to decrease when ArcAB is absent if this regulatory system promotes fermentation. The overall change in profile of mixed acids produced during fermentation seen in *arcA* and *arcB*, however, is more telling when considering the number of metabolic pathways affected. Again, global metabolic changes rather than just individual metabolites must be accounted for when analyzing ArcAB mutants.

Although ArcA regulates anaerobic processes such as fermentation, there are exceptions

to the classical description of ArcA as functional under anoxic conditions. Early studies focused on nitrate respiration found that ArcA-controlled genes encoding succinate and lactate dehydrogenases were less repressed in the presence of nitrate in low oxygen conditions (187, 188). In an experiment where trimethylamine-*N*-oxide was added to anaerobically cultured *E. coli* as a terminal electron acceptor, cells shifted from fermentation to anaerobic respiration, and ArcA activity was momentarily repressed (189). The reductive TCA cycle shares some enzymes with the oxidative TCA cycle, which is why repression of ArcA activity in the context of anaerobic respiration is necessary. A study by Federowicz *et al.* also highlights genes in pathways downregulated by ArcA are de-repressed while transitioning from fermentation to nitrate respiration (30). These results further underscore the complexity of metabolic regulatory circuits and demonstrates the ability of cells to prioritize metabolic pathways based on energetic output, among other factors.

Nitrogen Metabolism

Catabolic processes controlled by ArcA inevitably affect the flux of glycolytic and TCA intermediates into anabolic pathways needed for the synthesis of the four major macromolecules (amino acids, nucleotides, lipids, and carbohydrates). ArcAB is likewise associated with nitrogen metabolism, an essential nutrient critical to anabolism. The cell must balance activity of anabolic pathways with overlapping pathways utilized for energy production via chemiosmosis (30). Major disruptions in nitrogen homeostasis have been observed in *arcA* mutants, affecting the balance between energy production pathways and protein synthesis. An *arcA* deletion mutant of *E. coli* was shown to have a decreased intake rate of ammonia, an important source of nitrogen, relative to an isogenic wild-type strain under strict anaerobic conditions with glucose as the sole carbon source (36). Nitrogen metabolism is of course critical to amino acid synthesis, and ArcA

is an important regulator of amino acid fate. For instance, multiple studies have corroborated that ArcA upregulates arginine transporter gene transcription and downregulates the arginine degradation pathway (36, 59). Unexpectedly however, arginine was among the amino acids that accumulated in an *arcA E. coli* mutant strain. Loss of ArcA was subsequently associated with major metabolic dysregulation impacting the biosynthesis and utilization of amino acids which could not be predicted by examination of the ArcA regulon alone (36). Further, the rate of metabolic flux relative to translation was calculated to be higher in this *arcA* deletion mutant, indicating an imbalance of cellular activities critical to homeostasis and growth (36). When the proteome of wild-type cells was compared to that of *arcA* mutant cells in fermentative conditions, a larger portion of the proteome deemed "unused" or "unnecessary" was found in the mutant cells. The authors classified metabolic proteins as unnecessary if they had potential to be beneficial during adaptation to environmental conditions but were otherwise burdensome during fermentation. The wild-type cells were deemed to be more metabolically efficient as a result. Therefore, while cells can survive without an intact ArcAB system, they are at a clear disadvantage regarding balancing metabolic and translational efficiencies. In effect, ArcA regulation contributes to optimized cellular activity based on availability and utilization of metabolic precursors for energy production and biomass.

1.4.4 Response to Growth Limitation

The Stress Response

The ability of a cell to switch from generating energy for growth to conserving energy and making repairs under stress relies on careful metabolic regulation. Control of the bacterial stress response is indeed linked to ArcA-mediated regulation central carbon metabolism such as the TCA cycle (190). The general stress response involves a metabolic shift during less favorable

conditions, including nutrient deprivation and the entry into stationary phase (191). σ^S (or RpoS) is a sigma factor that coordinates the stress response in *E. coli* and influences the regulation of a wide range of genes that promote survival (192). Because multiple factors can lead to cellular stress, the complexity in connecting σ^S to simultaneous responses cannot be overstated (191, 193). With this in mind, σ^S activity has been shown to be influenced by central metabolic pathways of the cell, which in turn are regulated by σ^S. For example, mutation of pyruvate dehydrogenase, which provides acetyl-CoA for the TCA cycle, leads to an increase in σ^S levels (193). The relationship between metabolic enzymes and σ^S levels suggests an interesting connection to ArcA, an important repressor of the TCA cycle. ArcA exerts partial control over σ^S through the small activating RNA ArcZ, which binds *rpoS* transcripts (95). When ArcA is active, such as in anaerobic conditions, ArcZ is repressed and translation of RpoS is low. ArcZ has been proposed to support translation of *rpoS* while also repressing the Arc system. ArcAB was connected to the coordination of synthesis and proteolysis of RpoS (σ^S) with RssB, which facilitates degradation of RpoS by the protease ClpXP (134). During exponential phase, *rpoS* is directly repressed by ArcA and kept at basal levels (95, 134, 194). During rapid cell growth, quinones are expected to be reduced following flooding of the ETC with electrons, corresponding to ArcB kinase activity and phosphorylated ArcA. As cells enter stationary phase, phosphorylated ArcA levels are thought to diminish and σ^S levels in turn increase (134). Comparable to conditions in which high levels of oxygen result in oxidized quinones, nutrient-poor conditions might also result in oxidized quinones as fewer electrons pass through the ETC (134). Oxidized quinones would lower ArcB activity and subsequently lead to de-repression of σ^S under the current mechanistic model. Although ArcA represses *rpoS*, deletion of *arcA* results in increased sensitivity to dehydration in *E. coli* (194). This phenotype is striking as σ^S is thought

to be an important regulator active during dehydration tolerance and raises the question of how does ArcA coordinate with σ^S to resist the effects of dehydration. Expanding studies to include interrogation of ArcA alongside σ^S during various stressors will not only further untangle the connection of these two vast regulators but also provide more insight into cellular stress overall.

Starvation

Starvation is one potential trigger of the stress response, as noted above. Cells experience starvation when key nutrients such as amino acids become limited and cellular processes must be modified as a result. In culture, bacteria often begin to experience starvation when transitioning from exponential to stationary phase growth. ArcAB has been identified as an important metabolic regulator during stationary phase in which cells must balance a lack of available nutrients with a potentially harmful accumulation of metabolic byproducts (195). Nyström *et al.* demonstrated that gene expression during anaerobiosis and aerobic stationary phase was similar. Despite the availability of oxygen and usable carbon sources, cells shutdown the TCA cycle via ArcA during stationary phase. The authors concluded that during starvation in stationary phase, cells lessen respiratory activity to prevent oxidative damage and to conserve endogenous resources. ArcAB plays a protective role in this case by repressing aerobic pathways, ultimately aiding cells in the aging process (195). These results however may be dependent on carbon source availability as the finding that ArcAB is important for survival during stationary phase was not apparent when *arcA* mutant cells were cultured in rich LB medium instead of minimal medium (196, 197). Intriguingly, TCA cycle mutants did live longer than wildtype counterparts in a rich medium during stationary phase, which may be due to lower ROS levels (197). Because active ArcA can downregulate the genes of the TCA cycle, one might expect that loss of ArcA resulting in increased TCA cycle activity would lower levels of survival. The authors speculate

that in LB medium, starving cells must continue to rely on the TCA cycle to generate energy, so ArcA function would be counterintuitive. This same study also revealed that mutants lacking *lipA*, which encodes lipoyl synthase involved in lipoic acid biosynthesis, outlive wildtype cells in rich media but that this increased lifespan was in fact ArcA-dependent (197). *lipA* mutants are unable to convert pyruvate to acetyl-coA to enter the TCA cycle. The result is that pyruvate is converted to acetate, which can occur during fermentation and overflow metabolism, a concept described later. Therefore, ArcA repression of the TCA cycle would indeed be advantageous in conserving energy and resources to promote survival in the *lipA* mutant.

Iron Limitation

Iron is a critical nutrient which cells must acquire from the extracellular environment, and ArcAB is implicated in iron homeostasis in anaerobic conditions (198). Iron homeostasis and metabolism are closely connected as enzymes found in the TCA cycle and the ETC rely on the availability of iron for proper regulation and function (199, 200). Predictably, cells are likely to switch from using aerobic respiratory enzymes when iron is scarce and not available as a enzymatic cofactor (201, 202). Under conditions of iron starvation, cells then rely on alternative metabolic pathways, including fermentation. Accordingly, an *arcB* mutant of *Actinobacillus actinomycetemcomitans* grew poorly under iron-limiting conditions aerobically relative to an *arcB* complemented strain (203). This is a clear example in which sensing of environmental conditions through ArcAB leads to metabolic changes to optimize growth. When considering the regulatory response to iron, the regulons of Fur, the master regulator of iron metabolism, and ArcA have in fact been found to overlap (36, 204). ArcA specifically downregulates genes encoding enzymes that contain iron-sulfur clusters including succinate dehydrogenase and NADH:ubiquinone oxidoreductase (205, 206). Of note, all of these genes are also controlled by

at least one other regulator such as FNR, further demonstrating the ability of ArcA to interconnect multiple regulatory networks (205). ArcA is also well-established as a regulator of genes encoding cytochromes that utilize heme-bound iron. ArcA can upregulate *cydAB* and downregulate *cyoABCDE,* which both encode terminal oxidases of the ETC (59, 207). Interestingly, less ArcA protein is found in iron-limited conditions (208). Though as stated earlier, the regulatory outcomes of a transcription factor cannot be determined by protein abundance alone. Nevertheless, the relationship of ArcAB activity to iron availability and utilization is evidently intricate, and future research should focus on further integrating ArcA-controlled metabolism into iron homeostasis.

Overflow Metabolism

Optimal metabolism is not solely based on the availability of substrates; therefore, the role of ArcA in repression of the TCA cycle needs to be considered from other perspectives. For example, *E. coli* can perform fermentation during periods of rapid growth in the presence of oxygen to quickly produce ATP (209, 210). It is hypothesized that the growing cell membrane may be unable to accommodate room for respiratory enzymes, so the cell must utilize other metabolic processes (209). Not surprisingly, ArcAB has been implicated in this process, known as "overflow metabolism," as it controls multiple operons involved in these pathways (68, 176, 205). The term "overflow" refers to the increased production and release of metabolites such as acetate as the cell oxidizes substrates that could have otherwise been further catabolized through aerobic respiration. Because of the extensive regulatory network of ArcA, investigators have also noted that the connection between this system and an overflow of acetate could be an indirect relationship (176). Increased activity of the TCA cycle in *arcA* mutants may incidentally result in decreased acetate production because acetyl-CoA, a potential precursor of acetate, is continuing

to be used in the oxidative TCA cycle. At the cellular level, overflow metabolism is perhaps the most striking example in which ArcA is active in the presence of oxygen and an abundance of carbon sources.

1.4.5 Interactions with Other Regulatory Systems

Fumarate Nitrate Reductase (FNR)

Multiple transcription factors regulate metabolism during anaerobiosis, but FNR is the one most closely associated with ArcAB in *E. coli*. Together, ArcA and FNR control more than 80% of metabolic flux during anaerobiosis (30). Unlike ArcA, FNR uses iron sulfur clusters to directly senses molecular oxygen, which passes freely through the cellular membrane (75, 211, 212). Upon encountering oxygen-limited conditions, iron-sulfur clusters become reduced and FNR is activated. There is no concrete evidence that FNR can also be affected by other oxidizing agents that reduce the iron-sulfur cluster, implying a specificity for oxygen (211). As its name implies, FNR promotes the transition from aerobic respiration to anaerobic respiration with alternative terminal electron acceptors such as fumarate and nitrate. When fumarate and nitrate are available as electron acceptors during anaerobic respiration, FNR upregulates reductases encoded by the *frdABCD* and *nirBD* genes to properly utilize them as part of its role in controlling metabolism (30, 213). The apparent overlap between the ArcAB and FNR regulons was noted early on after it was reported that the expression of genes related to anaerobiosis was dependent on both systems (74, 96, 207, 214). For example, the binding of FNR at the promoter of *cydAB*, a component of the ETC, is contingent upon the presence of ArcA also binding in some cases (207). One group initially reported that 303 genes are regulated by both ArcAB and FNR, demonstrating extensive overlap of their regulons (56). FNR and ArcA dually contribute to repression of the tricarboxylic acid pathway (36). Both regulators repress the operons encoding α-ketoglutarate dehydrogenase,

succinyl coenzyme A synthetase, and succinate dehydrogenase, enzymes critical to the oxidative tricarboxylic acid pathway (36). Like ArcAB, FNR also promotes fermentation by upregulating genes involved in non-oxidative pyruvate catabolism (*pflB*) for example (213). Multiple hypotheses have been proposed to differentiate apart the seemingly redundant roles of these regulators (56). It is speculated that ArcAB is more critical in microaerobic conditions, while FNR becomes the major regulator as cells encounter strict anaerobic environments (72, 166, 175, 215). This notion is complicated by studies that show ArcA becomes increasingly phosphorylated as conditions become more anaerobic. Whether this directly correlates with increasing ArcA activity or if maximal ArcA function is reached before complete anaerobic conditions could inform functionality of ArcA *vs* FNR. Curiously, mutations of *arcA* and *arcB* are epistatic over mutation of *fnr* under nitrate respiratory conditions (187). Another theory for explaining how the two systems work in tandem is FNR mediating a fast initial response to low oxygen levels with ArcAB becoming active only after sustained exposure (216).

Despite the partial overlap between the ArcA and FNR regulons, the transcription factors also serve distinctive functions (37). At the cellular level, ArcA's major role is repression of catabolism while FNR activates chemiosmotic and anabolic pathways (30). In anaerobic conditions with glucose as the sole carbon source, there are only seven reported operons directly regulated by both ArcA and FNR in *E. coli* (59). There are additionally instances of ArcA and FNR having opposing activities on co-regulated genes (175, 205, 216). This is especially evident in the regulation of cytochromes of the ETC. ArcA is involved in the upregulation and downregulation of *cydAB* and *cyoABCDE*, respectively; however, FNR downregulates both of these operons (70, 217, 218). This multilayer regulation of cytochromes has again been attributed to the varying activity of both regulators under microaerobic and anaerobic conditions. Under

microaerobic conditions, ArcA-mediated transcription of *cydAB* ensures the presence of cytochrome *bd-I* oxidase, which has a higher affinity for oxygen than cytochrome bo_3 oxidase from *cyoABCDE* and therefore is useful for scavenging (207). When levels become anaerobic, FNR is then active to downregulate both cytochrome complexes as oxygen can no longer be utilized. In summary, ArcA and FNR activity is dependent on available substrates and electron acceptors, and they coordinate metabolism in complex networks with other regulators (205). The functionality of these intertwined regulators further illustrates the ability of bacterial cells to integrate multiple signals to optimize metabolic activity.

Phage Shock Protein System

The simplest two-component regulatory systems have one sensor and one response regulator. Cross-talk occurs when the sensor kinase of one system phosphorylates the response regulator of another system. Conventionally, coordinated cross-talk between bacterial two-component systems, also referred to as cross-regulation, is thought to be kept to a minimum to promote specificity during a response to a stimulus (219). An investigation into cross-talk of ArcAB with the two-component systems UhpBA, NtrBC, and PhoRB provided no evidence for physiologically relevant cross-talk between these tested systems (220). Evidence has been presented suggesting ArcB can phosphorylate the previously mentioned orphan response regulator RssB, but the significance of this interaction has not been fully elucidated (91, 134). Regulatory networks involving multiple kinases have been identified and may be useful in integrating multiple stimuli (221). Along these lines, studies have suggested that ArcB interacts with targets in addition to ArcA (134, 222). For instance, ArcB reportedly cooperates with the phage shock protein (Psp) system in *E. coli* cells (223, 224). While initially identified in the response to damage by bacteriophage, the Psp response is now associated with various agents that result in compromised

membrane integrity (reviewed by Joly *et al.* (225)). Homologs of the Psp system have been found in many organisms (57). In Gram-negative bacteria, where it was first identified, it is thought that the Psp system maintains the proton motive force when the inner membrane is damaged. It has been proposed that a not yet fully characterized direct interaction between ArcB and PspB, a membrane-bound component of the Psp system, is important for this function (224). The ArcB and PspB interaction was shown to be conditional on microaerobiosis. It was also proposed in the same study that the ArcAB regulon amplifies expression of the *psp* system. Although the initial stimulus of the Psp system has yet to be definitively identified, the contribution of ArcB to the activation of the Psp system in microaerobic conditions suggests that the redox state of the cell is an important aspect of Psp activation. Maintaining integrity of the cell envelope is critical for redox homeostasis, so contribution of redox status to Psp activity is logical. The connection between a system that ultimately senses changes in redox conditions (ArcAB) to a system that senses membrane damage (Psp) would be largely based on the notion that the proton motive force generated at the membrane needs to be maintained following envelope stress. In agreement with this concept, the Arc system has been referred to as a "protometer," describing how activation of ArcAB coincides with changes in the electrochemical gradient at the inner membrane (226).

Cell Envelope Maintenance

The role of ArcAB in response to perturbations at the cell envelope has also been demonstrated in *Shewanella oneidensis* in connection with the sigma factor σ^E (encoded by *rpoE*) (227). σ^E becomes active when envelope stress results in accumulation of misfolded outer membrane proteins and lipopolysaccharides in the periplasm and modulates envelope biogenesis as a result. Under stable conditions, σ^E is sequestered by the anti-sigma factor RseA. In *arcA* mutants of *S. oneidensis*, *rseA* gene expression is considerably elevated. Through a yet undefined

mechanism, ArcAB and RseA are accordingly theorized to cooperate in mediating σ^E activity. The relationship between ArcAB and σ^E has been further supported by evidence that proper functioning of the lipopolysaccharide transport system relies on both systems (228). *rpoE* is upregulated in Δ*arcA E. coli* mutants relative to the wild-type strain, indicating the connection extends to other species (36). Interestingly, these studies connect ArcA function specifically to the outer membrane. As ArcAB has now been linked to inner and outer membrane maintenance (albeit in different organisms), general envelope integrity preservation by this system may be necessary for optimal redox homeostasis. It is noteworthy that in clinical strains of *Klebsiella pneumoniae*, *arcB* is upregulated following exposure to polymyxin B, a cationic peptide used as a model for antimicrobial peptides of the immune system (94). This study highlights that metabolic rewiring was an important aspect of response to this antibiotic. Specifically, genes encoding respiratory enzymes repressed by ArcA are downregulated following polymyxin B exposure. As the cellular response to polymyxin B includes a metabolic shift to fermentation, it is not surprising that ArcAB was implicated as a mediator in the process (94). Polymyxins are well-recognized for perforating the outer membrane of bacterial cells, but the precise mechanism of how this leads to cell death is unclear. From inducing ROS damage to stiffening the membrane, a growing body of evidence implicates perturbations at the inner membrane by polymyxins (229–231). We can speculate that these changes can influence or impede ETC and specifically quinone activity at the membrane, which would in turn impact activation of the ArcB kinase. Damage by polymyxins has indeed been shown to impact enzyme activity at the respiratory chain (232). The Arc system has also been implicated in the response to multiple classes of antibiotics, including aminoglycosides and the cephalosporin cefixime that inhibits cell wall synthesis (88, 233, 234). This is notable as ArcAB has also been connected to cell envelope maintenance in *S. oneidensis* (227, 235, 236). These

findings further display the complex networks dedicated to responding to stressors. Whether ArcAB controls functions directly in structural maintenance of the cell envelope, or whether redox homeostasis is so tightly dependent on envelope integrity that ArcAB metabolic regulation is inextricably tied to perturbations, remains to be determined.

1.4.6 Response to Reactive Oxygen Species

Aerobic metabolism efficiently provides ATP to cells, but this benefit must be balanced with the cost of redox stress produced when using these pathways (237, 238). Cells have evolved sophisticated mechanisms for responding to these stressors and ultimately maintaining redox balance within the cell (239, 240). With the redox state of the cell closely linked to metabolism, involvement of ArcAB activity in maintaining redox balance within the cell across oxygen conditions are expected (182, 183). As noted above, ArcAB has been linked to the ratio of $NADH/NAD^+$ in the cell and by proxy also ATP/ADP (174). Redox homeostasis by ArcAB may also involve maintenance of the extracellular microenvironment, such as release of reactive oxygen species (ROS), in addition to ROS levels inside the cell (241). In conditions in which the cell is not using oxidative phosphorylation, ArcA regulation promotes glutathione export as well as extracellular superoxide production (173). As already described, ArcAB has been implicated in "overflow metabolism" in which low-yield metabolic pathways replace higher-yield pathways. This diversion also helps maintain redox balance within the cell (242). The role of ArcA in responding to various forms of redox stress not only highlights the broad array of cellular processes impacted by ArcAB but also serves as an indication for other potential mechanisms of ArcA activation.

Mechanisms of ROS Resistance

The cell must respond to ROS, which are oxygen and its derivatives including peroxides,

superoxide, and hydroxyl radicals, as they can damage bacterial DNA, proteins, and lipids (243). Accordingly, bacteria have evolved ways to scavenge and reduce ROS into less harmful products (239). ArcAB has been characterized by multiple studies to play a role in such ROS resistance. Indeed, in *E. coli* deletion of *arcA* or *arcB* resulted in increased susceptibility to hydrogen peroxide in aerobic conditions (244). In *Salmonella enterica* serovar Typhimurium, the ArcA regulon overlapped very little in comparison to the regulon of untreated aerobically grown cells following H_2O_2 treatment (60). Accordingly, the function of ArcA in the context of ROS may be difficult to predict utilizing established regulons defined in anaerobic conditions (30, 36, 59). The role of ArcAB in resisting hydrogen peroxide was shown to be independent from the ability to detoxify ROS since *arcA* and *arcB E. coli* mutants were shown to neutralize peroxide to wild-type levels (244). Similarly, the gene encoding superoxide dismutase in *Haemophilus influenzae* is not under the control of *arcA* despite *arcA* mutants being more susceptible to hydrogen peroxide (64). Other studies have since explored alternative mechanisms of ArcAB-mediated hydrogen peroxide resistance in *Salmonella enterica*, *S. oneidensis,* and *H. influenzae* (**Fig. 1.4)** (245, 236, 64). *S.* Typhimurium *arcA* mutants are more sensitive to the effects of hydrogen peroxide because ArcA downregulates a porin that enhances entry of this ROS (245). In *H. influenzae*, ArcA controlled expression of *dps* contributes to resistance via Dps-dependent protection against hydrogen peroxide-mediated DNA damage (64). Since ROS are also primary anti-bacterial effectors of innate immune cells, it is noteworthy that ArcAB has been described as promoting survival of *S.* Typhimurium in macrophages and neutrophils (246). Killing by the host cells in this study was not shown to be explicitly ROS-mediated, but ROS levels were not different in immune cells infected with wild-type or *arcA/arcB* mutant cells. Direct links between metabolic regulation by ArcA and oxidative stress have already been suggested based

on findings that resistance to hydrogen peroxide is restored via amino acid supplementation in *E.*

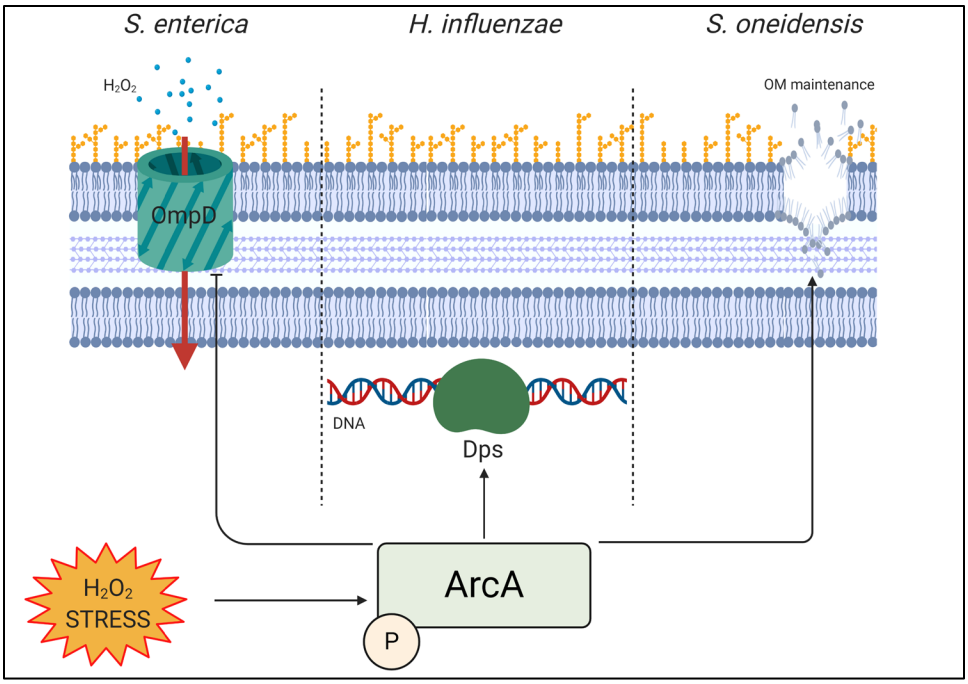

Figure 1.4: ArcA-mediated responses to hydrogen peroxide. Following reactive oxygen stress from exposure to hydrogen peroxide (H_2O_2), cells utilize ArcA to respond by downregulating porins of H_2O_2 (*S. enterica*), producing proteins such as Dps to protect DNA from oxidative damage (*H. influenzae*), and promote maintenance of the outer membrane following ROS damage (*S. oneidensis*).

coli (244). It has been demonstrated in *S.* Typhimurium that *arcA* mutants have a skewed $NADH/NAD^+$ ratio, which may result in a higher proportion of ferrous *vs.* ferric iron and thus more hydroxyl radical formation via Fenton chemistry(60, 247). Because of the pleiotropic effects of mutating *arcA* or *arcB*, it is unlikely that a single mechanism for ROS resistance exists. Strikingly, ArcA has been implicated in the regulation of *soxS,* a gene encoding an important mediator of the ROS response (36, 248). Considering the multiple studies indicating that ArcAB does not play a role in the neutralization of ROS such as hydrogen peroxide, the biological significance of ArcAB-controlled *soxS* expression remains unclear. Ubiquinone has also been identified an important antioxidant within the cell membrane preventing peroxidation of lipids by H_2O_2 (249). Based on the earlier description of quinones as the main signal for ArcAB activation, this finding may serve as a direction for future research investigating how ArcAB can respond to oxidative stress through interaction with other molecules.

Activation of ArcAB during ROS Response

ArcAB actively regulates the response to reactive oxygen derivatives yet is canonically known to be active in conditions in which oxygen consumption drops. This apparent contradiction could be a starting point for novel research exploring an unknown role for ArcAB in aerobic growth and may uncover other regulators of the system beyond the quinone pool. The mechanisms for a relationship between ArcA-mediated control of metabolism and the ROS response may already be evident. The metabolic pathways ArcA controls are large sources of internal ROS production and thus may need to be repressed when the cell faces an exogenous ROS threat (250, 251). In this scenario, ArcA would need to be active under aerobic conditions, which could rely on one of three mechanisms: 1) binding/regulatory activity by unphosphorylated ArcA; 2) an alternative kinase of ArcA; or 3) kinase activity of ArcB under oxidizing conditions. No direct evidence has been presented for points 2 or 3, but noteworthy evidence has been reported for point 1. There are existing examples of response regulators not needing phosphorylation to function (252). Unphosphorylated ArcA has indeed been shown to bind the same DNA fragments as phosphorylated ArcA in experiments examining plasmid recombination (253). Subsequent DNase footprinting however found that the binding pattern by unphosphorylated ArcA was different (59, 133, 134). Additionally, apparent activity of ArcA under aerobic conditions may be attributed to small amounts of phosphorylated ArcA (101). Most recently, it has been found that *S. enterica* ArcA becomes partially active in the presence of ROS in a phosphorylation-independent manner (254). Zhou and colleagues demonstrated that ROS exposure leads to disulfide bond formation in ArcA, allowing for ArcA dimers to form without activation from ArcB. The oxidized cysteines forming these bonds are reportedly highly conserved, suggesting this new mechanism may be conserved in other species as well. Barring

the existence other ArcB activators, ROS damage would ultimately have to impact quinone oxidation or abundance for ArcB to become active. One could theorize damage at the ETC affects the oxidation state of the quinone pool and ultimately its connection to ArcB. Future studies could also examine if high levels of ROS result in the activation or release of other ArcB regulators. With the capability of ROS to cause cell-wide damage and the capacity of ArcA to affect global change at the cellular level, the role of ArcA in maintaining metabolic homeostasis during ROS response in aerobic conditions cannot be overlooked.

1.4.7 Contribution to Pathogenesis

Cellular replication is one component of bacterial fitness during infection. Furthermore, it is intuitive that transcriptional regulation is critical for optimal fitness and pathogenesis in the host. Dynamic bacterial interactions with the host include responses to changes in nutrient availability, oxygenation, and immune defenses, all of which are heavily dependent on the site and stage of infection (255, 256). This may be especially true during the initial stages of infection and during dissemination from an initial site, in which the transition between environments can be dramatic. Examples of two-component regulatory systems in pathogenic bacteria are so ubiquitous that the regulatory pathways have now become attractive targets of antimicrobial therapies (Reviewed by Tiwari *et al.* (257), Rajput *et al.* (258), and Hirakawa *et al.* (259)). Likewise, the function of ArcAB in controlling metabolic functions in response to oxygen availability or consumption has prompted several groups to investigate the impact of the ArcAB system on infection processes and outcomes. Indeed, we have determined that *arcB* mutants of the opportunistic pathogens *Serratia marcescens* and *Citrobacter freundii* exhibit a significant loss of fitness as assessed by Tn-seq of bacteria recovered from an experimental bloodstream infection model (40, 41). *S. marcescens arcA* was also identified as a fitness gene in

the same study. Similarly, a loss of fitness was also associated with a *Klebsiella pneumoniae* *arcB* transposon insertion mutant in a murine lung infection model (260). Growing evidence from the literature supports the notion that ArcAB control of gene expression is required for optimal bacterial fitness in the host environment. The diversity of organisms and infection models described in the sections that follow suggests that the importance of ArcAB is widespread among bacterial pathogens. Understanding the function of the ArcAB system during infection will aid in constructing models of pathogenesis and may provide viable targets for future therapeutic development.

Bacterial Survival during Infection

A role for ArcAB in directly and indirectly supporting growth during infection has been identified in several important pathogens. Disruption of *arcA* in *S.* Typhimurium significantly reduces the recovery of bacteria from mice following oral inoculation or during systemic infection following intraperitoneal injection (246, 261). Mutation of *S.* Typhimurium *arcA* furthermore limits intracellular survival in epithelial cells, macrophages, and neutrophils (246). So important is ArcAB to the pathogenesis of this species that mutating *arcA* alongside *fnr* and *fliC* has been proposed in developing an attenuated live *S.* Typhimurium vaccine (262). A second example of ArcA contributions to gastrointestinal infections has been observed using *Vibrio cholerae* in which *arcA* mutants exhibit reduced virulence and colonization in an infant mouse cholera model (263, 264). ArcA function was also shown to increase pathogenesis in a porcine pneumonia model using *Actinobacillus pleuropneumoniae*, with *arcA* mutant bacteria exhibiting lower clinical scores and reduced bacterial recovery compared to wild-type *A. pleuropneumoniae* (265). Finally, multiple bacterial species have been shown to require ArcAB function for optimal fitness during bloodstream infections, as previously noted (40, 41). The mammalian bloodstream

presents an interesting paradox of oxygen availability in that the blood is an oxygen-rich environment, yet it is likely that little oxygen is available to extracellular pathogens in circulation as 98% of oxygen here is tightly bound to host hemoglobin within erythrocytes (266). Similarly, little is known about bacterial oxygen availability in the spleen and liver, which often harbor high concentrations of bacteria in murine models of bloodstream infections (267). *H. influenzae,* a natural inhabitant of the human nasopharynx, is also capable of causing invasive infections. *H. influenzae arcA* mutants required a higher lethal dose than wild-type bacteria following intraperitoneal injection of mice and decreased bloodstream recovery of an independent *arcA* mutant strain has also been observed (64, 268). All the bloodstream pathogens highlighted above can cause both localized and systemic infections and can be found as non-pathogenic colonizers of the human microbiota, further highlighting the need for pathogen adaptation during infection. For bacterial species that additionally occupy niches outside the mammalian host, such as *S. marcescens* and *C. freundii*, the transition to colonization from environmental reservoirs undoubtedly represents a shift in the metabolic requirements for fitness. The evidence for ArcAB function during pathogenic bacterial interactions solidifies the importance of this regulatory system and highlights the need for further investigation of the specific ArcAB-controlled metabolic pathways that contribute to each type of infection and in different infection niches.

Virulence

While metabolic coordination is likely to be a critical function of ArcAB transcriptional control during infection, additional ArcAB-regulated functions have also been implicated in pathogenesis. The *S.* Typhimurium gene *loiA* encodes a positive regulator of *Salmonella* pathogenicity island 1 (SPI-1) genes that are required for pathogenesis in a murine infection model and a loss of *Salmonella* cellular invasion and reduced mouse virulence was observed

when *loiA* was disrupted (261). Interestingly, expression of *loiA* is controlled by oxygen availability in an *arcA*- and *arcB*-dependent manner (261). Virulence genes encoded in SPI-1 were shown to be dependent on ArcA at the transcriptional and protein level in a subsequent *S.* Typhimurium study analyzing the proteome of this serovar in anaerobic conditions (269). These examples of regulation of SPI-1 effector genes by ArcAB in *Salmonella* are a clear demonstration of the diversity of ArcAB regulatory targets and expands the mechanisms by which this global regulator modulates infection processes. A second example of ArcAB-mediated control of virulence genes has been observed in *V. cholera*e. Mutation of *arcA* in *V. cholerae* results in a loss of cholera toxin production, the major virulence factor of this species and was further correlated to a loss of *ctxAB* (cholera toxin) and *tcpA* (toxin-coregulated pilus) gene expression in aerobic conditions (263). It was further suggested that the dysregulation of *V. cholerae* virulence genes was due to ArcA-dependent modulation of ToxT, a known transcriptional activator of *ctxAB* and *tcpA* expression (263). Finally, *arcA* mutants have been demonstrated to increase the sensitivity of *H. influenza*e to the bactericidal activity of human serum (140, 268). In nontypeable *H. influenzae* clinical isolate NT127, this loss of serum resistance was attributed to ArcA-dependent transcriptional modulation of the lipooligosaccharide glycosyltransferse gene *lic2B,* which participates in the lipooligosaccharide (LOS) biosynthesis pathway of this strain (140). ArcA and FNR have also been shown to participate in lipid A modifications in *Salmonella* Enteritidis based on oxygen availability (270).

1.4.8 Concluding Remarks

The two-component regulatory system ArcAB has been the subject of foundational research for more than three decades. The uniqueness of the structure of its sensor kinase ArcB and the complex binding architecture of the response regulator ArcA are some of the attributes

that have made this system a fascinating one for study. Future work is still needed to address the discrepancies between models of how quinones regulate ArcAB under differing oxygenation conditions (**Text Box 1.1**). Further development of techniques allowing for individual study of all three quinones within the same cell *in situ* will greatly aid in this matter. ArcA is a powerful repressor of central metabolic pathways, and this function is critical in mediating global metabolic changes not only during anaerobiosis but also in situations where the use of specific pathways is no longer efficient or even detrimental. From this perspective, ArcAB can incorporate feedback from the cell including electron acceptor availability, enzymatic capabilities, and redox homeostasis into a harmonized response. We have yet to fully characterize the operons under ArcA's control and how this control may extend to other conditions in which oxygen consumption is impacted. This is especially true in species beyond *E. coli* and *S. enterica*. These discoveries will be important in uncovering all the cellular functions including ROS response and cell envelope maintenance that are becoming increasingly

- Further characterization of ArcA oligomerization at target DNA binding sites and regulatory control by partially active ArcA
- Clarification of control of ArcB phosphatase activity and effects of sustained stimulus exposure on ArcA activity
- Continued profiling of quinone-based regulation of ArcB with respect to each quinone species
- Integration of ArcA regulons from more culture conditions into global regulatory networks with a focus on co-regulators such as FNR and σ^S
- Elucidation of the significance of ArcA-controlled metabolic pathways during pathogenesis

associated with ArcAB regulation. While the concept of this two-component system is strikingly straightforward, ArcAB and its vast regulon represent a sophisticated coordination of cellular processes. The numerous examples of ArcAB contributions to bacterial infections further suggests this global regulatory system plays an important role in responding to the host environment and additional work is needed to elucidate the specific nutrient and oxygenation requirements of each species to better understand the mechanisms of ArcAB function during infection.

1.4.9 Acknowledgements

We thank Drs. Dimitris Georgellis and Klaas Hellingwerf for their permission to adapt figures from their aforementioned manuscripts for this review. All figures were created with Biorender.com. This work was supported by Predoctoral Fellowship award 828854 to A. N. B. from the American Heart Association and Public Health Service awards AI148767 to M. T. A and AI134731 to H. L. T. M. and M. A. B. from the National Institutes of Health. The authors have no competing interests to declare.

Text Box 1.1: KEY AREAS FOR FUTURE RESEARCH

1.5 Supplemental Figures[2]

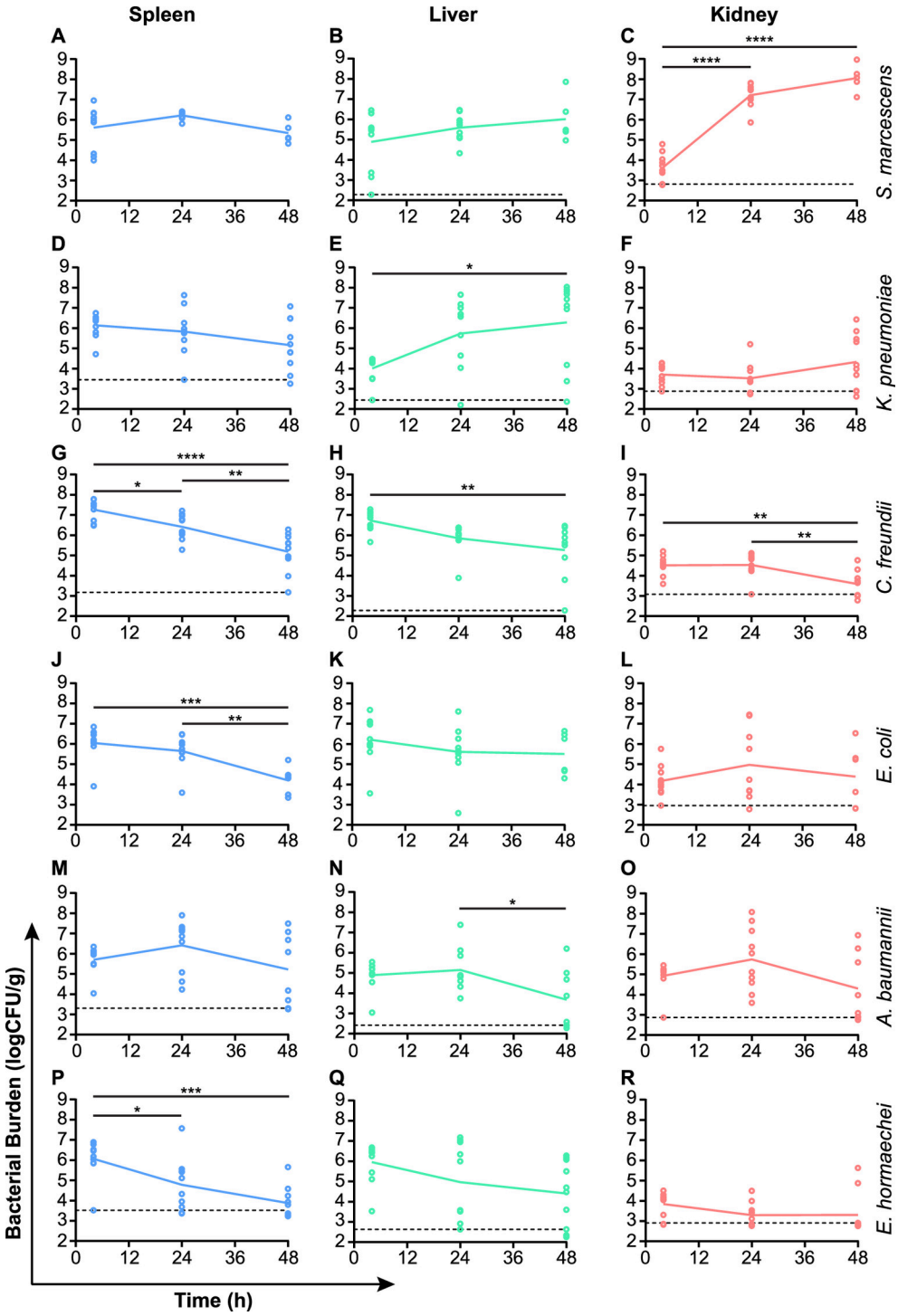

Supplemental Figure 1.5: Tissue colonization for six bacterial species in a murine BSI model. C57BL/6J mice were inoculated (n = 10/time point) with *S. marcescens* (A to C), *K. pneumoniae* (D to F), *C. freundii* (G to I), *E. coli* (J to L), *A. baumannii* (M to O), or *E. hormaechei* (P to R) via tail vein injection. Target doses for each species were as follows: for *A. baumannii*, 1×10^7 CFU; for *C. freundii*, 5×10^7 CFU; for *E. coli*, 5×10^6 CFU; for *E. hormaechei*, 1×10^8 CFU; for *K. pneumoniae*, 5×10^5 CFU; and for *S. marcescens*, 5×10^6 CFU. Bacterial loads in the indicated organs were monitored by viable counts for 48 h. Time points are connected by the mean infectious burden, and horizontal dashed lines indicate the limits of detection, where applicable. Each graph reports the combined results from two independent experiments. Values were log transformed, and significant differences (*, $P < 0.05$; **, $P < 0.01$; ***, $P < 0.001$; ****, $P < 0.0001$) in mean bacterial burdens were assessed by one-way analysis of variance (ANOVA) with Tukey's multiple-comparison test.

[2] Components of this section are modified from the following publication:
Anderson MA, Brown AN, Pirani A, Smith SN, Photenhauer AL, Sun Y, Snitkin ES, Bachman MA, Mobley HLT. Replication Dynamics for Six Gram-Negative Bacterial Species during Bloodstream Infection. *mBio*. 2021 July 6; PubMed PMID: 34225485.

1.6 References

1. Smith DA, Nehring SM. 2023. Bacteremia. StatPearls Publishing, Treasure Island (FL).
2. Chakraborty RK, Burns B. 2023. Systemic Inflammatory Response Syndrome. StatPearls Publishing, Treasure Island (FL).
3. Rudd KE, Johnson SC, Agesa KM, Shackelford KA, Tsoi D, Kievlan DR, Colombara DV, Ikuta KS, Kissoon N, Finfer S, Fleischmann-Struzek C, Machado FR, Reinhart KK, Rowan K, Seymour CW, Watson RS, West TE, Marinho F, Hay SI, Lozano R, Lopez AD, Angus DC, Murray CJL, Naghavi M. 2020. Global, regional, and national sepsis incidence and mortality, 1990–2017: analysis for the Global Burden of Disease Study. *The Lancet* 395:200–211.
4. Paoli CJ, Reynolds MA, Sinha M, Gitlin M, Crouser E. 2018. Epidemiology and Costs of Sepsis in the United States—An Analysis Based on Timing of Diagnosis and Severity Level*. *Crit Care Med* 46:1889–1897.
5. Chang DW, Tseng C-H, Shapiro MF. 2015. Rehospitalizations Following Sepsis: Common and Costly. *Crit Care Med* 43:2085–2093.
6. Rhee C, Jones TM, Hamad Y, Pande A, Varon J, O'Brien C, Anderson DJ, Warren DK, Dantes RB, Epstein L, Klompas M, for the Centers for Disease Control and Prevention (CDC) Prevention Epicenters Program. 2019. Prevalence, Underlying Causes, and Preventability of Sepsis-Associated Mortality in US Acute Care Hospitals. *JAMA Netw Open* 2:e187571.
7. Umemura Y, Ogura H, Takuma K, Fujishima S, Abe T, Kushimoto S, Hifumi T, Hagiwara A, Shiraishi A, Otomo Y, Saitoh D, Mayumi T, Yamakawa K, Shiino Y, Nakada T, Tarui T, Okamoto K, Kotani J, Sakamoto Y, Sasaki J, Shiraishi S, Tsuruta R, Masuno T, Takeyama N, Yamashita N, Ikeda H, Ueyama M, Gando S. 2021. Current spectrum of causative pathogens in sepsis: A prospective nationwide cohort study in Japan. *Int J Infect Dis* 103:343–351.
8. Sirijatuphat R, Sripanidkulchai K, Boonyasiri A, Rattanaumpawan P, Supapueng O, Kiratisin P, Thamlikitkul V. 2018. Implementation of global antimicrobial resistance surveillance system (GLASS) in patients with bacteremia. *PLOS ONE* 13:e0190132.
9. Wang Q, Li X, Tang W, Guan X, Xiong Z, Zhu Y, Gong J, Hu B. 2022. Differential Gene Sets Profiling in Gram-Negative and Gram-Positive Sepsis. *Front Cell Infect Microbiol* 12.
10. Rogers DE, Koenig MG, Holmes KK. 1965. The problem of gram-negative bacteremia and its management. *South Med J* 58:1391–1396.
11. Turner NA, Sharma-Kuinkel BK, Maskarinec SA, Eichenberger EM, Shah PP, Carugati M, Holland TL, Fowler VG. 2019. Methicillin-resistant *Staphylococcus aureus*: an overview of basic and clinical research. 4. *Nat Rev Microbiol* 17:203–218.
12. Tenover FC, McDougal LK, Goering RV, Killgore G, Projan SJ, Patel JB, Dunman PM. 2006. Characterization of a strain of community-associated methicillin-resistant *Staphylococcus aureus* widely disseminated in the United States. *J Clin Microbiol* 44:108–118.
13. Breijyeh Z, Jubeh B, Karaman R. 2020. Resistance of Gram-Negative Bacteria to Current Antibacterial Agents and Approaches to Resolve It. *Molecules* 25:1340.
14. Morris S, Cerceo E. 2020. Trends, Epidemiology, and Management of Multi-Drug Resistant Gram-Negative Bacterial Infections in the Hospitalized Setting. 4. *Antibiotics* 9:196.

15. Albrecht SJ, Fishman NO, Kitchen J, Nachamkin I, Bilker WB, Hoegg C, Samel C, Barbagallo S, Arentzen J, Lautenbach E. 2006. Reemergence of gram-negative health care-associated bloodstream infections. *Arch Intern Med* 166:1289–1294.
16. Opal SM, Cohen J. 1999. Clinical gram-positive sepsis: does it fundamentally differ from gram-negative bacterial sepsis? *Crit Care Med* 27:1608–1616.
17. Ramachandran G. 2014. Gram-positive and gram-negative bacterial toxins in sepsis. *Virulence* 5:213–218.
18. Tang BMP, McLean AS, Dawes IW, Huang SJ, Cowley MJ, Lin RCY. 2008. Gene-expression profiling of gram-positive and gram-negative sepsis in critically ill patients. *Crit Care Med* 36:1125–1128.
19. Hoerr V, Zbytnuik L, Leger C, Tam PPC, Kubes P, Vogel HJ. 2012. Gram-negative and Gram-Positive Bacterial Infections Give Rise to a Different Metabolic Response in a Mouse Model. *J Proteome Res* 11:3231–3245.
20. Zhang J, Chen L, Yang Y, Liu X, Yuan Y, Song S, Zhao Y, Mao J. 2023. Clinical and laboratory findings to differentiate late-onset sepsis caused by Gram-negative vs Gram-positive bacteria among perterm neonates: A retrospective cohort study. *Int Immunopharmacol* 116:109769.
21. Holmes CL, Anderson MT, Mobley HLT, Bachman MA. 2021. Pathogenesis of Gram-Negative Bacteremia. *Clin Microbiol Rev* 34.
22. Ree IMC, Fustolo-Gunnink SF, Bekker V, Fijnvandraat KJ, Steggerda SJ, Lopriore E. 2017. Thrombocytopenia in neonatal sepsis: Incidence, severity and risk factors. *PloS One* 12:e0185581.
23. Dritsakou K, Liosis G, Gioni M, Glynou E, Avdeliodi K, Papagaroufalis K. 2015. CRP levels in extremely low birth weight (ELBW) septic infants. *J Matern-Fetal Neonatal Med Off J Eur Assoc Perinat Med Fed Asia Ocean Perinat Soc Int Soc Perinat Obstet* 28:237–239.
24. Thaden JT, Li Y, Ruffin F, Maskarinec SA, Hill-Rorie JM, Wanda LC, Reed SD, Fowler VG. 2017. Increased Costs Associated with Bloodstream Infections Caused by Multidrug-Resistant Gram-Negative Bacteria Are Due Primarily to Patients with Hospital-Acquired Infections. *Antimicrob Agents Chemother* 61.
25. Kang C-I, Kim S-H, Park WB, Lee K-D, Kim H-B, Kim E-C, Oh M, Choe K-W. 2005. Bloodstream Infections Caused by Antibiotic-Resistant Gram-Negative Bacilli: Risk Factors for Mortality and Impact of Inappropriate Initial Antimicrobial Therapy on Outcome. *Antimicrob Agents Chemother* 49:760–766.
26. Waters J, Shorr AF. 2023. Bloodstream Infection and Gram-Negative Resistance: The Role for Newer Antibiotics. *Antibiotics* 12:977.
27. Ward B. 2015. Chapter 11 - Bacterial Energy Metabolism, p. 201–233. *In* Tang, Y-W, Sussman, M, Liu, D, Poxton, I, Schwartzman, J (eds.), Molecular Medical Microbiology (Second Edition). Academic Press, Boston.
28. André AC, Debande L, Marteyn BS. 2021. The selective advantage of facultative anaerobes relies on their unique ability to cope with changing oxygen levels during infection. *Cell Microbiol* 23:e13338.
29. Unden G, Bongaerts J. 1997. Alternative respiratory pathways of *Escherichia coli*: energetics and transcriptional regulation in response to electron acceptors. *Biochim Biophys Acta BBA - Bioenerg* 1320:217–234.

30. Federowicz S, Kim D, Ebrahim A, Lerman J, Nagarajan H, Cho B, Zengler K, Palsson B. 2014. Determining the Control Circuitry of Redox Metabolism at the Genome-Scale. *PLoS Genet* 10:e1004264.
31. Richardson AR. 2019. Virulence and Metabolism. *Microbiol Spectr* 7.
32. Schoen C, Kischkies L, Elias J, Ampattu BJ. 2014. Metabolism and virulence in *Neisseria meningitidis*. *Front Cell Infect Microbiol* 4:114.
33. Le Bouguénec C, Schouler C. 2011. Sugar metabolism, an additional virulence factor in enterobacteria. *Int J Med Microbiol IJMM* 301:1–6.
34. Anderson MT, Brown AN, Pirani A, Smith SN, Photenhauer AL, Sun Y, Snitkin ES, Bachman MA, Mobley HLT. 2021. Replication Dynamics for Six Gram-Negative Bacterial Species during Bloodstream Infection. *mBio* 12:e0111421.
35. King AN, de Mets F, Brinsmade SR. 2020. Who's in control? Regulation of metabolism and pathogenesis in space and time. *Curr Opin Microbiol* 55:88–96.
36. Iyer MS, Pal A, Srinivasan S, Somvanshi PR, Venkatesh KV. 2021. Global Transcriptional Regulators Fine-Tune the Translational and Metabolic Efficiency for Optimal Growth of *Escherichia coli*. *mSystems* 6.
37. Iyer MS, Pal A, Venkatesh KV. 2023. A Systems Biology Approach To Disentangle the Direct and Indirect Effects of Global Transcription Factors on Gene Expression in *Escherichia coli*. *Microbiol Spectr* e0210122.
38. Pettinari MJ, Nikel PI, Ruiz JA, Méndez BS. 2008. ArcA redox mutants as a source of reduced bioproducts. *J Mol Microbiol Biotechnol* 15:41–47.
39. Goodman AL, Wu M, Gordon JI. 2011. Identifying microbial fitness determinants by insertion sequencing using genome-wide transposon mutant libraries. 12. *Nat Protoc* 6:1969–1980.
40. Anderson MT, Mitchell LA, Zhao L, Mobley HLT. 2018. *Citrobacter freundii* fitness during bloodstream infection. *Sci Rep* 8:11792.
41. Anderson MT, Mitchell LA, Zhao L, Mobley HLT. 2017. Capsule Production and Glucose Metabolism Dictate Fitness during *Serratia marcescens* Bacteremia. *mBio* 8.
42. Subashchandrabose S, Smith SN, Spurbeck RR, Kole MM, Mobley HLT. 2013. Genome-Wide Detection of Fitness Genes in Uropathogenic *Escherichia coli* during Systemic Infection. *PLoS Pathog* 9.
43. Holmes CL, Wilcox AE, Forsyth V, Smith SN, Moricz BS, Unverdorben LV, Mason S, Wu W, Zhao L, Mobley HLT, Bachman MA. 2023. *Klebsiella pneumoniae* causes bacteremia using factors that mediate tissue-specific fitness and resistance to oxidative stress. bioRxiv https://doi.org/10.1101/2023.02.23.529827.
44. Shimizu K. 2013. Metabolic Regulation of a Bacterial Cell System with Emphasis on *Escherichia coli* Metabolism. *ISRN Biochem* 2013:645983.
45. Shi X, Wegener-Feldbrügge S, Huntley S, Hamann N, Hedderich R, Søgaard-Andersen L. 2008. Bioinformatics and Experimental Analysis of Proteins of Two-Component Systems in *Myxococcus xanthus*. *J Bacteriol* 190:613–624.
46. Schaller GE, Shiu S-H, Armitage JP. 2011. Two-Component Systems and Their Co-Option for Eukaryotic Signal Transduction. *Curr Biol* 21:R320–R330.
47. Gao R, Mack TR, Stock AM. 2007. Bacterial response regulators: versatile regulatory strategies from common domains. *Trends Biochem Sci* 32:225–234.
48. Gao R, Stock AM. 2009. Biological insights from structures of two-component proteins. *Annu Rev Microbiol* 63:133–154.

49. Groisman EA. 2016. Feedback Control of Two-Component Regulatory Systems. *Annu Rev Microbiol* 70:103–124.
50. Malpica R, Sandoval GRP, Rodríguez C, Franco B, Georgellis D. 2006. Signaling by the Arc Two-Component System Provides a Link Between the Redox State of the Quinone Pool and Gene Expression. *Antioxid Redox Signal* 8:781–795.
51. Iuchi S, Lin EC. 1988. *arcA* (dye), a global regulatory gene in *Escherichia coli* mediating repression of enzymes in aerobic pathways. *Proc Natl Acad Sci U S A* 85:1888–1892.
52. Iuchi S, Cameron DC, Lin EC. 1989. A second global regulator gene (*arcB*) mediating repression of enzymes in aerobic pathways of *Escherichia coli*. *J Bacteriol* 171:868–873.
53. Iuchi S, Matsuda Z, Fujiwara T, Lin EC. 1990. The *arcB* gene of *Escherichia coli* encodes a sensor-regulator protein for anaerobic repression of the *arc* modulon. *Mol Microbiol* 4:715–727.
54. Georgellis D, Lynch AS, Lin EC. 1997. *In vitro* phosphorylation study of the *arc* two-component signal transduction system of *Escherichia coli*. *J Bacteriol* 179:5429–5435.
55. Kwon O, Georgellis D, Lin EC. 2000. Phosphorelay as the sole physiological route of signal transmission by the arc two-component system of *Escherichia coli*. *J Bacteriol* 182:3858–3862.
56. Salmon KA, Hung S, Steffen NR, Krupp R, Baldi P, Hatfield GW, Gunsalus RP. 2005. Global Gene Expression Profiling in *Escherichia coli* K12 EFFECTS OF OXYGEN AVAILABILITY AND ArcA. *J Biol Chem* 280:15084–15096.
57. Huvet M, Toni T, Sheng X, Thorne T, Jovanovic G, Engl C, Buck M, Pinney JW, Stumpf MPH. 2011. The Evolution of the Phage Shock Protein Response System: Interplay between Protein Function, Genomic Organization, and System Function. *Mol Biol Evol* 28:1141–1155.
58. Jiang F, An C, Bao Y, Zhao X, Jernigan RL, Lithio A, Dan Nettleton, Li L, Wurtele ES, Nolan LK, Lu C, Li G. 2015. ArcA Controls Metabolism, Chemotaxis, and Motility Contributing to the Pathogenicity of Avian Pathogenic *Escherichia coli*. *Infect Immun* 83:3545–3554.
59. Park DM, Akhtar MdS, Ansari AZ, Landick R, Kiley PJ. 2013. The Bacterial Response Regulator ArcA Uses a Diverse Binding Site Architecture to Regulate Carbon Oxidation Globally. *PLoS Genet* 9.
60. Morales EH, Collao B, Desai PT, Calderón IL, Gil F, Luraschi R, Porwollik S, McClelland M, Saavedra CP. 2013. Probing the ArcA regulon under aerobic/ROS conditions in *Salmonella enterica* serovar Typhimurium. *BMC Genomics* 14:626.
61. Yun S, Shin JM, Kim O-C, Jung YR, Oh D-B, Lee SY, Kwon O. 2012. Probing the ArcA regulon in the rumen bacterium *Mannheimia succiniciproducens* by genome-wide expression profiling. *J Microbiol Seoul Korea* 50:665–672.
62. Evans MR, Fink RC, Vazquez-Torres A, Porwollik S, Jones-Carson J, McClelland M, Hassan HM. 2011. Analysis of the ArcA regulon in anaerobically grown *Salmonella enterica* sv. Typhimurium. *BMC Microbiol* 11:58.
63. Gao H, Wang X, Yang ZK, Chen J, Liang Y, Chen H, Palzkill T, Zhou J. 2010. Physiological Roles of ArcA, Crp, and EtrA and Their Interactive Control on Aerobic and Anaerobic Respiration in *Shewanella oneidensis*. *PLoS ONE* 5.
64. Wong SMS, Alugupalli KR, Ram S, Akerley BJ. 2007. The ArcA regulon and oxidative stress resistance in *Haemophilus influenzae*. *Mol Microbiol* 64:1375–1390.

65. Liu X, De Wulf P. 2004. Probing the ArcA-P modulon of *Escherichia coli* by whole genome transcriptional analysis and sequence recognition profiling. *J Biol Chem* 279:12588–12597.
66. Alvarez AF, Georgellis D. 2010. Chapter 12 - *In Vitro* and *In Vivo* Analysis of the ArcB/A Redox Signaling Pathway, p. 205–228. *In* Methods in Enzymology. Academic Press.
67. Cabezas CE, Laulié AM, Briones AC, Pardo-Esté C, Lorca DE, Cofré AA, Morales EH, Mora AY, Krüger GI, Bueno SM, Hidalgo AA, Saavedra CP. 2021. Activation of regulator ArcA in the presence of hypochlorite in *Salmonella enterica* serovar Typhimurium. *Biochimie* 180:178–185.
68. Peebo K, Valgepea K, Nahku R, Riis G, Õun M, Adamberg K, Vilu R. 2014. Coordinated activation of PTA-ACS and TCA cycles strongly reduces overflow metabolism of acetate in *Escherichia coli*. *Appl Microbiol Biotechnol* 98:5131–5143.
69. Portnoy VA, Scott DA, Lewis NE, Tarasova Y, Osterman AL, Palsson BØ. 2010. Deletion of Genes Encoding Cytochrome Oxidases and Quinol Monooxygenase Blocks the Aerobic-Anaerobic Shift in *Escherichia coli* K-12 MG1655. *Appl Environ Microbiol* 76:6529–6540.
70. Iuchi S, Chepuri V, Fu HA, Gennis RB, Lin EC. 1990. Requirement for terminal cytochromes in generation of the aerobic signal for the arc regulatory system in *Escherichia coli*: study utilizing deletions and lac fusions of *cyo* and *cyd*. *J Bacteriol* 172:6020–6025.
71. Nochino N, Toya Y, Shimizu H. 2020. Transcription Factor ArcA is a Flux Sensor for the Oxygen Consumption Rate in *Escherichia coli*. *Biotechnol J* 15:1900353.
72. Alexeeva S, Hellingwerf KJ, Teixeira de Mattos MJ. 2003. Requirement of ArcA for Redox Regulation in *Escherichia coli* under Microaerobic but Not Anaerobic or Aerobic Conditions. *J Bacteriol* 185:204–209.
73. de Graef MR, Alexeeva S, Snoep JL, Teixeira de Mattos MJ. 1999. The Steady-State Internal Redox State (NADH/NAD) Reflects the External Redox State and Is Correlated with Catabolic Adaptation in *Escherichia coli. J Bacteriol* 181:2351–2357.
74. Gunsalus RP, Park S-J. 1994. Aerobic-anaerobic gene regulation in *Escherichia coli*: control by the ArcAB and Fnr regulons. *Res Microbiol* 145:437–450.
75. Green J, Paget MS. 2004. Bacterial redox sensors. *Nat Rev Microbiol* 2:954–966.
76. Alvarez AF, Rodriguez C, Georgellis D. 2013. Ubiquinone and Menaquinone Electron Carriers Represent the Yin and Yang in the Redox Regulation of the ArcB Sensor Kinase. *J Bacteriol* 195:3054–3061.
77. van Beilen JWA, Hellingwerf KJ. 2016. All Three Endogenous Quinone Species of *Escherichia coli* Are Involved in Controlling the Activity of the Aerobic/Anaerobic Response Regulator ArcA. *Front Microbiol* 7:1339.
78. Rolfe MD, Beek AT, Graham AI, Trotter EW, Asif HMS, Sanguinetti G, de Mattos JT, Poole RK, Green J. 2011. Transcript Profiling and Inference of *Escherichia coli* K-12 ArcA Activity across the Range of Physiologically Relevant Oxygen Concentrations. *J Biol Chem* 286:10147–10154.
79. Iuchi S. 1993. Phosphorylation/dephosphorylation of the receiver module at the conserved aspartate residue controls transphosphorylation activity of histidine kinase in sensor protein ArcB of *Escherichia coli*. *J Biol Chem* 268:23972–23980.
80. Georgellis D, Kwon O, Lin EC. 2001. Quinones as the redox signal for the arc two-component system of bacteria. *Science* 292:2314–2316.

81. Serna A, Espinosa E, Camacho EM, Casadesús J. 2010. Regulation of Bacterial Conjugation in Microaerobiosis by Host-Encoded Functions ArcAB and SdhABCD. *Genetics* 184:947–958.
82. Cheng C, Chen J, Shan Y, Fang C, Liu Y, Xia Y, Song H, Fang W. 2013. *Listeria monocytogenes* ArcA contributes to acid tolerance. *J Med Microbiol* 62:813–821.
83. Longo P, Ota-Tsuzuki C, Nunes A, Fernandes B, Mintz K, Fives-Taylor P, Mayer M. 2009. Aggregatibacter actinomycetemcomitans *arcB* influences hydrophobic properties, biofilm formation and adhesion to hydroxyapatite. *Braz J Microbiol* 40:550–562.
84. Bose JL, Kim U, Bartkowski W, Gunsalus RP, Overley AM, Lyell NL, Visick KL, Stabb EV. 2007. Bioluminescence in *Vibrio fischeri* is controlled by the redox-responsive regulator ArcA. *Mol Microbiol* 65:538–553.
85. Lu J, Peng Y, Wan S, Frost LS, Raivio T, Glover JNM. 2019. Cooperative Function of TraJ and ArcA in Regulating the F Plasmid *tra* Operon. *J Bacteriol* 201.
86. Sun H, Song Y, Chen F, Zhou C, Liu P, Fan Y, Zheng Y, Wan X, Feng L. 2020. An ArcA-Modulated Small RNA in Pathogenic *Escherichia coli* K1. *Front Microbiol* 11:574833.
87. Li G-W, Burkhardt D, Gross C, Weissman JS. 2014. Quantifying absolute protein synthesis rates reveals principles underlying allocation of cellular resources. *Cell* 157:624–635.
88. Ćudić E, Surmann K, Panasia G, Hammer E, Hunke S. 2017. The role of the two-component systems Cpx and Arc in protein alterations upon gentamicin treatment in *Escherichia coli*. *BMC Microbiol* 17.
89. Gunsalus RP. 1992. Control of electron flow in *Escherichia coli*: coordinated transcription of respiratory pathway genes. *J Bacteriol* 174:7069–7074.
90. Capra EJ, Laub MT. 2012. The Evolution of Two-Component Signal Transduction Systems. *Annu Rev Microbiol* 66:325–347.
91. Yamamoto K, Hirao K, Oshima T, Aiba H, Utsumi R, Ishihama A. 2005. Functional Characterization *in Vitro* of All Two-component Signal Transduction Systems from *Escherichia coli**. *J Biol Chem* 280:1448–1456.
92. Iuchi S, Lin EC. 1992. Mutational analysis of signal transduction by ArcB, a membrane sensor protein responsible for anaerobic repression of operons involved in the central aerobic pathways in *Escherichia coli*. *J Bacteriol* 174:3972–3980.
93. Shalel-Levanon S, San K-Y, Bennett GN. 2005. Effect of ArcA and FNR on the expression of genes related to the oxygen regulation and the glycolysis pathway in *Escherichia coli* under microaerobic growth conditions. *Biotechnol Bioeng* 92:147–159.
94. Ramos PIP, Custódio MGF, Quispe Saji G del R, Cardoso T, da Silva GL, Braun G, Martins WMBS, Girardello R, de Vasconcelos ATR, Fernández E, Gales AC, Nicolás MF. 2016. The polymyxin B-induced transcriptomic response of a clinical, multidrug-resistant *Klebsiella pneumoniae* involves multiple regulatory elements and intracellular targets. *BMC Genomics* 17.
95. Mandin P, Gottesman S. 2010. Integrating anaerobic/aerobic sensing and the general stress response through the ArcZ small RNA. *EMBO J* 29:3094–3107.
96. Compan I, Touati D. 1994. Anaerobic activation of *arcA* transcription in *Escherichia coli*: roles of Fnr and ArcA. *Mol Microbiol* 11:955–964.
97. Ireland WT, Beeler SM, Flores-Bautista E, McCarty NS, Röschinger T, Belliveau NM, Sweredoski MJ, Moradian A, Kinney JB, Phillips R. 2020. Deciphering the regulatory genome of *Escherichia coli*, one hundred promoters at a time. *eLife* 9:e55308.

98. Jordan PA, Thomson AJ, Ralph ET, Guest JR, Green J. 1997. FNR is a direct oxygen sensor having a biphasic response curve. *FEBS Lett* 416:349–352.
99. Crack J, Green J, Thomson AJ. 2004. Mechanism of oxygen sensing by the bacterial transcription factor fumarate-nitrate reduction (FNR). *J Biol Chem* 279:9278–9286.
100. Marzan LW, Hasan CMM, Shimizu K. 2013. Effect of acidic condition on the metabolic regulation of *Escherichia coli* and its *phoB* mutant. *Arch Microbiol* 195:161–171.
101. Park DM, Kiley PJ. 2014. The influence of repressor DNA binding site architecture on transcriptional control. *mBio* 5:e01684-01614.
102. Kwon O, Georgellis D, Lynch AS, Boyd D, Lin ECC. 2000. The ArcB Sensor Kinase of *Escherichia coli*: Genetic Exploration of the Transmembrane Region. *J Bacteriol* 182:2960–2966.
103. Maslennikov I, Klammt C, Hwang E, Kefala G, Okamura M, Esquivies L, Mörs K, Glaubitz C, Kwiatkowski W, Jeon YH, Choe S. 2010. Membrane domain structures of three classes of histidine kinase receptors by cell-free expression and rapid NMR analysis. *Proc Natl Acad Sci U S A* 107:10902–10907.
104. Malpica R, Franco B, Rodriguez C, Kwon O, Georgellis D. 2004. Identification of a quinone-sensitive redox switch in the ArcB sensor kinase. *Proc Natl Acad Sci U S A* 101:13318–13323.
105. Mascher T, Helmann JD, Unden G. 2006. Stimulus Perception in Bacterial Signal-Transducing Histidine Kinases. *Microbiol Mol Biol Rev* 70:910–938.
106. Kinoshita-Kikuta E, Kinoshita E, Eguchi Y, Koike T. 2016. Validation of Cis and Trans Modes in Multistep Phosphotransfer Signaling of Bacterial Tripartite Sensor Kinases by Using Phos-Tag SDS-PAGE. *PLOS ONE* 11:e0148294.
107. Kato M, Mizuno T, Shimizu T, Hakoshima T. 1997. Insights into multistep phosphorelay from the crystal structure of the C-terminal HPt domain of ArcB. *Cell* 88:717–723.
108. Tsuzuki M, Ishige K, Mizuno T. 1995. Phosphotransfer circuitry of the putative multi-signal transducer, ArcB, of *Escherichia coli*: *in vitro* studies with mutants. *Mol Microbiol* 18:953–962.
109. Matsushika A, Mizuno T. 1998. A Dual-Signaling Mechanism Mediated by the ArcB Hybrid Sensor Kinase Containing the Histidine-Containing Phosphotransfer Domain in *Escherichia coli*. *J Bacteriol* 180:3973–3977.
110. Matsushika A, Mizuno T. 1998. The Structure and Function of the Histidine-Containing Phosphotransfer (HPt) Signaling Domain of the *Escherichia coli* ArcB Sensor. *J Biochem (Tokyo)* 124:440–445.
111. Iuchi S, Lin EC. 1992. Purification and phosphorylation of the Arc regulatory components of *Escherichia coli*. *J Bacteriol* 174:5617–5623.
112. Iuchi S, Weiner L. 1996. Cellular and Molecular Physiology of *Escherichia coli* in the Adaptation to Aerobic Environments. *J Biochem (Tokyo)* 120:1055–1063.
113. Ishige K, Nagasawa S, Tokishita S, Mizuno T. 1994. A novel device of bacterial signal transducers. *EMBO J* 13:5195–5202.
114. Nuñez Oreza LA, Alvarez AF, Arias-Olguín II, Torres Larios A, Georgellis D. 2012. The ArcB Leucine Zipper Domain Is Required for Proper ArcB Signaling. *PLoS ONE* 7.
115. Taylor BL, Zhulin IB. 1999. PAS Domains: Internal Sensors of Oxygen, Redox Potential, and Light. *Microbiol Mol Biol Rev* 63:479–506.

116. Matsushika A, Mizuno T. 2000. Characterization of three putative sub-domains in the signal-input domain of the ArcB hybrid sensor in *Escherichia coli*. *J Biochem (Tokyo)* 127:855–860.
117. Zhulin IB, Taylor BL, Dixon R. 1997. PAS domain S-boxes in archaea, bacteria and sensors for oxygen and redox. *Trends Biochem Sci* 22:331–333.
118. Georgellis D, Kwon O, Lin ECC, Wong SM, Akerley BJ. 2001. Redox Signal Transduction by the ArcB Sensor Kinase of *Haemophilus influenzae* Lacking the PAS Domain. *J Bacteriol* 183:7206–7212.
119. Nguyen M-P, Yoon J-M, Cho M-H, Lee S-W. 2015. Prokaryotic 2-component systems and the OmpR/PhoB superfamily. *Can J Microbiol* 61:799–810.
120. Toro-Roman A, Mack TR, Stock AM. 2005. Structural Analysis and Solution Studies of the Activated Regulatory Domain of the Response Regulator ArcA: A Symmetric Dimer Mediated by the α4-β5-α5 Face. *J Mol Biol* 349:11–26.
121. Lynch AS, Lin EC. 1996. Transcriptional control mediated by the ArcA two-component response regulator protein of *Escherichia coli*: characterization of DNA binding at target promoters. *J Bacteriol* 178:6238–6249.
122. Martínez-Hackert E, Stock AM. 1997. Structural relationships in the OmpR family of winged-helix transcription factors. *J Mol Biol* 269:301–312.
123. Kenney LJ. 2002. Structure/function relationships in OmpR and other winged-helix transcription factors. *Curr Opin Microbiol* 5:135–141.
124. Galperin MY. 2010. Diversity of structure and function of response regulator output domains. *Curr Opin Microbiol* 13:150–159.
125. Joyce AP, Havranek JJ. 2018. Deciphering the protein-DNA code of bacterial winged helix-turn-helix transcription factors. *Quant Biol* 6:68–84.
126. Peña-Sandoval GR, Georgellis D. 2010. The ArcB sensor kinase of *Escherichia coli* autophosphorylates by an intramolecular reaction. *J Bacteriol* 192:1735–1739.
127. Teran-Melo JL, Peña-Sandoval GR, Silva-Jimenez H, Rodriguez C, Alvarez AF, Georgellis D. 2018. Routes of phosphoryl group transfer during signal transmission and signal decay in the dimeric sensor histidine kinase ArcB. *J Biol Chem* 293:13214–13223.
128. West AH, Stock AM. 2001. Histidine kinases and response regulator proteins in two-component signaling systems. *Trends Biochem Sci* 26:369–376.
129. Drapal N, Sawers G. 1995. Purification of ArcA and analysis of is specific interaction with the *pfl* promoter-regulatory region. *Mol Microbiol* 16:597–607.
130. Strohmaier H, Noiges R, Kotschan S, Sawers G, Högenauer G, Zechner EL, Koraimann G. 1998. Signal transduction and bacterial conjugation: characterization of the role of ArcA in regulating conjugative transfer of the resistance plasmid R1. *J Mol Biol* 277:309–316.
131. Liu X, Peña Sandoval GR, Wanner BL, Jung WS, Georgellis D, Kwon O. 2009. Evidence against the physiological role of acetyl phosphate in the phosphorylation of the ArcA response regulator in *Escherichia coli*. *J Microbiol* 47:657.
132. Shen J, Gunsalus RP. 1997. Role of multiple ArcA recognition sites in anaerobic regulation of succinate dehydrogenase (*sdhCDAB*) gene expression in *Escherichia coli*. *Mol Microbiol* 26:223–236.
133. Jeon Y, Lee YS, Han JS, Kim JB, Hwang DS. 2001. Multimerization of Phosphorylated and Non-phosphorylated ArcA Is Necessary for the Response Regulator Function of the Arc Two-component Signal Transduction System. *J Biol Chem* 276:40873–40879.

134. Mika F, Hengge R. 2005. A two-component phosphotransfer network involving ArcB, ArcA, and RssB coordinates synthesis and proteolysis of σS (RpoS) in *E. coli. Genes Dev* 19:2770–2781.
135. Pellicer MT, Lynch AS, De Wulf P, Boyd D, Aguilar J, Lin EC. 1999. A mutational study of the ArcA-P binding sequences in the *aldA* promoter of *Escherichia coli*. *Mol Gen Genet MGG* 261:170–176.
136. McGuire AM, De Wulf P, Church GM, Lin EC. 1999. A weight matrix for binding recognition by the redox-response regulator ArcA-P of *Escherichia coli*. *Mol Microbiol* 32:219–221.
137. Favorov AV, Gelfand MS, Gerasimova AV, Ravcheev DA, Mironov AA, Makeev VJ. 2005. A Gibbs sampler for identification of symmetrically structured, spaced DNA motifs with improved estimation of the signal length. *Bioinformatics* 21:2240–2245.
138. Wang X, Gao H, Shen Y, Weinstock GM, Zhou J, Palzkill T. 2008. A high-throughput percentage-of-binding strategy to measure binding energies in DNA–protein interactions: application to genome-scale site discovery. *Nucleic Acids Res* 36:4863–4871.
139. Gao H, Wang X, Yang ZK, Palzkill T, Zhou J. 2008. Probing regulon of ArcA in *Shewanella oneidensis* MR-1 by integrated genomic analyses. *BMC Genomics* 9:42.
140. Wong SMS, St. Michael F, Cox A, Ram S, Akerley BJ. 2011. ArcA-Regulated Glycosyltransferase Lic2B Promotes Complement Evasion and Pathogenesis of Nontypeable *Haemophilus influenzae*. *Infect Immun* 79:1971–1983.
141. Georgellis D, Kwon O, De Wulf P, Lin EC. 1998. Signal decay through a reverse phosphorelay in the Arc two-component signal transduction system. *J Biol Chem* 273:32864–32869.
142. Peña-Sandoval GR, Kwon O, Georgellis D. 2005. Requirement of the receiver and phosphotransfer domains of ArcB for efficient dephosphorylation of phosphorylated ArcA *in vivo*. *J Bacteriol* 187:3267–3272.
143. Matsubara Masahiro, Mizuno Takeshi. 2000. The SixA phospho-histidine phosphatase modulates the ArcB phosphorelay signal transduction in *Escherichia coli*. *FEBS Lett* 470:118–124.
144. Ogino T, Matsubara M, Kato N, Nakamura Y, Mizuno T. 1998. An *Escherichia coli* protein that exhibits phosphohistidine phosphatase activity towards the HPt domain of the ArcB sensor involved in the multistep His-Asp phosphorelay. *Mol Microbiol* 27:573–585.
145. Hakoshima T, Ichihara H. 2007. Structure of SixA, a histidine protein phosphatase of the ArcB histidine-containing phosphotransfer domain in Escherichia coli. *Methods Enzymol* 422:288–304.
146. Schulte JE, Goulian M. 2018. The Phosphohistidine Phosphatase SixA Targets a Phosphotransferase System. *mBio* 9.
147. Roeder W, Somerville RL. 1979. Cloning the *trpR* gene. *Mol Gen Genet MGG* 176:361–368.
148. Kashef N, Hamblin MR. 2017. Can microbial cells develop resistance to oxidative stress in antimicrobial photodynamic inactivation? *Drug Resist Updat Rev Comment Antimicrob Anticancer Chemother* 31:31–42.
149. Alvarez AF, Malpica R, Contreras M, Escamilla E, Georgellis D. 2010. Cytochrome d But Not Cytochrome o Rescues the Toluidine Blue Growth Sensitivity of *arc* Mutants of *Escherichia coli*. *J Bacteriol* 192:391–399.

150. Georgellis D, Kwon O, Lin EC. 1999. Amplification of signaling activity of the *arc* two-component system of *Escherichia coli* by anaerobic metabolites. An *in vitro* study with different protein modules. *J Biol Chem* 274:35950–35954.
151. Rodriguez C, Kwon O, Georgellis D. 2004. Effect of d-Lactate on the Physiological Activity of the ArcB Sensor Kinase in *Escherichia coli*. *J Bacteriol* 186:2085–2090.
152. Lin ECC, Iuchi S. 1991. Regulation of Gene Expression in Fermentative and Respiratory Systems in *Escherichia coli* and Related Bacteria. *Annu Rev Genet* 25:361–387.
153. Nowicka B, Kruk J. 2010. Occurrence, biosynthesis and function of isoprenoid quinones. *Biochim Biophys Acta BBA - Bioenerg* 1797:1587–1605.
154. Collins MD, Jones D. 1981. Distribution of isoprenoid quinone structural types in bacteria and their taxonomic implication. *Microbiol Rev* 45:316–354.
155. Meganathan R, Kwon O. 2009. Biosynthesis of Menaquinone (Vitamin K2) and Ubiquinone (Coenzyme Q). *EcoSal Plus* 3.
156. 1965. Tentative rules nomenclature of quinones with isoprenoid side-chains. *Biochim Biophys Acta BBA - Gen Subj* 107:5–10.
157. Nitzschke A, Bettenbrock K. 2018. All three quinone species play distinct roles in ensuring optimal growth under aerobic and fermentative conditions in *E. coli* K12. *PloS One* 13:e0194699.
158. Borisov VB, Verkhovsky MI. 2015. Oxygen as Acceptor. *EcoSal Plus* 6.
159. Søballe B, Poole RK. 1999. Microbial ubiquinones: multiple roles in respiration, gene regulation and oxidative stress management. *Microbiol Read Engl* 145 (Pt 8):1817–1830.
160. Sharma P, Mattos MJT de, Hellingwerf KJ, Bekker M. 2012. On the function of the various quinone species in *Escherichia coli*. *FEBS J* 279:3364–3373.
161. Weiss SA, Jeuken LJC. 2009. Electrodes modified with lipid membranes to study quinone oxidoreductases. *Biochem Soc Trans* 37:707–712.
162. Sharma P, Stagge S, Bekker M, Bettenbrock K, Hellingwerf KJ. 2013. Kinase Activity of ArcB from *Escherichia coli* Is Subject to Regulation by Both Ubiquinone and Demethylmenaquinone. *PLoS ONE* 8.
163. Bekker M, Alexeeva S, Laan W, Sawers G, Teixeira de Mattos J, Hellingwerf K. 2010. The ArcBA Two-Component System of *Escherichia coli* Is Regulated by the Redox State of both the Ubiquinone and the Menaquinone Pool. *J Bacteriol* 192:746–754.
164. Bekker M, Kramer G, Hartog AF, Wagner MJ, de Koster CG, Hellingwerf KJ, Teixeira de Mattos MJ. 2007. Changes in the redox state and composition of the quinone pool of *Escherichia coli* during aerobic batch-culture growth. *Microbiology* 153:1974–1980.
165. Aussel L, Pierrel F, Loiseau L, Lombard M, Fontecave M, Barras F. 2014. Biosynthesis and physiology of coenzyme Q in bacteria. *Biochim Biophys Acta BBA - Bioenerg* 1837:1004–1011.
166. Alexeeva S, de Kort B, Sawers G, Hellingwerf KJ, de Mattos MJT. 2000. Effects of Limited Aeration and of the ArcAB System on Intermediary Pyruvate Catabolism in *Escherichia coli. J Bacteriol* 182:4934–4940.
167. Shestopalov AI, Bogachev AV, Murtazina RA, Viryasov MB, Skulachev VP. 1997. Aeration-dependent changes in composition of the quinone pool in *Escherichia coli. FEBS Lett* 404:272–274.
168. Martínez-Antonio A, Collado-Vides J. 2003. Identifying global regulators in transcriptional regulatory networks in bacteria. *Curr Opin Microbiol* 6:482–489.

169. Li Y, Yan J, Guo X, Wang X, Liu F, Cao B. 2022. The global regulators ArcA and CytR collaboratively modulate *Vibrio cholerae* motility. *BMC Microbiol* 22:22.
170. Kargeti M, Venkatesh KV. 2017. The effect of global transcriptional regulators on the anaerobic fermentative metabolism of Escherichia coli. *Mol Biosyst* 13:1388–1398.
171. Kothamachu VB, Feliu E, Wiuf C, Cardelli L, Soyer OS. 2013. Phosphorelays Provide Tunable Signal Processing Capabilities for the Cell. *PLoS Comput Biol* 9.
172. Perrenoud A, Sauer U. 2005. Impact of Global Transcriptional Regulation by ArcA, ArcB, Cra, Crp, Cya, Fnr, and Mlc on Glucose Catabolism in *Escherichia coli. J Bacteriol* 187:3171–3179.
173. Smirnova GV, Tyulenev AV, Muzyka NG, Oktyabrsky ON. 2020. Study of the relationship between extracellular superoxide and glutathione production in batch cultures of *Escherichia coli*. *Res Microbiol* 171:301-310.
174. Toya Y, Nakahigashi K, Tomita M, Shimizu K. 2012. Metabolic regulation analysis of wild-type and *arcA* mutant *Escherichia coli* under nitrate conditions using different levels of omics data. *Mol Biosyst* 8:2593–2604.
175. Shalel-Levanon S, San K-Y, Bennett GN. 2005. Effect of oxygen, and ArcA and FNR regulators on the expression of genes related to the electron transfer chain and the TCA cycle in *Escherichia coli. Metab Eng* 7:364–374.
176. Vemuri GN, Altman E, Sangurdekar DP, Khodursky AB, Eiteman MA. 2006. Overflow metabolism in *Escherichia coli* during steady-state growth: transcriptional regulation and effect of the redox ratio. *Appl Environ Microbiol* 72:3653–3661.
177. Waegeman H, Beauprez J, Moens H, Maertens J, De Mey M, Foulquié-Moreno MR, Heijnen JJ, Charlier D, Soetaert W. 2011. Effect of *iclR* and *arcA* knockouts on biomass formation and metabolic fluxes in *Escherichia coli* K12 and its implications on understanding the metabolism of *Escherichia coli* BL21 (DE3). *BMC Microbiol* 11:70.*i*
178. Förster AH, Gescher J. 2014. Metabolic Engineering of *Escherichia coli* for Production of Mixed-Acid Fermentation End Products. *Front Bioeng Biotechnol* 2.
179. Bidart GN, Ruiz JA, de Almeida A, Méndez BS, Nikel PI. 2012. Manipulation of the Anoxic Metabolism in *Escherichia coli* by ArcB Deletion Variants in the ArcBA Two-Component System. *Appl Environ Microbiol* 78:8784–8794.
180. Basan M, Hui S, Williamson JR. 2017. ArcA overexpression induces fermentation and results in enhanced growth rates of *E. coli*. *Sci Rep* 7:11866.
181. Liu M, Yao L, Xian M, Ding Y, Liu H, Zhao G. 2016. Deletion of *arcA* increased the production of acetyl-CoA-derived chemicals in recombinant *Escherichia coli.Biotechnol Lett* 38:97–101.
182. Ruiz JA, de Almeida A, Godoy MS, Mezzina MP, Bidart GN, Méndez BS, Pettinari MJ, Nikel PI. 2013. *Escherichia coli redox* mutants as microbial cell factories for the synthesis of reduced biochemicals. *Comput Struct Biotechnol J* 3.
183. Matsuoka Y, Kurata H. 2017. Modeling and simulation of the redox regulation of the metabolism in *Escherichia coli* at different oxygen concentrations. *Biotechnol Biofuels* 10:183.
184. Egoburo DE, Diaz Peña R, Alvarez DS, Godoy MS, Mezzina MP, Pettinari MJ. 2018. Microbial Cell Factories à la Carte: Elimination of Global Regulators Cra and ArcA Generates Metabolic Backgrounds Suitable for the Synthesis of Bioproducts in *Escherichia coli. Appl Environ Microbiol* 84:e01337-18.

185. Pettinari MJ, Egoburo DE. 2021. Chapter 23 - Manipulation of global regulators in *Escherichia coli* for the synthesis of biotechnologically relevant products, p. 437–453. *In* Singh, V (ed.), Microbial Cell Factories Engineering for Production of Biomolecules. Academic Press.
186. Covert MW, Knight EM, Reed JL, Herrgard MJ, Palsson BO. 2004. Integrating high-throughput and computational data elucidates bacterial networks. *Nature* 429:92–96.
187. Iuchi S, Aristarkhov A, Dong JM, Taylor JS, Lin EC. 1994. Effects of nitrate respiration on expression of the Arc-controlled operons encoding succinate dehydrogenase and flavin-linked L-lactate dehydrogenase. *J Bacteriol* 176:1695–1701.
188. Park S-J, Tseng C-P, Gunsalus RP. 1995. Regulation of succinate dehydrogenase *(sdhCDAB)* operon expression in *Escherichia coli* in response to carbon supply and anaerobiosis: role of ArcA and Fnr. *Mol Microbiol* 15:473–482.
189. Denby KJ, Rolfe MD, Crick E, Sanguinetti G, Poole RK, Green J. 2015. Adaptation of anaerobic cultures of *Escherichia coli* K-12 in response to environmental trimethylamine-N-oxide. *Environ Microbiol* 17:2477–2491.
190. Yoshida H, Shimada T, Ishihama A. 2018. Coordinated Hibernation of Transcriptional and Translational Apparatus during Growth Transition of *Escherichia coli* to Stationary Phase. *mSystems* 3:e00057-18.
191. Battesti A, Majdalani N, Gottesman S. 2011. The RpoS-Mediated General Stress Response in *Escherichia coli. Annu Rev Microbiol* 65:189–213.
192. Gottesman S. 2019. Trouble is coming: Signaling pathways that regulate general stress responses in bacteria. *J Biol Chem* 294:11685–11700.
193. Battesti A, Majdalani N, Gottesman S. 2015. Stress sigma factor RpoS degradation and translation are sensitive to the state of central metabolism. *Proc Natl Acad Sci U S A* 112:5159–5164.
194. Chen AI, Goulian M. 2018. A network of regulators promotes dehydration tolerance in *Escherichia coli. Environ Microbiol* 20:1283–1295.
195. Nyström T, Larsson C, Gustafsson L. 1996. Bacterial defense against aging: role of the *Escherichia coli* ArcA regulator in gene expression, readjusted energy flux and survival during stasis. *EMBO J* 15:3219–3228.
196. Gonidakis S, Finkel SE, Longo VD. 2010. *E. coli* hypoxia-inducible factor ArcA mediates lifespan extension in a lipoic acid synthase mutant by suppressing acetyl-CoA synthetase. *Biol Chem* 391:1139–1147.
197. Gonidakis S, Finkel SE, Longo VD. 2010. Genome-wide screen identifies *Escherichia coli* TCA cycle-related mutants with extended chronological lifespan dependent on acetate metabolism and the hypoxia-inducible transcription factor ArcA. *Aging Cell* 9:868–881.
198. Hidese R, Mihara H, Kurihara T, Esaki N. 2014. Global identification of genes affecting iron-sulfur cluster biogenesis and iron homeostasis. *J Bacteriol* 196:1238–1249.
199. Roche B, Aussel L, Ezraty B, Mandin P, Py B, Barras F. 2013. Iron/sulfur proteins biogenesis in prokaryotes: Formation, regulation and diversity. *Biochim Biophys Acta BBA - Bioenerg* 1827:455–469.
200. Cotter PA, Darie S, Gunsalus RP. 1992. The effect of iron limitation on expression of the aerobic and anaerobic electron transport pathway genes in *Escherichia coli. FEMS Microbiol Lett* 100:227–232.
201. Chareyre S, Barras F, Mandin P. 2019. A small RNA controls bacterial sensitivity to gentamicin during iron starvation. *PLOS Genet* 15:e1008078.

202. Folsom JP, Parker AE, Carlson RP. 2014. Physiological and Proteomic Analysis of *Escherichia coli* Iron-Limited Chemostat Growth. *J Bacteriol* 196:2748–2761.
203. Fong KP, Gao L, Demuth DR. 2003. *luxS* and *arcB* control aerobic growth of *Actinobacillus actinomycetemcomitans* under iron limitation. *Infect Immun* 71:298–308.
204. Tardat B, Touati D. 1993. Iron and oxygen regulation of *Escherichia coli* MnSOD expression: competition between the global regulators Fur and ArcA for binding to DNA. *Mol Microbiol* 9:53–63.
205. Shimizu K. 2016. Metabolic Regulation and Coordination of the Metabolism in Bacteria in Response to a Variety of Growth Conditions. *Adv Biochem Eng Biotechnol* 155:1–54.
206. Liu J, Chakraborty S, Hosseinzadeh P, Yu Y, Tian S, Petrik I, Bhagi A, Lu Y. 2014. Metalloproteins Containing Cytochrome, Iron–Sulfur, or Copper Redox Centers. *Chem Rev* 114:4366–4469.
207. Cotter PA, Melville SB, Albrecht JA, Gunsalus RP. 1997. Aerobic regulation of cytochrome d oxidase *(cydAB*) operon expression in *Escherichia coli:* roles of Fnr and ArcA in repression and activation. *Mol Microbiol* 25:605–615.
208. Zupok A, Gorka M, Siemiatkowska B, Skirycz A, Leimkühler S. 2019. Iron-Dependent Regulation of Molybdenum Cofactor Biosynthesis Genes in *Escherichia coli. J Bacteriol* 201.
209. Szenk M, Dill KA, de Graff AMR. 2017. Why Do Fast-Growing Bacteria Enter Overflow Metabolism? Testing the Membrane Real Estate Hypothesis. *Cell Syst* 5:95–104.
210. Basan M, Hui S, Okano H, Zhang Z, Shen Y, Williamson JR, Hwa T. 2015. Overflow metabolism in *Escherichia coli* results from efficient proteome allocation. *Nature* 528:99–104.
211. Kiley PJ, Beinert H. 1998. Oxygen sensing by the global regulator, FNR: the role of the iron-sulfur cluster. *FEMS Microbiol Rev* 22:341–352.
212. Crack JC, Green J, Thomson AJ, Brun NEL. 2014. Iron–Sulfur Clusters as Biological Sensors: The Chemistry of Reactions with Molecular Oxygen and Nitric Oxide. *Acc Chem Res* 47:3196–3205.
213. Kang Y, Weber KD, Qiu Y, Kiley PJ, Blattner FR. 2005. Genome-Wide Expression Analysis Indicates that FNR of *Escherichia coli* K-12 Regulates a Large Number of Genes of Unknown Function. *J Bacteriol* 187:1135–1160.
214. Sawers G, Suppmann B. 1992. Anaerobic induction of pyruvate formate-lyase gene expression is mediated by the ArcA and FNR proteins. *J Bacteriol* 174:3474–3478.
215. Levanon SS, San K-Y, Bennett GN. 2005. Effect of oxygen on the *Escherichia coli* ArcA and FNR regulation systems and metabolic responses. *Biotechnol Bioeng* 89:556–564.
216. Partridge JD, Sanguinetti G, Dibden DP, Roberts RE, Poole RK, Green J. 2007. Transition of *Escherichia coli* from aerobic to micro-aerobic conditions involves fast and slow reacting regulatory components. *J Biol Chem* 282:11230–11237.
217. Cotter PA, Gunsalus RP. 1992. Contribution of the *fnr* and *arcA* gene products in coordinate regulation of cytochrome o and d oxidase *(cyoABCDE* and *cydAB)* genes in *Escherichia coli. FEMS Microbiol Lett* 70:31–36.
218. Jiang GR, Nikolova S, Clark DP. 2001. Regulation of the *ldhA* gene, encoding the fermentative lactate dehydrogenase of *Escherichia coli. Microbiology* 147:2437–2446.
219. Laub MT, Goulian M. 2007. Specificity in Two-Component Signal Transduction Pathways. *Annu Rev Genet* 41:121–145.

220. Verhamme DT, Arents JC, Postma PW, Crielaard W, Hellingwerf KJ 2002. Investigation of *in vivo* cross-talk between key two-component systems of *Escherichia coli. Microbiology* 148:69–78.
221. Francis VI, Porter SL. 2019. Multikinase Networks: Two-Component Signaling Networks Integrating Multiple Stimuli. *Annu Rev Microbiol* 73:null.
222. Matsubara M, Kitaoka S, Takeda S, Mizuno T. 2000. Tuning of the porin expression under anaerobic growth conditions by His-to-Asp cross-phosphorelay through both the EnvZ-osmosensor and ArcB-anaerosensor in *Escherichia coli. Genes Cells* 5:555–569.
223. Jovanovic G, Lloyd LJ, Stumpf MPH, Mayhew AJ, Buck M. 2006. Induction and function of the phage shock protein extracytoplasmic stress response in *Escherichia coli. J Biol Chem* 281:21147–21161.
224. Jovanovic G, Engl C, Buck M. 2009. Physical, functional and conditional interactions between ArcAB and phage shock proteins upon secretin-induced stress in *Escherichia coli. Mol Microbiol* 74:16–28.
225. Joly N, Engl C, Jovanovic G, Huvet M, Toni T, Sheng X, Stumpf MPH, Buck M. 2010. Managing membrane stress: the phage shock protein (Psp) response, from molecular mechanisms to physiology. *FEMS Microbiol Rev* 34:797–827.
226. Bogachev AV, Murtazine RA, Shestopalov AI, Skulachev VP. 1995. Induction of the *Escherichia coli* cytochrome d by low delta mu H+ and by sodium ions. *Eur J Biochem* 232:304–308.
227. Liang H, Zhang Y, Wang S, Gao H. Mutual interplay between ArcA and σE orchestrates envelope stress response in *Shewanella oneidensis*. *Environ Microbiol* 23:652-668.
228. Xie P, Liang H, Wang J, Huang Y, Gao H. 2021. Lipopolysaccharide Transport System Links Physiological Roles of σE and ArcA in the Cell Envelope Biogenesis in *Shewanella oneidensis. Microbiol Spectr* e0069021.
229. Ayoub Moubareck C. 2020. Polymyxins and Bacterial Membranes: A Review of Antibacterial Activity and Mechanisms of Resistance. 8. *Membranes* 10:181.
230. Fu L, Wan M, Zhang S, Gao L, Fang W. 2020. Polymyxin B Loosens Lipopolysaccharide Bilayer but Stiffens Phospholipid Bilayer. *Biophys J* 118:138–150.
231. Sabnis A, Hagart KL, Klöckner A, Becce M, Evans LE, Furniss RCD, Mavridou DA, Murphy R, Stevens MM, Davies JC, Larrouy-Maumus GJ, Clarke TB, Edwards AM. 2021. Colistin kills bacteria by targeting lipopolysaccharide in the cytoplasmic membrane. *eLife* 10:e65836.
232. Deris ZZ, Akter J, Sivanesan S, Roberts KD, Thompson PE, Nation RL, Li J, Velkov T. 2014. A secondary mode of action of polymyxins against Gram-negative bacteria involves the inhibition of NADH-quinone oxidoreductase activity. *J Antibiot (Tokyo)* 67:147–151.
233. Kohanski MA, Dwyer DJ, Wierzbowski J, Cottarel G, Collins JJ. 2008. Mistranslation of membrane proteins and two-component system activation trigger aminoglycoside-mediated oxidative stress and cell death. *Cell* 135:679–690.
234. Horinouchi T, Maeda T, Kotani H, Furusawa C. 2020. Suppression of antibiotic resistance evolution by single-gene deletion. *Sci Rep* 10:4178.
235. Yuan J, Wei B, Lipton MS, Gao H. 2012. Impact of ArcA loss in *Shewanella oneidensis* revealed by comparative proteomics under aerobic and anaerobic conditions. *PROTEOMICS* 12:1957–1969.

236. Wan F, Mao Y, Dong Y, Ju L, Wu G, Gao H. 2015. Impaired cell envelope resulting from *arcA* mutation largely accounts for enhanced sensitivity to hydrogen peroxide in *Shewanella oneidensis. Sci Rep* 5.
237. Imlay JA. 2019. Where in the world do bacteria experience oxidative stress? *Environ Microbiol* 21:521–530.
238. Knoefler D, Leichert LIO, Thamsen M, Cremers CM, Reichmann D, Gray MJ, Wholey W-Y, Jakob U. 2014. About the dangers, costs and benefits of living an aerobic lifestyle. *Biochem Soc Trans* 42:917–921.
239. Imlay JA. 2015. Transcription factors that defend bacteria against reactive oxygen species. *Annu Rev Microbiol* 69:93–108.
240. Imlay JA, Sethu R, Rohaun SK. 2019. Evolutionary adaptations that enable enzymes to tolerate oxidative stress. *Free Radic Biol Med* 140:4–13.
241. Diaz JM, Hansel CM, Voelker BM, Mendes CM, Andeer PF, Zhang T. 2013. Widespread Production of Extracellular Superoxide by Heterotrophic Bacteria. *Science* 340:1223–1226.
242. van Hoek MJ, Merks RM. 2012. Redox balance is key to explaining full vs. partial switching to low-yield metabolism. *BMC Syst Biol* 6:22.
243. Ezraty B, Gennaris A, Barras F, Collet J-F. 2017. Oxidative stress, protein damage and repair in bacteria. 7. *Nat Rev Microbiol* 15:385–396.
244. Loui C, Chang AC, Lu S. 2009. Role of the ArcAB two-component system in the resistance of *Escherichia coli* to reactive oxygen stress. *BMC Microbiol* 9:183.
245. Calderón IL, Morales E, Caro NJ, Chahúan CA, Collao B, Gil F, Villarreal JM, Ipinza F, Mora GC, Saavedra CP. 2011. Response regulator ArcA of *Salmonella enterica* serovar Typhimurium downregulates expression of OmpD, a porin facilitating uptake of hydrogen peroxide. *Res Microbiol* 162:214–222.
246. Pardo-Esté C, Hidalgo AA, Aguirre C, Briones AC, Cabezas CE, Castro-Severyn J, Fuentes JA, Opazo CM, Riedel CA, Otero C, Pacheco R, Valvano MA, Saavedra CP. 2018. The ArcAB two-component regulatory system promotes resistance to reactive oxygen species and systemic infection by *Salmonella* Typhimurium. *PLoS ONE* 13.
247. Winterbourn C. 1995. Toxicity of iron and hydrogen peroxide: the Fenton reaction. *Toxicol Lett* 82–83:969–974.
248. Li Z, Demple B. 1994. SoxS, an activator of superoxide stress genes in *Escherichia coli.* Purification and interaction with DNA. *J Biol Chem* 269:18371–18377.
249. Søballe B, Poole RK. 2000. Ubiquinone limits oxidative stress in *Escherichia coli. Microbiol Read Engl* 146 (Pt 4):787–796.
250. Messner KR, Imlay JA. 2002. Mechanism of Superoxide and Hydrogen Peroxide Formation by Fumarate Reductase, Succinate Dehydrogenase, and Aspartate Oxidase. *J Biol Chem* 277:42563–42571.
251. González-Flecha B, Demple B. 1995. Metabolic Sources of Hydrogen Peroxide in Aerobically Growing *Escherichia coli. J Biol Chem* 270:13681–13687.
252. Desai SK, Kenney LJ. 2017. To ~P or Not to ~P? Non-canonical activation by two-component response regulators. *Mol Microbiol* 103:203–213.
253. Colloms SD, Alén C, Sherratt DJ. 1998. The ArcA/ArcB two-component regulatory system of *Escherichia coli* is essential for Xer site-specific recombination at *psi. Mol Microbiol* 28:521–530.

254. Zhou Y, Pu Q, Chen J, Hao G, Gao R, Ali A, Hsiao A, Stock AM, Goulian M, Zhu J. 2021. Thiol-based functional mimicry of phosphorylation of the two-component system response regulator ArcA promotes pathogenesis in enteric pathogens. *Cell Rep* 37:110147.
255. Passalacqua KD, Charbonneau M-E, O'Riordan MXD. 2016. Bacterial Metabolism Shapes the Host-Pathogen Interface. *Microbiol Spectr* 4.
256. Reniere ML. 2018. Reduce, Induce, Thrive: Bacterial Redox Sensing during Pathogenesis. *J Bacteriol* 200.
257. Tiwari S, Jamal SB, Hassan SS, Carvalho PVSD, Almeida S, Barh D, Ghosh P, Silva A, Castro TLP, Azevedo V. 2017. Two-Component Signal Transduction Systems of Pathogenic Bacteria As Targets for Antimicrobial Therapy: An Overview. *Front Microbiol* 8.
258. Rajput A, Seif Y, Choudhary KS, Dalldorf C, Poudel S, Monk JM, Palsson BO. 2021. Pangenome Analytics Reveal Two-Component Systems as Conserved Targets in ESKAPEE Pathogens. *mSystems* 6.
259. Hirakawa H, Kurushima J, Hashimoto Y, Tomita H. 2020. Progress Overview of Bacterial Two-Component Regulatory Systems as Potential Targets for Antimicrobial Chemotherapy. *Antibiotics* 9.
260. Bachman MA, Breen P, Deornellas V, Mu Q, Zhao L, Wu W, Cavalcoli JD, Mobley HLT. 2015. Genome-Wide Identification of *Klebsiella pneumoniae* Fitness Genes during Lung Infection. *mBio* 6:e00775.
261. Jiang L, Feng L, Yang B, Zhang W, Wang P, Jiang X, Wang L. 2017. Signal transduction pathway mediated by the novel regulator LoiA for low oxygen tension induced Salmonella Typhimurium invasion. *PLoS Pathog* 13:e1006429.
262. Zhao X, Zeng X, Dai Q, Hou Y, Zhu D, Wang M, Jia R, Chen S, Liu M, Yang Q, Wu Y, Zhang S, Huang J, Ou X, Mao S, Gao Q, Zhang L, Liu Y, Yu Y, Cheng A. 2021. Immunogenicity and protection efficacy of a *Salmonella enterica* serovar Typhimurium *fnr, arcA* and *fliC* mutant. *Vaccine* 39:588-595.
263. Sengupta N, Paul K, Chowdhury R. 2003. The Global Regulator ArcA Modulates Expression of Virulence Factors in *Vibrio cholerae. Infect Immun* 71:5583–5589.
264. Xi D, Yang S, Liu Q, Li Y, Li Y, Yan J, Wang X, Ning K, Cao B. 2020. The response regulator ArcA enhances biofilm formation in the *vpsT* manner under the anaerobic condition in *Vibrio cholerae. Microb Pathog* 104197.
265. Buettner FFR, Maas A, Gerlach G-F. 2008. An *Actinobacillus pleuropneumoniae arcA* deletion mutant is attenuated and deficient in biofilm formation. *Vet Microbiol* 127:106–115.
266. Pittman RN. 2011. Chapter 4, Oxygen TransportRegulation of Tissue Oxygenation. Morgan & Claypool Life Sciences, San Rafael.
267. Smith SN, Hagan EC, Lane MC, Mobley HLT. 2010. Dissemination and Systemic Colonization of Uropathogenic *Escherichia coli* in a Murine Model of Bacteremia. *mBio* 1.
268. De Souza-Hart JA, Blackstock W, Di Modugno V, Holland IB, Kok M. 2003. Two-Component Systems in *Haemophilus influenzae:* a Regulatory Role for ArcA in Serum Resistance. *Infect Immun* 71:163–172.
269. Wang Z, Sun J, Xia T, Liu Y, Fu J, Lo YK, Chang C, Yan A, Liu X. 2018. Proteomic Delineation of the ArcA Regulon in *Salmonella* Typhimurium During Anaerobiosis. *Mol Cell Proteomics MCP* 17:1937–1947.

270. Fernández PA, Velásquez F, Garcias-Papayani H, Amaya FA, Ortega J, Gómez S, Santiviago CA, Álvarez SA. 2018. Fnr and ArcA Regulate Lipid A Hydroxylation in *Salmonella* Enteritidis by Controlling *lpxO* Expression in Response to Oxygen Availability. *Front Microbiol* 9:1220.

Chapter 2 The Role of ArcAB during Gram-Negative Bacteremia[3]

2.1 Summary

Gram-negative facultative anaerobes often cause bacteremia, a systemic infection associated with severe clinical outcomes. ArcAB, a two-component regulatory system that represses aerobic respiration, is a key mediator of metabolic adaptation for such bacteria. Using targeted mutational analysis informed by global genetic screens, we identified the *arcA* gene as promoting fitness of *Citrobacter freundii*, *Klebsiella pneumoniae*, and *Serratia marcescens* but not *Escherichia coli* in a murine model of bacteremia. *arcA* mutants exhibit a dysregulated response to changes in oxygen availability, iron limitation, and membrane perturbations, which bacterial cells experience during infection. The genetic response of the *arcA* mutants to the cationic antimicrobial peptide polymyxin B supports an expanded role for ArcA as an activator in response to membrane damage. ArcA function is linked to electron transport chain activity based on its response to proton motive force uncoupling by carbonyl cyanide-*m*-chlorophenylhydrazone (CCCP). Differences in lactate, acetate, and lactate dehydrogenase activity between *arcA* mutant and wild-type cells following CCCP treatment support an ArcA-mediated shift to fermentation independent of oxygen availability. This study highlights the semi-conserved role of ArcA during bacteremia and consolidates infection phenotypes into a comprehensive model based on respiratory activity.

[3]Components of this section are modified from the following publication:
Brown AN, Anderson MT, Smith SN, Bachman MA, Mobley HLT. Conserved Metabolic Regulator ArcA Responds to Oxygen Availability, Iron Limitation, and Cell Envelope Perturbations during Bacteremia. *mBio*. 2023. *Accepted*.

2.2 Introduction

Metabolic flexibility is an established characteristic of opportunistic bacteria and may be a prerequisite for transitioning between non-pathogenic and pathogenic environments. Facultatively anaerobic bacteria are capable of respiration and fermentation and are the most commonly isolated pathogens from Gram-negative bacteremia patients (1, 2). However, the factors dictating metabolic shifts throughout infection, including during colonization and dissemination, are poorly understood. *Citrobacter freundii*, *Escherichia coli*, *Klebsiella pneumoniae*, and *Serratia marcescens* cause many community and hospital-acquired cases of bacteremia (3). Sepsis, the single highest cause of in-hospital mortality in the United States, commonly results from bacteremia (4). *E. coli* and *K. pneumoniae* are the two most frequently isolated Gram-negative pathogens in sepsis cases while *C. freundii* and *S. marcescens* are emerging bacteremia pathogens of increasing concern (5–8). The long-term goal of this work is to advance our understanding of the metabolic and regulatory pathways that these bacteria employ within the host bloodstream.

Our group previously utilized *C. freundii*, *E. coli*, *K. pneumoniae*, and *S. marcescens* transposon mutant libraries and TnSeq to identify genes critical to bacteremia (9–12). Genes encoding pathways of central carbon metabolism were among the significant fitness genes shared between species. Understanding the regulation of such processes is critical for establishing comprehensive models of pathogenesis (13). The TnSeq results were compared to identify shared transcriptional regulators of central metabolism contributing to bacterial fitness. Interruption of genes encoding the two-component system ArcAB resulted in a significant loss of fitness for *C. freundii*, *K. pneumoniae*, and *S. marcescens* but not *E. coli*. The response regulator ArcA is a transcription factor (14) that regulates aerobic and anaerobic transitions in *E. coli* in

coordination with FNR, IHFA-B, CRP, and Fis (15). ArcA was the only such regulator from this group that was implicated in bacteremia fitness across *C. freundii*, *K. pneumoniae*, and *S. marcescens*. ArcA is already known to be employed by *Haemophilus influenzae* and *Salmonella enterica* in systemic infections (16, 17). The most well-studied function of ArcA is repression of aerobic respiration pathways, including the citric acid cycle. Global regulation of metabolism by ArcA is critical for balancing catabolic efficiency (energy production) with fueling anabolism (biomass growth) (18–20). ArcA and its cognate sensor kinase ArcB function in conditions where oxygen utilization decreases (21) and in response to reactive oxygen species (22). Global regulators integrate multiple stimuli for metabolic reprogramming (19, 23), and several signals in the infection environment likely impact ArcA activity. Here, the role of ArcA in repressing respiration in the mammalian bloodstream is examined.

2.3 Conservation of ArcAB across Order Enterobacterales

ArcA conservation was assessed across Order *Enterobacterales* by mapping protein sequences with Consurf (24) to an Alpha Fold-predicted structure of ArcA (25, 26). 419 ArcA amino acids sequences (**Supplemental Table 8**) from 418 species across 8 families were identified in total (**Fig. 2.1A**) with 150 unique sequences remaining after identical sequence removal. Conservation analysis based on ArcA structure and sequence phylogeny calculated an average pairwise distance of 0.07, meaning approximately 7% of residues differ between any two ArcA sequences. On a scale of 1 to 9, the average conservation level of the 238 residues was 7.7, and more than 75% of residues scored in the "conserved" range of 6 to 9 (**Fig. S2.9**). The N-terminal receiver domain of ArcA was very well conserved including the 54th residue aspartate phosphorylated by ArcB (27) (**Fig. 2.1B)**. In contrast, the linker domain directly following the receiver domain was one of the least conserved regions. The C-terminal winged helix-turn-helix

(wHTH) DNA-binding domain α1-β1-α2-turn-α3-β2-β3 is broadly maintained in this model of ArcA (28, 29). The α3 helix binds the major groove of DNA while the "β2-β3 wing" binds the minor groove. The α1 and α2 helices bind to the DNA backbone as a hydrophobic core to provide structural support while the "turn" or "loop" of the HTH interacts with RNA polymerase (30). These structures are all widely conserved in the ArcA model presented here in agreement with characterization of other OmpR-like regulators (28). Such OmpR-like wHTH regulators are characterized by an antiparallel β-sheet on the N-terminal side of the binding domain that likely

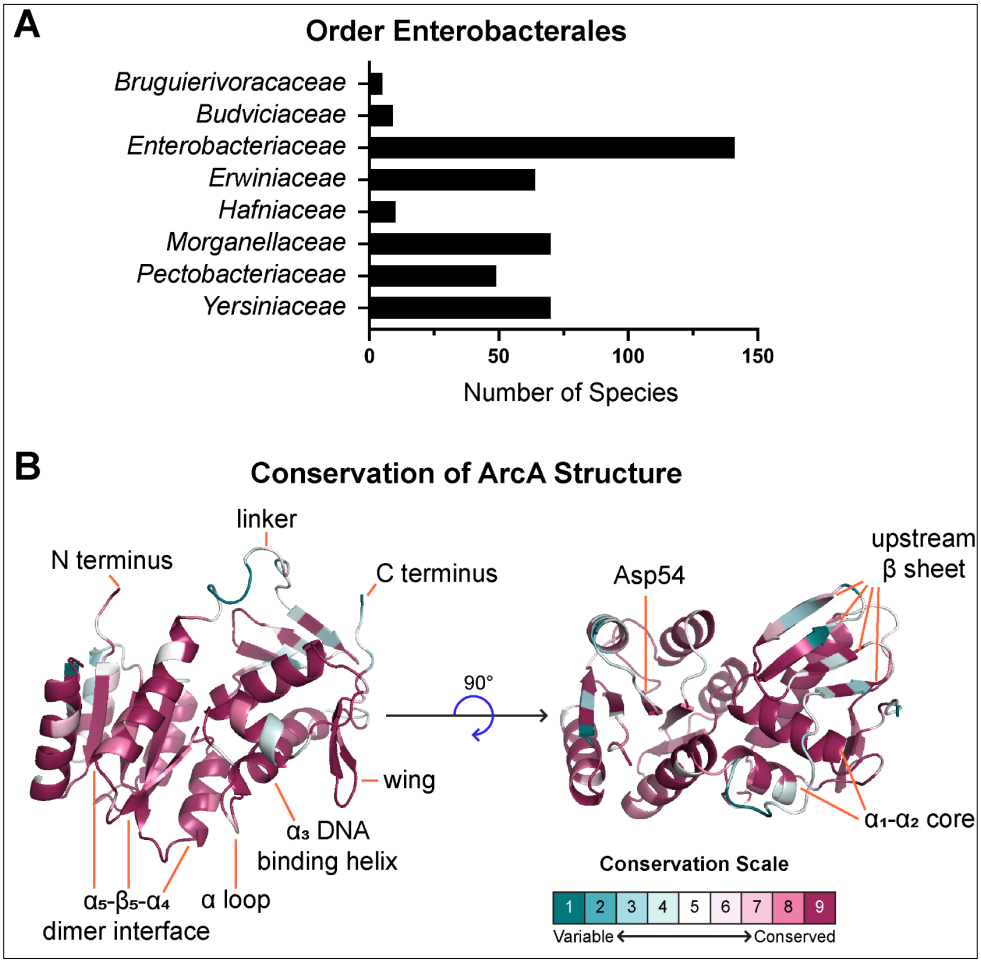

Figure 2.1: ArcA is structurally conserved across Order Enterobacterales. (A) 419 ArcA amino acid sequences of 418 species across 8 families in Order Enterobacterales were identified with BV-BRC and aligned (**File S1**). **(B)** The multi-sequence alignment was mapped onto a structure of ArcA with Consurf and visualized with pyMOL. The average grade of conservation for 238 residues on a scale of 1 to 9 was 7.7. The regions with the greatest variation in conservation are the linker domain and the N-terminal β sheet of the DNA binding domain. ArcB activates ArcA via phosphorylation of Asp^{54} which is highly conserved among the species examined in addition to the DNA binding helix and structures supporting it. Conservation of individual residues are visualized in **Fig. S2.9**.

determines binding specificity (28), and lower conservation of the β-sheet here suggests potential species-based differences in DNA binding capabilities. In concordance with the larger sequence comparison, ArcA homology in clinical strains of *C. freundii*, *E. coli*, *K. pneumoniae*, and *S. marcescens* ranged from 93.70% to 99.58% amino acid identity **(Fig. S2.10)** (31). Structural conservation coupled with the previous genetic screens prompted investigation of a shared role for ArcA during bloodstream infections.

2.4 Validation of *arcA* encoding a fitness factor in murine model of bacteremia

Competition experiments between wild-type strains and *arcA* mutant constructs **(Supplemental Table 7)** were conducted in a murine bacteremia model to assess how ArcA contributes to bacterial survival and replication, collectively referred to as fitness. Each species colonized the liver and spleen 24-hours post inoculation **(Fig. 2.2A).** *S. marcescens* is the only species to reliably colonize kidneys based on our previous findings (32) and achieved high bacterial burdens again here. A significant *arcA*-dependent fitness defect was observed in the liver and spleen for *C. freundii*, *K. pneumoniae*, and *S. marcescens* (**Fig. 2.2B)**. The largest fitness defect for *C. freundii* and *K. pneumoniae* was in the liver where *arcA* mutants were outcompeted 6.0-fold and 99.4-fold, respectively. The *S. marcescens arcA* mutant was most outcompeted in the kidneys (33.7-fold), indicating the link between ArcA and fitness in this model is organ-and species-specific. These results validate our previous TnSeq findings identifying fitness potential of ArcA among a substantial pool of transposon mutants (10–12). No significant fitness defect was observed for the *E. coli arcA* mutant in the spleen or the liver, a notable contrast to the other species. This finding is corroborated by earlier studies in which an *E. coli arcA* transposon mutant was not associated with a significant fitness defect in spleens (9, 33). Thus, although the ArcA sequence analysis demonstrates a high level of conservation, the

fundamental contribution of *E. coli* ArcA to bacterial fitness during infection differs substantially from the other species. We therefore chose to explore *in vitro* how ArcA contributes to fitness during bacteremia in *C. freundii, K. pneumoniae,* and *S. marcescens*.

Table 3: Strains and Constructs Used in Chapter 2

Species	Parent Strain	Genotype	Description	Reference
C. freundii	UMH14	wild-type strain		Anderson 2018 (11)
C. freundii	UMH14	Δ*arcA*	Δ*arcA*::*nptII* knock-out construct	This study
C. freundii	UMH14	Δ*arcA*::*arcA*	chromosomally complemented construct	This study
E. coli	CFT073	wild-type strain		Welch 2002 (34), Mobley 1990 (35)
E. coli	CFT073	Δ*arcA*	Δ*arcA*::*nptII* knock-out construct	This study
K. pneumoniae	KPPR1	wild-type		Broberg 2014 (36)
K. pneumoniae	KPPR1	Δ*arcA*	Δ*arcA*::*nptII* knock-out construct	This study
K. pneumoniae	KPPR1	Δ*arcA* + pBBR1MCS-5	*arcA* knock-out construct with empty vector pBBR1MCS-5	This study
K. pneumoniae	KPPR1	Δ*arcA* + pBBR1MCS-5+*arcA*	Δ*arcA*::*nptII* knock-out construct complemented with pBBR1MCS-5 + *arcA* gene	This study
S. marcescens	UMH9	wild-type construct		Anderson 2017 (10)
S. marcescens	UMH9	Δ*arcA*	Δ*arcA*::*nptII* knock-out construct	This study
S. marcescens	UMH9	Δ*arcA::arcA*	chromosomally complemented construct	This study

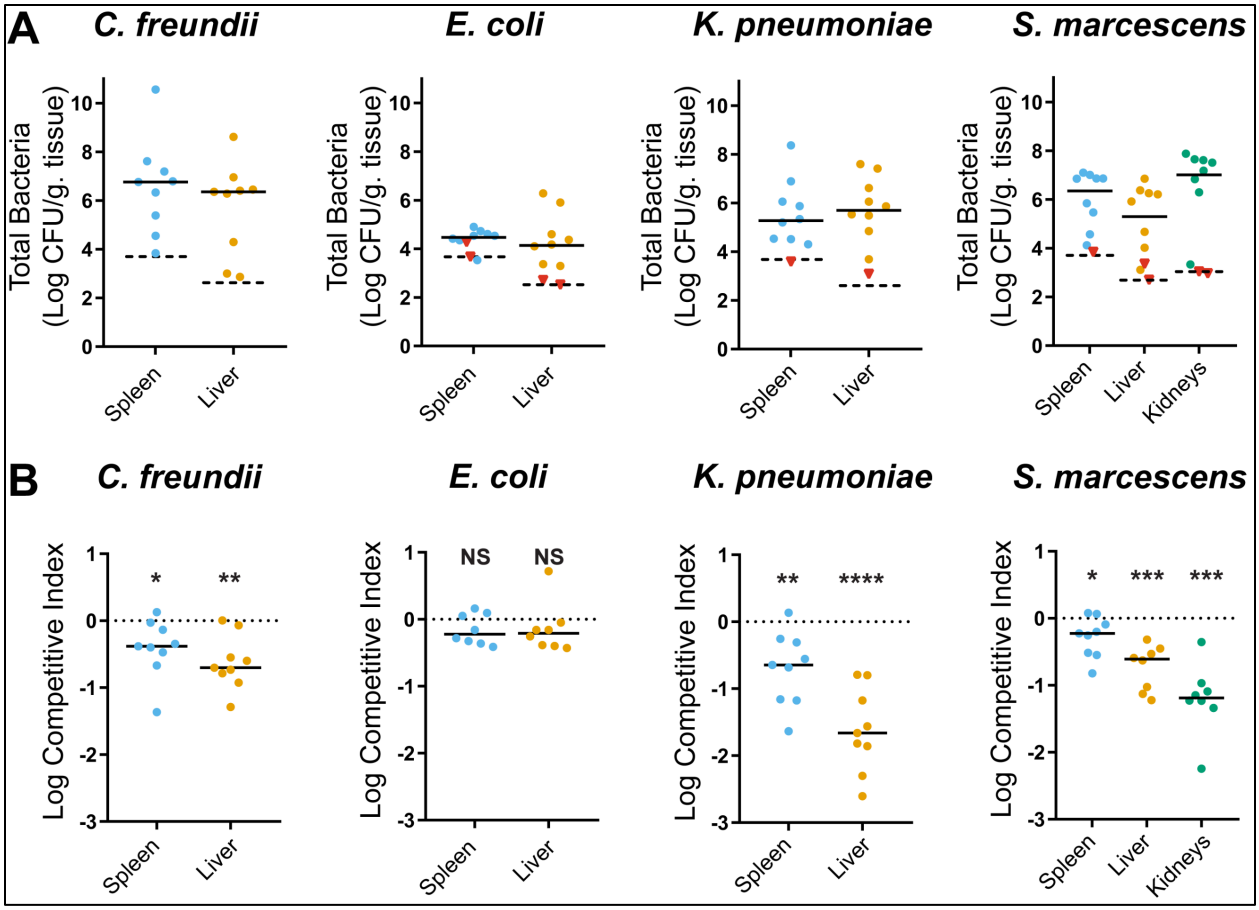

Figure 2.2: *arcA* encodes a fitness factor in a murine model of bacteremia. Wild-type (WT) strains and Δ*arcA* mutant constructs were cultured to mid-log phase in LB. Cells were washed in PBS and mixed 1:1 to prepare the inoculum for each species at an average target total CFU of 1 x 10^8 *(C. freundii*), 1 x 10^5 (*K. pneumoniae*), 1 x 10^7 (*Serratia marcescens*), and 2 x 10^6 (*E. coli*). Mice were sacrificed 24 hours post tail vein inoculation, and organs were harvested and plated on LB with and without antibiotics for differential CFU enumeration. **(A)** Total CFU were normalized to tissue weight for all organs. The limit of detection is denoted as a dashed black line, and red triangles are samples not included in calculating competitive indices due to limited CFU recovery. **(B)** Competitive indices (CI) were calculated by dividing the ratio of *arcA* mutant counts to WT counts in the inoculum (input) to that in the organs (output). Dots in the burden and CI graphs represents the organ from one mouse, and median values are presented as solid horizontal lines. Significance of log transformed CI was determined via a one-sample *t*-test with a null hypothetical value of zero, represented as a dotted a line. *p*-values: *≤0.05, **≤0.01, ***≤0.001, NS = not significant

2.5 *In vitro* growth of *arcA* mutants

In model species, the ArcB kinase is a sensor of anaerobiosis and activates ArcA via phosphorylation under such conditions. *arcA* mutant cells were thus hypothesized to exhibit growth defects in the absence of oxygen. As described in Chapter 1, growth defects associated with *arcA E. coli* mutants vary greatly and are highly dependent on experimental set-up. Wild-

type strains, *arcA* mutant constructs, and genetically complemented constructs or revertants were cultured anaerobically to study how ArcA influences bacterial replication across species (**Fig. 2.3A**). The difference in generation times between wild-type and *arcA* mutant constructs was

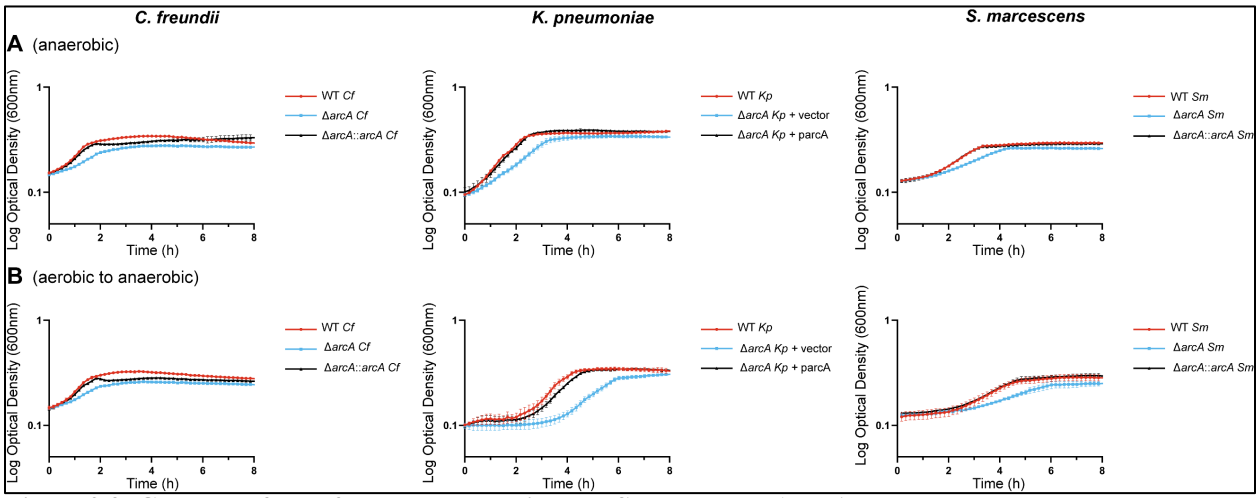

Figure 2.3: Growth defects of the *K. pneumoniae* and *S. marcescens* Δ*arcA* mutants are more pronounced during the aerobic to anaerobic transition. Wild-type strains and derivatives were cultured overnight in LB under **(A)** anaerobic or **(B)** aerobic conditions and then normalized based on OD_{600}. Fresh LB was inoculated with normalized overnight cultures in an anaerobic chamber. OD_{600} was then measured with a plate reader every 10 minutes. The graphs presented here are representative of three independent experiments. Each culture was grown in triplicate, and the average with standard deviation was plotted over time.

significant for *C. freundii* (73.5 *vs* 127.1 min.) and *S. marcescens* (113.0 *vs* 173.0 min.) but more modest for *K. pneumoniae* (59.6 *vs* 90.0 min.) **(Table 4)**. As opposed to simply responding to anaerobic conditions, ArcB more accurately senses a decrease in oxygen consumption within the cell (21). To induce a reduction in oxygen utilization, cells were cultured aerobically overnight and transferred to a strict anaerobic environment before subculturing (**Fig. 2.3B**). Shifted growth curves from this condition revealed a more substantial delay in the growth of the *K. pneumoniae* and *S. marcescens arcA* mutants compared to the wild-type strains. The *C. freundii*, *K. pneumoniae* and *S. marcescens arcA* mutant constructs had 57.5, 22.0, and 72.3 min. longer doubling time relative to the respective wild-type strains after transition from aerobic to anaerobic conditions (**Table 5**). The average doubling time following this transition was very similar to the strict anaerobic condition for the *C. freundii* and *K. pneumoniae* groups. These

values were considerably longer for *S. marcescens* cells, but the wild-type strain continued to grow faster than the *arcA* mutant construct. Differences in lag time, or the time to reach maximum growth rate, were also calculated (Δ_{LT}) as a metric of the ability of the cells to optimize growth performance (**Table 4**). The Δ_{LT} values for *C. freundii* and *K. pneumoniae* were greater in the anaerobic condition, indicating the *arcA* mutant took longer to reach its maximum growth rate relative to the wild-type strain. In contrast, the Δ_{LT} was 29.4 min. longer in the aerobic to anaerobic transition between the *S. marcescens* wild-type strain and *arcA* mutant construct in comparison to the anaerobic condition.

Replication of *arcA* mutants was also measured in M9 medium supplemented with glucose and casamino acids to determine if a carbohydrate carbon source alters *arcA*-dependance. The *C. freundii arcA* mutant exhibited a severe growth defect in the presence of glucose for anaerobic culture and aerobic to anaerobic transition culture (**Fig. S2.11**), for which both phenotypes were more pronounced than in LB medium (**Fig. 2.3**). Growth defects of the *K. pneumoniae arcA* mutant on the other hand were very similar in glucose-containing medium (**Fig. S2.11)** to those observed in LB (**Fig. 2.3**). In the presence of glucose, all three *S. marcescens* cultures displayed a biphasic growth pattern, with the *arcA* mutant displaying the largest growth defect when bacteria were shifted from aerobic to anaerobic conditions (**Fig. S2.11**). Overall, the presence of glucose as an available carbon source did not diminish the overall contribution of *arcA* in these three species and indeed exacerbated *arcA*-dependent replication defects for *C. freundii* and *S. marcescens*. The *in vitro* growth kinetics of *arcA* mutants determined here may in part provide a basis for the observed competitive disadvantage of *arcA* mutants during infection, considering that both peptide and monosaccharide carbon sources are likely abundant in the host. Furthermore, limited oxygen availability during infection

likely plays an important role in how ArcA modulates metabolism of these three species in the bloodstream and tissue environments. Given the complexity of the infection environment, the potential for ArcA to integrate other relevant signals was investigated.

Genotype	Anaerobic	Aerobic → Anaerobic
C. freundii		
WT	73.5 ± 5.7	72.0 ± 0.7
Δ*arcA*	127.1 ± 7.3	129.5 ± 9.8
Δ*arcA*::*arcA*	80.8 ± 1.2	80.3 ± 2.8
S. marcescens		
WT	59.6 ± 2.9	65.1 ± 4.0
Δ*arcA* + pBBR1MCS-5	90.0 ± 4.6	87.0 ± 3.9
Δ*arcA* + pBBR1MCS-5+*arcA*	67.8 ± 5.9	73.2 ± 6.8
K. pneumoniae		
WT	113.0 ± 2.7	135.6 ± 16.2
Δ*arcA*	173.0 ± 7.7	207.9 ± 34.0
Δ*arcA*::*arcA*	111.0 ± 6.9	134.7 ± 4.4

Table 4: Doubling times in LB medium (min.)

Table 5: Difference in lag times (wild-type strain *vs. arcA* mutants) in LB medium (min.)

Species	Anaerobic	Aerobic → Anaerobic
C. freundii	26.8 ± 5.8	10.0 ± 8.2
K. pneumoniae	83.6 ± 8.2	70.2 ± 8.2
S. marcescens	36.8 ± 20.9	60.2 ± 25.9

2.6 Growth in iron-limited medium

Iron is a critical cofactor for many respiratory enzymes including succinate dehydrogenase and NADH:ubiquinone oxidoreductase. These electron transport chain complexes require iron-sulfur clusters (37) and are transcriptionally repressed by ArcA (18, 19). We hypothesized ArcA would reprogram metabolism during iron limitation to suppress respiratory activity. This regulation would be important in the host where most iron is bound to hemoglobin and sequestered away from invading pathogens by iron-chelating proteins such as ferritin and transferrin (38, 39). Compared to untreated cultures **(Fig. 2.4A)**, *arcA* mutants grew more slowly than isogenic wild-type strains when cultured aerobically in LB supplemented with the non-utilizable iron chelator 2-2'-dipyridyl **(Fig. 2.4B)**. Addition of DMSO alone to LB did not impact culture growth (data not shown). *C. freundii* culture growth resembled a multiple-

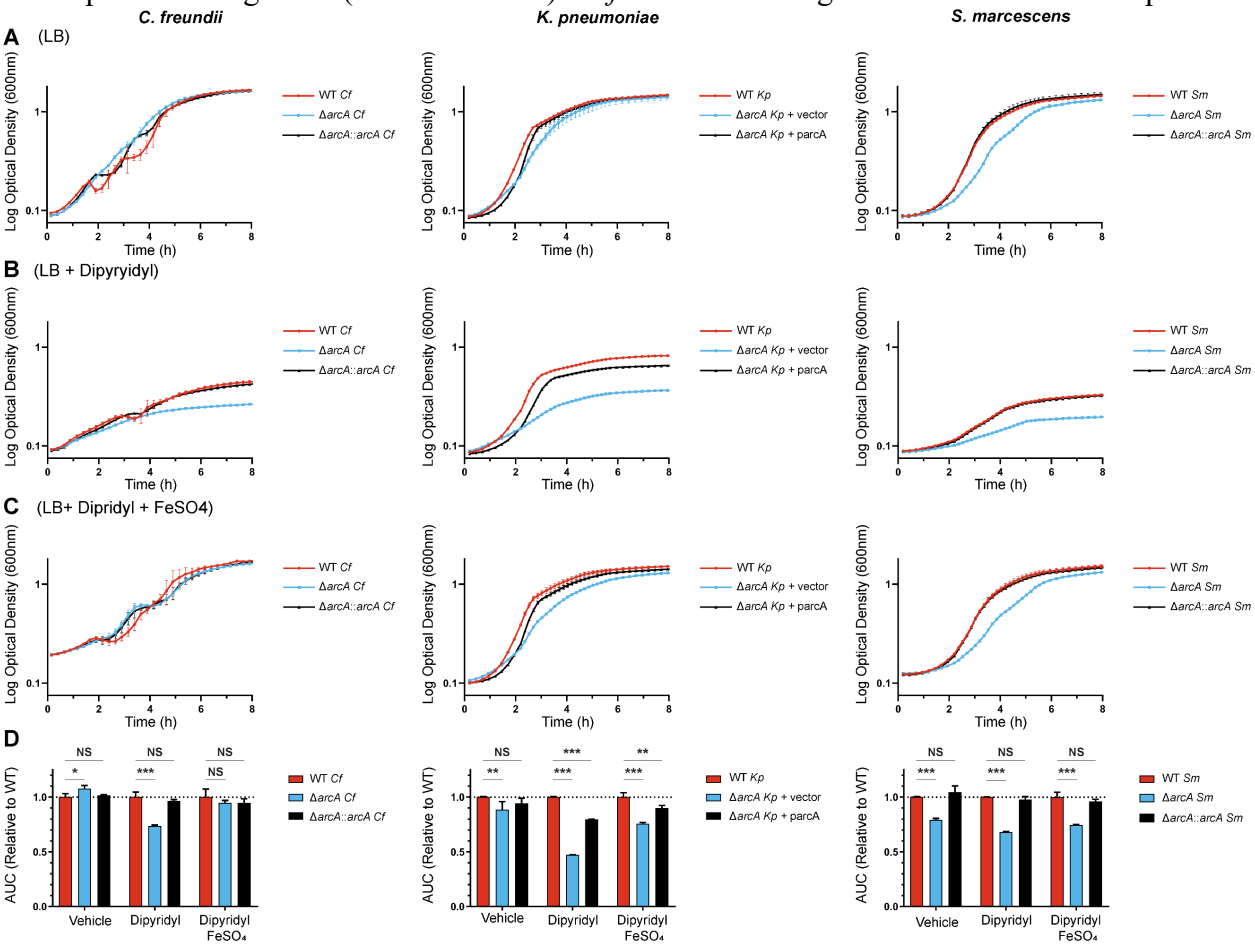

Figure 2.4: ArcA optimizes growth in an iron-limited medium under aerobic conditions. Overnight cultures incubated aerobically in LB were inoculated into fresh LB containing **(A)** DMSO, **(B)** dipyridyl, or **(C)** dipyridyl supplemented with $FeSO_4$. Cultures were incubated at 37°C in aerobic conditions and growth was tracked via OD_{600} by a plate reader every 15 minutes. Growth curves are the average of technical triplicates with standard deviation and are representative of three independent experiments. **(D)** Growth was assessed by calculating area under the curve (AUC) and comparing this value to the AUC of the wild-type in each condition. Bars represent the average of the technical triplicates of the representative growth curves with standard deviation. Significance was determined by comparing the wild-type strain with the mutant and complemented derivatives with Dunnett's multiple comparisons test. *p*-values: *≤0.05, **≤0.01, ***≤0.001, NS = not significant

phase growth pattern, which is due to a previously observed clumping phenomenon during exponential phase growth referred to as flocculation (also observable in **Supplementary Figure 2.13**). Density at stationary phase was considerably lower in the *arcA* mutant cultures than wild-type cultures for all species, which differs from the results of the previous anaerobic experiments where mutant cultures routinely reached the density of the wild-type cells despite any slower growth rates or extended lag periods. The phenotype also demonstrates a requirement for ArcA in the presence of oxygen. In all cases, growth kinetics of the three tested species returned to untreated conditions following supplementation of excess iron to dipyridyl-containing cultures (**Fig. 2.4C**). The requirement for ArcA in iron-limited environments is further supported by measuring total growth potential of each species via area under the curve **(Fig. 2.4D)**. These results ultimately provide an example in which ArcA contributes to growth optimization in response to host-mediated micronutrient limitation.

2.7 Susceptibility to human serum

The cell envelope provides the structural barrier necessary to maintain proton motive force from the electron transport chain during respiration. Through quinones, the electron transport chain impacts the kinase activity of ArcB (40, 41). ArcA regulates genes whose products maintain the cell envelope in coordination with other regulators such as σ_E (19, 42–44). The bactericidal effects of serum largely target the bacterial envelope (45), and I therefore investigated the role of ArcA in resisting this infection-relevant envelope stress. The viability of

wild-type and *arcA* mutants was quantified in the presence of pooled normal and heat-inactivated human serum. The *C. freundii arcA* mutant was 37.7-fold more susceptible to killing by intact serum relative to the wild-type strain (**Fig. 2.5A**). This phenotype was partially rescued in the Δ*arcA*::*arcA* revertant. In contrast, the *C. freundii* wild-type strain and derivatives grew in culture with heat-inactivated serum, but the *arcA* mutant did not grow as robustly. Neither the *K. pneumoniae* wild-type strain nor the mutant construct exhibited reduced viability when cultured with 90% human serum, which demonstrated a high level of serum resistance for this species (**Fig. 2.5B**). The wild-type and complemented *arcA* strain *K. pneumoniae* grew to similar levels in heat-inactivated serum while the *arcA* mutant showed a significantly reduced ability to replicate in serum. This observation was unexpected and may be due to disruption of heat-labile nutrients that *K. pneumoniae* utilizes in an ArcA-dependent manner. Serum-mediated cell death was observed in the *S. marcescens* cultures where the *arcA* mutant experienced 16.7 times more killing relative to the wild-type strain (**Fig. 2.5C**). The *S. marcescens* wild-type strain and derivatives cultured in the heat-inactivated serum experienced net growth rather than killing to similar levels as the *C. freundii* group. The wild-type *C. freundii* and *S. marcescens* cultures reached 3.9-fold and 3.2-fold higher CFU/mL levels over the 90 minute incubation in heat-inactivated serum while the *arcA* mutant cultures grew 2.7- and 2.3-fold, respectively. Longer incubations in the inactivated serum may reveal growth defects for the *C. freundii* and *S. marcescens arcA* mutants like the *K. pneumoniae* construct relative to their isogenic wild-type strains. Disparities in growth between mutant and wild-type strains in heat-inactivated serum suggests that nutrient limitation or another serum-specific growth condition likely contributes to these results. Nevertheless, ArcA influences complement resistance for *C. freundii* and *S.*

marcescens, demonstrating the connection of this response regulator to membrane integrity.

2.8 Response to polymyxin B

The host innate immune response includes cationic antimicrobial peptides (CAMPs) which permeabilize Gram-negative bacterial cell membranes (46). The model CAMP polymyxin B (PMB) was used to test if ArcA responds to CAMP-mediated cell membrane damage (47, 48). PMB treatment of mid-exponential phase cells demonstrated that *arcA* mutants of all three species were significantly more susceptible to killing than isogenic wild-type strains and complemented and revertant constructs **(Fig. 2.6A)**. Survival rates were 44-, 138-, and 76-fold higher in the wild-type strains relative to the *arcA* mutant constructs of *C. freundii*, *K. pneumoniae*, and *S. marcescens*, respectively. These results are especially notable for *K. pneumoniae* given the lack of *arcA*-dependent serum resistance (**Fig. 2.5B**) and imply ArcA also responds to *K. pneumoniae* membrane perturbation. Together, these data support previous findings that ArcA regulation is important for cellular processes supporting envelope health. To investigate further, an ArcA-specific genetic response to PMB was interrogated.

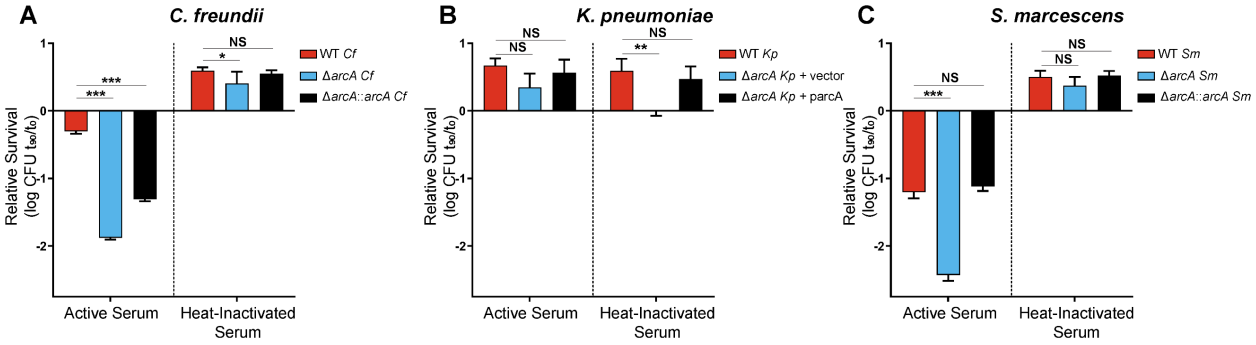

Figure 2.5: ArcA is required for serum resistance of *C. freundii* and *S. marcescens*. Overnight cultures incubated in LB medium were sub-cultured into LB medium and incubated aerobically until mid-log phase. Cells were normalized and resuspended in normal and heat-inactivated human serum to a final concentration of approximately 2 x 10^8 CFU/mL. Cultures were then incubated at 37°C for 90 minutes with sampling before and after incubation for CFU enumeration. Each species was treated with an empirically determined concentration of human serum at the following final concentrations: **(A)** *C. freundii*: 10%; **(B)** *K. pneumoniae*: 90%; **(C)** *S. marcescens*: 40%. Average values of technical triplicates with standard deviation are presented on each graph and are representative of three independent experiments. Significance was determined by comparing the wild-type strain with the mutant and complemented constructs with Dunnett's multiple comparisons test. *p*-values: *≤0.05, **≤0.01, ***≤0.001, NS = not significant

The genes differentially expressed by *K. pneumoniae* in response to polymyxin B have been previously identified via RNA-seq (49), and I hypothesized that a subset of these genes are regulated by ArcA. To explore this, the *K. pneumoniae* dataset was compared to the genes and operons directly controlled by ArcA in *E. coli* under anaerobic conditions (18). A list was generated of candidate genetic elements controlled by ArcA in response to PMB. After removal of genes with less than 80% shared amino acid identity between *E. coli* CFT073 and *K. pneumoniae* KPPR1, *acs*, *astC*, *fadE, feoB, lldP, putP,* and *ugpB* were selected for expression studies. qRT-PCR was used to measure gene expression of these targets in mid-exponential *K.*

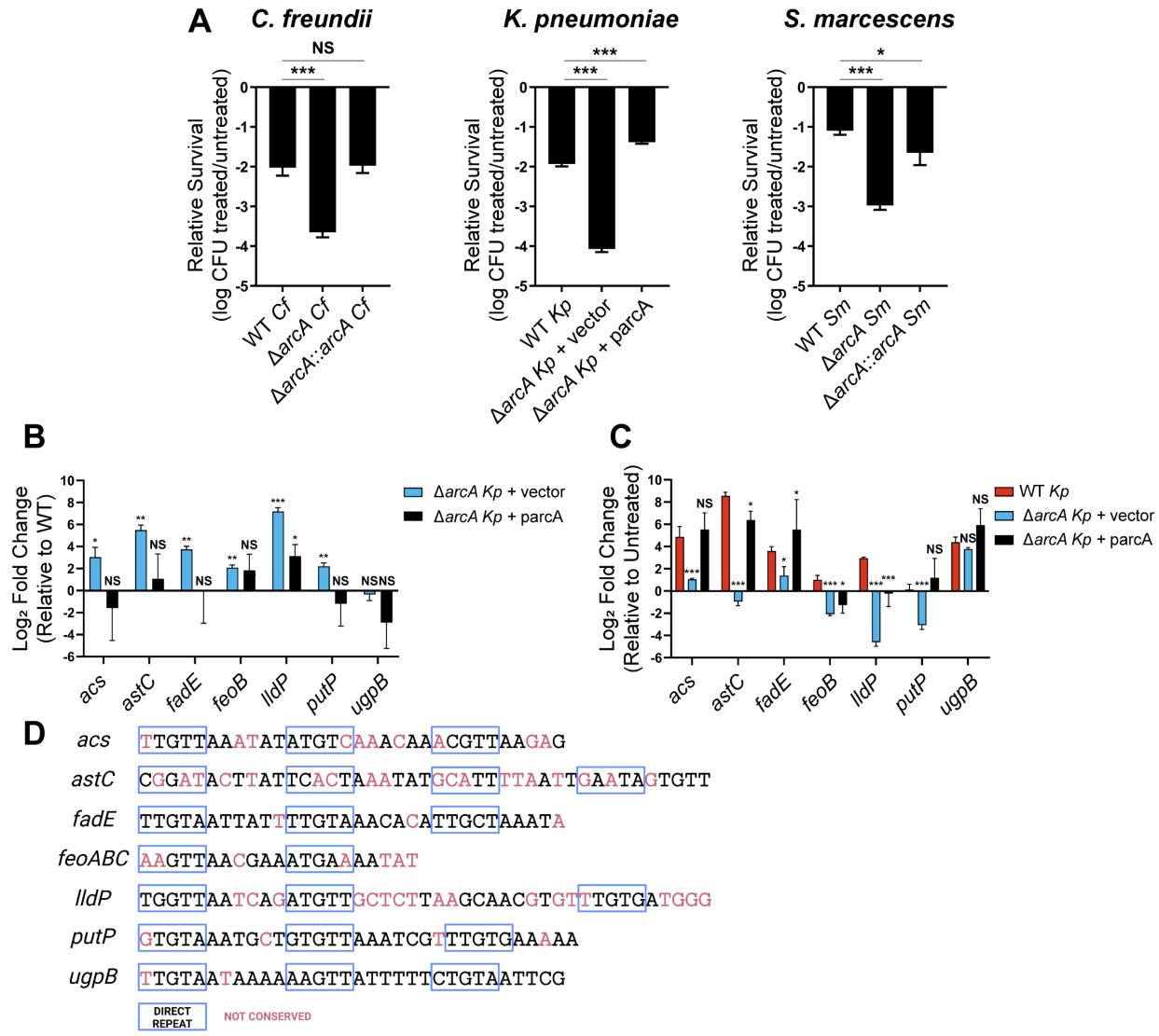

Figure 2.6: ArcA is involved in the polymyxin B response. (A) Overnight cultures grown in LB medium were sub-cultured into LB medium and incubated aerobically to mid-log phase. Cultures were normalized to an OD_{600} 0.2 and treated with polymyxin B for one hour at 37°C. Survival was assessed relative to untreated cultures, and the log transformed data are presented as an average of technical triplicates. Each graph is representative of three independent experiments. Significance was determined by comparing the wild-type strain with the mutant and complemented constructs with Dunnett's multiple comparisons test. **(B-C)** To measure expression of candidate ArcA-regulated genes in the *K. pneumoniae* wild-type strain and derivatives, mid-log phase cells grown in LB were normalized to approximately 2 x 10^8 CFU/mL in PBS. Cells were treated with 5μg/mL polymyxin B for 15 minutes followed by RNA extraction. RT-qPCR was performed to assess expression of *acs, astC, fade, feoB, lldP, ugpB* with *gap* serving as the housekeeping gene. Results are displayed as $\log_2$ fold change and are the average of 3 biological replicates with standard deviation. **(B)** In untreated conditions, expression of each gene by the mutant and complemented strains was compared to that of the wild-type strain following normalizing of Ct values to *gap* and log transformation. Significance was determined via a one-sample *t*-test with a null hypothetical value of zero. **C)** Expression of each gene was then compared between untreated and polymyxin B conditions for each genotype**.** Significance was determined by comparing the wild-type strain with the mutant and complemented constructs with Dunnett's multiple comparisons test. **(D)** FIMO was utilized to search for ArcA binding boxes from *E. coli* K-12 MG1255 (18) in the promoter regions of the seven genes evaluated in the expression studies. Sequences that had a *p*-value and *q*-value at or below 0.05 were considered significant. In the promoters of 6/7 *K. pneumoniae* genes, a putative ArcA binding sequence was identified. Underlined, red nucleotides were loci not conserved between *E. coli* and *K. pneumoniae* sequences. Direct repeats within sequences were labeled based on coordinates of direct repeats within corresponding promoters of *E. coli* genes and are denoted by blue boxes. *p*-values: *≤0.05, **≤0.01, ***≤0.001, NS = not significant

pneumoniae cells following sublethal treatment with PMB. In untreated control conditions, every gene except *ugpB* was more highly expressed in the *arcA* mutant relative to the wild-type strain (**Fig. 2.6B**). This result matches *E. coli* studies in which ArcA serves as a repressor for all of these genes except *feoB* under strict anaerobic conditions (18, 19). In all cases, genetic complementation reduced transcript levels compared to the *arcA* mutant. In the PMB treatment condition, *acs*, *astC*, *fadE, feoB, lldP*, and *ugpB* were upregulated 2.0-fold to more than 375-fold relative to untreated conditions in the wild-type cells **(Fig. 2.6C)**. *putP* exhibited minimal induction in response to PMB. The complemented construct yielded largely similar results to the wild-type strain excluding *feoB* and *lldP* for which intermediate phenotypes were noted. *acs* (1.9-fold) and *fadE* (6.4-fold) were also upregulated in *arcA* mutant cells, but these levels were significantly lower compared to wild-type. In contrast to wild-type, the following genes were downregulated in the *arcA* mutant following polymyxin B exposure: *astC* (2.6-fold), *feoB* (4.7-fold), *lldP* (24.9-fold), and *putP* (9.8-fold). In summary, six out of the seven genes were suppressed by ArcA in untreated conditions while ArcA served as an activator or mediator of de-

repression of the same genes in response to PMB-induced stress.

Promoters of the *K. pneumoniae* PMB-induced transcripts were analyzed to search for ArcA binding sites based on previously reported *E. coli* sites (18). A motif identification tool was used to identify putative binding sites in the homologous promoter regions of *K. pneumoniae*. Potential ArcA binding sequences were identified for six of the seven *K. pneumoniae* genes (**Fig. 2.6D**). A candidate upstream binding site was identified for *ugpB* but not *astC* despite the latter being differentially expressed in an ArcA-dependent manner in response to polymyxin B. Coordinates of the direct repeats bound by ArcA in the *E. coli* sequences were mapped onto the *K. pneumoniae* sequences. Most of the nucleotide differences between the *E. coli* and *K. pneumoniae* sequences were outside of the direct repeats, suggesting a pressure for conservation of these motifs. Putative ArcA binding sites were also readily identifiable for many of the same *C. freundii* and *S. marcescens* genes (**Fig. S4**). The PMB survival assay, expression data, and putative ArcA binding sites all provide evidence for a direct role of ArcA in responding to CAMPs, further highlighting its function during infection.

2.9 Adaptation to perturbations of the electron transport chain

Cell envelope damage can compromise maintenance of a proton gradient across the inner membrane by the electron transport chain (ETC). When a proton motive force (PMF) cannot be maintained, ATP production via chemiosmosis is not possible, and cells must rely on metabolic pathways independent of the ETC for energy production. The ability to switch to such processes following membrane damage likely requires metabolic regulators such as ArcA to repress respiratory complexes and pathways feeding the ETC (18, 50). Carbonylcyanide-*m*-chlorophenylhydrazone (CCCP) is a PMF uncoupler and was utilized to test the role of ArcA in optimizing growth following inhibition of aerobic respiration. Cells were cultured aerobically in

a minimal medium containing glucose with and without CCCP to test the hypothesis that ArcA activity supports growth when chemiosmosis is not possible despite the availability of electron donors and a terminal electron acceptor. The wild-type and *arcA* mutants of *K. pneumoniae and S. marcescens* grew nearly identically to their isogenic wild-type strains in an untreated minimal medium supplemented with glucose whereas the *C. freundii arcA* mutant experienced a relatively minor lag **(Fig. 2.7A**). Following CCCP treatment, *C. freundii*, *K. pneumoniae*, and *S. marcescens arcA* mutants had longer lag times of 8.0 h., 4.2 h., and 8.3 h relative to wild-type strains, respectively **(Fig. 2.7B)**. These delays in growth are mirrored by longer doubling times of the *C. freundii* (25.2 min.), *K. pneumoniae* (32.1 min.), and *S. marcescens* (18.7 min.) *arcA* mutants relative to the wild-type strains. The growth defects overall support a role of ArcA in optimizing growth in the presence of CCCP for all three species.

Growth in CCCP theoretically requires an ETC-independent mechanism for ATP production, such as fermentation. ArcA mediates the transition to fermentation, and *E. coli arcA* mutants excrete a different profile of fermentative products as compared to wild-type cells under microaerobic and anaerobic conditions (51–53). The *arcA* mutant bacteria described in this study were hypothesized to experience the same defects in mixed acid fermentative processes following PMF uncoupling (54–57). Acetate and lactate were quantified by HPLC in the supernatant of untreated and CCCP-treated cultures as metrics of fermentation (**Fig. S2.12-13**). Acetate levels decreased in wild-type *C. freundii* 6.2-fold but were 1.5 times higher in the *arcA* mutant relative to untreated conditions (**Fig. 2.7C**). In the *K. pneumoniae* and *S. marcescens* wild-type strains and *arcA* mutants, acetate levels were 1.4 to 2.2-fold higher in CCCP-treated

conditions (**Fig. 2.7C**). Lactate increased 20.7-fold in the wild-type *C. freundii* in CCCP but did not change in the *arcA* mutant (**Fig. 2.7D**). Almost no differences in excreted lactate were observed between the untreated and CCCP cultures of wild-type *K. pneumoniae* and *S. marcescens* (**Fig. 2.7D**). In *E. coli arcA* mutant cultures, supernatant acetate levels stay the same or decrease whereas lactate levels increase (52, 53, 58). Fermentation induced by CCCP or an absence of oxygen may favor production of different fermentative end-products, and ArcA-

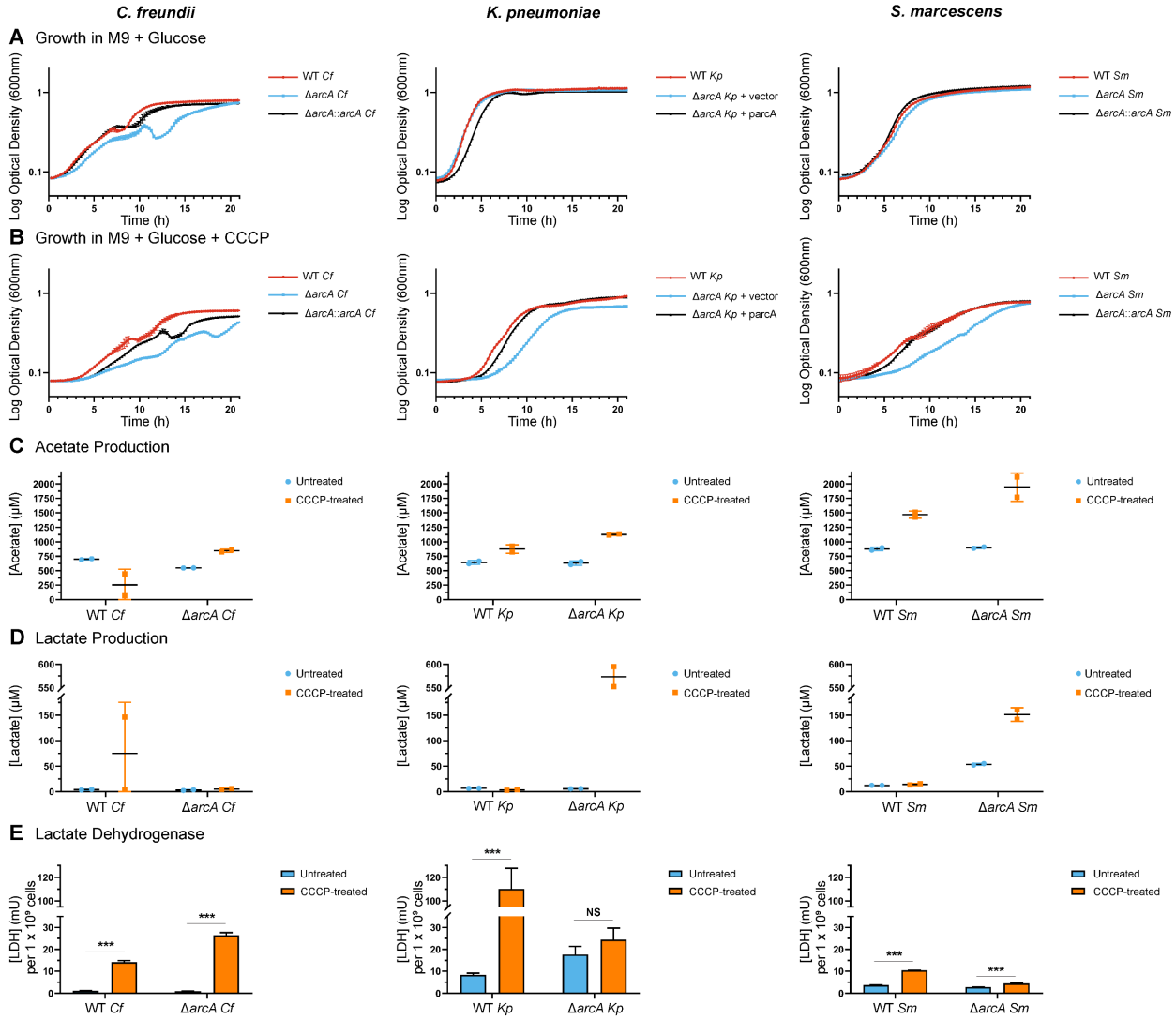

mediated fermentation is likely species-specific.

Figure 2.7: **ArcA modulates metabolism in response to disruption of proton motive force by the uncoupler carbonylcyanide-m-chlorophenylhydrazone (CCCP).** The ability of wild-type and Δ*arcA* mutant cells to respond to disruption of ATP synthesis via oxidative phosphorylation despite the availability of glucose and oxygen was tested. Overnight cultures incubated aerobically in LB to minimize growth differences between strain derivatives and were inoculated into M9 minimal medium with 0.4% glucose without **(A)** or with **(B)** CCCP (*C. freundii*, 15μM CCCP; *K. pneumoniae*, 20μM CCCP; *S. marcescens*, 25μM CCCP). CCCP concentrations were selected based on empirical testing in which growth was stunted but not completely inhibited. Cultures were incubated at 37°C under aerobic conditions and growth was tracked via OD_{600} by a plate reader every 15 minutes. Growth curves are the average of technical triplicates with standard deviation and are representative of three independent experiments. **(C)** Targeted metabolomics by LC-MS was utilized to quantitate acetate from supernatants of wild-type and *arcA* mutant cultures in early exponential phase from the same conditions as the growth curves. The average of two biological samples with standard deviation are presented in each graph. **(D)** d-Lactate dehydrogenase (d-LDH) was measured from cell lysates of cultures grown in M9 minimal medium with 0.4% glucose without or with CCCP at the same concentrations as the growth curve conditions. d-LDH levels were quantified with Amplite® Fluorimetric D-Lactate Dehydrogenase Assay Kit (AAT Bioquest) by comparing sample readings to known standards. d-LDH levels were normalized per 1 x 10^9 cells. The average of three technical replicates with standard deviation is presented as representative of three independent experiments. LDH levels were compared between cells in untreated and treated conditions using Šídák's multiple comparisons test to determine significance. (**E**) Targeted metabolomics was repeated to quantify lactate with the same experimental set-up as acetate (**C**). See methodology for details, **Fig. S5** for sampling metrics, and **Fig. S6** for LC-MS acetate and lactate samples. *p*-values: *≤0.05, **≤0.01, ***≤0.001, NS = not significant

Targeted metabolomics revealed a different fermentative profile following CCCP treatment of wild-type and *arcA* strains, but conclusions from these studies are limited by the potential recycling of secondary metabolites by cells. D-lactate dehydrogenase levels (LDH) were thus measured as an additional metric of fermentation to continue testing the hypothesis that *arcA* mutants exhibit a dysregulated response to CCCP treatment. LDH activity significantly increased in the *C. freundii* wild-type strain (13.5-fold) and *arcA* mutant construct (30.3-fold) cultured with CCCP relative to untreated conditions, indicating fermentation was induced but that ArcA may play an inhibitory role of LDH (**Fig. 2.7E**). Relative LDH levels also increased in wild-type *K. pneumoniae* (13.2-fold) and *S. marcescens* (2.8-fold) CCCP cultures, and LDH increases were ArcA-dependent for *K. pneumoniae* and partially so for *S. marcescens* (**Fig. 2.7E**). The inverse correlation of higher LDH levels in wild-type cells to lower lactate concentrations in their supernatant (**Fig. 2.7D**) is not clear but might be explained by unknown effects of CCCP or lactate oxidation at the ETC (59). Nevertheless, differences in LDH levels between wild-type and *arcA* mutant cultures provides further evidence ArcA plays a role in the

transition to fermentation following uncoupling of PMF.

2.10 Discussion

The response regulator ArcA is highly conserved among *Enterobacterales* species and was demonstrated for the first time here to promote fitness of *C. freundii*, *K. pneumoniae*, and *S. marcescens* during bacteremia. *arcA* mutants exhibited a dysregulated response to changes in oxygen and iron availability, conditions likely to be encountered during infection. ArcA was found to be part of the response to membrane damage caused by the CAMP polymyxin B, demonstrating an expanded role for ArcA linked to disruption of ETC activity. ArcA mediated a shift to fermentation in response to PMF uncoupling, independent of oxygen availability, as measured by LDH activity. The proposed model detailing how ArcA responds to low oxygen, limited iron, and membrane damage is summarized in **Fig. 2.8**. Ultimately, any stimulus that results in decreased flow of electrons through the ETC may produce a phenotype in which ArcA is activated.

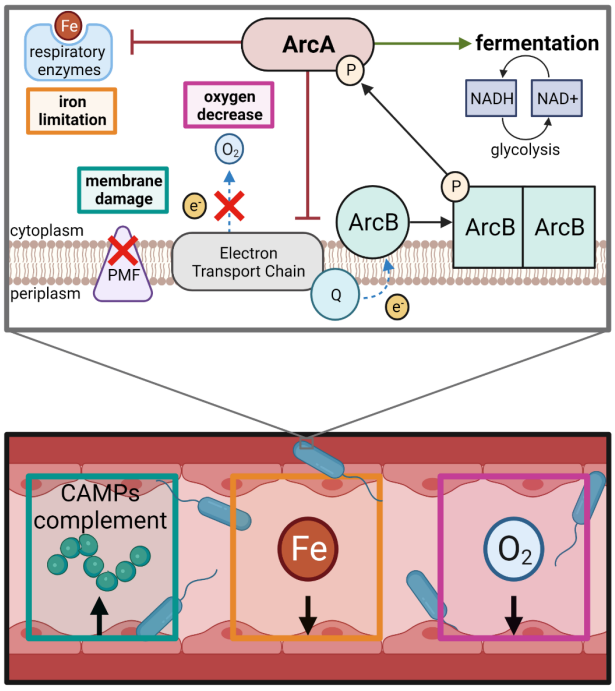

Figure 2.8: Response regulator ArcA supports fitness during Gram-negative bacteremia. Within the mammalian bloodstream, bacteria encounter decreased iron (Fe) availability, oxygen (O_2) levels, and elements of the host innate immune response such as cationic antimicrobial peptides (CAMPs) which can cause membrane damage. ArcA mediates the transition to fermentation in response to such conditions unfavorable for respiration including the inability to maintain a proton motive force (PMF). Quinones (Q) of the electron transport chain transfer electrons to sensor kinase ArcB instead of to pathways which lead to oxygen as the terminal electron acceptor. ArcB then phosphorylates and activates ArcA in response to decreased electron transport chain activity, providing a mechanism by which ArcA can respond to multiple stimuli impacting metabolic activity within the cell.

Bacteria entering the bloodstream directly from the environment or another infection site expectedly encounter increasingly anaerobic conditions during dissemination. Ambient oxygen levels of approximately 21.1% decrease from 13.2% in arterial blood to 5.4% in the liver with only small amounts being dissolved as 98% is hemoglobin-bound (60) (61). The *in vitro* growth defects of the *K. pneumoniae* and *S. marcescens arcA* mutants were evident by a sizeable shift in growth curves in the aerobic to anaerobic transition. Our group has calculated the average population doubling times of *C. freundii* (66 min.), *K. pneumoniae* (39 min.), and *S. marcescens* (61 min.) in murine spleens (32), leading to the hypothesis that bacterial cells' ability to maintain rapid replication rates is an important factor in combating host clearance mechanisms and establishing infection during bacteremia. This study captures the response of ArcA to changes in oxygen utilization and showcases the need for ArcA regulation to maintain such rapid growth. During urinary tract infections, *E. coli* utilizes the TCA cycle while glycolysis is dispensable (62, 63). If *E. coli* favors the same pathways during bacteremia, ArcA would be expendable as a repressor of the TCA cycle, explaining the lack of fitness defect of the *E. coli arcA* mutant during bacteremia. Our previous TnSeq screens identified genes encoding 6-phosphofructokinase, phosphate acetyltransferase, and acetate kinase as contributing to fitness for *C. freundii* and *S. marcescens* during bacteremia, suggesting glycolysis is utilized in infection (10, 11).

ArcA maximizes replication of *C. freundii*, *K. pneumoniae*, and *S. marcescens* in iron-limited conditions and reportedly regulates iron homeostasis alongside FNR and Fur in *E. coli* (64). Stunted growth of *arcA* mutants in iron limitation occurred under aerobic conditions, further showing ArcA responds to decreased oxygen utilization rather than absence of oxygen. Fermentation is the preferred metabolic pathway during iron starvation, and Chareyre *et al.*

demonstrated iron deprivation leads to post-transcriptional repression of respiratory complexes by small RNA RhyB (65, 66). The *nuo* and *shd* operons encoding these complexes are strongly repressed by ArcA (18, 19), indicating coordination between RhyB and ArcA during iron limitation may exist. The link between iron and oxygen is observed in higher order species as human Hypoxia Inducible Factor (HIF), a transcriptional activator induced by low oxygen levels, also promotes glycolytic activity during iron limitation (67–69).

These studies are the first to our knowledge linking ArcA to CAMP sensitivity. Upregulation of six genes by ArcA following PMB treatment was unexpected given its well established role in repressing five of them but not unprecedented (18–20). In a *Salmonella enterica* study, 38 genes were regulated in the opposite direction by ArcA when the regulon of cells cultured anaerobically were compared with cultures treated with H_2O_2 (70). Future studies can determine if ArcA directly or indirectly upregulates the PMB-responsive genes, which do not encode pathways of aerobic respiration. A "core" ArcA regulon may exist in which ArcA invariably represses central carbon metabolic pathways alongside a "conditional" regulon where its role is contextual. More transcriptomic and DNA footprinting studies will be critical for defining the direct and indirect ArcA regulons in infection-relevant conditions.

CAMPs damage the inner membrane and inhibit respiratory enzymes (71, 72), implying PMB disrupts PMF maintenance or damages the ETC. *arcA* mutants grew more slowly in CCCP, connecting ArcA to ETC perturbations. CCCP induced higher LDH levels in all three species, indicating a shift to fermentation, and this increase was at least partially ArcA-dependent for *K. pneumoniae* and *S. marcescens*. Targeted metabolomics revealed CCCP-induced lactate and acetate production is ArcA-and species-dependent. Acetate and lactate pathways contribute to the maintenance redox balance during glycolysis (57). Based on ArcA maintaining intracellular

redox balance (14), acetate and lactate production might reflect balancing of redox levels in the presence of CCCP. Cells that are more efficient in carbon cycling may reuse end products of fermentation rather than secrete them into the supernatant. To this end, an *arcA* mutant of *E. coli* undergoing anaerobic fermentation had a 15.8% lower growth rate relative to the wild-type strain (19). Approaches including carbon tracing and untargeted metabolomics can further characterize the global metabolic changes in these species in response to proton motive force uncoupling.

I conclude that ArcA responds to low oxygen conditions, decreased iron levels, and host-mediated membrane damage during bacteremia in three related Gram-negative bacterial species. Activation of ArcA in response to low iron and membrane damage was not tested, so control of ArcA function in these contexts remains to be established. Although a phosphomimetic *arcA* mutant has not been constructed, an *arcA* over-expression system may be useful in such *in vitro* experiments as well as in the bacteremia model. Increased fitness of such a bacterial construct overexpressing *arcA* in a longitudinal murine study could inform conclusions regarding the importance of promoting fermentation *versus* repressing respiration. It also remains possible that differences in ArcB activity between species explain some of the ArcA-mediated phenotypes that proved to be differential. Additionally, ArcA has recently been shown to become partially active independently of ArcB under oxidizing conditions, providing evidence of additional regulatory mechanisms that require further study (73). Future ArcA studies will be important in understanding the complex regulation of central carbon pathways utilized in the bloodstream environment and may reveal other shared or unique metabolic capabilities.

2.11 Supplemental Figures

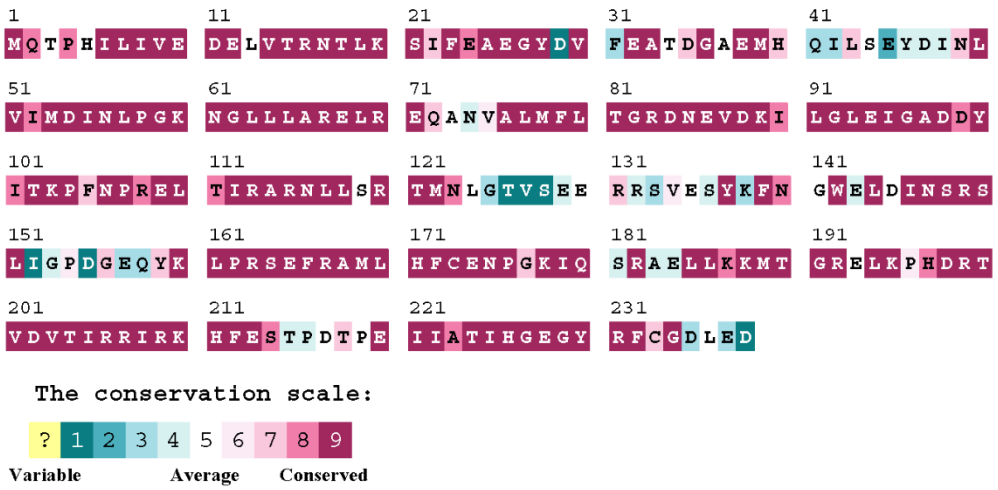

Supplemental Figure 2.10: A majority of ArcA residues are evolutionarily conserved across Order *Enterobacterales*. Consurf (24) was utilized to map an alignment of 419 ArcA amino acid sequences from 418 species in Order *Enterobacterales* onto a predicted structure of ArcA from AlphaFold (25, 26). Evolutionary rates were calculated via the JTT model of substitution (74) based on an alignment from MUSCLE (75). A phylogenetic tree was constructed from the alignment using Neighbor Joining with ML distance. Rate4site then calculated residue specific conservation scores with Bayesian method providing confidence intervals. Residue conservation scores were visualized on a structure of ArcA with pyMOL (76) (**Fig. 1B**).

```
C. freundii  MQTPHILIVEDELVTRNTLKSIFEAEGYDVFEATDGAEMHQILSEYDINLVIMDINLPGK  60
E. coli      MQTPHILIVEDELVTRNTLKSIFEAEGYDVFEATDGAEMHQILSEYDINLVIMDINLPGK  60
K. pneumoniae MQTPHILIVEDELVTRNTLKSIFEAEGYDVFEATDGAEMHQILSENDINLVIMDINLPGK  60
S. marcescens MQTPHILIVEDELVTRNTLKSIFEAEGYIVHEANDGAEMHNILSENDINLVIMDINLPGK  60
              ************************** *.**.******:**** **************

C. freundii  NGLLLARELREQANVALMFLTGRDNEVDKILGLEIGADDYITKPFNPRELTIRARNLLSR  120
E. coli      NGLLLARELREQANVALMFLTGRDNEVDKILGLEIGADDYITKPFNPRELTIRARNLLSR  120
K. pneumoniae NGLLLARELREQADVALMFLTGRDNEVDKILGLEIGADDYITKPFNPRELTIRARNLLSR  120
S. marcescens NGLLLARELREQASVALMFLTGRDNEVDKILGLEIGADDYITKPFNPRELTIRARNLLSR  120
              ************.*********************************************

C. freundii  TMNLGTVSEERRSVESYKFNGWELDINSRSLIGPDGEQYKLPRSEFRAMLHFCENPGKIQ  180
E. coli      TMNLGTVSEERRSVESYKFNGWELDINSRSLIGPDGEQYKLPRSEFRAMLHFCENPGKIQ  180
K. pneumoniae TMNLGTVSEERRSVESYKFNGWELDINSRSLVSPNGEQYKLPRSEFRAMLHFCENPGKIQ  180
S. marcescens TMNLGSLGEERRLVESYKFNGWELDINSRSLISPAGEQYKLPRSEFRAMLHFCENPGKIQ  180
              *****::.**** ******************:.* ************************

C. freundii  SRAELLKKMTGRELKPHDRTVDVTIRRIRKHFESTPDTPEIIATIHGEGYRFCGDLQD    238
E. coli      SRAELLKKMTGRELKPHDRTVDVTIRRIRKHFESTPDTPEIIATIHGEGYRFCGDLED    238
K. pneumoniae SRAELLKKMTGRELKPHDRTVDVTIRRIRKHFESTPDTPEIIATIHGEGYRFCGDLQE    238
S. marcescens SRGELLKKMTGRELKPHDRTVDVTIRRIRKHFESTPDTPEIIATIHGEGYRFCGDLEE    238
              **.**************************************************::
```

Supplemental Figure 2.9: ArcA is highly conserved at the amino acid level. The amino acid sequences of ArcA from *C. freundii*, *E. coli, K. pneumoniae*, and *S. marcescens* were aligned with Clustal Omega (21988835). Symbols beneath the alignment are representative of the following: asterisk (*) – amino acid conserved across all species; colon (:) – strongly similar – Gonnet PAM 250 matrix score >0.5; period (.) – weakly similar – Gonnet PAM 250 matrix score <0.5 and >0; space ( ) – residues not conserved based on amino acid properties. The red arrow at position 54 identifies the conservation of an aspartate residue in all four species which is known participate in the canonical ArcB-ArcA phosphorelay (27).

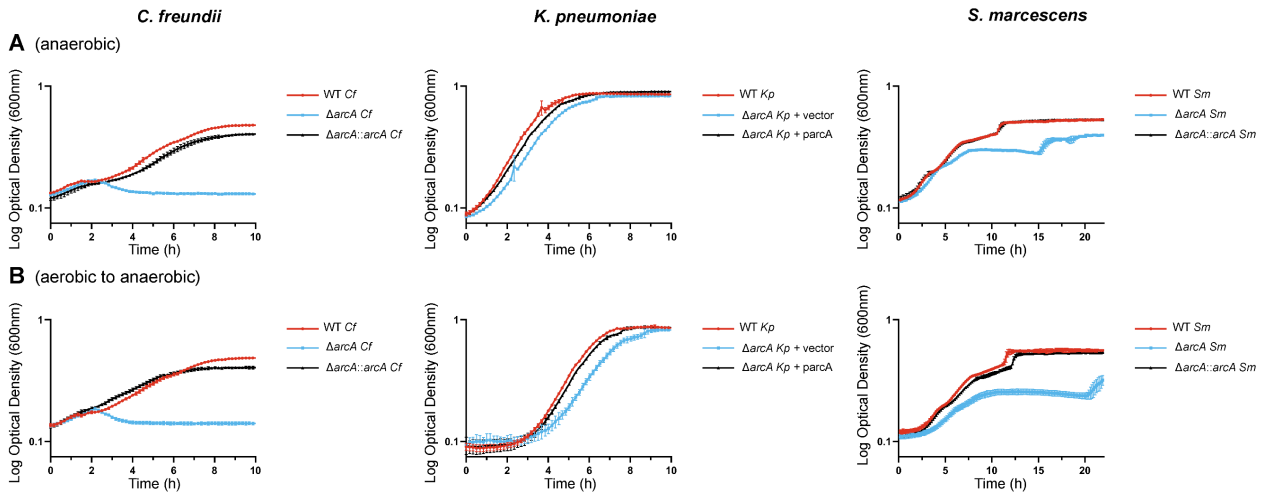

Supplemental Figure 2.12: Growth of bacterial strains in M9 + glucose + casamino acids in anaerobic conditions. Strains were cultured overnight in LB under anaerobic or aerobic conditions and then normalized based on OD_{600} in PBS. M9 minimal medium with 0.4% glucose and 0.1% casamino acids was inoculated with normalized overnight cultures and incubated in an anaerobic chamber. OD_{600} was measured with a plate reader every 10 minutes. Results are representative of three independent experiments. Each strain was grown in triplicate, and the average with standard deviation was plotted above.

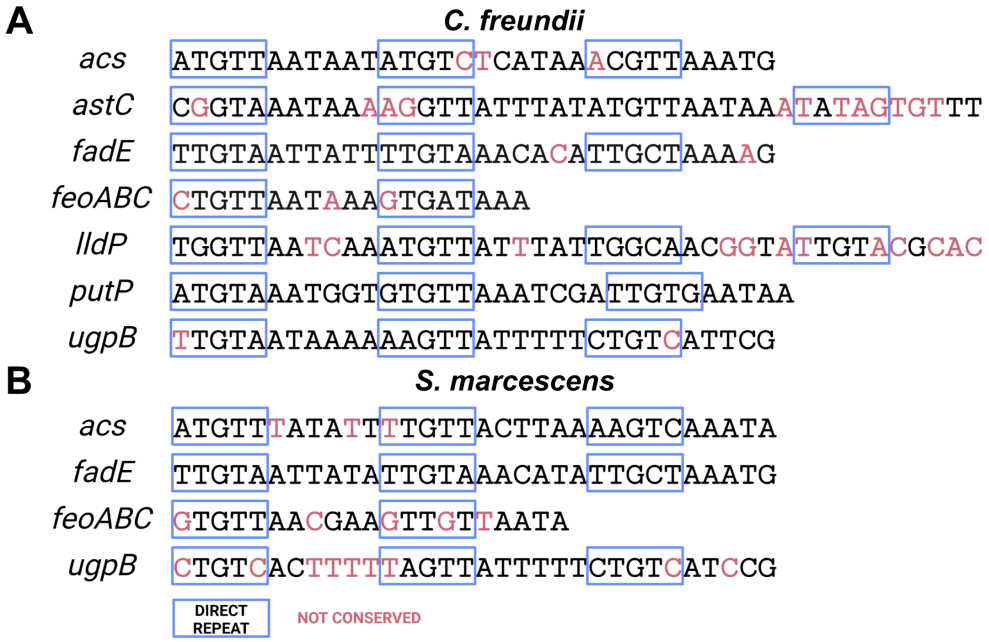

Supplemental Figure 2.11: Putative ArcA binding sequences of C. freundii and S. marcescens. FIMO was utilized to search for ArcA binding boxes from *E. coli* MG1655 in the promoter regions of the seven genes evaluated in the *K. pneumoniae* expression studies. Sequences having a p-value and q-value at or below 0.05 were considered significant and analyzed more closely. **(A)** In the promoters of 7/7 *C. freundii* genes, a putative ArcA binding sequence was identified. **(B)** In the promoters of 4/7 *S. marcescens* genes, a putative ArcA binding sequence was identified. Red nucleotides were loci not conserved between the *E. coli* and the corresponding species' nucleotide sequences. Direct repeats within sequences were labeled based on coordinates of direct repeats within corresponding promoters of *E. coli* genes and are denoted by blue boxes.

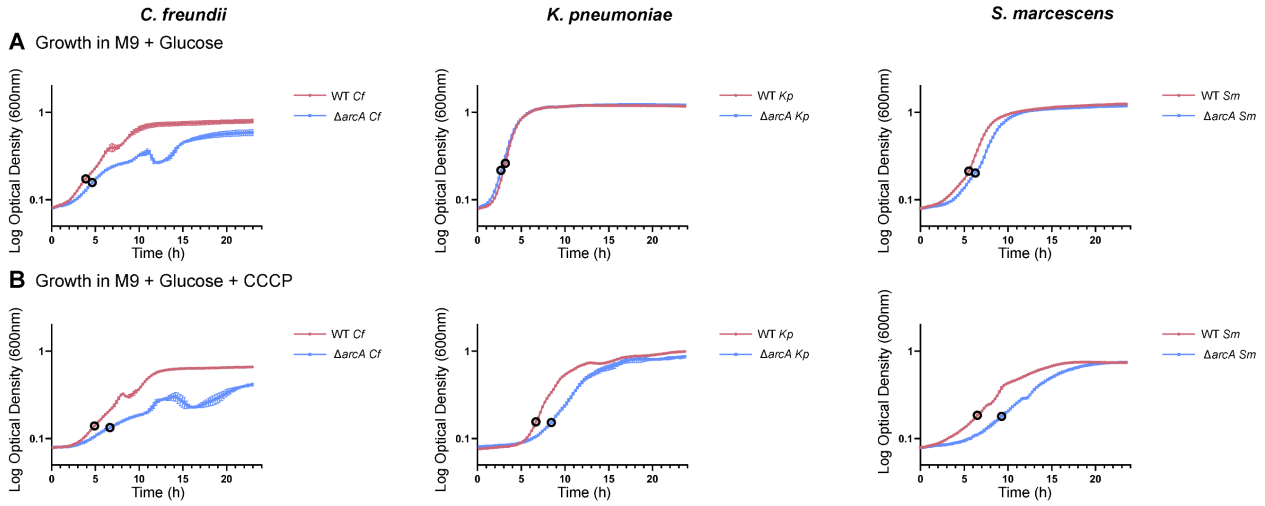

Supplemental Figure 2.13 Sampling points for targeted metabolomics. Overnight cultures incubated aerobically in LB were inoculated into M9 minimal medium with 0.4% glucose without (**A**) or with (**B**) CCCP (*C. freundii* - 15µM CCCP, *K. pneumoniae* - 20µM CCCP, *S. marcescens* - 25µM CCCP). Wild-type and Δ*arcA* cultures were incubated at 37°C in aerobic conditions and growth was tracked via OD_{600} by a plate reader every 15 minutes in quintuplet replicates. Upon reaching early exponential phase, cultures from two wells for each strain in both media were removed for processing. The remaining three wells with culture were allowed to continue to grow. Sampling points are representative by open, black circles. Supernatants from the removed cultures were used in targeted metabolomics to quantitate acetate and lactate as described in the methodology section (**Fig. 2.7**).

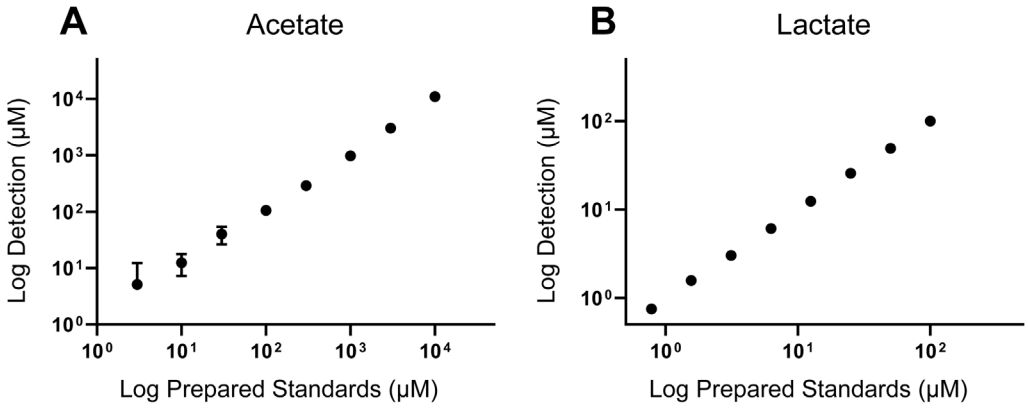

Supplemental Figure 2.14: Acetate and lactate standards for LC-MS. Acetate and lactate were measured via separate LC-MS protocols as described in methodology. Standards of acetate and lactate were included alongside experimental samples to allow for metabolite quantification. **(A)** Prepared acetate controls ranging from 3µM to 3000µM were quantified in duplicate using an Agilent 1290 LC coupled to an Agilent 6490 triple quadrupole MS. **(B)** Prepared lactate controls ranging from 0.7813µM to 100µM were quantified in duplicate on an Infinity Lab II UPLC coupled with a 6545 QTof mass spectrometer using a JetStream ESI source in negative mode. The averages of each control are plotted with standard deviation.

2.12 Materials and Methods

Bacterial strains and culture conditions

Bacterial strains and constructs utilized in this study are listed in **Table 1**. *E. coli* TOP10 cells were used for routine cloning purposes. Overnight culture was performed in LB (77) and experimental cultures were grown in LB or M9 medium (78) containing 100µM $CaCl_2$, 1mM $MgSO_4$, 0.4% D-glucose, and 0.1% casamino acids as indicated. Cultures were maintained at 37°C with 200RPM shaking unless noted otherwise. Anaerobic cultures were maintained in a 37°C anaerobic chamber maintained at 10% H_2, 5% CO_2 and 85% N_2.

Strain engineering

C. freundii, E. coli, K. pneumoniae, and *S. marcescens arcA* mutants were generated using Lambda red mutagenesis as previously described (10, 79, 80) with the oligonucleotides from **Supplemental Table 7**. Chromosomal mutations were confirmed by PCR-amplification and sequencing of the mutant allele.

Genetic reversion and complementation

The *C. freundii* and *S. marcescens* Δ*arcA*::*npII* alleles were reverted to wild-type via recombineering to confirm that phenotypes observed in the *arcA::npt* mutant constructs are due to loss of *arcA*. Primers were designed to amplify the portion of the *arcA* gene replaced by the antibiotic resistance cassette in the Δ*arcA*::*npII* mutants with the same homologous ends as the inserts from the first round of Lambda red recombineering. *C. freundii* and *S. marcescens arcA* mutant strains were transformed with the resultant *arcA*-containing PCR products. Recovery of cells was performed in LB without selection at 30°C. Transformants were passaged overnight in LB at 30°C serially for two (*S. marcescens*) or three (*C. freundii*) days to enrich for revertants since *arcA* mutants were observed to grow more slowly relative to wild-type cells. Cultures were

plated each day on LB without selection, and colonies were screened based on reversion to the wild-type colony size as *arcA* mutants exhibit a small colony phenotype. Reversion was confirmed by observing loss of kanamycin resistance and Sanger sequencing of PCR products amplified from the *arcA* locus.

The *K. pneumoniae* Δ*arcA*::*npII* mutant was complemented *in trans* with pBBR1MCS-5. Primers ANB21F and ANB21R and were used to amplify the *arcA* ORF and 539 base pairs upstream of the start of the gene with Easy A polymerase (Agilent). The PCR product and pBBR1MCS-5 parent plasmid were separately digested with SacI and XbaI. Ligation of the two digested fragments was achieved with T4 DNA ligase (NEB) followed by electroporation into *E. coli* TOP10 (Thermo Fischer). Plasmid construction was confirmed by Sanger sequencing. KPPR1 *ΔarcA::npII* was transformed with complementation plasmid by electroporation the complementation or empty vector control plasmids were maintained in the presence of gentamicin (10 μg/ml).

Murine bacteremia model

Overnight LB cultures of wild-type and *arcA* mutant constructs were sub-cultured into fresh LB and cultured at 37°C with 200 RPM shaking. Mid-log cells were washed and resuspended with PBS and normalized by OD_{600} to approximate CFU/mL of 1 x 10^9 (*C. freundii*), *E. coli*: 2 x 10^7 (*E. coli*), 1 x 10^6 (*K. pneumoniae*), and 1 x 10^8 (*S. marcescens*). Wild-type and *arcA* mutant cells were injected into 6-8 weeks old male and female C57BL/6 mice (Jackson Laboratory) via tail-veins as previously described (82). Inocula and organ homogenates were plated on LB agar with and without kanamycin (50 μg/ml) for differential CFU determinations. Competitive indices were calculated by dividing the ratio of mutant to wild-type CFU in organs by the inocula ratio. Competitive indices were log-transformed, and significance

was determined by a one-sample *t*-test with a hypothetical null value of zero. Murine experiments were performed in compliance with an animal protocol (PRO00010856) approved by the University of Michigan Institutional Animal Care & Use Committee.

***In vitro* growth**

Aerobic and anaerobic overnight cultures were normalized by OD_{600}, washed and resuspended in PBS, and subcultured 1:100 into the desired media. For aerobic growth studies, 300µL from each culture was added in triplicate to a honeycomb plate. Iron-limited M9 media with and without iron supplementation were prepared as follows: *C. freundii* – 0.6mM 2,2'-dipyridyl (0.6% DMSO) and 3.0mM $FeSO_4$; *K. pneumoniae* – 0.2mM 2,2'-dipyridyl (0.2% DMSO) and 0.1mM $FeSO_4$; *S. marcescens* – 0.4mM 2,2'-dipyridyl (0.4% DMSO) and 0.2mM $FeSO_4$. Growth was assessed by comparing area under the curve to wild-type strains with significance determined by Dunnett's multiple comparisons test. M9 media were prepared with carbonylcyanide-*m*-chlorophenylhydrazone (CCCP) at 15µM (*C. freundii*), 20µM (*K. pneumoniae*) and 25µM (*S. marcescens*). Plates were incubated on a Bioscreen-C plate reader with the following settings: 37°C, intermediate continuous shaking, OD_{600} measurement every 15 minutes. For anaerobic growth studies, 200µL from each prepared culture was added in triplicate to a 96 well plate, which was incubated in an anaerobic plate reader (BioTek Powerwave HT) per the following settings: 37°C, static, OD_{600} measurement taken every 10 minutes.

Survival assays

Pooled human complement serum (Innovative Research) stored at -80C was thawed directly prior to use and heat-inactivated at 56°C for 45 minutes, where indicated. Washed mid-log cells were resuspended to a final density of $2x10^8$ CFU/ml in PBS and added to serum in 96-

well plates. Serum sensitivity was tested at concentrations of 10% (*C. freundii*), 90% (*K. pneumoniae*), or 20% (*S. marcescens*). Bacterial viability was determined after a static 90-min exposure at 37°C by CFU enumeration relative to time zero. For polymyxin B studies, cells were collected by centrifugation and resuspended in PBS to an OD_{600} of 0.2. Polymyxin B (RPI) was added to cells in 96-well plates at final concentrations of 5.0µg/mL (*C. freundii*), 50µg/mL (*K. pneumoniae*), or 100µg/mL (*S. marcescens*). Plates were incubated statically for 1 hour at 37°C followed by enumeration of viable bacteria relative to untreated conditions. For both assays, Dunnett's multiple comparisons test was used to assess statistical significance following log transformation of data.

Gene expression

Mid-exponential phase aerobic bacteria were normalized to 2 x 10^8 CFU/mL in PBS. 10mL of resuspended culture was added to a 125mL flask, and 1.0mL of resuspended culture was kept as an untreated control. Polymyxin B (50uL) was added for a final concentration of 5µg/mL. Flasks were incubated at 37°C and 200 RPM shaking for 15 minutes. 1.0mL of treated and untreated culture were added directly to 2mL of RNA protect solution (Qiagen), and RNA was extracted with the RNeasy Mini Kit (Qiagen) following manufacturer's instructions. RNA samples were treated with RQ1 DNase (Promega) and repurified with the RNeasy Mini Kit (Qiagen). cDNA was generated with iScript cDNA Synthesis Kit (Bio-Rad) and diluted 1:10 with water. RT-qPCR was performed with Power SYBR Green (Thermo Fischer) followed by calculation of relative gene expression with the $2^{-\Delta\Delta Ct}$ (Livak) method (83). In untreated conditions, gene expression was compared to the wild-type strain following log transformation, and significance was determined via a one-sample t-test with a null hypothetical value of zero. Expression of each gene was compared between untreated and polymyxin B conditions, and significance was

determined by comparing the wild-type strain with the mutant and complemented strains with Dunnett's multiple comparisons test.

Metabolite quantification

Aerobic and anaerobic overnight cultures were normalized by OD600, washed and resuspended in PBS, and subcultured into M9 media with carbonylcyanide-*m*-chlorophenylhydrazone (CCCP) at 15µM (*C. freundii*), 20µM (*K. pneumoniae*) and 25µM (*S. marcescens*). 300µL from each culture was added to five wells in a honeycomb plate. Plates were incubated on a Bioscreen-C plate reader with the following settings: 37°C, intermediate continuous shaking, OD600 measurement every 15 minutes. OD_{600} readings were monitored in real time via the Bioscreen-C plate reader. Upon reaching early exponential phase, 300uL was removed from two wells for each strain and condition and immediately transferred to ice. An aliquot of each sample was removed for CFU enumeration before cells were pelleted in a 4°C microcentrifuge. The supernatant was transferred to a new tube and immediately stored at -80°C. Supernatant samples were processed by the University of Michigan Metabolomics Core to quantify acetate and lactate. Growth is reported as the average of the unsampled wells for each genotype and condition.

Short chain fatty acids (SCFAs), including acetate, were measured using a modified version of a previously described protocol (84). SCFAs in the sample supernatant were derivatized using 3-nitrophenylhydrazine and an EDAC-6% pyridine solution. Samples were analyzed via LC-MS alongside acetate controls ranging from 3µ to 3000µM using an Agilent (Santa Clara, CA) 1290 LC coupled to an Agilent 6490 triple quadrupole MS. The chromatographic column was a Waters (Milford, MA) HSS T3, 2.1 mm x 100 mm, 1.7 µm particle size. Quantitation was performed using Agilent MassHunter Quantitative Analysis

software version 8.0 by measuring the ratio of peak area of the 3-NPH derivatized SCFA species to its closest internal standard.

Lactate quantification was performed starting with the addition of an extraction solvent containing ^{13}C Lactate to each supernatant sample. Following a series of mixing and centrifugation, supernatant was collected and dried using a nitrogen blower. Samples were reconstituted alongside a series of calibration standards. Ion pairing reverse phase LC-MS analysis was then performed using an Infinity Lab II UPLC coupled with a 6545 QTof mass spectrometer (Agilent Technologies, Santa Clara, CA) and a JetStream ESI source in negative mode. Chromatographic separation was performed on an Agilent ZORBAX RRHD Extend 80Å C18, 2.1 × 150 mm, 1.8 µm column with an Agilent ZORBAX SB-C8, 2.1 mm × 30 mm, 3.5 µm guard column. Data were processed using MassHunter Quantitative analysis version B.07.00.

Lactate dehydrogenase measurement

Bacteria were cultured as described for metabolite quantification and early exponential phase cells were collected via centrifugation at 4°C. The supernatant was removed, and cells were washed once then resuspended in PBS at 4°C prior to sonication. Cells were lysed by sonication with a taper microtip Z192740-1EA (Sigma-Aldrich) with the following protocol: 1 min. 40s. sonication at 40% amplitude with 4 s. bursts divided by 10 s. pauses to avoid overheating. Lactate dehydrogenase was measured in triplicate from cleared lysates with the Amplite® Fluorimetric D-Lactate Dehydrogenase (LDH) Assay Kit from AAT Bioquest per the manufacturer's instructions. Fluorescence (excitation: 540nm; emission: 590nM) was measured after one hour incubation at room temperature protected from light with a Synergy H1 plate reader. LDH was quantified in samples based on standards ranging from 1µM/mL LDH to 200µM/mL. LDH concentration per 1 x 10^9 cells was subsequently normalized based on CFU

enumeration and compared for each strain between untreated and CCCP-treated conditions. Significance was determined by comparing LDH levels for strains in untreated and treated conditions using Šídák's multiple comparisons test.

***In silico* analyses**

ArcA amino acids sequences (n=419) from 418 *Enterobacterales* species were collated from BV-BRC (85) (**Supplemental Table 8**). A multi-sequence alignment was generated with MUSCLE via EMBL-EBI (75, 86). An ArcA predicted structure AF-P0A9Q1-F1 from Alpha Fold in agreement with a previously partially solved structure was retrieved via UniProt to serve as a template for conservation mapping (25, 26, 87, 88). Consurf calculated conservation scores from the multiple sequence alignment based on the sequence extracted from the predicted structure via a JTT evolutionary model (24, 74). A phylogenetic tree was constructed from the provided alignment via Neighbor Joining with ML distance. Rate4site then calculated residue specific conservation scores with Bayesian method providing confidence intervals, which were mapped onto the predicted ArcA structure with visualization of this projection provided by PyMOL (76). The ArcA amino acid sequences of *C. freundii* UMH14, *E.* coli CFT073, K. *pneumoniae* KPPR1, and *S. marcescens* UMH9 were aligned with Clustal Omega (31). A percent identity matrix was generated to calculate pairwise percent identities for all possible combinations of the four species. The output of amino acid alignment between all four species was then examined to assess conservation. Similarity of non-conserved residues was defined according to set parameters with a Gonnet PAM 250 matrix score of >0.5 signifying “strongly similar” and a score <0.5 and >0 for “weakly similar” residues.

ArcA binding sequences in the promoters of *acs*, *astC*, *fadE*, *feoB*, *lldP*, *putP*, and *ugpB* from *E. coli* K-12 MG1655 were used as the input motif with which to scan the promoters of the

same genes in *C. freundii*, *K. pneumoniae*, and *S. marcescens* (18). Sequences identified by FIMO Version 5.5.1 from MEME Suite were reported as potential ArcA binding sequences when *p*-values and *q*-values (false discovery rate) were both ≤0.05 (89). Nucleotides of the *E. coli* sequence and the sequences of the other species were compared to assess homology. Putative direct repeats were mapped onto the proposed ArcA sequences based on the coordinates reported in the *E. coli* sequences.

2.13 Acknowledgements

This work was supported by Predoctoral Fellowship award 828854 to A. N. B. from the American Heart Association and Public Health Service award AI134731 to H. L. T. M. and M. A. B. from the National Institutes of Health. We thank Mobley and Bachman laboratory members for their continual feedback and Dr. Maria Sandkvist for her expertise and insight with experimental planning and interpretation. We also thank the laboratories of Dr. Nicole Koropatkin and Dr. Eric Martens for technical support and equipment used during the anaerobic studies. The Biomedical Research Core Facilities at the University of Michigan are acknowledged for DNA sequencing and metabolomics. The summary figure was created with BioRender.com. We lastly acknowledge the use of C57BL/6 mice in the bacteremia model.

2.14 References

1. André AC, Debande L, Marteyn BS. 2021. The selective advantage of facultative anaerobes relies on their unique ability to cope with changing oxygen levels during infection. *Cell Microbiol* 23:e13338.
2. Thaden JT, Li Y, Ruffin F, Maskarinec SA, Hill-Rorie JM, Wanda LC, Reed SD, Fowler VG. 2017. Increased Costs Associated with Bloodstream Infections Caused by Multidrug-Resistant Gram-Negative Bacteria Are Due Primarily to Patients with Hospital-Acquired Infections. *Antimicrob Agents Chemother* 61.
3. Holmes CL, Anderson MT, Mobley HLT, Bachman MA. 2021. Pathogenesis of Gram-Negative Bacteremia. *Clin Microbiol Rev* 34.

4. Rhee C, Jones TM, Hamad Y, Pande A, Varon J, O'Brien C, Anderson DJ, Warren DK, Dantes RB, Epstein L, Klompas M, for the Centers for Disease Control and Prevention (CDC) Prevention Epicenters Program. 2019. Prevalence, Underlying Causes, and Preventability of Sepsis-Associated Mortality in US Acute Care Hospitals. *JAMA Netw Open* 2:e187571.
5. Umemura Y, Ogura H, Takuma K, Fujishima S, Abe T, Kushimoto S, Hifumi T, Hagiwara A, Shiraishi A, Otomo Y, Saitoh D, Mayumi T, Yamakawa K, Shiino Y, Nakada T, Tarui T, Okamoto K, Kotani J, Sakamoto Y, Sasaki J, Shiraishi S, Tsuruta R, Masuno T, Takeyama N, Yamashita N, Ikeda H, Ueyama M, Gando S. 2021. Current spectrum of causative pathogens in sepsis: A prospective nationwide cohort study in Japan. *Int J Infect Dis* 103:343–351.
6. Rhee C, Kadri SS, Dekker JP, Danner RL, Chen H-C, Fram D, Zhang F, Wang R, Klompas M. 2020. Prevalence of Antibiotic-Resistant Pathogens in Culture-Proven Sepsis and Outcomes Associated With Inadequate and Broad-Spectrum Empiric Antibiotic Use. *JAMA Netw Open* 3:e202899.
7. Zhang Y, Wang Q, Yin Y, Chen H, Jin L, Gu B, Xie L, Yang C, Ma X, Li H, Li W, Zhang X, Liao K, Man S, Wang S, Wen H, Li B, Guo Z, Tian J, Pei F, Liu L, Zhang L, Zou C, Hu T, Cai J, Yang H, Huang J, Jia X, Huang W, Cao B, Wang H. 2018. Epidemiology of Carbapenem-Resistant *Enterobacteriaceae* Infections: Report from the China CRE Network. *Antimicrob Agents Chemother* 62:e01882-17.
8. Denisuik AJ, Garbutt LA, Golden AR, Adam HJ, Baxter M, Nichol KA, Lagacé-Wiens P, Walkty AJ, Karlowsky JA, Hoban DJ, Mulvey MR, Zhanel GG. 2019. Antimicrobial-resistant pathogens in Canadian ICUs: results of the CANWARD 2007 to 2016 study. *J Antimicrob Chemother* 74:645–653.
9. Subashchandrabose S, Smith SN, Spurbeck RR, Kole MM, Mobley HLT. 2013. Genome-Wide Detection of Fitness Genes in Uropathogenic *Escherichia coli* during Systemic Infection. *PLoS Pathog* 9.
10. Anderson MT, Mitchell LA, Zhao L, Mobley HLT. 2017. Capsule Production and Glucose Metabolism Dictate Fitness during *Serratia marcescens* Bacteremia. *mBio* 8.
11. Anderson MT, Mitchell LA, Zhao L, Mobley HLT. 2018. *Citrobacter freundii* fitness during bloodstream infection. *Sci Rep* 8:11792.
12. Holmes CL, Wilcox AE, Forsyth V, Smith SN, Moricz BS, Unverdorben LV, Mason S, Wu W, Zhao L, Mobley HLT, Bachman MA. 2023. *Klebsiella pneumoniae* causes bacteremia using factors that mediate tissue-specific fitness and resistance to oxidative stress. bioRxiv https://doi.org/10.1101/2023.02.23.529827.
13. King AN, de Mets F, Brinsmade SR. 2020. Who's in control? Regulation of metabolism and pathogenesis in space and time. *Curr Opin Microbiol* 55:88–96.
14. Brown AN, Anderson MT, Bachman MA, Mobley HLT. 2022. The ArcAB Two-Component System: Function in Metabolism, Redox Control, and Infection. *Microbiol Mol Biol Rev* 86:e00110-21.
15. Kargeti M, Venkatesh KV. 2017. The effect of global transcriptional regulators on the anaerobic fermentative metabolism of *Escherichia coli*. *Mol Biosyst* 13:1388–1398.
16. De Souza-Hart JA, Blackstock W, Di Modugno V, Holland IB, Kok M. 2003. Two-Component Systems in *Haemophilus influenzae*: a Regulatory Role for ArcA in Serum Resistance. *Infect Immun* 71:163–172.

17. Pardo-Esté C, Hidalgo AA, Aguirre C, Briones AC, Cabezas CE, Castro-Severyn J, Fuentes JA, Opazo CM, Riedel CA, Otero C, Pacheco R, Valvano MA, Saavedra CP. 2018. The ArcAB two-component regulatory system promotes resistance to reactive oxygen species and systemic infection by *Salmonella* Typhimurium. *PLoS ONE* 13.
18. Park DM, Akhtar MdS, Ansari AZ, Landick R, Kiley PJ. 2013. The Bacterial Response Regulator ArcA Uses a Diverse Binding Site Architecture to Regulate Carbon Oxidation Globally. *PLoS Genet* 9.
19. Iyer MS, Pal A, Srinivasan S, Somvanshi PR, Venkatesh KV. 2021. Global Transcriptional Regulators Fine-Tune the Translational and Metabolic Efficiency for Optimal Growth of *Escherichia coli*. *mSystems* 6.
20. Federowicz S, Kim D, Ebrahim A, Lerman J, Nagarajan H, Cho B, Zengler K, Palsson B. 2014. Determining the Control Circuitry of Redox Metabolism at the Genome-Scale. *PLoS Genet* 10:e1004264.
21. Nochino N, Toya Y, Shimizu H. 2020. Transcription Factor ArcA is a Flux Sensor for the Oxygen Consumption Rate in *Escherichia coli*. *Biotechnol J* 15:1900353.
22. Loui C, Chang AC, Lu S. 2009. Role of the ArcAB two-component system in the resistance of *Escherichia coli* to reactive oxygen stress. *BMC Microbiol* 9:183.
23. Iyer MS, Pal A, Venkatesh KV. 2023. A Systems Biology Approach To Disentangle the Direct and Indirect Effects of Global Transcription Factors on Gene Expression in *Escherichia coli*. *Microbiol Spectr* e0210122.
24. Ashkenazy H, Abadi S, Martz E, Chay O, Mayrose I, Pupko T, Ben-Tal N. 2016. ConSurf 2016: an improved methodology to estimate and visualize evolutionary conservation in macromolecules. *Nucleic Acids Res* 44:W344-350.
25. Jumper J, Evans R, Pritzel A, Green T, Figurnov M, Ronneberger O, Tunyasuvunakool K, Bates R, Žídek A, Potapenko A, Bridgland A, Meyer C, Kohl SAA, Ballard AJ, Cowie A, Romera-Paredes B, Nikolov S, Jain R, Adler J, Back T, Petersen S, Reiman D, Clancy E, Zielinski M, Steinegger M, Pacholska M, Berghammer T, Bodenstein S, Silver D, Vinyals O, Senior AW, Kavukcuoglu K, Kohli P, Hassabis D. 2021. Highly accurate protein structure prediction with AlphaFold. *Nature* 596:583–589.
26. Varadi M, Anyango S, Deshpande M, Nair S, Natassia C, Yordanova G, Yuan D, Stroe O, Wood G, Laydon A, Žídek A, Green T, Tunyasuvunakool K, Petersen S, Jumper J, Clancy E, Green R, Vora A, Lutfi M, Figurnov M, Cowie A, Hobbs N, Kohli P, Kleywegt G, Birney E, Hassabis D, Velankar S. 2022. AlphaFold Protein Structure Database: massively expanding the structural coverage of protein-sequence space with high-accuracy models. *Nucleic Acids Res* 50:D439–D444.
27. Kwon O, Georgellis D, Lin EC. 2000. Phosphorelay as the sole physiological route of signal transmission by the *arc* two-component system of *Escherichia coli*. *J Bacteriol* 182:3858–3862.
28. Nguyen M-P, Yoon J-M, Cho M-H, Lee S-W. 2015. Prokaryotic 2-component systems and the OmpR/PhoB superfamily. *Can J Microbiol* 61:799–810.
29. Martínez-Hackert E, Stock AM. 1997. Structural relationships in the OmpR family of winged-helix transcription factors. *J Mol Biol* 269:301–312.
30. Morgan SJ, French EL, Plecha SC, Krukonis ES. 2019. The wing of the ToxR winged helix-turn-helix domain is required for DNA binding and activation of toxT and ompU. *PLOS ONE* 14:e0221936.

31. Sievers F, Wilm A, Dineen D, Gibson TJ, Karplus K, Li W, Lopez R, McWilliam H, Remmert M, Söding J, Thompson JD, Higgins DG. 2011. Fast, scalable generation of high-quality protein multiple sequence alignments using Clustal Omega. *Mol Syst Biol* 7:539.
32. Anderson MT, Brown AN, Pirani A, Smith SN, Photenhauer AL, Sun Y, Snitkin ES, Bachman MA, Mobley HLT. 2021. Replication Dynamics for Six Gram-Negative Bacterial Species during Bloodstream Infection. *mBio* 12:e0111421.
33. Hullahalli K, Waldor MK. Pathogen clonal expansion underlies multiorgan dissemination and organ-specific outcomes during murine systemic infection. *eLife* 10:e70910.
34. Welch RA, Burland V, Plunkett G, Redford P, Roesch P, Rasko D, Buckles EL, Liou S-R, Boutin A, Hackett J, Stroud D, Mayhew GF, Rose DJ, Zhou S, Schwartz DC, Perna NT, Mobley HLT, Donnenberg MS, Blattner FR. 2002. Extensive mosaic structure revealed by the complete genome sequence of uropathogenic *Escherichia coli*. *Proc Natl Acad Sci U S A* 99:17020–17024.
35. Mobley HL, Green DM, Trifillis AL, Johnson DE, Chippendale GR, Lockatell CV, Jones BD, Warren JW. 1990. Pyelonephritogenic *Escherichia coli* and killing of cultured human renal proximal tubular epithelial cells: role of hemolysin in some strains. *Infect Immun* 58:1281–1289.
36. Broberg CA, Wu W, Cavalcoli JD, Miller VL, Bachman MA. 2014. Complete Genome Sequence of *Klebsiella pneumoniae* Strain ATCC 43816 KPPR1, a Rifampin-Resistant Mutant Commonly Used in Animal, Genetic, and Molecular Biology Studies. *Genome Announc* 2.
37. Py B, Barras F. 2010. Building Fe–S proteins: bacterial strategies. 6. *Nat Rev Microbiol* 8:436–446.
38. Nairz M, Weiss G. 2020. Iron in infection and immunity. *Mol Aspects Med* 75:100864.
39. Gao G, Li J, Zhang Y, Chang Y-Z. 2019. Cellular Iron Metabolism and Regulation, p. 21–32. *In* Chang, Y-Z (ed.), Brain Iron Metabolism and CNS Diseases. Springer, Singapore.
40. Georgellis D, Kwon O, Lin EC. 2001. Quinones as the redox signal for the *arc* two-component system of bacteria. *Science* 292:2314–2316.
41. Malpica R, Franco B, Rodriguez C, Kwon O, Georgellis D. 2004. Identification of a quinone-sensitive redox switch in the ArcB sensor kinase. *Proc Natl Acad Sci U S A* 101:13318–13323.
42. Xie P, Liang H, Wang J, Huang Y, Gao H. 2021. Lipopolysaccharide Transport System Links Physiological Roles of σE and ArcA in the Cell Envelope Biogenesis in *Shewanella oneidensis*. *Microbiol Spectr* e0069021.
43. Gao H, Wang X, Yang ZK, Palzkill T, Zhou J. 2008. Probing regulon of ArcA in *Shewanella oneidensis* MR-1 by integrated genomic analyses. *BMC Genomics* 9:42.
44. Liang H, Zhang Y, Wang S, Gao H. 2021. Mutual interplay between ArcA and σE orchestrates envelope stress response in *Shewanella oneidensis*. *Environ Microbiol* 23:652–668.
45. Miajlovic H, Smith SG. 2014. Bacterial self-defence: how *Escherichia coli* evades serum killing. *FEMS Microbiol Lett* 354:1–9.
46. Huan Y, Kong Q, Mou H, Yi H. 2020. Antimicrobial Peptides: Classification, Design, Application and Research Progress in Multiple Fields. *Front Microbiol* 11.
47. Ridyard KE, Overhage J. 2021. The Potential of Human Peptide LL-37 as an Antimicrobial and Anti-Biofilm Agent. *Antibiotics* 10:650.

48. Napier BA, Burd EM, Satola SW, Cagle SM, Ray SM, McGann P, Pohl J, Lesho EP, Weiss DS. 2013. Clinical Use of Colistin Induces Cross-Resistance to Host Antimicrobials in *Acinetobacter baumannii*. *mBio* 4.
49. Ramos PIP, Custódio MGF, Quispe Saji G del R, Cardoso T, da Silva GL, Braun G, Martins WMBS, Girardello R, de Vasconcelos ATR, Fernández E, Gales AC, Nicolás MF. 2016. The polymyxin B-induced transcriptomic response of a clinical, multidrug-resistant *Klebsiella pneumoniae* involves multiple regulatory elements and intracellular targets. *BMC Genomics* 17.
50. Unden G, Bongaerts J. 1997. Alternative respiratory pathways of *Escherichia coli*: energetics and transcriptional regulation in response to electron acceptors. *Biochim Biophys Acta BBA - Bioenerg* 1320:217–234.
51. Förster AH, Gescher J. 2014. Metabolic Engineering of *Escherichia coli* for Production of Mixed-Acid Fermentation End Products. *Front Bioeng Biotechnol* 2.
52. Egoburo DE, Diaz Peña R, Alvarez DS, Godoy MS, Mezzina MP, Pettinari MJ. 2018. Microbial Cell Factories à la Carte: Elimination of Global Regulators Cra and ArcA Generates Metabolic Backgrounds Suitable for the Synthesis of Bioproducts in *Escherichia coli*. *Appl Environ Microbiol* 84:e01337-18.
53. Bidart GN, Ruiz JA, de Almeida A, Méndez BS, Nikel PI. 2012. Manipulation of the Anoxic Metabolism in *Escherichia coli* by ArcB Deletion Variants in the ArcBA Two-Component System. *Appl Environ Microbiol* 78:8784–8794.
54. Keevil CW, Hough JS, Cole JA. 1979. Regulation of Respiratory and Fermentative Modes of Growth of *Citrobacter freundii* by Oxygen, Nitrate and Glucose. *J Gen Microbiol* 113:83–95.
55. Grimont PAD, Grimont F. 2015. Klebsiella, p. 1–26. *In* Bergey's Manual of Systematics of Archaea and Bacteria. John Wiley & Sons, Ltd.
56. Pederson CS, Breed RS. 1928. THE FERMENTATION OF GLUCOSE BY ORGANISMS OF THE GENUS *SERRATIA*. *J Bacteriol* 16:163–185.
57. Clark DP. 1989. The fermentation pathways of *Escherichia coli*. *FEMS Microbiol Lett* 63:223–234.
58. Waegeman H, Beauprez J, Moens H, Maertens J, De Mey M, Foulquié-Moreno MR, Heijnen JJ, Charlier D, Soetaert W. 2011. Effect of *iclR* and *arcA* knockouts on biomass formation and metabolic fluxes in *Escherichia coli* K12 and its implications on understanding the metabolism of *Escherichia coli* BL21 (DE3). *BMC Microbiol* 11:70.
59. Matsushita K, Kaback HR. 1986. D-Lactate oxidation and generation of the proton electrochemical gradient in membrane vesicles from *Escherichia coli* GR19N and in proteoliposomes reconstituted with purified D-lactate dehydrogenase and cytochrome o oxidase. *Biochemistry* 25:2321–2327.
60. Carreau A, El Hafny-Rahbi B, Matejuk A, Grillon C, Kieda C. 2011. Why is the partial oxygen pressure of human tissues a crucial parameter? Small molecules and hypoxia. *J Cell Mol Med* 15:1239–1253.
61. Pittman RN. 2011. Chapter 4, Oxygen Transport. Morgan & Claypool Life Sciences, San Rafael.
62. Alteri CJ, Smith SN, Mobley HLT. 2009. Fitness of *Escherichia coli* during Urinary Tract Infection Requires Gluconeogenesis and the TCA Cycle. *PLoS Pathog* 5.
63. Alteri CJ, Mobley HLT. 2012. *Escherichia coli* physiology and metabolism dictates adaptation to diverse host microenvironments. *Curr Opin Microbiol* 15:3–9.

64. Beauchene NA, Mettert EL, Moore LJ, Keleş S, Willey ER, Kiley PJ. 2017. O_2 availability impacts iron homeostasis in *Escherichia coli*. *Proc Natl Acad Sci* 114:12261–12266.
65. Chareyre S, Barras F, Mandin P. 2019. A small RNA controls bacterial sensitivity to gentamicin during iron starvation. *PLOS Genet* 15:e1008078.
66. Baez A, Sharma AK, Bryukhanov A, Anderson ED, Rudack L, Olivares-Hernández R, Quan D, Shiloach J. 2022. Iron availability enhances the cellular energetics of aerobic *Escherichia coli* cultures while upregulating anaerobic respiratory chains. *New Biotechnol* 71:11–20.
67. Wang GL, Semenza GL. 1993. General involvement of hypoxia-inducible factor 1 in transcriptional response to hypoxia. *Proc Natl Acad Sci U S A* 90:4304–4308.
68. Shah YM, Xie L. 2014. Hypoxia-Inducible Factors Link Iron Homeostasis and Erythropoiesis. *Gastroenterology* 146:630–642.
69. Hu C-J, Wang L-Y, Chodosh LA, Keith B, Simon MC. 2003. Differential Roles of Hypoxia-Inducible Factor 1α (HIF-1α) and HIF-2α in Hypoxic Gene Regulation. *Mol Cell Biol* 23:9361–9374.
70. Morales EH, Collao B, Desai PT, Calderón IL, Gil F, Luraschi R, Porwollik S, McClelland M, Saavedra CP. 2013. Probing the ArcA regulon under aerobic/ROS conditions in *Salmonella enterica* serovar Typhimurium. *BMC Genomics* 14:626.
71. Sabnis A, Hagart KL, Klöckner A, Becce M, Evans LE, Furniss RCD, Mavridou DA, Murphy R, Stevens MM, Davies JC, Larrouy-Maumus GJ, Clarke TB, Edwards AM. 2021. Colistin kills bacteria by targeting lipopolysaccharide in the cytoplasmic membrane. *eLife* 10:e65836.
72. Deris ZZ, Akter J, Sivanesan S, Roberts KD, Thompson PE, Nation RL, Li J, Velkov T. 2014. A secondary mode of action of polymyxins against Gram-negative bacteria involves the inhibition of NADH-quinone oxidoreductase activity. *J Antibiot (Tokyo)* 67:147–151.
73. Zhou Y, Pu Q, Chen J, Hao G, Gao R, Ali A, Hsiao A, Stock AM, Goulian M, Zhu J. 2021. Thiol-based functional mimicry of phosphorylation of the two-component system response regulator ArcA promotes pathogenesis in enteric pathogens. *Cell Rep* 37:110147.
74. Darriba D, Taboada GL, Doallo R, Posada D. 2011. ProtTest 3: fast selection of best-fit models of protein evolution. *Bioinforma Oxf Engl* 27:1164–1165.
75. Edgar RC. 2004. MUSCLE: a multiple sequence alignment method with reduced time and space complexity. *BMC Bioinformatics* 5:113.
76. Schrodinger. 2015. The PyMOL Molecular Graphics System, Version 2.5.4.
77. Bertani G. 1951. Studies on Lysogenesis I: The Mode of Phage Liberation by Lysogenic *Escherichia coli*. *J Bacteriol* 62:293–300.
78. Jeffrey H. Miller. 1972. Experiments in molecular genetics. 9780879691066, United States.
79. Yu D, Ellis HM, Lee EC, Jenkins NA, Copeland NG, Court DL. 2000. An efficient recombination system for chromosome engineering in *Escherichia coli*. *Proc Natl Acad Sci U S A* 97:5978–5983.
80. Thomason LC, Sawitzke JA, Li X, Costantino N, Court DL. 2014. Recombineering: genetic engineering in bacteria using homologous recombination. *Curr Protoc Mol Biol* 106:1.16.1-39.
81. Kovach ME, Elzer PH, Steven Hill D, Robertson GT, Farris MA, Roop RM, Peterson KM. 1995. Four new derivatives of the broad-host-range cloning vector pBBR1MCS, carrying different antibiotic-resistance cassettes. *Gene* 166:175–176.

82. Smith SN, Hagan EC, Lane MC, Mobley HLT. 2010. Dissemination and Systemic Colonization of Uropathogenic *Escherichia coli* in a Murine Model of Bacteremia. *mBio* 1.
83. Schmittgen TD, Livak KJ. 2008. Analyzing real-time PCR data by the comparative C(T) method. *Nat Protoc* 3:1101–1108.
84. Yue M, Kim JH, Evans CR, Kachman M, Erb-Downward JR, D'Souza J, Foxman B, Adar SD, Curtis JL, Stringer KA. 2020. Measurement of Short-Chain Fatty Acids in Respiratory Samples: Keep Your Assay above the Water Line. *Am J Respir Crit Care Med* 202:610–612.
85. Olson RD, Assaf R, Brettin T, Conrad N, Cucinell C, Davis JJ, Dempsey DM, Dickerman A, Dietrich EM, Kenyon RW, Kuscuoglu M, Lefkowitz EJ, Lu J, Machi D, Macken C, Mao C, Niewiadomska A, Nguyen M, Olsen GJ, Overbeek JC, Parrello B, Parrello V, Porter JS, Pusch GD, Shukla M, Singh I, Stewart L, Tan G, Thomas C, VanOeffelen M, Vonstein V, Wallace ZS, Warren AS, Wattam AR, Xia F, Yoo H, Zhang Y, Zmasek CM, Scheuermann RH, Stevens RL. 2023. Introducing the Bacterial and Viral Bioinformatics Resource Center (BV-BRC): a resource combining PATRIC, IRD and ViPR. *Nucleic Acids Res* 51:D678–D689.
86. Madeira F, Pearce M, Tivey ARN, Basutkar P, Lee J, Edbali O, Madhusoodanan N, Kolesnikov A, Lopez R. 2022. Search and sequence analysis tools services from EMBL-EBI in 2022. *Nucleic Acids Res* 50:W276-279.
87. UniProt Consortium. 2021. UniProt: the universal protein knowledgebase in 2021. *Nucleic Acids Res* 49:D480–D489.
88. Toro-Roman A, Mack TR, Stock AM. 2005. Structural Analysis and Solution Studies of the Activated Regulatory Domain of the Response Regulator ArcA: A Symmetric Dimer Mediated by the α4-β5-α5 Face. *J Mol Biol* 349:11–26.
89. Grant CE, Bailey TL, Noble WS. 2011. FIMO: scanning for occurrences of a given motif. *Bioinforma Oxf Engl* 27:1017–1018.

Chapter 3 Utilization of Respiration Components during Bacteremia

3.1 Summary

C. freundii, *K. pneumoniae*, and *E. coli* require energy production to meet the relatively high growth rates we have identified for them previously in the murine spleen during bacteremia. The contribution of ArcA to fitness during bacteremic infection by *C. freundii* and *K. pneumoniae* but not *E. coli* serves as an important indication of which metabolic pathways the bacteria utilize within this host environment. Here I demonstrate that *C. freundii* does not utilize certain metabolic machinery and related processes of aerobic and anaerobic respiration. This finding is in agreement with expectations from the previous ArcA studies that *C. freundii* relies chiefly on fermentation in the murine bacteremia model. Requirement of ubiquinone in specific organs by *E. coli* suggests this species utilizes both aerobic and anaerobic respiration to meet energetic needs during infection. Ubiquinone was found to be critical for *K. pneumoniae* in both the spleen and liver and provides a new context for the seemingly paradoxical requirement of ArcA for this species. Overall, this chapter continues to serve as a foundation for generating hypotheses regarding bacterial metabolic activity during bacteremia at the pathway level.

3.2 Introduction

Successfully identifying the requirement of ArcA, a transcription factor, for fitness optimization naturally implicates the members of its regulon in potentially contributing to fitness. To date, ArcA has largely been characterized as a repressor through occluding other regulators promoters (1). Existing Tn-seq data sets thus do not necessarily inform the potential

contribution to fitness of many of ArcA's target genes/operons because loss of function of a repressed genetic element in theory would not impact fitness negatively. To this end, very few genes in model ArcA regulons have been identified as fitness factors by Tn-seq (2–7). Using the existing Tn-seq data to generate further hypotheses regarding metabolic requirements for bacteremia based on what is known about regulation by ArcA thus requires examination of components of the pathways not regulated by this transcription factor. From here, our understanding of the metabolic networks fueling bacteremia can deepen.

The facultative anaerobes utilizing ArcA are capable of diverse metabolic processes (8). The fitness defect associated with *arcA* in *C. freundii*, *K. pneumoniae,* and *S. marcescens* suggests that some of these processes, namely aerobic and anaerobic respiration, are dispensable. This hypothesis is naturally challenged by the limitations of the murine model. Because the competitive index was only measured at 24 h.p.i. (**Fig. 2.2**), the temporal role of ArcA remains to be determined. The metabolic pathways used during initial colonization may differ from those employed during dissemination or in response to mounting nutritional immunity. The use of aerobic and anaerobic respiration during bacteremia can thus not be discounted based on the requirement of ArcA at some stage(s) of infection, and this possibility can especially not be ignored for *E. coli* for which ArcA was not found to be a fitness factor in the bacteremia model. The transposon sequencing screens which identified *arcA* as a gene contributing to fitness for multiple species can also be used to identify specific metabolic components contributing to infection development. Here, the contribution of genes encoding synthesis pathways and cellular structures pertinent to respiration are examined.

3.3 Bacterial ubiquinone synthesis

Aerobic respiration requires the electron transport chain to participate in chemiosmosis

through a series of electron transfers by which dispensed energy is used to create a proton gradient. One of the operons most strongly repressed by ArcA is *nuoABCEFGHIJKLMN* (2), which encodes the first respiratory complex (9). Nevertheless, Tn-seq results show genes encoding NADH::quinone oxidoreductases may contribute to fitness for *C. freundii*, *E. coli*, and *K. pneumoniae* (4, 5, 7). A key set of molecules that link the initial respiratory complexes receiving electrons from NADH and $FADH_2$ with downstream components of the ETC are quinones (10). *ubiH* encodes an enzyme in the synthesis pathway of ubiquinone (11), which is the dominant quinone of aerobic respiration. Based on validation of *arcA* as encoding a fitness factor for *C. freundii* and *K. pneumoniae* but not *E. coli*, loss of *ubiH* would be expected to decrease the fitness of *E. coli* but not *C. freundii* or *K. pneumoniae*. Competition experiments between wild-type strains and *ubiH* mutant constructs (**Table 6**) were thus conducted in a murine bacteremia model to assess if ubiquinone and by proxy aerobic respiration are necessary for fitness at any point of infection. Each species colonized the liver and spleen 24-hours post inoculation (**Fig. 3.1A**). Loss of *ubiH* did not result in a fitness defect in either organ for *C. freundii*, and the competitive index in the liver on the contrary trended towards a fitness advantage (**Fig. 3.1B**). In *E. coli* a modest yet significant fitness defect was found for the *ubiH* mutant construct in the liver but not the spleen (**Fig. 3.1B**). Unexpectedly, *ubiH* was outcompeted 8.5-fold in the liver and 2.2-fold in the spleen for *K. pneumoniae* (**Fig. 3.1B**).

Given the variation in competitive indices associated with *ubiH* loss, growth of *ubiH* constructs was studied alongside isogenic wild-type strains *in vitro* to identify any further species differences. Under aerobic conditions the *ubiH* mutants for all species grew more slowly and with an hours-long lag relative to the wild-type strains as expected (**Fig. 3.2A**). The delayed growth of *ubiH* constructs under aerobic conditions further underscores the ability of these

species to switch to other metabolic pathways to meet energy production needs. Any growth differences between *ubiH* mutants and wild-type cultures were ameliorated under anaerobic conditions (**Fig. 3.2B**). This finding is important because it demonstrates the specificity of targeting aerobic but not anaerobic respiration by interrupting ubiquinone synthesis. In a rich medium such as LB, alternative electron acceptors would be available for anaerobic respiration in the absence of oxygen, and the growth curves under strict anaerobiosis suggest anaerobic respiration pathways remain intact in the *ubiH* mutants. The requirement of ubiquinone synthesis in supporting bacterial fitness in infection of the bloodstream environment is evidently variable by species and organ. UbiH and by extension ubiquinone production was dispensable in *C. freundii* bacteremia as expected, so the necessity of other elements of the electron transport chain necessary for aerobic and anaerobic respiration was investigated.

Table 6: Strains and Constructs Used in Chapter 3

Species	Parent Strain	Genotype	Description	Reference*
C. freundii	UMH14	wild-type strain		Anderson 2018 (11)
C. freundii	UMH14	Δ*atp* operon	Δ*atp* operon::*nptII* knock-out construct	This study (AB/GS)
C. freundii	UMH14	Δ*entB* receptor	Δ*atp* operon::*nptII* knock-out construct	This study (AB/GS)
C. freundii	UMH14	Δ*hscBA*	Δ*hscBA*::*nptII* knock-out construct	This study (AB/GS)
C. freundii	UMH14	Δ*lpdA*	ΔlpdA::*nptII* knock-out construct	This study (AB/GS)
C. freundii	UMH14	Δ*menA*	Δ*menA*::*nptII* knock-out construct	This study (GS)
C. freundii	UMH14	Δ*ubiG*	Δ*ubiG*::*nptII* knock-out construct	This study (GS)
C. freundii	UMH14	Δ*ubiH*	Δ*ubiH*::*nptII* knock-out construct	This study (GS)
E. coli	CFT073	wild-type strain		Welch 2002 (77), Mobley 1990 (78)
E. coli	CFT073	Δ*ubiH*	Δ*ubiH*::*nptII* knock-out construct	This study (AB/GS)
K. pneumoniae	KPPR1	wild-type		Broberg 2014 (79)
K. pneumoniae	KPPR1	Δ*ubiH*	Δ*ubiH*::*nptII* knock-out construct	This study (GS)

* Lambda-red constructs designed and engineered by Aric Brown (AB) and/or Dr. Geoffrey Severin (GS)

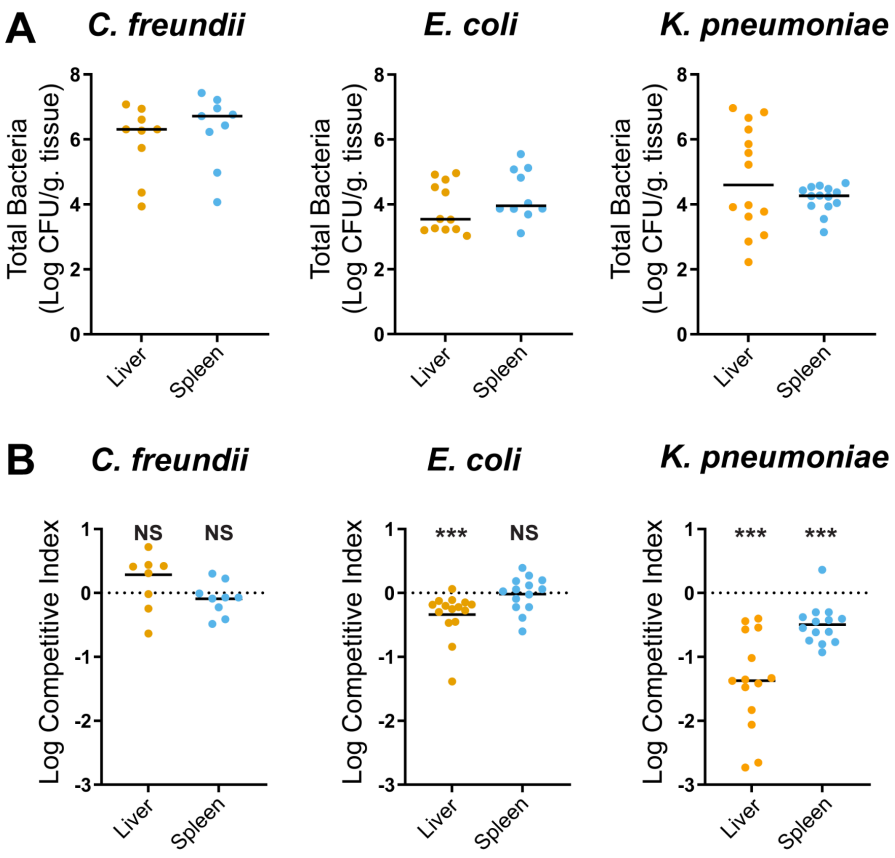

Figure 3.1: Contribution of *ubiH* to bacteremia fitness is species-dependent and site-specific. Wild-type (WT) strains and Δ*arcA* mutant constructs were cultured to mid-log phase in LB. Cells were washed in PBS and mixed 1:1 to prepare the inoculum for each species at an average target total CFU of 1 x 10^8 *(C. freundii*), 1 x 10^5 (*K. pneumoniae*), and 2 x 10^6 (*E. coli*). Mice were sacrificed 24 hours post tail vein inoculation, and organs were harvested and plated on LB with and without antibiotics for differential CFU enumeration. **(A)** Total CFU were normalized to tissue weight for all organs. **(B)** Competitive indices (CI) were calculated by dividing the ratio of *arcA* mutant counts to WT counts in the inoculum (input) to that in the organs (output). Dots in the burden and CI graphs represents the organ from one mouse, and median values are presented as solid horizontal lines. Significance of log transformed CI was determined via a one-sample *t*-test with a null hypothetical value of zero, represented as a dotted a line. *p*-values: *≤0.05, **≤0.01, ***≤0.001, NS = not significant

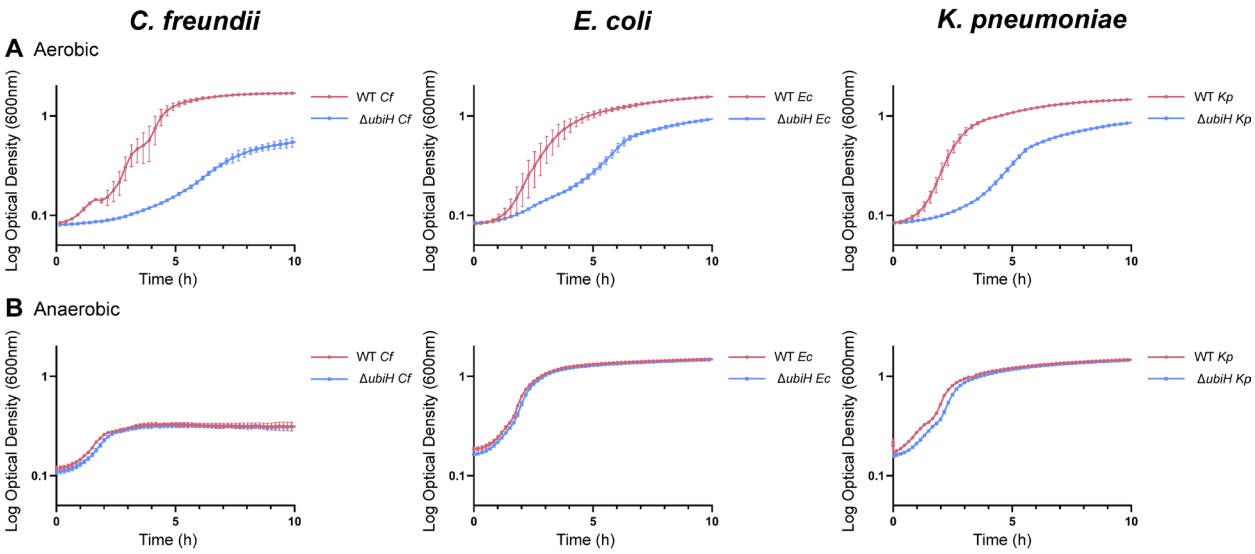

Figure 3.2: *ubiH* mutants exhibit growth defects under aerobic but not anaerobic conditions. Strains were cultured overnight in LB under anaerobic or aerobic conditions and then normalized based on OD600 in PBS. LB was inoculated with normalized overnight cultures, and plates were incubated at 37° under the same oxygenation condition as the corresponding overnight culture. OD600¬ was measured with a plate reader every 15 (aerobic) or 10 (anaerobic) minutes. Aerobic plates were incubated with shaking in between readings while anaerobic plates were stored statically. Results are representative of three independent experiments. Each strain was grown in triplicate, and the average with standard deviation was plotted above.

3.4 Respiration by *C. freundii*

Quinone production is an extensive process that involves synthesis of two distinct structures, a polar head group and an apolar isoprenoid tail (15). The three main facultative anaerobe quinones, ubiquinone, menaquinone, and demethylmenaquinone, share many precursor molecules and processing enzymes (16). Furthermore, quinone intermediates may retain some levels of activity, making individual quinone mutants difficult to characterize. To support the finding that ubiquinone is dispensable for *C. freundii* bacteremia, a second ubiquinone synthesis mutant, *ubiG*, was tested in the murine bacteremia model. *ubiG* encodes an enzyme that is involved in two separate steps of ubiquinone synthesis as opposed to UbiH which only catalyzes one reaction step (16). High bacterial burdens were achieved in a competition between wild-type *C. freundii* and a *C. freundii ubiG* mutant in the murine bacteremia model (**Fig. 3.3A**), and no significant fitness defect was observed in the liver or spleen (**Fig. 3.3B**). Similarly, the

contribution of anaerobic respiration to bacteremic fitness for *C. freundii* was tested by competing a synthesis mutant of the main quinone of anaerobic respiration, menaquinone, against the wild-type strain. Bacterial burdens in competitions between wild-type *C. freundii* and a *menA* mutant reached expected levels in the liver and spleen (**Fig. 3.3A**). Average competitive indices showed *menA* does not contribute to fitness in either organ site to a statistical degree (**Fig. 3.3B**). The growth of the *menA* mutant construct was also studied under aerobic and anaerobic mutants to assess oxygen-dependent growth defects (**Fig. S3.6)**. In contrast to the *ubiH* mutant (**Fig. 3.2**), the *menA* mutant had a growth advantage over the wild-type strain under aerobic conditions (**Fig. S3.6A**) but reached a lower final density than the wild-type strain under anaerobic conditions (**Fig. S3.6B**).

The last mutant of the electron transport chain tested in the murine bacteremia model was a deletion mutant of the operon encoding the ATP synthase complex, *atpIBEFHAGDC* (17).

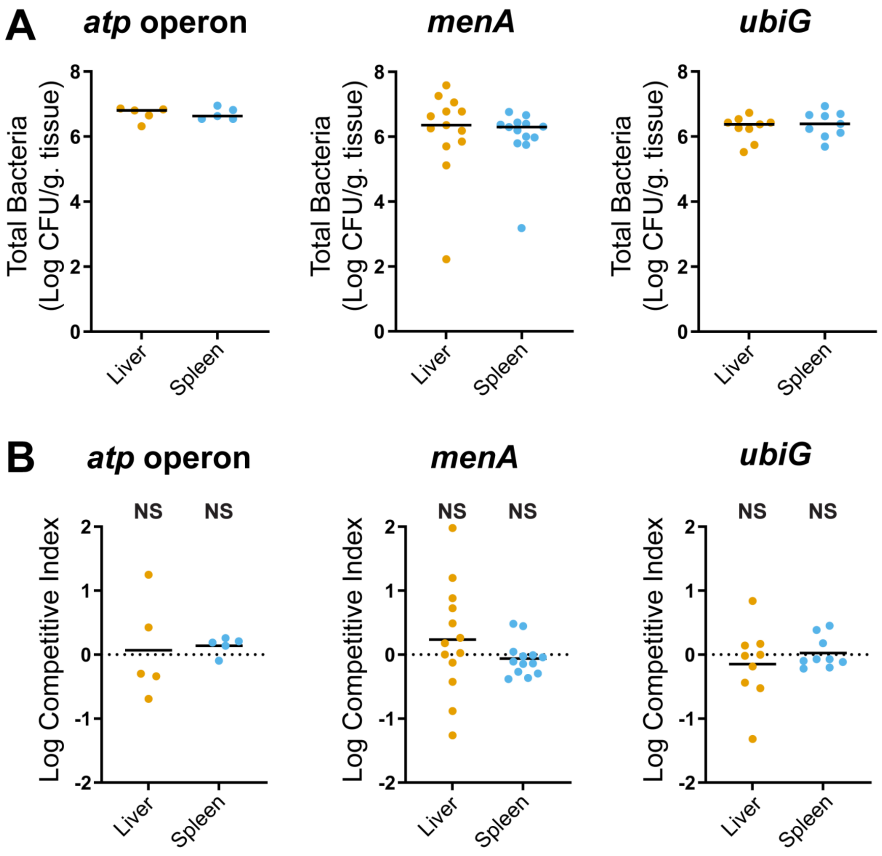

Figure 3.3: Key components of the electron transport chain are dispensable for *C. freundii* fitness in the liver and spleen during bacteremia. Wild-type (WT) strains and Δ*atpIBEFHAGDC*, Δ*menA*, and Δ*ubiG* mutant constructs were cultured to mid-log phase in LB. Cells were washed in PBS and mixed 1:1 to prepare the inoculum for each species at an average target total CFU of 1 x 10^8Mice were sacrificed 24 hours post tail vein inoculation, and organs were harvested and plated on LB with and without antibiotics for differential CFU enumeration. **(A)** Total CFU were normalized to tissue weight for all organs. **(B)** Competitive indices (CI) were calculated by dividing the ratio of *arcA* mutant counts to WT counts in the inoculum (input) to that in the organs (output). Dots in the burden and CI graphs represents the organ from one mouse, and median values are presented as solid horizontal lines. Significance of log transformed CI was determined via a one-sample *t*-test with a null hypothetical value of zero, represented as a dotted a line. *p*-values: *≤0.05, **≤0.01, ***≤0.001, NS = not significant

This enzyme is a shared feature of aerobic and anaerobic respiration that yields ATP proportional to the proton motive force generated at the electron transport chain (9). If *C. freundii* undergoes neither aerobic respiration nor anaerobic respiration during bacteremia, ATP synthase should be dispensable. In support of this hypothesis, the *atp* operon *C. freundii* mutant was not outcompeted by wild-type during bacteremia in the liver or spleen (**Fig. 3AB**). This set of competition experiments supports the conclusion that *C. freundii* does not rely on respiration during bacteremia and that other metabolic pathways including fermentation dominate. This finding agrees with the requirement of ArcA during infection for this species in the same organ **(Fig. 2.2B**).

The electron transport chain is the site of the bulk of ATP production during aerobic and anaerobic respiration, but many upstream processes are needed to support the production of electron carriers such as NADH and maintenance of the ETC itself. A hypothesis explored in Chapter 2 was the need for ArcA to repress respiration when iron was not available to the cell as many important TCA and ETC enzymes require iron in some form as a cofactor (18, 19). If respiration components require iron yet are dispensable in the bloodstream environment where iron is scarce, mechanisms acquiring iron and transferring it to these components should also be dispensable. To this end, the fitness of a *C. freundii* mutant lacking a FepA-like ferric siderophore receptor (CUC46_RS02895) was determined. Siderophores are an important molecule for iron scavenging by bacteria during the host (20). By testing the fitness of a receptor

required to bring a siderophore bound to iron back into the cell, cross-feeding by wild-type cells is avoided. Iron already within the cell needs to be carefully transported to avoid adverse reactions such as Fenton chemistry. For instance, a set of chaperones are required to bring iron-sulfur clusters to respiratory complexes in the ETC (21). *hscBA* encodes one of these chaperons, and a *C. freundii hscBA* mutant was also competed against wild-type *C. freundii* with the expectation that *hscBA* mutants should not exhibit a defect. The murine experiments competing the siderophore receptor mutant and *hscBA* mutant separately against wild-type cells achieved necessary burdens in the liver and spleen for fitness determination (**Fig. 3.4A**). Neither mutant was outcompeted in the liver or spleen (**Fig. 3.4B**), which indicates mechanisms supporting iron acquisition and usage by *C. freundii* should be studied further given the potential for compensatory or other preferred strategies. These results further imply *C. freundii* does not respire during bacteremia and furthers our understanding of how this pathogen is able to

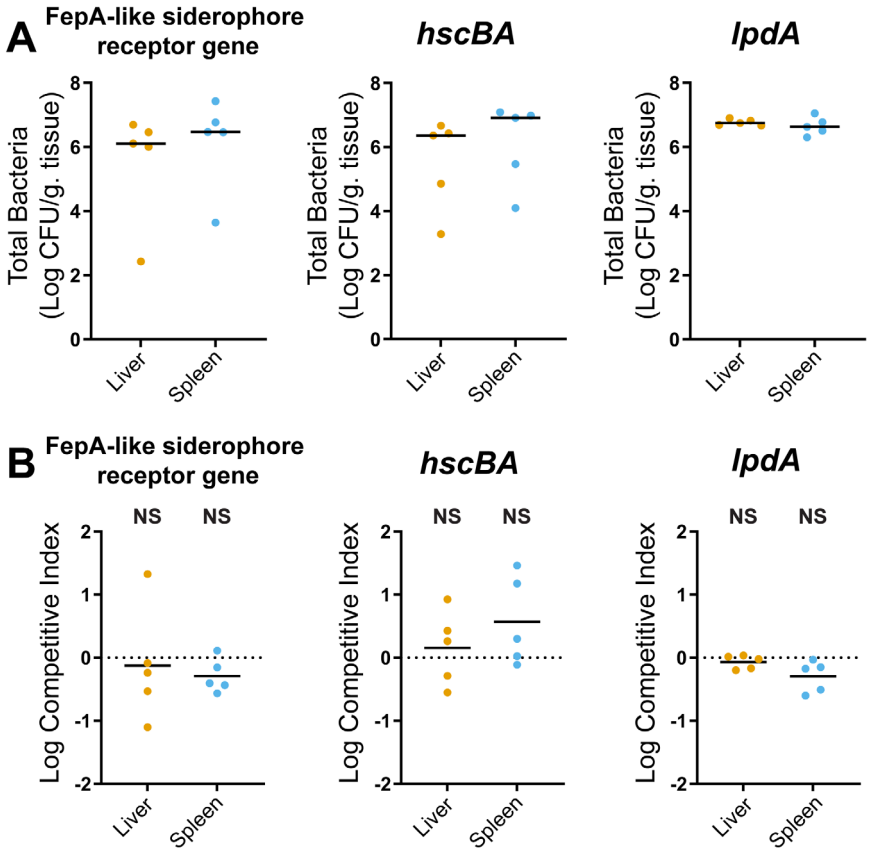

Figure 3.4: *C. freundii* mutants lacking a siderophore receptor, an iron sulfur cluster chaperone, and an enzyme of the pyruvate dehydrogenase are not outcompeted by the wild-type strain in the liver and spleen during bacteremia. Wild-type (WT) strains and ΔFep-like siderophore receptor, Δ*hscBA*, and Δ*lpdA* mutant constructs were cultured to mid-log phase in LB. Cells were washed in PBS and mixed 1:1 to prepare the inoculum for each species at an average target total CFU of 1 x 10^8Mice were sacrificed 24 hours post tail vein inoculation, and organs were harvested and plated on LB with and without antibiotics for differential CFU enumeration. **(A)** Total CFU were normalized to tissue weight for all organs. **(B)** Competitive indices (CI) were calculated by dividing the ratio of *arcA* mutant counts to WT counts in the inoculum (input) to that in the organs (output). Dots in the burden and CI graphs represents the organ from one mouse, and median values are presented as solid horizontal lines. Significance of log transformed CI was determined via a one-sample *t*-test with a null hypothetical value of zero, represented as a dotted a line. *p*-values: *≤0.05, **≤0.01, ***≤0.001, NS = not significant

successfully colonize the host bloodstream environment.

The electron transport chain performs chemiosmosis via the reduction potential provided by the electrons delivered to complex I and complex II by NADH and $FADH_2$ (8). These electron carriers are generated from their oxidized form from energy released by a series of catabolic reactions. The bulk of electron carriers fueling aerobic and anaerobic respiration are reduced via the citric acid cycle. An important complex linking pyruvate, an end product of glycolysis, with the citric acid cycle is the pyruvate dehydrogenase complex (22). *lpdA* encodes an enzyme that is a part of this complex. A mutant lacking *lpdA* would be unable to shuttle catabolites of glycolysis into the citric acid cycle and thus would not be able to complete aerobic or anaerobic respiration (23). For *C. freundii, lpdA* should be dispensable in the liver and spleen during bacteremia based on the previous results demonstrating other components of aerobic and anaerobic respiration are expendable. In a murine model competing *C. freundii* wild-type and *lpdA* mutant, adequate bacterial burdens were achieved in both organ sites (**Fig3.4A**), and the *lpdA* mutant construct was not outcompeted by the wild-type strain as predicted (**Fig3.4B**). In summary, disruption of multiple cellular processes supporting respiration by *C. freundii* do not contribute to fitness during bacteremia.

3.5 Discussion

C. freundii, *E coli,* and *K. pneumoniae* are all Gram-negative facultative anaerobes capable of aerobic and anaerobic respiration as well as fermentation. Understanding how they regulate utilization of these competing pathways during bacteremia is necessary to fully understand their pathogenesis. Competition experiments in the murine bacteremia model with a mutant of the enzyme UbiH of the ubiquinone synthesis pathway showcased the importance of studying multiple species and anatomical sites when examining metabolic pathways *in vivo*. The lack of a *C. freundii* fitness phenotype in the spleen and liver following loss of *ubiH* aligned more straightforwardly with the *arcA* mutant results. Repression of respiration by ArcA theoretically negates the requirement for quinones, and the absence of a *ubiH*-mediated fitness defect supports the hypothesis that *C. freundii* does not rely on aerobic respiration in the murine model. The finding that *ubiH* is dispensable in the spleen but not the liver for *E. coli* in the context of *arcA* not contributing to fitness in either site may provide evidence that different metabolic pathways are being utilized. ArcA represses key enzymes of both aerobic and anaerobic respiration. As ubiquinone is the major quinone of aerobic respiration, the combination of the *arcA* and *ubiH* results could imply *E. coli* respires aerobically in the liver and anaerobically in the spleen. Both processes align with previous studies illustrating *E. coli* during urinary tract infection which employs the tricarboxylic acid cycle. I would further hypothesize that in contrast with *C. freundii*, an *E. coli menA* mutant would experience a fitness defect in the spleen. The significant competitive defects of the *K. pneumoniae ubiH* mutant in the spleen and liver were the most surprising when considering the biggest *arcA* defect was for *K. pneumoniae*. Although unexpected, these results still inform the potential metabolic pathways *K. pneumoniae* utilizes during bacteremia. It is possible that this species utilizes aerobic respiration and

fermentation at different stages of infection. Another possibility is *K. pneumoniae* chiefly performs aerobic respiration and ArcA represses this pathway transiently. It may be advantageous to not perform aerobic respiration at full capacity when external ROS from the host are threatening. Balancing maximally efficient energy production with inevitable internal ROS production may be a strategy to survive in the infection environment (24). As reviewed in the introduction, ArcA has been implicated in responding to ROS in other contexts. In a similar context, ubiquinone itself can also play a role in resisting oxidative stress (25). The set of *ubiH* experiments overall demonstrates the utility of comparing global metabolic regulators with localized pathway components in refining working models of pathogenesis.

The influence of ArcA but not UbiH on fitness during *C. freundii* infection leads to the hypothesis that aerobic respiration is not the dominant pathway for this species in this bacteremia model. A lack of phenotype with loss of *ubiG* and *atpIBEFHAGDC* further supported this theory. In consideration of the potential compensatory mechanisms provided by the other quinone species, *E. coli* mutants which lack UQ may respiration partially rescued by DMK (16). The neutrality of the *atpIBEFHAGDC* mutation in regards to fitness coupled with the absence of a competitive defect for an enzyme in the menaquinone synthesis pathway, MenA, also indicated anaerobic respiration was not the process *C. freundii* was relying on for energy production. A caveat of this result is the *menA* mutant lacks demethylmenaquinone in addition to menaquinone due to a shared synthesis pathway, but additional loss of quinones (MK and DMK) is not likely to restore fitness associated with losing just one (MK). The dispensability of electron transport elements of aerobic and anaerobic respiration allows for further inferences regarding upstream processes leading to the ETC (**Fig. 3.5)**. The TCA cycle is a critical pathway for providing electron carriers for the ETC for both respiratory options. Preventing entry of carbon skeletons

from glycolysis into the TCA should not affect fitness if the TCA cycle is not being utilized for production of NADH/$FADH_2$. The strategy of not utilizing the TCA for energy production may be metabolically advantageous in the host environment. Indeed, loss of only one of the eight TCA enzymes, oxoglutarate dehydrogenase, resulted in a significant splenic fitness defect in the *C. freundii* Tn-seq study (5), demonstrating the potential dispensability of the TCA cycle overall during *C. freundii* bacteremia. SspA, a stringent response protein, was found to contribute to fitness in *C. freundii*, *K. pneumoniae*, and *S. marcescens* (5–7). One theory for SspA induction is amino acid starvation (26). If bacterial cells in the bloodstream are not able to receive amino acids (or short peptides) from the host environment, preserving amino acids for synthesis may be beneficial. Further *C. freundii* studies should test the hypothesis that this species favors fermentation over either respiratory process by further competing *C. freundii* mutants lacking key glycolytic or respiratory enzymes in the murine model of bacteremia.

Iron scavenging is a well-studied process for bacteria in infection sites including the bloodstream. With iron being a requirement for many critical enzymes, the ability to accumulate iron is a high priority as is evidenced by the numerous mechanisms bacteria have for acquisition (20). The lack of a fitness defect associated with loss of the FepA-like ferric siderophore receptor presents multiple possibilities. *C. freundii* may be acquiring iron through other mechanisms, or its iron requirements do not necessitate the procurement of additional iron within the host environment during the tested timeframe. Another hypothesis that aligns with the ArcA study is *C. freundii* is not utilizing respiratory enzymes, so the bacterial cells do not need iron in the form of iron-sulfur clusters that such enzymes utilize. This interpretation is supported by the dispensability of the HscBA chaperone that plays a role in shielding iron-sulfur clusters from aberrant oxidation before incorporation into the respiratory complexes. Future studies should

examine if other enzymes that utilize iron in various forms and the machinery that manages intracellular iron pools are also dispensable in *C. freundii* bacteremia and if this extends to other anatomical sites where iron abundancy differs. Such studies would also benefit from interrogating the fitness of *C. freundii* mutants in which multiple iron acquisition mechanisms are disrupted and respiratory enzymes mutated. In summary, examination of fitness of genes involved aerobic and anaerobic respiration during bacteremia has shown related species of family *Enterobacteriaceae* rely on different metabolic pathways during infection in an organ-specific manner.

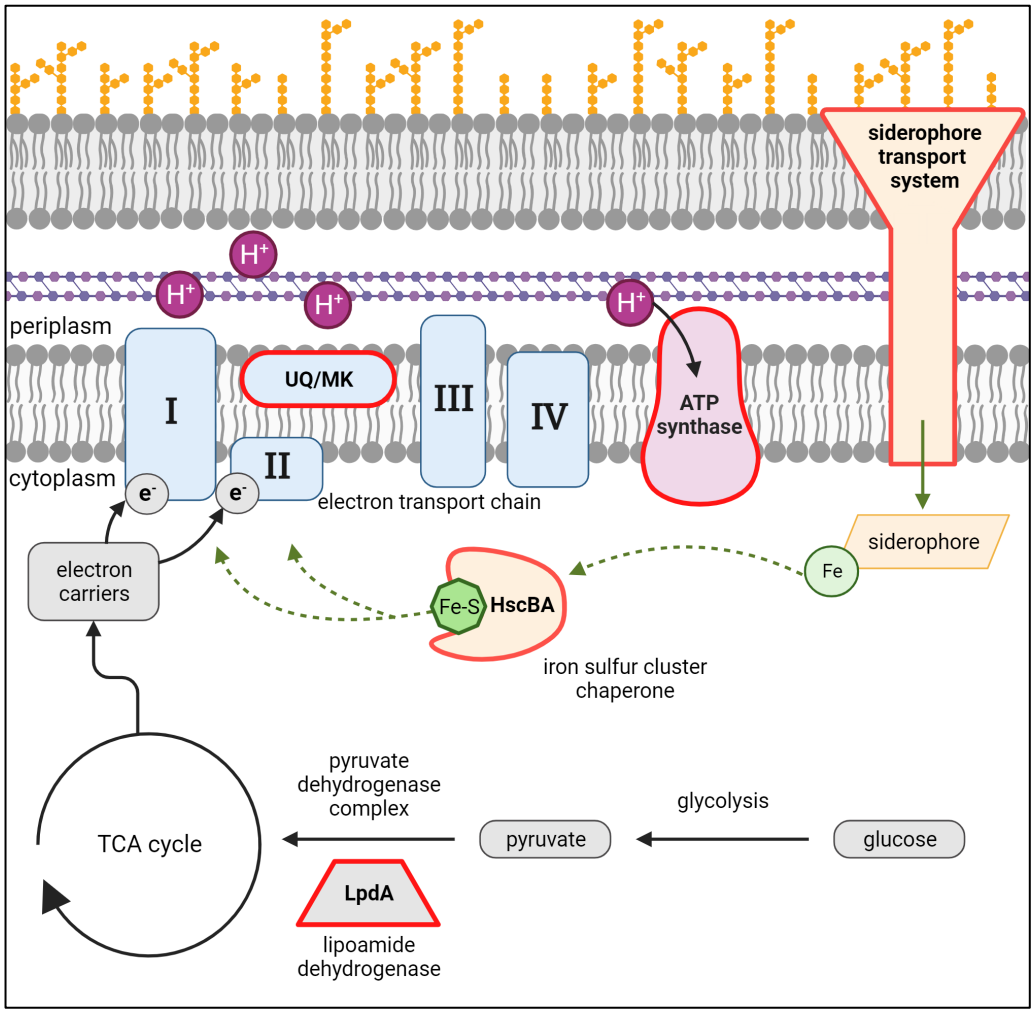

Figure 3.5: Aerobic and anaerobic respiration and cellular processes underpinning them are dispensable during *C. freundii* bacteremia. Ubiquinone (UQ) and menaquinone (MK) are the dominant quinones of aerobic and anaerobic respiration, respectively, and play key roles in facilitating electron transfer between complexes I/II of the electron transport chain and cytochrome oxidases. Complex I and II require iron-sulfur clusters to function, and HscBA serves as a chaperone for these clusters to ensure proper delivery to the complexes. Iron is a limiting nutrient within the host environment, and the FepA-like ferric siderophore receptor imports siderophores bound to iron, which can then be used as a cofactor such as in an iron-sulfur cluster. LpdA is an enzyme of the pyruvate dehydrogenase complex and plays a role in ultimately feeding pyruvate into the TCA cycle to generate electron carriers for the electron transport chain. All of these cellular components, which are boxed in red, are dispensable in the spleen and liver during *C. freundii* bacteremia.

3.6 Supplemental Figures

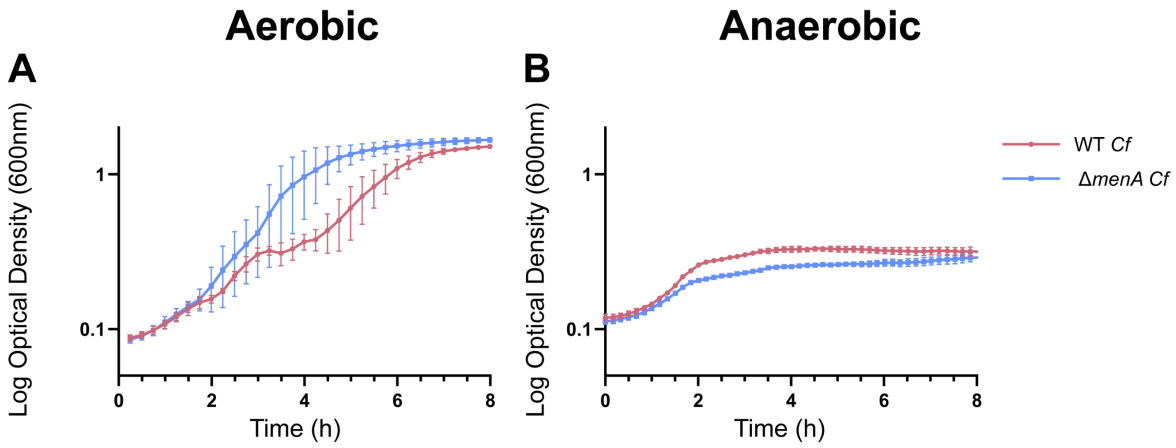

Supplemental Figure 3.6: The *C. freundii menA* mutant construct exhibits a growth advantage under aerobic conditions but a growth defect under anaerobic conditions. The *C. freundii* wild-type strain and *menA* mutant construct were cultured overnight in LB under aerobic (**A**) or anaerobic (**B**) conditions and then normalized based on OD_{600} in PBS. LB was inoculated with normalized overnight cultures, and plates were incubated at 37° under the same oxygenation condition as the corresponding overnight culture. OD_{600} was measured with a plate reader every 15 (aerobic) or 10 (anaerobic) minutes. Aerobic plates were incubated with shaking in between readings while anaerobic plates were stored statically. Results are representative of three independent experiments. Each strain was grown in triplicate, and the average with standard deviation was plotted above.

3.7 Materials and Methods

The murine model of bacteremia was performed as described in the Materials and Methods section of Chapter 2 except only female C57BL/6 mice were utilized. Aerobic and anaerobic growth curves were generated as described in Chapter 2 with LB. Constructs were created with the oligonucleotides in **Supplemental Table 7.**

3.8 Acknowledgements

Sara Smith, Margaret Gaca, and Stephanie Himpsl are acknowledged for assisting with the murine experiments. Dr. Geoffrey Severin is thanked for collaborating for the mouse experiments, experimental design and data interpretation for the anaerobic growth curves, and for providing additional mouse competition and aerobic growth data as noted. Some of the bacteremia model work was completed in conjunction with laboratory of Dr. Michael Bachman as part of a multiple-species study. I also thank Dr. Eric Martens for technical support and equipment used during the anaerobic studies. The summary figure was created with BioRender.com. I lastly acknowledge the use of C57BL/6 mice in the bacteremia model.

3.9 References

1. Park DM, Kiley PJ. 2014. The influence of repressor DNA binding site architecture on transcriptional control. *mBio* 5:e01684-01614.
2. Park DM, Akhtar MdS, Ansari AZ, Landick R, Kiley PJ. 2013. The Bacterial Response Regulator ArcA Uses a Diverse Binding Site Architecture to Regulate Carbon Oxidation Globally. *PLoS Genet* 9.
3. Iyer MS, Pal A, Srinivasan S, Somvanshi PR, Venkatesh KV. 2021. Global Transcriptional Regulators Fine-Tune the Translational and Metabolic Efficiency for Optimal Growth of Escherichia coli. *mSystems* 6.
4. Subashchandrabose S, Smith SN, Spurbeck RR, Kole MM, Mobley HLT. 2013. Genome-Wide Detection of Fitness Genes in Uropathogenic *Escherichia coli* during Systemic Infection. *PLoS Pathog* 9.
5. Anderson MT, Mitchell LA, Zhao L, Mobley HLT. 2018. *Citrobacter freundii* fitness during bloodstream infection. *Sci Rep* 8:11792.
6. Anderson MT, Mitchell LA, Zhao L, Mobley HLT. 2017. Capsule Production and Glucose Metabolism Dictate Fitness during *Serratia marcescens* Bacteremia. *mBio* 8.
7. Holmes CL, Wilcox AE, Forsyth V, Smith SN, Moricz BS, Unverdorben LV, Mason S, Wu W, Zhao L, Mobley HLT, Bachman MA. 2023. *Klebsiella pneumoniae* causes bacteremia using factors that mediate tissue-specific fitness and resistance to oxidative stress. bioRxiv https://doi.org/10.1101/2023.02.23.529827.
8. Ward B. 2015. Chapter 11 - Bacterial Energy Metabolism, p. 201–233. *In* Tang, Y-W, Sussman, M, Liu, D, Poxton, I, Schwartzman, J (eds.), Molecular Medical Microbiology (Second Edition). Academic Press, Boston.
9. Unden G, Dünnwald P. 2008. The Aerobic and Anaerobic Respiratory Chain of *Escherichia coli* and *Salmonella enterica*: Enzymes and Energetics. *EcoSal Plus* 3:10.1128/ecosalplus.3.2.2.

10. Sharma P, Mattos MJT de, Hellingwerf KJ, Bekker M. 2012. On the function of the various quinone species in *Escherichia coli*. *FEBS J* 279:3364–3373.
11. Meganathan R, Kwon O. 2009. Biosynthesis of Menaquinone (Vitamin K2) and Ubiquinone (Coenzyme Q). *EcoSal Plus* 3.
12. Welch RA, Burland V, Plunkett G, Redford P, Roesch P, Rasko D, Buckles EL, Liou S-R, Boutin A, Hackett J, Stroud D, Mayhew GF, Rose DJ, Zhou S, Schwartz DC, Perna NT, Mobley HLT, Donnenberg MS, Blattner FR. 2002. Extensive mosaic structure revealed by the complete genome sequence of uropathogenic *Escherichia coli*. *Proc Natl Acad Sci U S A* 99:17020–17024.
13. Mobley HL, Green DM, Trifillis AL, Johnson DE, Chippendale GR, Lockatell CV, Jones BD, Warren JW. 1990. Pyelonephritogenic *Escherichia coli* and killing of cultured human renal proximal tubular epithelial cells: role of hemolysin in some strains. *Infect Immun* 58:1281–1289.
14. Broberg CA, Wu W, Cavalcoli JD, Miller VL, Bachman MA. 2014. Complete Genome Sequence of *Klebsiella pneumoniae* Strain ATCC 43816 KPPR1, a Rifampin-Resistant Mutant Commonly Used in Animal, Genetic, and Molecular Biology Studies. *Genome Announc* 2.
15. Nowicka B, Kruk J. 2010. Occurrence, biosynthesis and function of isoprenoid quinones. *Biochim Biophys Acta BBA - Bioenerg* 1797:1587–1605.
16. van Beilen JWA, Hellingwerf KJ. 2016. All Three Endogenous Quinone Species of *Escherichia coli* Are Involved in Controlling the Activity of the Aerobic/Anaerobic Response Regulator ArcA. *Front Microbiol* 7:1339.
17. Kasimoglu E, Park SJ, Malek J, Tseng CP, Gunsalus RP. 1996. Transcriptional regulation of the proton-translocating ATPase (*atpIBEFHAGDC*) operon of *Escherichia coli*: control by cell growth rate. *J Bacteriol* 178:5563–5567.
18. Roche B, Aussel L, Ezraty B, Mandin P, Py B, Barras F. 2013. Iron/sulfur proteins biogenesis in prokaryotes: Formation, regulation and diversity. *Biochim Biophys Acta BBA - Bioenerg* 1827:455–469.
19. Cotter PA, Darie S, Gunsalus RP. 1992. The effect of iron limitation on expression of the aerobic and anaerobic electron transport pathway genes in *Escherichia coli*. *FEMS Microbiol Lett* 100:227–232.
20. Caza M, Kronstad JW. 2013. Shared and distinct mechanisms of iron acquisition by bacterial and fungal pathogens of humans. *Front Cell Infect Microbiol* 3:80.
21. Vickery LE, Cupp-Vickery JR. 2007. Molecular chaperones HscA/Ssq1 and HscB/Jac1 and their roles in iron-sulfur protein maturation. *Crit Rev Biochem Mol Biol* 42:95–111.
22. de Kok A, Hengeveld AF, Martin A, Westphal AH. 1998. The pyruvate dehydrogenase multi-enzyme complex from Gram-negative bacteria. *Biochim Biophys Acta BBA - Protein Struct Mol Enzymol* 1385:353–366.
23. Li M, Ho PY, Yao S, Shimizu K. 2006. Effect of lpdA gene knockout on the metabolism in *Escherichia coli* based on enzyme activities, intracellular metabolite concentrations and metabolic flux analysis by 13C-labeling experiments. *J Biotechnol* 122:254–266.
24. Anand A, Chen K, Yang L, Sastry AV, Olson CA, Poudel S, Seif Y, Hefner Y, Phaneuf PV, Xu S, Szubin R, Feist AM, Palsson BO. 2019. Adaptive evolution reveals a tradeoff between growth rate and oxidative stress during naphthoquinone-based aerobic respiration. *Proc Natl Acad Sci* 116:25287–25292.

25. Søballe B, Poole RK. 2000. Ubiquinone limits oxidative stress in *Escherichia coli*. *Microbiol Read Engl* 146 (Pt 4):787–796.
26. Williams MD, Ouyang TX, Flickinger MC. 1994. Starvation-induced expression of SspA and SspB: the effects of a null mutation in *sspA* on *Escherichia coli* protein synthesis and survival during growth and prolonged starvation. *Mol Microbiol* 11:1029–1043.

Chapter 4 Conclusions and Future Directions

4.1 Using ArcA to guide future research

ArcA has long been touted as one of the most powerful regulators of metabolism and is considered the chief regulator of aerobic respiration. This study has demonstrated that ArcA is well-conserved among species but that its role in supporting pathogenesis varies. Clear differences between species emphasize the need to study non-model organisms not only to address public health but also to further basic science. Out of the four species that were studied with the murine bacteremia model, *E. coli* was the only one to not present a fitness defect associated with mutating *arcA*. Notably, almost all the biochemical research and many genetic studies have utilized *E. coli* as the model organism for ArcAB research. The experiments presented here highlight not only the value of studying ArcA function under more conditions but also across species. The conclusion that ArcA can activate the same genes it is known to repress expands the potential functions of ArcA greatly. The high level of conservation of ArcA demonstrated here and by others suggests that while ArcAB may inherently respond to the same intracellular conditions (1), other features of the cell such as membrane structure and nutrient requirements that are specific to species/strains impact how external stimuli ultimately influence intracellular conditions.

Although global regulator networks are complex and highly dependent on culture conditions, this work provides another example of the utility of studying global regulators in guiding examination of bacterial metabolic pathways during infection. Global regulators such as ArcA orient metabolism at the cellular level. Metabolic pathways do not operate independently

of one another, and key information regarding regulation energy and biomass production can be obscured without broader context. For instance, studying a single TCA enzyme in the bacteremia model does not necessarily inform the utilization of respiration overall. It is possible that another branch of the TCA cycle or production of intermediates are enough to yield the electron carriers which fuel the ETC. In this way, the study of global regulators allows for the screening of entire metabolic processes and pathways at once, which also requires the consideration of compensatory mechanisms as metabolic regulatory networks often comprise multiple regulators. Future studies of ArcA in the host environment need to adopt an "omics" approach to appreciate metabolic activity more fully in *arcA* mutants relative to wild-type cells. Because enzymes are regulated at the transcriptional and post-translational levels, transcriptomic studies via RNA-seq are not sufficient to predict metabolite production as they do not fully inform reaction directionality (flux) (2). Proteomics and carbon tracing studies complimenting these sequencing DNA sets are thus necessitated to research how ArcA regulation contributes to specific metabolic reactions in a defined condition. These methodologies will also allow for closer interrogating of the coordination of ArcA with other global and local regulators of metabolism. For example, FNR was found to be dispensable in three of the Tn-seq screens but is considered the partner regulator of ArcA (3–7). If these results validate, another hypothesis to test is if repression of ArcA is more important than activation by FNR in the host environment.

Despite having the same "toolbox" of major metabolic pathways at their disposal, facultative anaerobes rely on different pathways to various extents in the bacteremia model here. Revisiting why facultative anaerobes cause the largest proportion of Gram-negative bacteremia cases with this perspective poses new questions. A leading hypothesis of why they are so successful is their ability to survive in the environment and in the host through metabolic

adaptation (8). However, *A. baumanii* and *P. aeruginosa* are also environmental pathogens capable of successfully colonizing the bloodstream but on the other hand are strict aerobes (9, 10). *Neisseria gonorrhoeae* is a facultative anaerobe yet is restricted to human hosts (11). Given these examples, it is quite notable that a vast majority of Gram-negative pathogens are indeed facultative anaerobes capable of living in the environment and in the host. Metabolic flexibility may be beneficial in that they can transition between metabolic pathways during infection, or it may perhaps refer to the use of different pathways during infection. These species are possibly better described as being metabolically advantaged. This notion would explain why opportunistic bacteria which are facultatively anaerobic are the most common pathogens yet do not necessarily rely on the same metabolic capabilities as one another. In this case, ArcA would not mediate the transition from respiration to fermentation but instead support fermentation during the duration of infection. It remains to be determined if ArcA supports the transition from the environment to the host or transition(s) within the host environment itself. From my work, regulation of metabolism of ArcA appears to be critical only in a subset of species in establishing and optimizing infection. Despite being known for responding to anoxic conditions, ArcAB is responsive in an environment with at least some oxygen available, emphasizing the finding ArcA responds to multiple stimuli beyond absence of oxygen. The ArcA regulon has only been defined in *E. coli*, *Salmonella enterica*, and *Shewenella oneidensis*. There is thus unknown potential for novel, species-specific roles for ArcA in *C. freundii*, *K. pneumoniae*, and *S. marcescens*. A source of species differences that was observed in the *arcA* growth studies and further highlighted by *ubiH* murine competition experiments is oxygen requirement. Shared roles of ArcA among species does not necessitate ArcA is used by these species under the same conditions.

The final consideration of what has been learned studying ArcA in the context of metabolism is how it relates to the concept of virulence. Indeed, ArcA has been shown to contribute to regulation of virulence factors in other species as described in Chapter 1. Here, the importance of ArcA in infection was defined by how it contributed to bacterial fitness with CFU burden serving as the readout. Although highly relevant, abundance of bacterial cells does not necessarily correlate with the ability to cause disease or disease severity. There is certainly more to discover regarding how regulation by ArcA influences pathogenesis during bacteremia regarding providing energy as well as regulating the virulence mechanisms themselves.

4.2 Study limitations

The culmination of this work has revealed novel functions for a global regulator of metabolism of multiple clinical species and provides important information about the metabolic pathways such species utilize during bacteremia. Experimental set-up must be carefully considered when applying these results more broadly. Many experiments were performed under ambient oxygen conditions. This parameter may call into question the applicability of some of the phenotypes to the infection model. In the mouse, bacterial cells likely encounter decreased oxygen levels as described, which can affect metabolism and thus the contribution of ArcA. The 24-hour murine model does not provide temporal information about how ArcA contributes to fitness. Future studies can perform a time course to capture more data points longitudinally to generate hypotheses regarding initial colonization and dissemination as has been previously done by our group (12).

Establishing ArcA conservation and shared phenotypes provided critical pieces of information in understanding how this regulator contributes to fitness. This study compared species with representative strains. ArcA function was not examined among different strains of

the same species but is likely necessary. For instance, an *E. coli* strain not as adept at acquiring iron as the CFT073 strain studied here may rely more heavily on ArcA function when facing iron-limitation within the host environment. As emphasized by the *K. pneumoniae* polymyxin B gene expression study, this work relied on the availability of a published ArcA regulon in *E. coli*. By not comparing the *K. pneumoniae* polymyxin B transcriptome to the ArcA regulon of *K. pneumoniae*, critical genes/operons could have been missed for study. As a result, a criticism of this work is that it identifies ArcA regulation as being important to infection but does not establish directly what that regulation is. An important aspect of regulation not addressed by these studies is the activation and repression of ArcA *in vivo*. Global regulators including ArcA are thought to "push" cells in a certain direction with local regulators taking over at individual pathways or reactions. Any competing feedback from external stimuli and internal signaling needs to be responded to in a coordinated fashion; studying the mechanisms by which ArcA is activated and repressed is thus critical for identifying how bacteria function at the cellular level. Global changes to metabolism are costly, and thus regulation of ArcA in addition to regulation by ArcA should be a key focus of future research.

4.3 Additional mechanisms of ArcA activation

4.3.1 ArcB-independent activation

The complex ArcA-mediated phenotypes observed in these studies suggest additional mechanisms of ArcAB activation exist. Canonical ArcAB models are defined under strict anaerobic conditions, but most of the *in vitro* experiments performed were under ambient oxygen levels. Existing studies coupled with the data from these studies allow for generation of new hypotheses regarding ArcAB activation. The first study demonstrated that ArcA can become partially active independently of ArcB via intramolecular disulfide bonding in oxidizing

conditions (**Fig. 4.1A)** (1). ArcA has been linked to oxidative stress in the host environment previously (13). It is thus conceivable that ArcA can respond to host conditions without ArcB through confirmational changes resulting in partial activity. To determine if this occurs, future studies should examine if *arcB* mutants of *C. freundii*, *K. pneumoniae*, and *S. marcescens* display the same phenotypes as their *arcA* counterparts. If ArcA is acting independently of ArcB in these conditions in wild-type cells, the *arcB* mutants should not behave like *arcA* mutants, barring the control of other response regulators by ArcB.

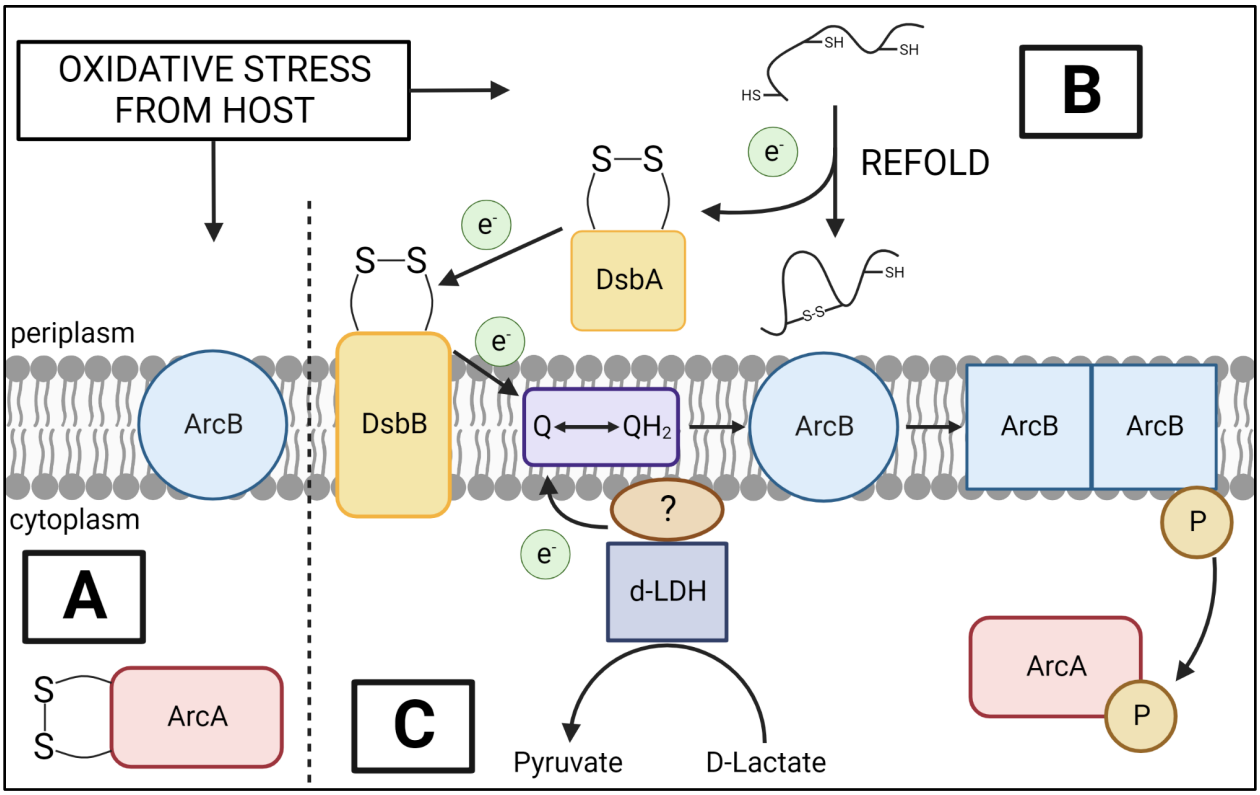

Figure 4.1: Proposed mechanisms of noncanonical activation of ArcAB. (A) Oxidative stress resulting in internal disulfide bond formation of ArcA. **(B)** Activation of ArcB via the DsbAB system which allows for refolding of oxidized periplasmic proteins. **(C)** Oxidation of D-lactate by lactate dehydrogenase may transfer electrons to the quinone pool via an unknown mechanism, resulting in accumulating of reduced quinones that reduce ArcB.

4.3.2 DsbAB

If ArcA ultimately represses respiration, it is not clear how electrons can continue to flow through the ETC to quinones for sustained ArcB activation. Electrons are no longer being carried

to the ETC by NADH and $FADH_2$. This paradox may be addressed by the disposal of electrons at the cell envelope when bacteria encounter exogenous ROS such as from the host immune system. Periplasmic proteins are particularly sensitive to oxidative stress, and metabolic processes do exist to bolster protection in this microenvironment (14). The DsbAB system can act as a receptacle for radicals causing disulfide bond breakages in these proteins (15). DsbAB passes the electrons to quinones to replace its capacity for further electron acceptance. Reduced quinones in this instance could then potentially pass the electrons to ArcB as they do in other reducing conditions resulting in ArcB kinase activation and ArcA phosphorylation (**Fig. 4.1B**). This mechanism would ultimately allow the cell to detect oxidative stress occurring in the periplasm and respond immediately in conjunction with already known responses like switching respiratory complexes (14). ArcB does not have an extensive periplasmic domain (16, 17), so it is currently thought that direct sensing of external conditions by ArcB is not possible. Future work can examine the DsbAB system and its potential connection to ArcAB through study of mutants in wild-type and *arcA*/*arcB* mutant backgrounds.

4.3.3 Lactate

Early studies of the Arc system considered the possibility that certain metabolites could be an activating signal for ArcB (18–21). Although some of these products did enhance ArcB kinase activity or prohibited phosphatase activity, they were ultimately ruled out as the dominant regulator due to their absence in standard aerobiosis. The metabolomic studies here reaffirming the effects of ArcAB on lactate and acetate production may spark continued research of the connection of fermentation products to this two-component system. D-lactate production may still be explored as a potential activator of ArcB kinase activity based on the link of ArcA to fermentation in the presence of oxygen as established here (**Fig. 4.1C**). The enzyme DLD can

convert pyruvate to D-lactate in conjunction with FAD in an NADH-independent manner in contrast to LDH (22). Electrons are transferred to ubiquinone in this case, resulting in its reduction to ubiquinol. Despite the connection of DLD to quinones not being yet fully known, this mechanism could serve as a positive feedback loop in sustaining ArcA activity as ubiquinol is a known activator of ArcB (23). This connection of ArcAB to lactate is especially lucrative when you consider the bloodstream environment during infection. D-lactate from the host microbiome has also been implicated in preventing dissemination by pathogens from the gut (24), and increased levels of L-lactate are a known marker of sepsis (25). The *lpdA* gene encoding the importer of L-lactate (not to be confused with the lactate dehydrogenase enzyme LdhA) was shown in this study for *K. pneumoniae* to be upregulated in response to polymyxin B. A connection to explore is if membrane damage prompts the cell to scavenge for alternative carbon sources like L-lactate. A recent study has demonstrated *H. pylori* requires the L-lactate importer to be resistant to complement in the stomach (26). Precedence thus exists for studying nutrient acquisition as a defense against components of the host immune system, and given the role of ArcA in nutrient utilization, this association should not be overlooked.

4.4 Targeting ArcA as a therapeutic

The antibiotic resistance crisis has accelerated the need for effective treatments of infections by Gram-negative pathogens (27). Two-component systems are lucrative targets for drug development from multiple perspectives (28–30). Two-component systems are not found in animals (31), so chances of cross-reactivity with host cells are decreased. Targeting a global regulator such as ArcA provides the opportunity to impact multiple bacterial processes at once. Importantly, it may be difficult to target the metabolic enzymes themselves given the high level of conservation of central carbon pathways across kingdoms of life, so directing therapeutics

towards unique regulators may be a more fruitful strategy. As opposed to broad-spectrum antibiotics that can negatively affect important commensal microbes of the host microbiome, a drug targeting ArcA should not directly affect strict anaerobes that make up an important part of the microbiome, which do not encode *arcA*. Small molecules directly binding ArcA may also be more effective against multiple species based on the high levels of structural conservation in Order *Enterobacterales* of which many important pathogens are a member. An interesting consideration of selecting ArcA as a drug target is the potential for resistance. Recent approaches to small molecule research for therapeutics has focused on targeting virulence factors that do not directly affect growth rate as a method for decreasing selective pressure (32). Resistance to conventional antibiotics arises due to selective pressure on a bacterial population based on growth, which is why antibiotics are particularly effective against acute infections when bacteria are quickly replicating. As ArcA function impacts growth, considering selection for suppressor mutants following ArcA targeting should not be overlooked. To counter this possibility, however, is evidence that the potential for evolution of resistance decreases in an *arcA* mutant (33). In fact, re-sensitization or loss of resistance to antibiotics is a known trait of *arcA* mutants (34). Like small molecule and phage therapies, targeting ArcA may thus be of most benefit when used in conjunction with existing antibiotic treatments. The results of the study here also provide context for the conditions in which screening of ArcA therapies should be performed. Ultimately, inhibiting ArcA function during infection is only effective when ArcA is active. Uncovering the function of ArcA in pathogenesis further is thus significant for consideration of this global regulator as a target for countering infection.

4.5 References

1. Zhou Y, Pu Q, Chen J, Hao G, Gao R, Ali A, Hsiao A, Stock AM, Goulian M, Zhu J. 2021. Thiol-based functional mimicry of phosphorylation of the two-component system response regulator ArcA promotes pathogenesis in enteric pathogens. *Cell Rep* 37:110147.
2. Iyer MS, Pal A, Srinivasan S, Somvanshi PR, Venkatesh KV. 2021. Global Transcriptional Regulators Fine-Tune the Translational and Metabolic Efficiency for Optimal Growth of *Escherichia coli*. *mSystems* 6.
3. Anderson MT, Mitchell LA, Zhao L, Mobley HLT. 2017. Capsule Production and Glucose Metabolism Dictate Fitness during *Serratia marcescens* Bacteremia. *mBio* 8.
4. Anderson MT, Mitchell LA, Zhao L, Mobley HLT. 2018. *Citrobacter freundii* fitness during bloodstream infection. *Sci Rep* 8:11792.
5. Holmes CL, Anderson MT, Mobley HLT, Bachman MA. 2021. Pathogenesis of Gram-Negative Bacteremia. *Clin Microbiol Rev* 34.
6. Gunsalus RP, Park S-J. 1994. Aerobic-anaerobic gene regulation in *Escherichia coli*: control by the ArcAB and Fnr regulons. *Res Microbiol* 145:437–450.
7. Federowicz S, Kim D, Ebrahim A, Lerman J, Nagarajan H, Cho B, Zengler K, Palsson B. 2014. Determining the Control Circuitry of Redox Metabolism at the Genome-Scale. *PLoS Genet* 10:e1004264.
8. André AC, Debande L, Marteyn BS. 2021. The selective advantage of facultative anaerobes relies on their unique ability to cope with changing oxygen levels during infection. *Cell Microbiol* 23:e13338.
9. Subashchandrabose S, Smith S, DeOrnellas V, Crepin S, Kole M, Zahdeh C, Mobley HLT. 2016. *Acinetobacter baumannii* Genes Required for Bacterial Survival during Bloodstream Infection. *mSphere* 1:e00013-15.
10. Pont S, Janet-Maitre M, Faudry E, Cretin F, Attrée I. 2022. Molecular Mechanisms Involved in *Pseudomonas aeruginosa* Bacteremia. *Adv Exp Med Biol* 1386:325–345.
11. Schoen C, Kischkies L, Elias J, Ampattu BJ. 2014. Metabolism and virulence in *Neisseria meningitidis*. *Front Cell Infect Microbiol* 4:114.
12. Anderson MT, Brown AN, Pirani A, Smith SN, Photenhauer AL, Sun Y, Snitkin ES, Bachman MA, Mobley HLT. 2021. Replication Dynamics for Six Gram-Negative Bacterial Species during Bloodstream Infection. *mBio* 12:e0111421.
13. Pardo-Esté C, Castro-Severyn J, Krüger GI, Cabezas CE, Briones AC, Aguirre C, Morales N, Baquedano MS, Sulbaran YN, Hidalgo AA, Meneses C, Poblete-Castro I, Castro-Nallar E, Valvano MA, Saavedra CP. 2019. The Transcription Factor ArcA Modulates Salmonella's Metabolism in Response to Neutrophil Hypochlorous Acid-Mediated Stress. *Front Microbiol* 10:2754.
14. Chakraborty S, Liu L, Fitzsimmons L, Porwollik S, Kim J-S, Desai P, McClelland M, Vazquez-Torres A. 2020. Glycolytic reprograming in *Salmonella* counters NOX2-mediated dissipation of ΔpH. 1. *Nat Commun* 11:1783.
15. Arts IS, Gennaris A, Collet J-F. 2015. Reducing systems protecting the bacterial cell envelope from oxidative damage. *FEBS Lett* 589:1559–1568.
16. Kwon O, Georgellis D, Lynch AS, Boyd D, Lin ECC. 2000. The ArcB Sensor Kinase of *Escherichia coli*: Genetic Exploration of the Transmembrane Region. *J Bacteriol* 182:2960–2966.

17. Malpica R, Franco B, Rodriguez C, Kwon O, Georgellis D. 2004. Identification of a quinone-sensitive redox switch in the ArcB sensor kinase. *Proc Natl Acad Sci U S A* 101:13318–13323.
18. Rolfe MD, Beek AT, Graham AI, Trotter EW, Asif HMS, Sanguinetti G, de Mattos JT, Poole RK, Green J. 2011. Transcript Profiling and Inference of *Escherichia coli* K-12 ArcA Activity across the Range of Physiologically Relevant Oxygen Concentrations. *J Biol Chem* 286:10147–10154.
19. Iuchi S. 1993. Phosphorylation/dephosphorylation of the receiver module at the conserved aspartate residue controls transphosphorylation activity of histidine kinase in sensor protein ArcB of *Escherichia coli*. *J Biol Chem* 268:23972–23980.
20. Alvarez AF, Malpica R, Contreras M, Escamilla E, Georgellis D. 2010. Cytochrome d But Not Cytochrome o Rescues the Toluidine Blue Growth Sensitivity of arc Mutants of Escherichia coli. *J Bacteriol* 192:391–399.
21. Georgellis D, Kwon O, Lin EC. 1999. Amplification of signaling activity of the arc two-component system of *Escherichia coli* by anaerobic metabolites. An in vitro study with different protein modules. *J Biol Chem* 274:35950–35954.
22. Matsushita K, Kaback HR. 1986. D-Lactate oxidation and generation of the proton electrochemical gradient in membrane vesicles from *Escherichia coli* GR19N and in proteoliposomes reconstituted with purified D-lactate dehydrogenase and cytochrome o oxidase. *Biochemistry* 25:2321–2327.
23. Georgellis D, Kwon O, Lin EC. 2001. Quinones as the redox signal for the *arc* two-component system of bacteria. *Science* 292:2314–2316.
24. McDonald B, Zucoloto AZ, Yu I-L, Burkhard R, Brown K, Geuking MB, McCoy KD. 2020. Programing of an Intravascular Immune Firewall by the Gut Microbiota Protects against Pathogen Dissemination during Infection. *Cell Host Microbe* 28:660-668.e4.
25. Lee SM, An WS. 2016. New clinical criteria for septic shock: serum lactate level as new emerging vital sign. *J Thorac Dis* 8:1388–1390.
26. Hu S, Ottemann KM. 2023. *Helicobacter pylori* initiates successful gastric colonization by utilizing L-lactate to promote complement resistance. *Nat Commun* 14:1695.
27. Waters J, Shorr AF. 2023. Bloodstream Infection and Gram-Negative Resistance: The Role for Newer Antibiotics. *Antibiotics* 12:977.
28. Tiwari S, Jamal SB, Hassan SS, Carvalho PVSD, Almeida S, Barh D, Ghosh P, Silva A, Castro TLP, Azevedo V. 2017. Two-Component Signal Transduction Systems of Pathogenic Bacteria As Targets for Antimicrobial Therapy: An Overview. *Front Microbiol* 8.
29. Rajput A, Seif Y, Choudhary KS, Dalldorf C, Poudel S, Monk JM, Palsson BO. 2021. Pangenome Analytics Reveal Two-Component Systems as Conserved Targets in ESKAPEE Pathogens. *mSystems* 6.
30. Hirakawa H, Kurushima J, Hashimoto Y, Tomita H. 2020. Progress Overview of Bacterial Two-Component Regulatory Systems as Potential Targets for Antimicrobial Chemotherapy. *Antibiotics* 9.
31. Stock AM, Robinson VL, Goudreau PN. 2000. Two-Component Signal Transduction. *Annu Rev Biochem* 69:183–215.
32. Maura D, Hazan R, Kitao T, Ballok AE, Rahme LG. 2016. Evidence for Direct Control of Virulence and Defense Gene Circuits by the *Pseudomonas aeruginosa* Quorum Sensing Regulator, MvfR. 1. *Sci Rep* 6:34083.

33. Horinouchi T, Maeda T, Kotani H, Furusawa C. 2020. Suppression of antibiotic resistance evolution by single-gene deletion. Sci Rep 10:4178.
34. Arrieta-Ortiz ML, Pan M, Kaur A, Srinivas V, Dash A, Immanuel SRC, Baliga NS. 2020. Disrupting the ArcA regulatory network increases tetracycline susceptibility of TetR *Escherichia coli*. *bioRxiv* 2020.08.31.275693.

Appendix

Supplemental Table 7: Oligonucleotide primers utilized in this study

Primer Set	Forward Primer (5'-3')	Reverse Primer (5'-3')	Description
***C. freundii* UMH14**			
ANB0009	ATGCAGACCCCGCACATTCTTATCGT TGAAGACGAGTTAGTAACACGCAATG TAGGCTGGAGCTGCTTCG	AATCCTGCAGGTCGCCGCAGAAACGG TAGCCTTCACCGTGAATGGTGGCGCA TATGAATATCCTCCTTAGT	λ-red kanamycin cassette insert for mutagenesis of *arcA*
ANB0012	CTACCCACGACCAAGCTAATG	CAGAGTGACGAGTTTCGCTTAT	Confirmation of Δ*arcA* mutation
ANB0054	ATGCAGACCCCGCACATTCTTATCGT TGAAGACGAGTTAGTAACACGCAACA CGTTGAAAAGCATTTTCG	AATCCTGCAGGTCGCCGCAGAAACGG TAGCCTTCACCGTGAATGGTGGCGAT AATTTCTGGCGTATCCGG	*C. freundii* chromosomal complementation with *arcA*
ANB0055	CGGCATGTCTTAGCCTGTTAT	TCCCAGCCATTGAACTTGTAG	Screening for Δ*arcA*::*arcA* complemented mutant
gsp260/1	GCACCGTATTAACCCGCTGCGTCTGG GCTACATTACTGAGGTGTAGGCTGGA GCTGCTTC	TTATTCGCTTTTGGCGGTGGTATGCAC CATATAGTTCACAATATGAATATCCT CCTTAGT	λ-red kanamycin cassette insert for mutagenesis of *ubiG*
gsp262/3	CCGTCAGGCTGATATACTCATTTGC	TCTAAGGTAAGGAAAGTTCTTATGAT CTGG	Confirmation of Δ*ubiG* mutation
gsp264/5	GTGACATTGAAGCATTAATGGCTGCG GCGCGACTGCAATGATGTAGGCTGGA GCTGCTTC	TTATCAGGCCTACTTCTTTAATTCGGC CTACAGGTTATATATATGAATATCCT CCTTAGT	λ-red kanamycin cassette insert for mutagenesis of *ubiH*
gsp266/7	CGGCATTCGTATTGAGGATGACATC	CCTGAAAATAGGACAATCAAAAACC GTAG	Confirmation of Δ*ubiH* mutation
gsp293/4	TGATGGGGCTGATAAAGCCCCATTTT TATTGGCGCTAAATGTGTAGGCTGGA GCTGCTTC	CTGTTGGCAAAATCATCAATTGTTAA TTGATATTTG/5TCAGATATGAATATC CTCCTTAGT	λ-red kanamycin cassette insert for mutagenesis of *menA*
gsp295/6	ACAATTGATGCCGAATATGTGAGC	AGATGTCACAAAGCTCGGATGTATC	Confirmation of Δ*menA* mutation
gsp476/7	CACATTGGTACTCGTGGCTAAAAGAA CAGCAGGACATACAGTGTAGGCTGGA GCTGCTTC	TGTTTCCCTCTCCCCGTAGCGAGGAG AGGGAGAAACGTTAATATGAATATCC TCCTTAGT	λ-red kanamycin cassette insert for mutagenesis of CUC46_RS02895
gsp474/5	TTGACTGCCACCACGCCTC	AGGCACAGTTTTGATACCGTATTCAC	Confirmation of CUC46_RS02895 mutation
gsp436/7	CCCGTGAACAACAGAGAATCGATGCC CTGAGAATGTTATGGTGTAGGCTGGA GCTGCTTC	AAAATAACAATCTTTGGCATATTAAA CCTCGTCCACAGACATATGAATATCC TCCTTAGT	λ-red kanamycin cassette insert for mutagenesis of *hscBA*
gsp434/5	GGTACGCAGTTAGATTTCGTCAAAG CCTTCACGTACGATGCAGTGG	CCTTCACGTACGATGCAGTGG	Confirmation of Δ*hscBA* mutation
gsp394/5	CGCGGCATACCTCGAAGGGAGCAGG AGTAAAAACGTGATGGTGTAGGCTGG AGCTGCTTC	CTGGAAACCAGACTGGCCTTTGTGCT TTTCAAGCCGGTGCATATGAATATCC TCCTTAGT	λ-red kanamycin cassette insert for mutagenesis of *atpIBEFHAGDC* operon
gsp396/471	GCATAAAAGTGATAAATGTGGCGTAG	AGTGGCGCTGACTGATAAACC	Confirmation of *atpIBEFHAGDC* opern mutant mutation
gsp398/9	GACCCGGTGGACGACGGGTATAAATT AAGAGGTCATGATGGTGTAGGCTGGA GCTGCTTC	AAACGCCTCCGAAGAGGCGTTTTCAC AAAAGCGGGAAGACATATGAATATC CTCCTTAGT	λ-red kanamycin cassette insert for mutagenesis of *lpdA*
gsp400/1	TCATGAAGTCAGTGAGGTTATTGTGC	GTCGCGACAATCATGCCAAC	Confirmation of Δ*lpdA* mutation
***E. coli* CFT073**			
ANB0017	TCAGGCAGGTCAGGGACTTTTGTACT TCCTGTTTCGATTTAGTTGGCAATTTG TAGGCTGGAGCTGCTTCG	CGATGAATTACGTATCTGGAAATAAG ATAGAAAAATAAAAACGGCGCTAAA CATATGAATATCCTCCTTAGT	λ-red kanamycin cassette insert for mutagenesis of *arcA*
ANB0018	TGTTGTTGACGTTGATGGAAAG	GACCCGTAATATCGACTGGTATG	Confirmation of Δ*arcA* mutation

gsp350/1	GGGCACGACGCTGGCGCTGGCTATTTCCCGGTTAAGTCACGTGTAGGCTGGAGCTGCTTC	ACATCGCGTGCTGGGGTAAATAATTCCATCGTCATCAGCCATATGAATATCCTCCTTAGT	λ-red kanamycin cassette insert for mutagenesis of *ubiH*
gsp352/3	GAACCAGGGCTGTATATTGCG	CATCCGCCGCCAGAGG	Confirmation of Δ*ubiH* mutation
***K. pneumoniae* KPPR1**			
ANB0010	ATGCAGACCCCGCACATTCTTATCGTTGAAGACGAGTTGGTAACACGCAATGTAGGCTGGAGCTGCTTCG	TTATTCCTGCAGGTCGCCACAGAAACGGTAGCCTTCACCGTGAATGGTAGCATATGAATATCCTCCTTAGT	λ-red kanamycin cassette insert for mutagenesis of *arcA*
ANB0013	GGGACTTTGGTACTTCCTGTT	CGTGGACTGGTATGCGTTAT	Confirmation of Δ*arcA* mutation
ANB0021	CCCCTCTAGAAATTGCGTTTTCTTACCC	CCCCGAGCTCGCTGAGCGTCCTGATGTTTTT	For cloning *arcA* into pBBR1MCS-5
M13	CGCCAGGGTTTTCCCAGTCACGAC	CAGGAAACAGCTATsGAC	Confirmation of pBBR1MCS-5 + *arcA* construct
ANB0040	CGCAGAGTACATGGCTTACA	TTACCGTTAACGACCAGATGAC	For qPCR of *gapA*
ANB0029	CAATCCATAACCGACCCTGATAC	TGCGAAGGAGGTGTTCTTTAC	For qPCR of *acs*
ANB0026	CTATGGCCTGTTCAAGGAGAT	GCCAGGTTACTGAGGGTTT	For qPCR of *astC*
ANB0022	GCTAACGACTTCGCCATCA	TCAAGTCCGCCATACTCTTTC	For qPCR of *fadE*
ANB0030	GTGACCGTTGAGCGTAAAGA	AGATGGTGGTCAGGGAGTAG	For qPCR of *feoB*
ANB0028	TCGGATCTGTTCCGCTTTAC	CACGGGATCATCCAGGTTAAA	For qPCR of *lldP*
ANB0023	GTGGTCCTGTTCTCGGTAATG	AACTGCTTCCAGACGATCAC	For qPCR of *putP*
ANB0027	TGCTCGAAGAGATGAACAAGAA	GGACGAGGCAGTGGTAATG	For qPCR of *ugpB*
pKD4_ubiH_4140_F/R	TGGCCATCTCCCGTTTGACCGGCGGCGCGCTGCCGGTCCACCTCATTGAAGCGCAGGATCCGCATGTGTAGGCTGGAGCTGCTTC	ACGGGGAACCCAACCGAGGGTACGCTGCGCCAGCGCATCGCGCGCCGGGGTAAATAATTCCAATGGGAATTAGCCATGGTCC	λ-red kanamycin cassette insert for mutagenesis of ubiH
ubiH_4140_flanking_F/R	GGCGAGATTGACGAGCTTAT	CCACACTTCCATACCGTGATAG	Confirmation of Δ*ubiH* mutation
***S. marcescens* UMH9**			
ANB0008	TATGCAGACCCCGCACATTCTGATTGTCGAAGACGAGTTAGTCACTCGTATGTAGGCTGGAGCTGCTTCG	GCCGTGAATGGTGGCGATGATTTCCGGCGTGTCCGGCGTCGATTCGAAGTCATATGAATATCCTCCTTAGT	λ-red kanamycin cassette insert for mutagenesis of *arcA*
ANB0011	TCTCTGCCCTCCTCTAAGAAA	CGTGGGCTGAGACGAAATAA	Confirmation of Δ*arcA* mutation
ANB0044	TATGCAGACCCCGCACATTCTGATTGTCGAAGACGAGTTAGTCACTCGTAACACCCTGAAGAGCATTTTC	GCCGTGAATGGTGGCGATGATTTCCGGCGTGTCCGGCGTCGATTCGAAGTGTTTGCGAATGCGACGGATGG	Chromosomal complementation with *arcA*
ANB0045	TCGGCACACGCTGTTATATT	ACCGTTGAACTTGTAGCTCTC	Screening for Δ*arcA*::*arcA* complemented mutant

Supplemental Table 8: Order Enterobacterales genomes and ArcA ORFs analyzed for conservation modeling

Species	Genome	Accession	BRC ID
Citrobacter freundii	*Citrobacter freundii* strain UMH14	CP024680	fig|546.464.peg.4775
Klebsiella aerogenes	*Klebsiella aerogenes* strain Ka37751	CP041925	fig|548.605.peg.4297
Pantoea agglomerans	*Pantoea agglomerans* strain FDAARGOS 1447 strain Not applicable	CP077366	fig|549.416.peg.3740
Enterobacter cloacae	*Enterobacter cloacae* RS35	JAMQCM010000001	fig|550.3788.peg.725
Pectobacterium carotovorum	*Pectobacterium carotovorum* strain WPP14	CP051652	fig|554.82.peg.565
Escherichia coli	*Escherichia coli* CFT073	CP058222	fig|562.94315.peg.4412
Escherichia fergusonii	*Escherichia fergusonii* strain FDAARGOS_1499 strain Not applicable	CP083638	fig|564.206.peg.2836
Atlantibacter hermannii	*Atlantibacter hermannii* strain 78-1320	CP049608	fig|565.16.peg.1578
Pseudescherichia vulneris	*Pseudescherichia vulneris* strain 4928STDY7071515	LR607338	fig|566.7.peg.3637
Hafnia alvei	*Hafnia alvei* strain LE8	LAZF01000055	fig|569.30.peg.3623
Klebsiella oxytoca	*Klebsiella oxytoca* strain FDAARGOS_500 strain Not applicable	CP033844	fig|571.376.peg.4322
Klebsiella pneumoniae	*Klebsiella pneumoniae* strain KPPR1	KN150814	fig|573.1355.peg.814
Raoultella planticola	*Raoultella planticola* A2-F21	CP093334	fig|575.107.peg.2369
Raoultella terrigena	*Raoultella terrigena* strain JH01	CP050508	fig|577.26.peg.4690
Morganella morganii	*Morganella morganii* strain MGYG-HGUT-02512	LR699007	fig|582.306.peg.3544
Proteus vulgaris	*Proteus vulgaris* strain ATCC 49132	KN150745	fig|585.9.peg.355
Providencia rettgeri	*Providencia rettgeri* strain AR_0082	CP029736	fig|587.78.peg.117
Providencia stuartii	*Providencia stuartii* CMC-4104	CP095443	fig|588.252.peg.638
Serratia liquefaciens	*Serratia liquefaciens* S1	CP048784	fig|614.156.peg.567
Serratia marcescens	*Serratia marcescens* strain UMH9	CP018923	fig|615.524.peg.4802
Serratia odorifera	*Serratia odorifera* strain FDAARGOS_353	NJFR01000003	fig|618.3.peg.5061
Shigella boydii	*Shigella boydii* strain ESBL-W3-2	NIYS01000040	fig|621.169.peg.324
Shigella dysenteriae	*Shigella dysenteriae* SWHEFF_49	CP055055	fig|622.549.peg.572
Shigella sonnei	*Shigella sonnei* strain SE6-1	CP055292	fig|624.2249.peg.1245
Xenorhabdus nematophila	*Xenorhabdus nematophila* strain SII	CP060401	fig|628.33.peg.2748
Yersinia enterocolitica	*Yersinia enterocolitica* strain IP26014	CQAE01000002	fig|630.69.peg.1701
Yersinia intermedia	*Yersinia intermedia* strain FDAARGOS_730 strain Not applicable	CP046293	fig|631.40.peg.3867
Yersinia bercovieri	*Yersinia bercovieri* strain IZSPB_Y87	JAJAVX010000003	fig|634.18.peg.1594
Edwardsiella tarda	*Edwardsiella tarda* strain KC-Pc-HB1	CP023706	fig|636.15.peg.1015
Arsenophonus nasoniae	*Arsenophonus nasoniae* strain FIN	CP038613	fig|638.17.peg.3615
Plesiomonas shigelloides	*Plesiomonas shigelloides* strain 7A	CP087711	fig|703.94.peg.687
Cronobacter sakazakii	*Cronobacter sakazakii* CS-931	CP027107	fig|28141.1048.peg.2650
Serratia proteamaculans	*Serratia proteamaculans* strain CCUG 14510	WBKI01000003	fig|28151.36.peg.2912
Yersinia kristensenii	*Yersinia kristensenii* strain ATCC BAA-2637	CP032482	fig|28152.31.peg.692
Pectobacterium atrosepticum	*Pectobacterium atrosepticum* strain 21a	CP009125	fig|29471.25.peg.3966

Yersinia rohdei	*Yersinia rohdei* YRA	CP009787	fig|29485.3.peg.3332
Yersinia ruckeri	*Yersinia ruckeri* strain KMM821	CP071802	fig|29486.164.peg.528
Photorhabdus luminescens	*Photorhabdus luminescens* strain PB45.5	LOIC01000019	fig|29488.15.peg.1018
Citrobacter amalonaticus	*Citrobacter amalonaticus* FDAARGOS_165	CP014070	fig|35703.153.peg.4641
Xenorhabdus bovienii	*Xenorhabdus bovienii* 18M	JAKMXG010000003	fig|40576.59.peg.543
Xenorhabdus beddingii	*Xenorhabdus beddingii* strain DSM 4764	MUBK01000003	fig|40578.4.peg.2578
Ewingella americana	*Ewingella americana* strain CCUG 14506T	VXKG01000002	fig|41202.12.peg.2224
Serratia entomophila	*Serratia entomophila* A1	CP082787	fig|42906.9.peg.607
Serratia fonticola	*Serratia fonticola* strain DSM 4576	CP011254	fig|47917.8.peg.2420
Kluyvera ascorbata	*Kluyvera ascorbata* strain WCH1410	LSME01000011	fig|51288.6.peg.592
Tatumella citrea	*Tatumella citrea* strain ATCC 39140	CP015581	fig|53336.8.peg.3555
Xenorhabdus japonica	*Xenorhabdus japonica* strain DSM 16522	FOVO01000002	fig|53341.3.peg.2148
Raoultella ornithinolytica	*Raoultella ornithinolytica* strain NCTC9164	CABDWD010000002	fig|54291.184.peg.4618
Pectobacterium betavasculorum	*Pectobacterium betavasculorum* strain NCPPB 2795	JQHM01000003	fig|55207.5.peg.2192
Pantoea cypripedii	*Pantoea cypripedii* strain WS4375	JAGGMY010000001	fig|55209.9.peg.1905
Brenneria nigrifluens	*Brenneria nigrifluens* strain ATCC 13028	CP034036	fig|55210.5.peg.663
Erwinia persicina	*Erwinia persicina* strain Cp2	CP082141	fig|55211.39.peg.3725
Erwinia rhapontici	*Erwinia rhapontici* strain BY21311	CP085627	fig|55212.15.peg.4077
Brenneria rubrifaciens	*Brenneria rubrifaciens* strain 6D370	CP034035	fig|55213.4.peg.3201
Rahnella inusitata	*Rahnella inusitata* strain Se8.10.12	CP065024	fig|58169.7.peg.4246
Pantoea dispersa	*Pantoea dispersa* strain Lsch	CP082346	fig|59814.204.peg.695
Lelliottia amnigena	*Lelliottia amnigena* strain FDAARGOS_1445 strain Not applicable	CP079896	fig|61646.100.peg.4039
Pluralibacter gergoviae	*Pluralibacter gergoviae* strain FDAARGOS_186	CP020388	fig|61647.65.peg.1773
Kluyvera intermedia	*Kluyvera intermedia* strain N2-1	CP045845	fig|61648.20.peg.3784
Serratia ficaria	*Serratia ficaria* strain NCTC12148	LT906479	fig|61651.3.peg.698
Serratia rubidaea	*Serratia rubidaea* strain FDAARGOS_926 strain Not applicable	CP065640	fig|61652.34.peg.2077
Erwinia tracheiphila	*Erwinia tracheiphila* BHKY	CP089932	fig|65700.171.peg.5261
Pantoea stewartii	*Pantoea stewartii* strain ZJ-FGZX1	CP049115	fig|66269.21.peg.3643
Edwardsiella ictaluri	*Edwardsiella ictaluri* S07-698	CP084521	fig|67780.67.peg.620
Citrobacter farmeri	*Citrobacter farmeri* strain CF_355	RHWV01000002	fig|67824.9.peg.2432
Citrobacter rodentium	*Citrobacter rodentium* DSM 16636	CP082833	fig|67825.30.peg.226
Erwinia aphidicola	*Erwinia aphidicola* X001	JAMKCQ010000001	fig|68334.9.peg.2351
Enterobacter cancerogenus	*Enterobacter cancerogenus* strain JY65	CP081105	fig|69218.53.peg.866
Lelliottia nimipressuralis	*Lelliottia nimipressuralis* strain MEZLN61	JAJNQS010000018	fig|69220.16.peg.1776
Pectobacterium cacticida	*Pectobacterium cacticida* CFCC10813	CP109947	fig|69221.4.peg.3298
Erwinia mallotivora	*Erwinia mallotivora* EP39	VFIH01000003	fig|69222.13.peg.3036
Musicola paradisiaca	*Dickeya paradisiaca* strain A3967	JAAWVW010000007	fig|69223.13.peg.3828
Erwinia psidii	*Erwinia psidii* strain IBSBF 435	RHHM01000002	fig|69224.3.peg.2450
Brenneria alni	*Brenneria alni* strain NCPPB 3934	MJLZ01000001	fig|71656.4.peg.143

Lonsdalea quercina	*Lonsdalea quercina* strain ATCC 29281	FNQS01000004	fig|71657.5.peg.3292
Pectobacterium odoriferum	*Pectobacterium odoriferum* strain JK2.1	CP034938	fig|78398.23.peg.4174
Erwinia pyrifoliae	*Erwinia pyrifoliae* strain EpK1/15	CP023567	fig|79967.6.peg.3390
Buttiauxella agrestis	*Buttiauxella agrestis* strain MCE	JPRU01000002	fig|82977.3.peg.2974
Budvicia aquatica	*Budvicia aquatica* FDAARGOS_387	PDDX01000001	fig|82979.7.peg.1985
Obesumbacterium proteus	*Obesumbacterium proteus* strain PCM_1214	SITL01000116	fig|82983.11.peg.3336
Pragia fontium	*Pragia fontium* strain NCTC12284	LR134531	fig|82985.7.peg.733
Buttiauxella ferragutiae	*Buttiauxella ferragutiae* H4-C11	CP093332	fig|82989.7.peg.639
Buttiauxella izardii	*Buttiauxella izardii* strain CCUG 35510	QZWH01000022	fig|82991.3.peg.2222
Buttiauxella warmboldiae	*Buttiauxella warmboldiae* strain CCUG 35512	RPOH01000029	fig|82993.3.peg.1757
Serratia grimesii	*Serratia grimesii* strain BXF1	LT883155	fig|82995.6.peg.606
Leclercia adecarboxylata	*Leclercia adecarboxylata* strain USDA-ARS-USMARC-60222	CP013990	fig|83655.10.peg.3885
Pantoea endophytica	*Pantoea endophytica* 596	PJRT01000009	fig|92488.12.peg.4638
Erwinia toletana	*Erwinia toletana* strain WS4403	JAGGMQ010000001	fig|92490.6.peg.2977
Edwardsiella hoshinae	*Edwardsiella hoshinae* strain FDAARGOS_940 strain Not applicable	CP065626	fig|93378.7.peg.1234
Klebsiella cf. planticola B43	*Klebsiella cf.* planticola B43	BADH01000249	fig|95610.3.peg.1317
Salmonella enterica	*Salmonella enterica* subsp. enterica serovar Typhimurium str. LT2	AE006468	fig|99287.836.peg.4870
Proteus penneri	*Proteus penneri* S178-2	CP059690	fig|102862.26.peg.162
Providencia alcalifaciens	*Providencia alcalifaciens* strain FDAARGOS_408	CP023536	fig|126385.6.peg.334
Serratia quinivorans	*Serratia quinivorans* strain NCTC13188	LR134494	fig|137545.6.peg.603
Serratia symbiotica	*Serratia symbiotica* strain 24.1	WSPN01000025	fig|138074.16.peg.1474
Cedecea neteri	*Cedecea neteri* strain FDAARGOS_392	CP023525	fig|158822.21.peg.4140
Cedecea lapagei	*Cedecea lapagei* strain NCTC11466	LR134201	fig|158823.5.peg.3932
Enterobacter hormaechei	*Enterobacter hormaechei* strain FDAARGOS 1435 strain Not applicable	CP077392	fig|158836.1174.peg.186
Leminorella richardii	*Leminorella richardii* strain NCTC12151	LS483470	fig|158841.3.peg.2731
Moellerella wisconsensis	*Moellerella wisconsensis* W65	CP093242	fig|158849.12.peg.2757
Providencia rustigianii	*Providencia rustigianii* strain NCTC12026	UGUA01000002	fig|158850.7.peg.648
Yokenella regensburgei	*Yokenella regensburgei* strain DSM 5079	RBIZ01000005	fig|158877.9.peg.3378
Samsonia erythrinae	*Samsonia erythrinae* strain DSM 16730	SMBY01000006	fig|160434.3.peg.2512
Photorhabdus akhurstii	*Photorhabdus akhurstii* strain 0813-124 phase II strain not applicable	CP020335	fig|171438.4.peg.729
Pectobacterium brasiliense	*Pectobacterium brasiliense* strain 1692	CP047495	fig|180957.62.peg.2130
Proteus hauseri	*Proteus hauseri* strain 15H5D-4a	CP026364	fig|183417.5.peg.1993
Shigella flexneri	*Shigella flexneri* 2a str. 301	NC_004337	fig|198214.7.peg.5224
Dickeya dadantii	*Dickeya dadantii* FZ06	CP094943	fig|204038.53.peg.4202
Dickeya dianthicola	*Dickeya dianthicola* strain ME23	CP031560	fig|204039.55.peg.4126
Dickeya zeae	*Dickeya zeae* strain PL65	CP025799	fig|204042.48.peg.3916
Kosakonia cowanii	*Kosakonia cowanii* strain FBS 223	CP035129	fig|208223.19.peg.3797
Escherichia albertii	*Escherichia albertii* Sample 167	CP070290	fig|208962.289.peg.3731
[Curtobacterium] plantarum	*[Curtobacterium] plantarum* strain LMG 16222	RHDS01000003	fig|221276.3.peg.2191

Photorhabdus kayaii	*Photorhabdus kayaii* strain M-HU2	WSFE01000008	fig|230088.4.peg.1769
Photorhabdus thracensis	*Photorhabdus temperata* subsp. thracensis strain DSM 15199	CP011104	fig|230089.6.peg.1205
Photorhabdus laumondii	*Photorhabdus luminescens* subsp. laumondii TTO1	NC_005126	fig|243265.5.peg.610
Klebsiella variicola	*Klebsiella variicola* strain LEMB11	CP045783	fig|244366.435.peg.3686
Atlantibacter subterranea	*Atlantibacter subterranea* LH84-a	CP100494	fig|255519.10.peg.580
Yersinia aleksiciae	*Yersinia aleksiciae* strain 404/81	CGBL01000002	fig|263819.5.peg.602
Yersinia pseudotuberculosis	*Yersinia pseudotuberculosis* IP 32953	CP009712	fig|273123.14.peg.2083
Kosakonia radicincitans	*Kosakonia radicincitans* strain DSM 107547	CP040392	fig|283686.18.peg.4733
Xenorhabdus innexi	*Xenorhabdus innexi* strain HGB1681 (deposited as PTA-6826 in the American Type Culture Collection)	LT699767	fig|290109.7.peg.1758
Xenorhabdus budapestensis	*Xenorhabdus budapestensis* strain C-7-2	CP072455	fig|290110.7.peg.756
Xenorhabdus ehlersii	*Xenorhabdus ehlersii* strain DSM 16337	NIBT01000013	fig|290111.5.peg.823
Xenorhabdus szentirmaii	*Xenorhabdus szentirmaii* strain US123	NIUA01000001	fig|290112.3.peg.2482
Citrobacter koseri	*Citrobacter koseri* ATCC BAA-895	NC_009792	fig|290338.8.peg.2844
Photorhabdus asymbiotica	*Photorhabdus asymbiotica* strain ATCC 43949	NC_012962	fig|291112.3.peg.612
Enterobacter ludwigii	*Enterobacter ludwigii* strain EN-119	CP017279	fig|299767.18.peg.3638
Serratia ureilytica	*Serratia ureilytica* strain T6	CP071320	fig|300181.112.peg.4220
Providencia heimbachae	*Providencia heimbachae* strain NCTC12003	LS483422	fig|333962.4.peg.670
Xenorhabdus indica	*Xenorhabdus indica* strain DSM 17382	NKHP01000006	fig|333964.4.peg.3588
Providencia vermicola	*Providencia vermicola* strain DSM 17385	JAGSPI010000009	fig|333965.22.peg.2916
Sodalis glossinidius	*Sodalis glossinidius* str. 'morsitans'	NC_007712	fig|343509.12.peg.1055
Yersinia frederiksenii	*Yersinia frederiksenii* ATCC 33641	KN150731	fig|349966.8.peg.3358
Yersinia mollaretii	*Yersinia mollaretii* ATCC 43969	CP054043	fig|349967.11.peg.1808
Xenorhabdus stockiae	*Xenorhabdus stockiae* strain DSM 17904	NJAJ01000009	fig|351614.4.peg.4274
Xenorhabdus vietnamensis	*Xenorhabdus vietnamensis* strain DSM 22392	MUBJ01000001	fig|351656.5.peg.120
Xenorhabdus koppenhoeferi	*Xenorhabdus koppenhoeferi* strain DSM 18168	FPBJ01000035	fig|351659.4.peg.2814
Xenorhabdus doucetiae	*Xenorhabdus doucetiae* strain FRM16 = DSM 17909	FO704550	fig|351671.5.peg.776
Xenorhabdus griffiniae	*Xenorhabdus griffiniae* strain VH1	JADEUF010000012	fig|351672.10.peg.563
Xenorhabdus cabanillasii	*Xenorhabdus cabanillasii* strain DSM 17905	QTUB01000001	fig|351673.4.peg.792
Xenorhabdus miraniensis	*Xenorhabdus miraniensis* strain DSM 17902	NITZ01000017	fig|351674.5.peg.1433
Xenorhabdus mauleonii	*Xenorhabdus mauleonii* strain DSM 17908	FORG01000007	fig|351675.7.peg.4663
Xenorhabdus kozodoii	*Xenorhabdus kozodoii* strain DSM 17907	NJCX01000021	fig|351676.4.peg.1830
Xenorhabdus hominickii	*Xenorhabdus hominickii* strain ANU1	CP016176	fig|351679.5.peg.2656
Siccibacter turicensis	*Siccibacter turicensis* strain #493	RYYT01000003	fig|357233.20.peg.2153
Franconibacter helveticus	*Franconibacter helveticus* strain CS-23	QISR01000003	fig|357240.5.peg.2262
Yersinia similis	*Yersinia similis* strain 228	CP007230	fig|367190.3.peg.2178
Morganella psychrotolerans	*Morganella psychrotolerans* strain CCUG 53682T	VXKB01000005	fig|368603.12.peg.3308
Trabulsiella odontotermitis	*Trabulsiella odontotermitis* strain TbO1.1	LIFU01000002	fig|379893.8.peg.1897
Phytobacter diazotrophicus	*Phytobacter diazotrophicus* strain UAEU22	CP051548	fig|395631.4.peg.5027

Cronobacter turicensis	*Cronobacter turicensis* strain HA18060	JAANQI010000007	fig|413502.31.peg.3185
Mangrovibacter plantisponsor	*Mangrovibacter plantisponsor* strain DSM 19579	QGTS01000006	fig|451513.3.peg.2419
Serratia nematodiphila	*Serratia nematodiphila* strain DH-S01 strain not collected	CP038662	fig|458197.18.peg.609
Erwinia tasmaniensis	*Erwinia tasmaniensis* Et1/99	NC_010694	fig|465817.9.peg.746
Biostraticola tofi	*Biostraticola tofi* strain DSM 19580	SMCR01000002	fig|466109.3.peg.1351
Pantoea anthophila	*Pantoea anthophila* strain 11-2	JXXL01000005	fig|470931.3.peg.988
Pantoea deleyi	*Pantoea deleyi* LMG24200	CP071405	fig|470932.14.peg.3200
Pantoea eucalypti	*Pantoea eucalypti* strain LMG 24197	CP045720	fig|470933.11.peg.3400
Pantoea vagans	*Pantoea vagans* strain LMG 24199	CP038853	fig|470934.52.peg.3289
Photorhabdus cinerea	*Photorhabdus cinerea* strain DSM 19724	PUJW01000008	fig|471575.3.peg.2070
Pantoea eucrina	*Pantoea eucrina* strain XL123	CP083448	fig|472693.28.peg.466
Pantoea brenneri	*Pantoea brenneri* strain IIFCSG-B1	JACBPK010000005	fig|472694.20.peg.3540
Pantoea septica	*Pantoea septica* strain MGYG-HGUT-02423	CABMKO010000002	fig|472695.24.peg.1116
Pantoea conspicua	*Pantoea conspicua* strain LMG 24534	MLFN01000002	fig|472705.4.peg.266
Kosakonia oryzae	*Kosakonia oryzae* Ola 51	CP014007	fig|497725.17.peg.4503
Escherichia coli	*Escherichia coli* str. K-12 substr. MG1655	NC_000913	fig|511145.12.peg.4550
Proteus mirabilis	*Proteus mirabilis* HI4320	NC_010554	fig|529507.6.peg.3640
Enterobacter mori	*Enterobacter mori* ACYC.E9L	CP091779	fig|539813.36.peg.608
Hafnia paralvei	*Hafnia paralvei* AVS0177	CP083737	fig|546367.124.peg.3833
Kosakonia arachidis	*Kosakonia arachidis* strain KACC 18508	CP045300	fig|551989.5.peg.2352
Cedecea davisae	*Cedecea davisae* DSM 4568	KE161030	fig|566551.12.peg.450
Dickeya poaceiphila	*Dickeya poaceiphila* NCPPB 569	CP042220	fig|568768.7.peg.563
Shimwellia pseudoproteus	*Shimwellia pseudoproteus* strain DSM 3038	WBXP01000001	fig|570012.3.peg.191
Pantoea allii	*Pantoea allii* strain PNA 200-10	QGHF01000002	fig|574096.8.peg.1134
Photorhabdus temperata	*Photorhabdus temperata* DSM 14550	JAJAFX010000019	fig|574560.22.peg.1346
Rahnella variigena	*Rahnella variigena* strain CIP 105588	NSDJ01000001	fig|574964.4.peg.1314
Dickeya parazeae	*Dickeya dadantii* Ech586	NC_013592	fig|590409.4.peg.3636
Proteus terrae	*Proteus cibarius* strain ZN2	CP047349	fig|626774.13.peg.540
Shimwellia blattae	*Shimwellia blattae* DSM 4481 = NBRC 105725	CP001560	fig|630626.3.peg.3264
Erwinia billingiae	*Erwinia billingiae* Eb661	NC_014306	fig|634500.5.peg.950
Enterobacter asburiae	*Enterobacter asburiae* LF7a	NC_015968	fig|640513.3.peg.770
Tatumella morbirosei	*Tatumella morbirosei* LMG 23360	JPKR02000003	fig|642227.6.peg.2359
Erwinia amylovora	*Erwinia amylovora* CFBP1430	NC_013961	fig|665029.3.peg.2847
Mixta calida	*Mixta calida* strain DE0300	VEKN01000005	fig|665913.5.peg.3504
Mixta gaviniae	*Pantoea gaviniae* strain DSM 22758	CP026377	fig|665914.6.peg.849
Edwardsiella anguillarum	*Edwardsiella tarda* 080813	AFJH01000040	fig|667120.5.peg.1713
Yersinia nurmii	*Yersinia nurmii* strain CIP110231T	CPYD01000008	fig|685706.3.peg.2447
[Enterobacter] lignolyticus	*Enterobacter lignolyticus* SCF1	NC_014618	fig|701347.4.peg.3795
Brenneria salicis	*Brenneria salicis* ATCC 15712 = DSM 30166	QNRY01000006	fig|714314.6.peg.980

Rahnella aquatilis	*Rahnella aquatilis* CIP 78.65 = ATCC 33071	CP003244	fig|745277.3.peg.3743
Photorhabdus kleinii	*Photorhabdus kleinii* DSM 23513	JAJAFY010000011	fig|768034.3.peg.638
Serratia plymuthica	*Serratia plymuthica* AS9	NC_015567	fig|768492.3.peg.622
Photorhabdus heterorhabditis	*Photorhabdus heterorhabditis* strain VMG	LJCS01000012	fig|880156.5.peg.1572
Xenorhabdus khoisanae strain MCB	*Xenorhabdus khoisanae* strain MCB	LFCV01000130	fig|880157.4.peg.3603
Enterobacter bugandensis	*Enterobacter bugandensis* strain STN0717-56	AP022508	fig|881260.71.peg.631
Enterobacter soli	*Enterobacter soli* strain A23	JAGGDT010000007	fig|885040.7.peg.4881
Gibbsiella quercinecans	*Gibbsiella quercinecans* strain FRB97	CP014136	fig|929813.7.peg.1951
Yersinia entomophaga	*Yersinia entomophaga* strain MH96	CP010029	fig|935293.3.peg.2878
Rosenbergiella nectarea	*Rosenbergiella nectarea* strain 8N4	FOGC01000001	fig|988801.3.peg.2430
Providencia thailandensis	*Providencia thailandensis* strain KCTC 23281	BMYH01000004	fig|990144.3.peg.2496
Photorhabdus khanii	*Photorhabdus khanii* strain HGB 1456	WHZZ01000007	fig|1004150.3.peg.4866
Photorhabdus tasmaniensis	*Photorhabdus tasmaniensis* strain T327	PUJU01000046	fig|1004159.3.peg.4053
Photorhabdus caribbeanensis	*Photorhabdus caribbeanensis* strain HG29	RCWB01000018	fig|1004165.3.peg.2949
Photorhabdus hainanensis	*Photorhabdus hainanensis* strain DSM 22397	RCWD01000068	fig|1004166.3.peg.5252
Kosakonia oryzendophytica	*Kosakonia oryzendophytica* strain REICA_082	FMAY01000002	fig|1005665.7.peg.2626
Kosakonia oryziphila	*Kosakonia oryziphila* strain REICA_142	FMBC01000001	fig|1005667.7.peg.2343
Trabulsiella guamensis	*Trabulsiella guamensis* ATCC 49490	JMTB01000059	fig|1005994.3.peg.1694
Tatumella ptyseos	*Tatumella ptyseos* ATCC 33301	ATMJ01000012	fig|1005995.3.peg.674
Leminorella grimontii	*Leminorella grimontii* ATCC 33999 = DSM 5078	JMPN01000016	fig|1005999.13.peg.2401
Xenorhabdus ishibashii	*Xenorhabdus ishibashii* strain DSM 22670	NJAK01000001	fig|1034471.3.peg.2450
Yersinia pestis	*Yersinia pestis* A1122	CP002956	fig|1035377.4.peg.554
Cronobacter condimenti	*Cronobacter condimenti* 1330 strain LMG 26250	CP012264	fig|1073999.7.peg.657
Cronobacter universalis	*Cronobacter universalis* NCTC 9529	CP012257	fig|1074000.5.peg.653
Pantoea rodasii	*Pantoea rodasii* strain DSM 26611	PIQI01000031	fig|1076549.5.peg.5222
Pantoea rwandensis	*Pantoea rwandensis* strain LMG 26275	MLFR01000004	fig|1076550.4.peg.1521
Pantoea wallisii	*Pantoea wallisii* strain LMG 26277	MLFS01000024	fig|1076551.3.peg.2337
Lonsdalea iberica	*Lonsdalea quercina* subsp. iberica strain LMG 26264	LUTP01000001	fig|1082703.3.peg.69
Lonsdalea britannica	*Lonsdalea britannica* strain 477	CP023009	fig|1082704.5.peg.598
Dickeya solani	*Dickeya solani* strain PPO 9019	JWLS01000006	fig|1089444.22.peg.4111
Pantoea ananatis	*Pantoea ananatis* PA13	CP003085	fig|1095774.3.peg.3722
Brenneria goodwinii	*Brenneria goodwinii* strain FRB141	CP014137	fig|1109412.17.peg.4923
Budvicia diplopodorum	*Budvicia diplopodorum* strain D9	WOYF01000002	fig|1119056.3.peg.1823
Photorhabdus australis	*Photorhabdus asymbiotica* subsp. australis DSM 17609	JONO01000047	fig|1122960.3.peg.3524
Photorhabdus stackebrandtii	*Photorhabdus stackebrandtii* strain DSM 23271	PUJV01000001	fig|1123042.3.peg.261
Klebsiella michiganensis	*Klebsiella michiganensis* strain THO-011	AP022547	fig|1134687.230.peg.4908
Providencia sneebia	*Providencia sneebia* DSM 19967	AKKN01000013	fig|1141660.3.peg.3081
Providencia burhodogranariea	*Providencia burhodogranariea* DSM 19968	AKKL01000046	fig|1141662.3.peg.3343
Serratia inhibens	*Serratia inhibens* PRI-2C strain PRI-2c	CP015613	fig|1154756.11.peg.587

Kosakonia sacchari	*Kosakonia sacchari* strain BO-1	CP016337	fig|1158459.5.peg.2340
Cronobacter malonaticus	*Cronobacter malonaticus* LMG 23826	CP013940	fig|1159491.22.peg.3415
Cronobacter dublinensis	*Cronobacter dublinensis* subsp. dublinensis LMG 23823	CP012266	fig|1159554.7.peg.648
Cronobacter muytjensii	*Cronobacter muytjensii* ATCC 51329	CP012268	fig|1159613.6.peg.3201
Erwinia piriflorinigrans	*Erwinia piriflorinigrans* CFBP 5888	CAHS01000017	fig|1161919.3.peg.3092
Lonsdalea populi	*Lonsdalea populi* strain N-5-1	CP065534	fig|1172565.28.peg.429
Pectobacterium wasabiae	*Pectobacterium wasabiae* CFBP 3304	CP015750	fig|1175631.8.peg.984
Salmonella bongori	*Salmonella bongori* N268-08	CP006608	fig|1197719.3.peg.4636
Pectobacterium aroidearum	*Pectobacterium aroidearum* strain L6	CP065044	fig|1201031.21.peg.719
Yersinia massiliensis	*Yersinia massiliensis* CCUG 53443	CAKR01000016	fig|1205683.4.peg.2188
Photorhabdus noenieputensis	*Photorhabdus noenieputensis* DSM 25462	JAJQTM010000001	fig|1208607.5.peg.1306
Kluyvera cryocrescens	*Kluyvera cryocrescens* NBRC 102467	BCTM01000015	fig|1218112.3.peg.2530
Sodalis praecaptivus	*Sodalis sp.* HS1	CP006569	fig|1239307.3.peg.3762
Dickeya oryzae	*Dickeya sp.* ZYY5	ML762921	fig|1240404.3.peg.1439
Raoultella electrica	*Raoultella electrica* strain DSM 102253	CP041247	fig|1259973.4.peg.4415
Edwardsiella piscicida	*Edwardsiella piscicida* 18EpOKYJ	CP090968	fig|1263550.90.peg.559
Yersinia pekkanenii	*Yersinia pekkanenii* strain A125KOH2	CQAZ01000006	fig|1288385.3.peg.957
[Pantoea] beijingensis	*[Pantoea] beijingensis* JZB2120001	CP071409	fig|1324864.3.peg.3192
Phaseolibacter flectens	*Pseudomonas flectens* ATCC 12775	JAEE01000001	fig|1336237.3.peg.584
Yersinia wautersii	*Yersinia wautersii* strain WP-931201	CVMG01000012	fig|1341643.4.peg.2033
Tatumella saanichensis	*Tatumella sp.* NML 06-3099	ATMI01000002	fig|1344012.3.peg.310
Buttiauxella brennerae	*Buttiauxella brennerae* ATCC 51605	LXER01000029	fig|1354251.4.peg.3252
Buttiauxella gaviniae	*Buttiauxella gaviniae* ATCC 51604	LXEP01000015	fig|1354253.4.peg.1622
Buttiauxella noackiae	*Buttiauxella noackiae* ATCC 51607	LXEO01000046	fig|1354255.3.peg.2970
Kluyvera georgiana	*Kluyvera georgiana* ATCC 51603	LXEU01000068	fig|1354264.4.peg.3547
Xenorhabdus poinarii	*Xenorhabdus poinarii* G6	FO704551	fig|1354304.4.peg.2896
Proteus myxofaciens	*Cosenzaea myxofaciens* ATCC 19692	LXEN01000102	fig|1354337.7.peg.2286
Izhakiella capsodis	*Izhakiella capsodis* strain N6PO6	FOVC01000003	fig|1367852.4.peg.348
Entomohabitans teleogrylli	*Erwinia sp.* SCU-B244	LLXO01000007	fig|1384589.3.peg.1664
Pseudocitrobacter faecalis	*Pseudocitrobacter faecalis* strain CCM 8478	BNAA01000004	fig|1398493.8.peg.2352
Dickeya aquatica	*Dickeya aquatica* strain 174/2	LT615367	fig|1401087.6.peg.3966
Franconibacter pulveris	*Franconibacter pulveris* 1160	AXSZ01000019	fig|1406822.4.peg.1138
Chania multitudinisentens	*Serratia fonticola* RB-25	CP007044	fig|1441930.4.peg.3364
Yersinia aldovae	*Yersinia aldovae* 670-83	CP009781	fig|1453495.3.peg.3122
Mixta theicola	*Pantoea theicola* strain QC88-366	NWUO01000007	fig|1458355.3.peg.2341
Klebsiella quasipneumoniae	*Klebsiella quasipneumoniae* strain KqPF26	CP065838	fig|1463165.411.peg.4395
Pantoea coffeiphila	*Pantoea coffeiphila* strain 1480	JAFBFW010000005	fig|1465635.4.peg.3682
Hafnia psychrotolerans	*Hafnia psychrotolerans* strain CGMCC 1.12806	BMFZ01000005	fig|1477018.4.peg.2466
Phytobacter (Metakosakonia) massiliensis	*Metakosakonia massiliensis* strain MGYG-HGUT-01426	CABKSF010000003	fig|1485952.4.peg.3407

Enterobacillus tribolii	*Enterobacillus tribolii* strain DSM 103736	QRAP01000005	fig|1487935.3.peg.2556
Siccibacter colletis	*Cronobacter sp.* 1383	JMSQ01000004	fig|1499086.3.peg.746
Escherichia marmotae	*Escherichia marmotae* strain H1-003-0086-C-F	CACSXJ020000004	fig|1499973.35.peg.1505
Pectobacterium actinidiae	*Pectobacterium carotovorum* subsp. actinidiae KKH3	JRMH01000001	fig|1507808.3.peg.3521
Brenneria roseae	*Brenneria roseae* subsp. americana strain LMG 27715	QDKJ01000001	fig|1508507.3.peg.115
Rahnella victoriana	*Rahnella victoriana* JZ-GX1	CP089919	fig|1510570.11.peg.909
Rahnella bruchi	*Rahnella bruchi* strain DSM 27398	QZWI01000006	fig|1510573.3.peg.2647
Rahnella woolbedingensis	*Rahnella woolbedingensis* strain DSM 27399	RAHH01000009	fig|1510574.3.peg.1961
Rouxiella chamberiensis	*Rouxiella chamberiensis* strain 130333	JRWU01000004	fig|1513468.4.peg.3423
Serratia myotis	*Serratia myotis* L7-1	CP099707	fig|1521427.3.peg.582
Mangrovibacter yixingensis	*Mangrovibacter yixingensis* strain SaN21-3	JAIVKM010000003	fig|1529639.10.peg.3160
Arsenophonus apicola	*Arsenophonus endosymbiont* of Apis mellifera strain ArsBeeUS	CP084222	fig|1541805.5.peg.2797
Rosenbergiella epipactidis	*Rosenbergiella epipactidis* YCCK 550	JAKIVJ010000003	fig|1544694.17.peg.1724
Rosenbergiella collisarenosi	*Rosenbergiella collisarenosi* S294	JAKZKA010000002	fig|1544695.12.peg.1666
Rosenbergiella australiborealis	*Rosenbergiella australiborealis* strain CdVSA20.1	JABBFO010000001	fig|1544696.9.peg.1039
Erwinia iniecta	*Erwinia iniecta* strain B120	JRXE01000048	fig|1560201.3.peg.4528
Erwinia endophytica	*Erwinia endophytica* strain A41C3	RQVV01000057	fig|1563158.3.peg.3773
Citrobacter pasteurii	*Citrobacter pasteurii* strain FDAARGOS 1424 strain Not applicable	CP077262	fig|1563222.16.peg.4339
Dickeya undicola	*Dickeya sp.* 2B12	JSYG01000001	fig|1577887.3.peg.41
Pantoea pleuroti	*Pantoea pleuroti* strain JZB 2120015	SBFD01000014	fig|1592631.3.peg.1402
Mixta intestinalis	*Mixta intestinalis* strain SRCM103226	CP028271	fig|1615494.3.peg.4524
Enterobacter kobei	*Enterobacter sp.* 35730	JZYS01000031	fig|1619247.3.peg.3065
Erwinia gerundensis	*Erwinia gerundensis* strain AR	CP073262	fig|1619313.17.peg.2797
Kosakonia pseudosacchari	*Kosakonia pseudosacchari* strain BDA62-3	CP063425	fig|1646340.7.peg.671
Rouxiella silvae	*Rouxiella silvae* strain 213	MRWD01000007	fig|1646373.3.peg.4559
Rouxiella badensis	*Rouxiella badensis* strain SER3	CP049603	fig|1646377.6.peg.4002
Mangrovibacter phragmitis	*Mangrovibacter phragmitis* strain MP23	LYRP01000022	fig|1691903.4.peg.3195
Citrobacter cronae	*Citrobacter cronae* strain Colony478	CP069763	fig|1748967.19.peg.1772
Pseudenterobacter timonensis	*Enterobacter sp.* MT20	FCOP01000011	fig|1755099.3.peg.1663
Dickeya fangzhongdai	*Dickeya fangzhongdai* DSM 101947	CP025003	fig|1778540.117.peg.4072
Enterobacter roggenkampii	*Enterobacter cloacae* complex 'Hoffmann cluster IV' strain DSM 16690	CP017184	fig|1812935.7.peg.617
Pantoea hericii	*Pantoea hericii* strain JZB2120024	SCKV01000003	fig|1815628.3.peg.1971 fig|1815628.3.peg.1972
Scandinavium goeteborgense	*Scandinavium goeteborgense* CCUG 66741	CP054058	fig|1851514.13.peg.3811
Phytobacter palmae	*Kosakonia sp.* S29	FONB01000001	fig|1855371.3.peg.4864
Xenorhabdus eapokensis	*Xenorhabdus eapokensis* DL20	MKGQ01000005	fig|1873482.4.peg.3175
Xenorhabdus thuongxuanensis	*Xenorhabdus sp.* 30TX1	MKGR01000028	fig|1873484.3.peg.1993
Pantoea sesami	*Pantoea sesami* strain Si-M154	FQWJ01000003	fig|1881110.4.peg.2471
Pantoea alhagi	*Pantoea alhagi* strain LTYR-11Z	CP019706	fig|1891675.3.peg.787

[Kluyvera] intestini	*[Kluyvera] intestini* strain GT-16	MKZW03000001	fig|1898961.6.peg.3277
Pectobacterium parmentieri	*Pectobacterium parmentieri* strain IFB5427 strain not applicable	CP027260	fig|1905730.20.peg.4268
Lelliottia jeotgali	*Lelliottia sp.* PFL01	CP018628	fig|1907578.3.peg.650
Citrobacter europaeus	*Citrobacter europaeus* strain 67A	PQSZ01000006	fig|1914243.6.peg.4516
Nissabacter archeti	*Nissabacter archeti* strain JGM97	JAERKB010000005	fig|1917880.6.peg.3303
Izhakiella australiensis	*Izhakiella sp.* D4N98 strain D4N98	MRUL01000006	fig|1926881.3.peg.4607
Pantoea latae	*Pantoea sp.* AS1 strain AS1	MWUE01000013	fig|1964541.4.peg.442
Phytobacter ursingii	*Phytobacter ursingii* strain type strain: ATCC27989 strain ATCC27989T	CABDWT010000002	fig|1972431.3.peg.1082
Proteus alimentorum	*Proteus sp.* 08MAS0041	NBVR01000018	fig|1973495.3.peg.437
Proteus columbae	*Proteus sp.* 08MAS2615	NGVR01000021	fig|1987580.3.peg.698
Klebsiella quasivariicola	*Klebsiella quasivariicola* strain 08A119	CP084768	fig|2026240.29.peg.4617
Providencia huaxiensis	*Providencia huaxiensis* WCHPr000369	CP031123	fig|2027290.27.peg.76
Photorhabdus bodei	*Photorhabdus bodei* strain LJ24-63	NSCM01000044	fig|2029681.3.peg.4279
Serratia oryzae	*Serratia oryzae* strain S32	SOZF01000016	fig|2034155.6.peg.767
Pectobacterium zantedeschiae	*Pectobacterium zantedeschiae* strain 9M	NWTM01000002	fig|2034769.10.peg.3338
Pectobacterium polaris	*Pectobacterium polaris* strain PZ1	CP046377	fig|2042057.37.peg.748
Franconibacter daqui	*Franconibacter daqui* strain CGMCC 1.15944	BMKJ01000003	fig|2047724.3.peg.2763
Proteus cibi	*Proteus sp.* FJ2001126-3	PENW01000019	fig|2050966.3.peg.3266
Proteus faecis	*Proteus faecis* FZP1097	JAMOJQ010000004	fig|2050967.9.peg.2353
Klebsiella grimontii	*Klebsiella grimontii* strain SB6415	CABGGT010000022	fig|2058152.15.peg.5629
Chimaeribacter arupi	*Chimaeribacter arupi* 2016-Iso1	PJZK01000002	fig|2060066.9.peg.2593
Chimaeribacter californicus	*Chimaeribacter californicus* 2015-Iso6	PJZF01000002	fig|2060067.5.peg.2850
Chimaeribacter coloradensis	*Chimaeribacter coloradensis* 2016-Iso4	PJZH01000003	fig|2060068.4.peg.2950
Pectobacterium peruviense	*Pectobacterium peruviense* strain A97-S13-F16	PYUO01000011	fig|2066479.5.peg.451
Enterobacter sichuanensis	*Enterobacter sp.* WCHECl1597	POVL01000004	fig|2071710.3.peg.2956
Lelliottia aquatilis	*Lelliottia aquatilis* strain TZW17	JAENMQ010000002	fig|2080838.5.peg.2689
Pectobacterium punjabense	*Pectobacterium punjabense* strain SS95	CP038498	fig|2108399.7.peg.3945
Klebsiella huaxiensis	*Klebsiella huaxiensis* WCHKl090001	CP036175	fig|2153354.10.peg.4959
[Erwinia] mediterraneensis	*Erwinia sp.* Marseille-P5165	LR026978	fig|2161819.3.peg.2090
Limnobaculum parvum	*Limnobaculum parvum* HYN0051	CP029185	fig|2172103.7.peg.2484
Pectobacterium aquaticum	*Pectobacterium aquaticum* A212-S19-A16	CP086253	fig|2204145.13.peg.3728
Dickeya lacustris	*Dickeya sp.* S29	QNUT01000054	fig|2259638.3.peg.1510
Edaphovirga cremea	*Rahnella sp.* DSM 105170	QOVA01000003	fig|2267246.3.peg.2847
Yersinia hibernica	*Yersinia sp.* CFS1934	CP032487	fig|2339259.3.peg.715
Kalamiella piersonii	*Erwiniaceae bacterium* IIIF1SW-P2	RARB01000004	fig|2364647.3.peg.3532
Enterobacter oligotrophicus	*Enterobacter oligotrophica* strain CCA6	AP019007	fig|2478464.3.peg.3020
Pectobacterium polonicum	*Pectobacterium polonicum* strain DPMP315	RJTN01000003	fig|2485124.3.peg.3100
Pseudocitrobacter vendiensis	*Pseudocitrobacter vendiensis* type strain: CPO20170097	CALSBS010000004	fig|2488306.3.peg.1444
Pectobacterium versatile	*Pectobacterium sp.* CFBP6051	RMBU01000033	fig|2488639.3.peg.2045

Klebsiella africana	*Klebsiella africana* strain 200023	CP084874	fig|2489010.4.peg.4369
Enterobacter chengduensis	*Enterobacter chengduensis* WCHECl-C4 = WCHECh050004	CP043318	fig|2494701.30.peg.799
Enterobacter huaxiensis	*Enterobacter huaxiensis* 090008 = WCHEHu090008	CP043342	fig|2494702.15.peg.3945
Enterobacter quasiroggenkampii	*Enterobacter sp.* WCHEn090040	RXSJ01000003	fig|2497436.3.peg.2540
Enterobacter chuandaensis	*Enterobacter chuandaensis* C210219	JAMGKO010000006	fig|2497875.8.peg.4212
Jinshanibacter zhutongyuii	*Pragia sp.* CF-458	CP034752	fig|2498113.3.peg.2984
Serratia microhaemolytica	*Yersiniaceae bacterium* ZS-11	SBEF01000034	fig|2500534.3.peg.2425
Kosakonia quasisacchari	*Kosakonia sp.* WCHEs120001 strain WCHKQ120001	SJOP01000005	fig|2529380.3.peg.4151
Enterobacter wuhouensis	*Enterobacter sp.* WCHEs120002 strain WCHEW120002	SJOO01000004	fig|2529381.3.peg.3267
Enterobacter quasihormaechei	*Enterobacter sp.* WCHEs120003 strain WCHEQ120003	SJON01000004	fig|2529382.3.peg.3131
Citrobacter arsenatis	*Citrobacter sp.* LY-1	CP037864	fig|2546350.3.peg.699
Cedecea colo	*Cedecea colo* strain ZA	SOYS01000004	fig|2552946.3.peg.2990
Mixta tenebrionis	*Mixta sp.* BIT-26	VHQI01000002	fig|2562439.3.peg.2009
Citrobacter tructae	*Citrobacter sp.* SNU WT2	CP038469	fig|2562449.3.peg.2643
Escherichia alba	*Escherichia alba* strain B35	WMJZ01000002	fig|2562891.3.peg.1757
Bruguierivorax albus	*Biostraticola sp.* BGMRC 2031	SZPQ01000001	fig|2575567.3.peg.1692
Jejubacter calystegiae	*Izhakiella sp.* KSNA2	CP040428	fig|2579935.4.peg.1883
Klebsiella indica	*Klebsiella sp.* TOUT106	VCHQ01000024	fig|2582917.3.peg.2115
Klebsiella pasteurii	*Klebsiella pasteurii* 15Km1352	JAPJJB010000013	fig|2587529.12.peg.1797
Affinibrenneria salicis	*Brenneria sp.* L3-3HA	VYKJ01000001	fig|2590031.3.peg.340
Serratia rhizosphaerae	*Serratia sp.* KUDC3025	CP041764	fig|2597702.3.peg.1398
Yersinia canariae	*Yersinia sp.* NCTC 14382	CP043727	fig|2607663.3.peg.716
Escherichia ruysiae	*Escherichia ruysiae* C61-1	JAMSJK010000003	fig|2608867.59.peg.3171
Citrobacter telavivensis	*Citrobacter sp.* NMI7905_11	WHIY01000005	fig|2653933.3.peg.4990
Pantoea jilinensis	*Pantoea jilinensis* strain D25	CP077746	fig|2676834.3.peg.3330
Acerihabitans arboris	*Enterobacteriales bacterium* SAP-6	WUBS01000001	fig|2691583.3.peg.221
Sodalis ligni	*Sodalis sp.* dw_23	WXYM01000003	fig|2697027.3.peg.5040
Serratia bockelmannii	*Serratia bockelmannii* sma21	JAPFKJ010000002	fig|2703793.13.peg.3213
Serratia nevei	*Serratia nevei* 9rpt1	JAMYWQ010000039	fig|2703794.6.peg.3357
Rahnella contaminans	*Rahnella sp.* Lac-M11	JAADJS010000002	fig|2703882.3.peg.2202
Rouxiella aceris	*Rahnella sp.* SAP-1	JAADJU010000006	fig|2703884.3.peg.4027
Rahnella aceris	*Rahnella aceris* S2-A69	CP093328	fig|2703885.11.peg.4081
Brenneria izadpanahii	*Brenneria sp.* Ir50	CP050854	fig|2722756.3.peg.705
Kluyvera sichuanensis	*Kluyvera sp.* SCKS090646	JABBJF010000010	fig|2725494.3.peg.2675
Insectihabitans xujianqingii	*Insectihabitans xujianqingii* CWB-B4	JADRCP010000001	fig|2738837.5.peg.521
Serratia surfactantfaciens	*Serratia surfactantfaciens* YD25	CP016948	fig|2741499.12.peg.4935
Mixta mediterraneensis	*Mixta sp.* Marseille-Q2057	JACFXY010000001	fig|2758443.3.peg.1877
Escherichia whittamii	*Escherichia whittamii* strain C2-3	JAINCF010000051	fig|2762229.4.peg.3901
Xenorhabdus lircayensis	*Xenorhabdus sp.* VLS	JACOII010000037	fig|2763499.4.peg.1950

Escherichia hominis	*Escherichia sp.* L7	JACRWJ010000029	fig|2764324.3.peg.961
Pantoea Psp39-30	Pantoea Psp39-30	JACSWU010000114	fig|2767592.3.peg.327
Pectobacterium quasiaquaticum	*Pectobacterium quasiaquaticum* A398-S21-F17	CP065178	fig|2774015.5.peg.3519
Pectobacterium parvum	*Pectobacterium parvum* strain FN20211	CP087392	fig|2778550.7.peg.4009
Rahnella laticis	*Rahnella sp.* SAP-17	JADOBI010000003	fig|2787622.4.peg.3192
Jinshanibacter allomyrinae	*Budviciaceae bacterium* BWR-B9	JADRCR010000002	fig|2791986.4.peg.1980
Enterobacter vonholyi	*Enterobacter vonholyi* KD11A-1	JAMDPD010000017	fig|2797505.4.peg.3128
Enterobacter dykesii	*Enterobacter dykesii* strain 120147	JAHEVX010000005	fig|2797506.3.peg.3182
Tenebrionibacter intestinalis	*Enterobacterales bacterium* BIT-L3	JAEPBH010000023	fig|2799638.3.peg.1771
Photorhabdus aegyptia	*Photorhabdus aegyptia* strain BKT4.5	JAGJDU010000126	fig|2805098.4.peg.617
Leclercia pneumoniae	*Leclercia sp.* 4-9-1-25	CP071383	fig|2815358.3.peg.602
Tenebrionicola larvae	*Enterobacteriaceae bacterium* YMB-R21	JAGFEW010000025	fig|2815733.3.peg.1862
Rahnella perminowiae	*Rahnella perminowiae* C60	JAFMOT010000178	fig|2816244.8.peg.259
Rahnella bonaserana	*Rahnella sp.* H11b	JAFMOW010000067	fig|2816248.3.peg.2625
Rahnella rivi	*Rahnella sp.* FC061912-K	JAFMOX010000054	fig|2816249.3.peg.798
Rahnella ecdela	*Rahnella sp.* FRB 231	JAFMOY010000133	fig|2816250.3.peg.1785
Enterobacter quasimori	*Enterobacter quasimori* strain 120130	JAHEVU010000004	fig|2838947.3.peg.3337
Erwinia phyllosphaerae	*Erwiniaceae bacterium* CMYE1	JAHSPF010000015	fig|2853256.3.peg.786
Photorhabdus antumapuensis	*Photorhabdus sp.* UCH-936	JAHZMK010000044	fig|2862867.10.peg.3384
Pectobacterium colocasium	*Pectobacterium sp.* LJ1	CP084032	fig|2878098.10.peg.3978
Musicola keenii	*Musicola keenii* A3967	JAACFQ010000007	fig|2884250.3.peg.3828
Yersinia artesiana	*Yersinia artesiana* IP39904	CABHYL010000022	fig|2890315.10.peg.1363
Yersinia proxima	*Yersinia proxima* strain IP38950	CABHYW010000001	fig|2890316.18.peg.17
Yersinia alsatica	*Yersinia alsatica* SCPM-O-B-7604	CP104006	fig|2890317.4.peg.652
Pseudocitrobacter corydidari	*Pseudocitrobacter sp.* G163CM	CP087880	fig|2891570.3.peg.2951
Huaxiibacter chinensis	*Enterobacteriaceae bacterium* 155047	JAJVHF010000002	fig|2899785.5.peg.1584
Brenneria tiliae	*Brenneria sp.* WC1b.1 WC1b.1T	JAKPCB010000100	fig|2914984.4.peg.3427
Leclercia tamurae	*Leclercia sp.* H6S3	JAMHKS010000065	fig|2926467.3.peg.760
Silvania hatchlandensis	*Enterobacteriaceae bacterium* H19S6	JAMGZK010000051	fig|2926469.3.peg.3435
Silvania confinis	*Enterobacteriaceae bacterium* H4N4	JAMGZJ010000068	fig|2926470.3.peg.202
Scandinavium hiltneri	*Scandinavium sp.* H11S7	JALIGE010000070	fig|2926519.4.peg.4141
Scandinavium manionii	*Scandinavium manionii* SB 3.3	JALIGD010000043	fig|2926520.8.peg.3932
Scandinavium tedordense	*Scandinavium sp.* TWS1a strain TWS1a.2	JALIGG010000053	fig|2926521.3.peg.3818
Winslowiella arboricola	*Erwiniaceae bacterium* BAC15a-03b BAC15a-03bT	JAODIM010000041	fig|2978220.3.peg.2897